

Neutron-Physical Simulation of Fast Nuclear Reactor Cores

Investigation of New and Emerging Nuclear Reactor Systems

Zur Erlangung des Grades eines Doktors der Naturwissenschaften (Dr. rer. nat.)

genehmigte Dissertation von Friederike Renate Frieß, M.Sc., aus Cuxhaven

Tag der Einreichung: 13.6.2017, Tag der Prüfung: 12.7.2017

Juli 2017 — Darmstadt — D 17

1. Gutachten: Prof. Dr. Barbara Drossel
2. Gutachten: Prof. Dr. Wolfgang Liebert



TECHNISCHE
UNIVERSITÄT
DARMSTADT

Institut für Festkörperphysik
Fachbereich Physik

Neutron-Physical Simulation of Fast Nuclear Reactor Cores
Investigation of New and Emerging Nuclear Reactor Systems

Genehmigte Dissertation von Friederike Renate Frieß, M.Sc., aus Cuxhaven

1. Gutachten: Prof. Dr. Barbara Drossel
2. Gutachten: Prof. Dr. Wolfgang Liebert

Tag der Einreichung: 13.6.2017

Tag der Prüfung: 12.7.2017

Juli 2017 — Darmstadt — D 17

Contents

1. Introduction	1
1.1. Basics of (Fast) Nuclear Reactors	2
1.2. Generation IV Nuclear Power Plants	4
1.3. Special Applications for Fast Nuclear Reactors	5
1.3.1. Disposition of Weapon-grade Plutonium	5
1.3.2. Powering Remote Energy Grids	6
1.3.3. Partitioning and Transmutation	8
1.4. Research Synopsis	12
2. Material Assessment & Non-Proliferation	15
2.1. Fissile Materials in the Nuclear Fuel Cycle	15
2.2. The Existing Non-Proliferation Regime	16
2.3. General Considerations on Assessing Proliferation Risk	17
2.4. Spent Fuel Standard	18
2.5. Figures of Merit	19
3. Theoretical Basis	23
3.1. Neutron Flux Distribution	23
3.2. Source Efficiency	26
3.3. Material Depletion	27
3.4. Spallation Reaction	28
3.5. Interaction of Radiation and Tissue	30
4. Simulation Methods	33
4.1. Monte Carlo Calculation of the Neutron Flux	33
4.2. Depletion Calculation	34
4.2.1. Solution Approach for Depletion Calculations	34
4.2.2. The Depletion Codes MCMATH and VESTA	35
4.3. Spallation Source	36
4.3.1. Implementation in MCNPX	36
4.3.2. Calculation of the Source Efficiency	37
4.4. Dose Rate Calculations	38
5. Plutonium Breeding and Disposition in the Russian Fast Reactor BN-800	41
5.1. History of Russian Fast Reactors	41
5.2. BN-800 Reactor Simulation Model	42
5.2.1. Description of the Reactor Design	42
5.2.2. Simulation Parameters	45
5.3. Results of the BN-800 Simulation	46
5.3.1. Evolution of the Plutonium Vector	46
5.3.2. Plutonium Breeding in the Blankets	47
5.3.3. Dose Rates from Spent Fuel Elements	49
5.4. Summary	51

6. Plutonium Production in Small, Fast Reactors	53
6.1. Nuclear Batteries — The Smallest Nuclear Reactors	53
6.2. SMR Reactor Simulation Model	54
6.2.1. Description of the Reactor Design	55
6.2.2. Simulation Parameters	58
6.3. Results of the SMR Simulation	58
6.3.1. Neutron Flux and Criticality	59
6.3.2. Material Attractiveness	60
6.4. Summary	63
7. Partitioning and Transmutation Fuel Cycle	65
7.1. The History of Accelerator-Driven Systems in Europe	66
7.2. Accelerator-Driven System Reactor Models	67
7.2.1. The MYRRHA Reactor Model	67
7.2.2. The EFIT Reactor Model	72
7.2.3. Simulation Parameters	75
7.3. Model Verification	76
7.3.1. Criticality of the Reactor Cores	76
7.3.2. Position of the Spallation Source in the Core	77
7.3.3. Neutron Flux in the Reactor Cores	78
7.3.4. Source Efficiency	80
7.3.5. Transmutation of Minor Actinides and Plutonium	81
7.4. Aging of the Transuranium Vector	83
7.4.1. The Reactivity Swing During Reactor Operation	83
7.4.2. Irradiation History and Criticality	85
7.4.3. Plutonium Vectors from a European P&T Scenario	87
7.5. Characteristics of the Spent Fuel Elements	89
7.5.1. Activity	90
7.5.2. Heat Development	92
7.5.3. Gamma Dose Rate	94
7.6. Inventory of Long-lived Fission Products	97
7.6.1. Importance for Long-term Safety Analysis	97
7.6.2. Concentration of Long-lived Fission Products in the Spent P&T-Fuel	101
7.6.3. Total Inventory in a Simplified Scenario	103
7.7. Summary	106
8. Conclusion	109
Bibliography	115
A. Acronyms	127
B. MCNPX Input Files	129
C. Specific Activities	131

Zusammenfassung

An der Kernenergie scheiden sich die Geister: Befürworter führen die Vorzüge einer erprobten Technologie für die (fast) CO₂-freie Stromerzeugung ins Feld. Kritiker hingegen sehen vor allem das ungelöste Abfallproblem, das Risiko schwerer Unfälle und die Verbreitung von kernwaffenfähigem Material. Ungefähr seit der Jahrtausendwende wird von neuen Reaktoren gesprochen, die diese Probleme nicht oder nur in deutlich verminderter Form mit sich bringen sollen: die Reaktoren der sogenannten vierten Generation. Die Hälfte der von einer entsprechenden Interessengruppe vorgeschlagenen Reaktortypen sind dabei schnelle Reaktoren. In schnellen Reaktoren werden, im Gegensatz zu thermischen Reaktoren, die Neutronen im Reaktorkern nicht moderiert, das heißt abgebremst. Schnelle Reaktoren befinden sich seit den 1950er Jahren in der Entwicklung.

Aufgrund verschiedener Probleme, wie den hohen Kosten, der Proliferationsgefahr und den Sicherheitsrisiken der komplizierten Technologie, werden zur Leistungserzeugung bislang fast ausschließlich thermische Reaktoren verwendet. Dies mag einer der Gründe sein, warum seit ungefähr 15 Jahren schnelle Reaktoren vermehrt für neue Anwendungsfelder beworben werden. Wichtige Beispiele sind

- die Entsorgung von waffengrädigem Plutonium aus ausgemusterten Militärbeständen: Im Falle des zweiten wichtigen Kernwaffenstoffes, dem hoch angereicherten Uran, gibt es eine verhältnismäßig leichte Methode der Entsorgung. Es lässt sich mit Natururan mischen und als Brennstoff für Kernreaktoren verwenden. Für die Entsorgung waffengrädigen Plutoniums gibt es hingegen keine allgemein akzeptierte Lösung. Eine Option wäre die Bestrahlung im schnellen Reaktor. Dadurch ändert sich die Plutoniumzusammensetzung (Isotopenvektor), und hochradioaktive Spaltprodukte werden dem Waffenmaterial hinzugefügt. Die hierdurch entstehende Strahlung erschwert den Zugriff. Beide Aspekte zusammen sollen das verbliebene Plutonium proliferationsresistenter machen.
- die dezentrale Energieversorgung abgelegener Gegenden mit nur kleinem Energiebedarf: Viele kleine Kommunen, beispielsweise in Kanada und Alaska, aber auch in Ländern des geografischen Südens, sind bei ihrer Energieversorgung auf teure Dieselgeneratoren angewiesen. Eine Lösung verspricht das Konzept sogenannter *nuklearer Batterien*, also sehr kleiner Kernreaktoren mit sehr lange im Kern verbleibendem Brennstoff. Zusätzlich liegen die Investitionskosten pro Reaktor im Vergleich zu großen Leistungsreaktoren deutlich niedriger. Diese Eigenschaften sollen die kleinen Reaktoren auch für Schwellenländer attraktiv machen, trotz höherer Kosten pro installierter Kilowattstunde.
- die Behandlung von radioaktivem Abfall, der möglicherweise weitreichendste Ansatz: Die wiederholte Bestrahlung der abgebrannten Brennelemente in spezialisierten Reaktoren (Transmutation) soll unter anderem die zu gewährleistenden Einschlusszeiten für ein immer noch notwendiges Endlager auf einige hundert Jahre im Vergleich zu vorher einer Million Jahren reduzieren. Zwischen den einzelnen Bestrahlungsschritten ist eine Aufteilung der abgebrannten Brennelemente in verschiedene Stoffströme notwendig (Partitionierung). Das Gesamtkonzept wird dementsprechend auch Partitionierung und Transmutation (P&T) genannt.

Die Diskussion über den möglichen Nutzen der schnellen Reaktoren wird von Interessengruppierungen der Nuklearindustrie und der Nuklearforschung bestimmt. Es fehlt eine unabhängige wissenschaftliche Analyse der Versprechen. Die vorliegende Arbeit untersucht die drei genannten Anwendungsgebiete anhand eigener Reaktorsimulationen, um Beiträge zu einer möglichst umfassenden Beurteilung zu liefern. Computermodelle für die untersuchten Reaktortypen wurden mit öffentlich zugänglichen Daten angefertigt. Mit Hilfe von Monte-Carlo-Simulationen der Neutronenverteilung im Kern wurden Abbrandrechnungen mit den Programmen MCNPX, VESTA und MCMATH durchgeführt, die Aufschluss über die Entwicklung der Brennstoffzusammensetzung geben. Der Gehalt an Spaltprodukten und Transuranen ermöglicht direkte Rückschlüsse auf die

Waffentauglichkeit des entstehenden Materials, aber auch auf weitere Eigenschaften, die für die Weiterverarbeitung oder Endlagerung relevant sind. Das Datenmaterial kann dann auch für Folgerechnungen zur Bestimmung der Dosisrate herangezogen werden. Eine hohe Dosisrate erfordert entsprechenden Strahlenschutz bei der Handhabung. Ab einer gewissen Grenze, üblicherweise mehr als ein Sievert pro Stunde, wird das Material als sich-selbst-sichernd angesehen.

Als Beispiel für Plutonium-Disposition wurde der russische schnelle Brüter BN-800 modelliert, der seit 2015 in Betrieb ist. Für die Entsorgung des waffengrädigen Plutoniums zeigt sich, dass die zuvor in einem russisch-amerikanischen Abkommen formal festgesetzten Kriterien erfüllt werden. Das Verhältnis von Plutonium-240 zu Plutonium-239 im bestrahlten Plutonium ist größer als 0,1. Außerdem liegt das Plutonium in abgebrannten Brennelementen vor, die auch nach einer Abklingzeit von 30 Jahren noch eine Dosisrate von mehr als einem Sievert pro Stunde emittieren. Allerdings wird gleichzeitig in den Brutelementen an der Peripherie des Kerns extrem waffentaugliches Material (Gehalt an Plutonium-239 mehr als 93 %) erbrütet, das zudem nur durch eine sehr geringe Strahlungsbarriere vor Zugriff geschützt ist. Gerade wenn der BN-800, wie von Russland geplant, an andere Länder weiterverkauft werden soll, muss die mögliche Proliferationsgefahr beachtet werden.

Der Toshiba 4S wurde aufgrund seines fortgeschrittenen Designs und der geringen Leistung von 10 MWe bei einer gleichzeitigen Kernlaufzeit von 30 Jahren als Beispiel für eine nukleare Batterie gewählt. Was die Proliferationssicherheit angeht, zeigen sich ähnliche Probleme wie beim BN-800. Als starkes Argument wird immer wieder der für 30 Jahre versiegelte Kern genannt. Auch das Öffnen des Kerns und der Wechsel der Brennelemente soll nur mit speziellen Geräten möglich sein, die speziell zu dieser Gelegenheit zum Reaktorstandort transportiert würden. Allerdings wird im Reaktor selbst eine überdurchschnittlich große Menge an Plutonium erbrütet. Bereits nach zwei Jahren enthält der Kern ausreichend Material für eine Kernwaffe (>8 kg). Eine für militärische Zwecke eher gut geeignete Plutoniumzusammensetzung ist für schnelle Reaktoren charakteristisch. Das Plutonium aus dem 4S-Reaktor hat allerdings eine herausragende Qualität mit einem Anteil an Plutonium-239 von mehr als 97 %. Mit Hilfe dieses Reaktortyps ließe sich leicht eine Option des Zugriffs auf Kernwaffenmaterial aufbauen. Im Falle eines offenen Ausbruchs aus Nichtverbreitungsverpflichtungen, insbesondere im Rahmen des Nichtverbreitungsvertrages¹, hätte ein Staat schnellen Zugang zu militärisch exzellent nutzbarem Material.

Das bei weitem komplexeste System, das hier betrachtet wird, ist der beschleuniger-getriebene unterkritische Reaktor (ADS, aus dem Englischen: *Accelerator-driven System*), der für P&T ausgelegt ist. In ihm sollen gewisse Anteile des radioaktiven Abfalls verbrannt werden. Auf dem Weg zu der möglichen Implementierung eines P&T-Szenarios sind noch viele technologische Hürden zu nehmen. Das gilt insbesondere für den ADS selbst. So wurde bis jetzt kein beschleuniger-getriebener Reaktor, auch kein Versuchsreaktor, in Betrieb genommen. Zusätzlich stellt sich die grundsätzliche Frage nach dem Nutzen der Technologie. Im Rahmen dieser Arbeit wurden relevante Aspekte näher untersucht.

Als Grundlage für die Computersimulationen wurden die europäischen Reaktordesigns MYRRHA (*Multi-purpose hYbrid Research Reactor for High-tech Applications*) und EFIT (*European Industrial Sized Transmutation Facility*) gewählt, da für diese detaillierte Designdaten vorliegen. Weiterhin wurden die europäischen Szenarien zur P&T-Implementierung in Anlehnung an PATEROS (*Partitioning and Transmutation European Roadmap for Sustainable Nuclear Energy*) verwendet.

Im Rahmen von PATEROS wurden Brennstoffzusammensetzungen über den zeitlichen Verlauf möglicher P&T-Szenarien publiziert. Es zeigt sich auf der Basis der durchgeführten Simulationen, dass der Anteil an spaltbaren Isotopen stets signifikant höher ist als in der Brennstoffzusammensetzung, für die der EFIT-Reaktor laut Design ausgelegt ist. Kritikalitätsrechnungen ergeben dementsprechend einen deutlich zu hohen Wert für die Kritikalität des Systems mit $k_{eff} = 1,6$. Ein

¹ Vertrag über die Nichtverbreitung von Kernwaffen (NVV), im Englischen: Treaty on the Non-Proliferation of Nuclear Weapons (NPT).

solch hoher Wert ist im Betrieb technisch nicht möglich. Die Diskrepanz zwischen dem untersuchten Reaktordesign EFIT und den Szenarien, für deren Verwendung EFIT geplant ist, ist evident und stellt die bislang vorgelegte P&T-Szenarienentwicklung insgesamt in Frage. Die hohe Kritikalität des Systems erfordert eine Reduzierung der minoren Aktinide im Brennstoff und verlängert damit mögliche Umsetzungszeiträume eines P&T-Szenarios.

Zusätzlich unterscheiden sich die Charakteristika abgebrannter Brennelemente aus ADS von abgebrannten Brennelementen aus heute üblichen thermischen Kernreaktoren hinsichtlich Wärmeentwicklung, Aktivität und Dosisrate. Welche Auswirkungen das auf die notwendige Weiterverarbeitung hat, ist noch nicht klar. So ist beispielsweise die Wärmeentwicklung – ein bestimmender Faktor beim Transport zu einer Wiederaufarbeitungsanlage und bei der Dimensionierung des Endlagers – um mindestens eine Größenordnung höher.

Als Argumentationsgrundlage für den Nutzen von P&T wird normalerweise die dadurch mögliche deutliche Reduktion des Radiotoxizitätsindex basierend auf der Ingestionsdosisrate herangezogen. Diese Berechnungen gehen jedoch von der nur vordergründig konservativen Annahme einer Aufnahme des kompletten Endlagerinventars in den menschlichen Körper aus. Bei dieser Art der Bewertung sind die bestimmenden Faktoren Plutonium und die minoren Aktiniden, hauptsächlich Neptunium, Americium und Curium. Im Rahmen einer Langzeitsicherheitsanalyse eines atomaren Endlagers muss dem gegenüber allerdings auch die Mobilität der verschiedenen Isotope berücksichtigt werden. Die Wahrscheinlichkeit, durch natürliche Ursachen aus dem unterirdischen Endlager an die Oberfläche transportiert zu werden, ist für bestimmte, langlebige Spaltprodukte deutlich höher als für Transurane. Demzufolge dominieren diese auf Zeitskalen von mehreren 10.000 Jahren auch die Gesamtdosis, die vom Endlager ausgeht.

Relevant sind vor allem Zirkonium-93, Technetium-99, Iod-129 und Cäsium-135. Die Rechnungen zeigen, dass alle diese Isotope auch im P&T-Brennstoff generiert werden. Meist entstehen ähnliche Mengen wie in Leichtwasserreaktoren. Allerdings vervierfacht sich der Anteil an Cäsium-135. Hochgerechnet auf ein mögliches deutsches P&T-Szenario würde sich die endzulagernde Menge an Cäsium-135 im Vergleich zum derzeit beschlossenen Ausstiegsszenario mit direkter Endlagerung mehr als verdoppeln. Nur die direkt endzulagernden Brennstäbe betrachtet, würde sich die endzulagernde Menge an langlebigen Spaltprodukten von knapp 26 Tonnen auf etwa 40 Tonnen erhöhen.

Grundsätzlich würde man sich demnach die Reduzierung der minoren Aktinide im Endlager durch eine Erhöhung der langlebigen Spaltprodukte erkaufen. Neben Cäsium-135 ist für die Endlagersicherheit auch die deutliche Erhöhung des Technetium-99- und Iod-129-Gehalts von Bedeutung. Somit stellt sich ganz grundsätzlich die Frage, inwieweit eine P&T-Behandlung des radioaktiven Abfalls überhaupt nützt, wenn sich die Menge an sehr langlebigen endlager-relevanten Isotopen deutlich erhöht.

Die behandelten Beispiele zeigen, dass der Einsatz von schnellen Reaktoren zumindest fragwürdig ist. Der Nutzen ist nicht immer klar, gleichzeitig bergen sie eine hohe (latente) Proliferationsgefahr. Im Nichtverbreitungsvertrag ist das *"unveräußerliche Recht (...) der Verwendung der Kernenergie"* festgeschrieben. Solange schnelle Reaktorsysteme technologisch und wirtschaftlich attraktiv erscheinen, können mögliche Proliferateure diese Argumente nutzen, um sich zugleich eine Zugriffsoption auf waffentaugliches Material zu schaffen oder zumindest offen zu halten. Die auch im ADS vorhandene Proliferationsgefahr wurde nicht weiter diskutiert, weil sich für eine mögliche Umsetzung von P&T bereits viel grundlegendere Fragen stellen – wie der Einfluss auf das Endlager oder realistische Umsetzungszeiträume. Festzuhalten ist, dass das P&T-Konzept den Betrieb einer Vielzahl an kerntechnischen Anlagen mit einem schnellen Neutronenspektrum über einen Zeitraum von mindestens einem Jahrhundert erforderte.



1 Introduction

Nuclear energy production is an often fiercely discussed topic. While some see it as viable option to produce energy low on carbon dioxide emissions, for others safety and security risks posed by nuclear technology are at the forefront. The anticipated risks and potentials vary depending on the considered reactor design. One class of nuclear reactors that has been around nearly since the beginning of nuclear energy production is the fast (breeder) reactor. Compared to the more common thermal reactors, the free neutrons present in a fast reactor have a higher energy and are moving at higher velocities.

In the 1950s and 1960s, the Soviet Union and the United States were already aiming at closing their nuclear fuel cycle through the use of fast breeder reactors (Cochran 2010). In thermal reactors only a few percent of the uranium isotopes contained in the fuel can be used for energy production. This is different in fast breeder reactors. During operation, plutonium – which can also be used for energy production – is produced by neutron absorption of uranium isotopes. It is argued that the uranium resources can be used far more efficiently in a fast neutron spectrum. Extracting up to 60 times more energy than in a thermal reactor seems possible (World Nuclear Association 2017a). Using fast breeder technology, the present uranium stocks could last significantly longer (Mueller 2013; Gen IV International Forum 2016).

If the plutonium produced in the reactor is to be used for the fabrication of fresh fuel elements, several reprocessing and fabrication steps are necessary. These are not only costly, but also technologically challenging. Consequently, apart from several attempts and ample advertisement, the operational record of fast reactors is short. The largest fraction of nuclear energy is produced in light water reactors. Advocates often talk of 400 reactor years of experience for fast reactors (World Nuclear Association 2017a). Yet, this is a low number compared to the more than 16,000 years of commercial nuclear power plant operation (World Nuclear Association 2017c).

Currently, only two fast reactors are operating on a commercial base: the Russian BN-600 and the Russian BN-800 (World Nuclear Association 2017a). Furthermore, several of the fast reactor programs cannot be seen as a success. The French sodium-cooled breeder Superphénix was shut down in 1998 with a lifetime load factor of only 7% (IPFM 2010). The Japanese fast breeder prototype Monju was connected to the grid in 1995. Due to safety inspection violations, the reactor could not be restarted since 2012. In between, it was operational for only 250 days (Takubo et al. 2016). The German fast breeder in Kalkar never became critical and the site is now used as an amusement park (IAEA 2006, p. 359; Obbink 2017). Several other reactor projects can be added to the list of failed fast breeders.

Since fast reactor programs need massive investments over long periods of time without the guarantee of a successful outcome, all current fast breeder programs are state-driven. In the last decades, at least in western countries, no further efforts for the deployment of fast reactors were undertaken. By comparison, some countries, such as Russia or India, are still aiming at closing their nuclear fuel cycle. Several other countries abandoned or at least postponed their fast reactor ambitions.

In recent years though, other possible applications for fast reactors have been discussed prominently. One example is the disposition of excess weapon-grade plutonium in the Russian BN-800. Others are the energy production in remote areas using small, modular reactors (SMRs) and the treatment of the spent fuel by partitioning and transmutation (P&T). These applications will be investigated in this thesis.

This introductory chapter starts with explaining the underlying working principles of fast reactors and the delineation to thermal ones in section 1.1. International research efforts concentrate on a few reactor designs that were chosen by the Generation IV Forum. The research objective and the reactor designs are introduced in section 1.2. The concepts of plutonium disposition, SMRs and P&T are explained in section 1.3. The chapter concludes with the research synopsis.

1.1 Basics of (Fast) Nuclear Reactors

Except for the until now only hypothetically working fusion reactors, energy is generated in nuclear reactors by induced fission. Heavy isotopes, usually uranium isotopes, are hit by free neutrons and split into two smaller nuclei, a few additional neutrons and other particles. On average, each fission releases 200 MeV of energy. The free neutrons can then induce further fissions in the next generation. Not all neutrons generated in one generation are available to cause new fission. There are other reactions, such as absorption, taking place or the neutrons leak from the core. The neutron life cycle in a reactor is described by the effective multiplication factor k_{eff} or criticality of the system (United States Department of Energy 1993b, p. 32)

$$k_{eff} = \frac{\# \text{ of neutrons in generation } n + 1}{\# \text{ of neutrons in generation } n}. \quad (1.1)$$

The effective multiplication factor can be derived from the infinite multiplication factor which only accounts for material intrinsic corrections factors. Examples are the fast fission factor or the resonance escape probability. For the effective multiplication factor k_{eff} , factors are added that represent leakage out of the core geometry. Usually, the larger the core, the lower is the fraction of neutrons leaking. For critical reactor operation, the neutron chain reaction should be self-sustaining without excursion, meaning a more or less constant number of neutrons per generation in the core. In this case, $k_{eff} = 1$. For lower values, the chain reactions dies while for higher values, there is an exponential increase in the number of neutrons. Subsequently, the number of fissions and released energy per generation rises. This kind of behavior is desired in a nuclear weapon.

Almost all energy produced today in nuclear power plants comes from thermal reactors. In these nuclear power plants, the most likely energy for neutrons is around 0.025 eV which is the peak of the Maxwell-Boltzmann distribution at room temperature. The neutrons, however, originate mostly from nuclear fission which produces neutrons with much higher energies in the range of 1 MeV. To get a thermal spectrum, the neutrons are slowed down by a moderator (e.g. water or graphite). The probability of a certain reaction is described by the reaction cross section σ and depending on the energy of the incident neutron. For a certain neutron flux distribution $\Phi(E)$, the effective neutron cross section σ_{eff} can be defined as

$$\sigma_{eff} = \frac{\int \sigma(E)\Phi(E)dE}{\int \Phi(E)dE}. \quad (1.2)$$

Table 1.1 gives values related to reactor operation for important uranium and plutonium isotopes. Cross sections are given in barn ($= 10^{-24}\text{cm}^2$). For the thermal incident neutrons, an energy of 0.025 eV is assumed, whereas for the fast spectrum neutrons the neutrons flux distribution from a liquid metal fast breeder reactor is taken. As can be clearly seen, in a thermal spectrum the fission of uranium-235 is more probable than the fission of uranium-238. But natural uranium only contains about 0.7 % of uranium-235. Consequently, for the use in thermal reactors, the uranium is usually enriched to 3 %-4 % uranium-235. This also implies that most of the energy contained in the uranium isotopes cannot be used for energy generation. The lower cross sections for the fast spectrum result in a higher neutron flux for a comparable power output.

Table 1.1.: Average fission and capture cross sections for a thermal and a fast neutron spectrum in barn (Holdren et al. 1995, p. 44).

Isotope	$\sigma_{f, \text{ther.}}$	$\sigma_{c, \text{ther.}}$	$\nu_{\text{ther.}}$	$\eta_{\text{ther.}}$	$\sigma_{f, \text{fast}}$	$\sigma_{c, \text{fast}}$	ν_{fast}	η_{fast}
U-233	62.3	7.6	2.50	2.23	2.63	0.26	2.53	2.30
U-235	46.1	10.3	2.42	1.98	1.82	0.53	2.49	1.93
U-238	0.1	0.9	2.80	0.28	0.05	0.26	2.47	0.40
Pu-239	110	61.3	2.88	1.85	1.79	0.45	2.94	2.35

The situation changes in a fast neutron spectrum, where more fissile material can be produced by neutron absorption of fertile materials. The ratio of the fissile material production rate to the fissile material destruction rate is called the conversion ratio (CR), or, in case of net fissile material production, breeding ratio (BR) of a reactor.

The effectiveness of breeding is not only affected by the probability of fission and absorption, but also by the general neutron economy in the core. Since conversion of fissile isotopes does not produce additional neutrons, the average number of neutrons released per fission must be sufficiently high to sustain the chain reaction. This is expressed by the condition for the number of neutrons produced per absorbed neutrons η is greater than two. It is defined as

$$\eta = \nu / (1 + \alpha) > 2 \quad (1.3)$$

with the average number of neutrons produced per fission ν and the ratio of capture to fission reactions α . The higher the value of η , the more leakages and parasitic captures are possible while still breeding in a continuous mode (Rouault 2010). These values are also listed in Table 1.1. It can be seen that – considering only the isotopes used in today’s nuclear fuel – sustained breeding in a nuclear reactor is only possible with plutonium-239 in a fast neutron spectrum. Uranium-233 fulfills the requirements even in a thermal spectrum, which is the basis for the often proposed but yet to be realized uranium-thorium fuel cycle. Uranium-233 does not occur naturally but can be bred from thorium.

Typically, in fast reactors higher burn-up of the fuel is possible before discharge. It is not possible to operate a reactor core until all fissile material is transformed into other, non-fissile, isotopes. With increasing burn-up, lesser isotopes are fissioned while at the same time the number of parasitic elements, such as fission products, increases leading to a lower multiplication factor. This is called the reactivity swing and can only be compensated in a small range e.g. by removing control rods or neutron poisons present at the beginning of reactor operation. In general, higher burn-ups allow for a more economic operation of the reactor. Fewer refueling periods and a reduced material flow can in turn reduce the costs for fuel fabrication and reprocessing of the spent fuel. This, however, comes with some disadvantages. On the one hand, the increased content of fissile material in the fuel complicates ensuring safety during fuel storage and reprocessing. On the other hand, the higher burn-up also increases the fraction of fission products in the spent fuel leading to a higher specific activity. For the Russian fast breeder BN-600, specific activities four to five times as high as for typical light water reactor fuel are reported in Orlov et al. (1974). This should be taken into account when designing and analyzing fuel cycle schemes and reprocessing facilities.

When full burn-up is reached, the fuel elements are removed from the core and are replaced by new ones. The spent fuel elements still contain relevant amounts of fissile and fertile material, which is to be used in future fuel elements. In order to do so, the elements need to be reprocessed, meaning separation of the different materials. The uranium and plutonium can then further be used for manufacturing of new fuel elements or sent to direct disposal. Thermal reactors are dominantly used in a once-through or open fuel cycle. The spent fuel is not re-used but only reprocessed to be

sent into a deep geological repository. The better utilization of uranium resources in fast reactors can only be noted when they are used in a so-called closed nuclear fuel cycle.

Even with a cooling period of several years after discharge from the core, the elements are highly radioactive and their processing needs sophisticated technology. Beside the fact that the plutonium is present in separated form for a certain time during the process of fuel fabrication, the mentioned facilities allow processing of highly radioactive material. In section 2.1, implications of a closed nuclear fuel cycle on security and non-proliferation will be explained in more detail.

1.2 Generation IV Nuclear Power Plants

The technology of nuclear power plants has evolved through different design generations: The first nuclear power plants built in the 1950s and 1960 are called the Generation I nuclear power plants. In this first generation, the control of the chain reaction was the main objective. Generation II plants, which followed soon after, were standard light water reactors, mostly built from the 1970s onwards and still comprising the largest part of the nuclear reactor fleet. Compared to the first generation, safety aspects became more important. Current light water reactor designs with improved safety and performance features are referred to as Generation III or even III+ nuclear power plants (Stock 2013). Research and development (R&D) efforts are directed toward the Generation IV nuclear reactor designs. The Generation IV International Forum (GIF) unites several countries that are actively engaged in research and development activities on the new reactor designs (Gen IV International Forum 2016).

For the Generation IV reactor designs, different objectives were defined by the founders of GIF. The next generation of nuclear power plants is supposed to win wide public acceptance by advanced performance regarding the following aspects (Gen IV International Forum 2009; Kelly 2014):

Sustainability: Generation IV nuclear facilities can be used for nuclear waste management and thus reduce the burden of long-term storage of high-level nuclear waste. They allow for an efficient use of the present resources and provide sustainable energy production with only small greenhouse gas emissions.

Economics: unlike current nuclear power plants, Generation IV nuclear facilities are economically competitive to other energy resources. The financial risk of building them is comparable to other means of energy production.

Safety and Reliability: Generation IV nuclear facilities have outstanding performances in regard to their safe and reliable operation. Their very low likelihood of core damage will make off-site emergency response obsolete.

Proliferation Resistance and Physical Protection: Generation IV reactors are designed in a way that offers the least desirable pathway for acquiring weapon-usable nuclear material. Meanwhile, the physical protection against terroristic acts is increased.

These objectives are considered to be challenging even by the GIF. It is unclear to which extent they can be reached, but they are the guidelines for the design process. On the basis of these objectives, six different systems into which R&D efforts should be pooled were selected by the forum:

- The Very High Temperature Reactor (VHTR) is cooled by helium gas and moderated by graphite. It allows a very high outlet temperature of up to 1000°C and is thus well suited for the co-generation of electricity, hydrogen and process heat. The VHTR is either planned in a pebble bed or prismatic block type. Several reactors using this concept have already been built, but there are still open questions, for example in regard to their claimed inherent safety (Englert et al. 2017).
- The Sodium-Cooled Fast Reactor (SFR) is the type of the Russian BN-600 and BN-800 reactors, at the time the only two commercially operating fast reactors world-wide. They use sodium

as a coolant and allow high power densities. The small, fast reactor analyzed in chapter 6 is sodium-cooled.

- The Super-Critical Water Cooled Reactor (SCWR) operates above the thermodynamic critical point of water. This reactor type might allow for a thermodynamic efficiency of up to 50 %, but is still very much in an early design stage. No demonstration reactor of this type has been built yet.
- The Gas-Cooled Fast Reactor (GFR) is a fast spectrum reactor offering high temperatures as desired for the industrial use of the generated heat. It exists only in conceptual designs today.
- Lead-Cooled Fast Reactors (LFR) are widely used for energy generation in Russian submarines, because of their compact configuration. Accelerator-driven systems often rely on lead-cooled reactors.
- The Molten-Salt Reactors (MSR) are under development since the 1950s. Their unique characteristic is that the fuel is dissolved in the coolant, a molten salt mixture. This concept promises on-line processing of the spent fuel, for example to remove impurities. Together with the gas-cooled fast reactor, the molten-salt reactor is one of the reactor systems furthest from actual deployment.

These six systems are supposed to address the future energy market in a comprehensive way. Besides electricity generation, they allow for industrial applications such as hydrogen production, process heat, and the management of the actinide stockpiles. Depending on their design stage, they are planned to become commercially available from now on (Stock 2013). Several of the reactor designs are based on established concepts of reactors that have already been built and studied. The dominance of fast neutron spectrum reactors in the selection should be noted. Within the context of this work, reactor concepts that are cooled with liquid metal are further investigated.

1.3 Special Applications for Fast Nuclear Reactors

Fast reactors are primarily advertised for energy generation and industrial applications such as heat generation. But in these cases, the economics of the nuclear energy production compared to other options such as coal, gas or renewables are one driving factor for the decision to use nuclear power plants. Over the last years, more and more applications for fast reactors where financial deliberations play a less important role have been discussed. Important examples are presented in the following section. The first one is the disposition of excess weapon-grade plutonium. The second one is the energy supply of remote locations using small reactor cores with exceptional long core lifetimes. The last one is the incineration of minor actinides present in spent nuclear fuel.

1.3.1 Disposition of Weapon-grade Plutonium

With the growing fear of "*nuclear terrorism (...) as one of the greatest threats to global security*" (Obama 2012), the global stockpile of weapon-usable material raises more and more concerns. The reduction of nuclear warheads and their dismantlement after the end of the Cold War by the United States and Russia led to huge inventories of surplus weapon-usable material. This material, either high enriched uranium (HEU) or weapon-grade plutonium, is not needed for military purposes anymore and poses a severe security risk. High enriched uranium can be down-blended to low enriched uranium by approved methods to be then used as nuclear reactor fuel. There does not exist a generally accepted path on how to deal with the weapon-grade plutonium stocks.

Weapon-grade plutonium has a different isotopic composition than reactor-grade plutonium. Even though these terms imply the contrary, all plutonium compositions can be used for nuclear weapons. They are, as will be explained in section 2.5, only more or less suitable. The disposition of plutonium usually means transforming it into a form that impedes easy access to the fissile material.

In 2000, the United States and the Russia signed the Plutonium Management and Disposition Agreement (PMDA) in which both states commit to the disposition of 34 tons of excess weapon-grade plutonium each (Governments of the United States and Russia 2000). The benefit to nuclear security is, however, small as long as PMDA is not seen as a first step toward larger reductions. The 34 tons comprise only about one quarter of the total Russian stockpile of weapon-grade plutonium and about one third of the total U.S. plutonium stockpile (IPFM 2007, p. 33).

The agreement explicitly notes the irradiation of the excess plutonium as fuel in nuclear reactors or the immobilization of the plutonium as options to disposition (PMDA, Article III). The United States originally planned to immobilize a part of the excess material and irradiate the rest in its light water reactors. As soon as 2001, the immobilization option was canceled and all excess plutonium was to be used in mixed oxide (MOX) fuel to save on costs (Sokova 2010). In retrospective, this might not have been the most reasonable decision since the costs for the construction the Mixed Oxide Fuel Fabrication Facility (MFFF) at the Savannah River Site in South Carolina have increased by more than five times by now. This led to the fact that the U.S. started to consider alternatives for plutonium disposition in 2014 and halted construction of the facility (IPFM 2013, p. 20; Podvig 2016). As a result, Russian President Vladimir Putin rightfully criticized the United States for not fulfilling its agreed-upon obligations in April 2016 (Podvig 2016).

Russia planned to use her thermal and fast reactor fleet for irradiation of the excess plutonium. The time schedule agreed-upon by both sides was outdated after only a few years while the anticipated costs had risen manifold (IPFM 2007, p. 34). Due to the various obstacles encountered, the original agreement was amended in 2010 (Governments of the United States and Russia 2010). The new agreement postponed the start of the disposition efforts to 2018 and reduced the required disposition rate to 1.3 tons per year. Also, the option to use the Russian VVER¹ was replaced by the use of the new BN-800 fast reactor. The BN-800 is one key element in Russia's strategy to close her nuclear fuel cycle using fast breeder reactors, reflecting her opinion that plutonium is a resource (Digges 2016).

Since it is counterintuitive to use breeder reactors for disposition purposes, additional provisions were included in the PMDA: during the disposition of weapon-grade plutonium, the reactor has to be operated with a breeding ratio below one. Russia is not allowed to reprocess blanket or spent fuel materials based on weapon-grade plutonium during the disposition process except for research purposes and under the limitation that they do not result in accumulation of new weapon-grade material (Governments of the United States and Russia 2010).

In June 2016, Sergei Kireyenko, the head of the Russian state nuclear cooperation Rosatom, claimed that Russia, unlike the United States, fulfilled her obligations under the agreement (Digges 2016). Beside the "*unfriendly actions of the United States*", this was one reason why the Russian Federation announced the suspension of the PMDA in October 2016 (IPFM Blog 2016). Even though there was no change in the U.S. posture due to the suspension of the agreement, the future of the U.S. weapon-grade plutonium disposition program is unclear (Tabirian 2016). As of January 2017, the U.S. Department of State still lists the PMDA as being into force (Bureau of International Security and Nonproliferation 2017).

1.3.2 Powering Remote Energy Grids

Several countries consider the deployment of small nuclear power plants as an option to increase the share of nuclear energy in their total energy production (IAEA 2012b; Kelly 2013, p. 6ff). The International Atomic Energy Agency (IAEA) emphasizes the importance of nuclear energy for reasons of energy security, mitigation of the climate change and the economy in general. It also developed a program on "*Near Term & Small and Medium Sized Reactor Technology Development*"

¹ VVER from *Vodo-Vodyanoi Energetichesky Reaktor*; Water-Water Power Reactor (water cooled and moderated).

supporting its member states in their R&D and deployment efforts (Amano 2013; IAEA 2013). Commonly, and thus not matching the IAEA definition, SMR is used as an abbreviation for small, modular reactors: SMRs consist of standardized elements and have an energy output of less than 300 MWe. Today's base-load nuclear power plants have a power output of up to 1600 MWe and are conceivably bigger than SMRs.

One rationale of using small modular reactors is the desire to reduce installation and operational costs, while at the same time having the possibility to generate power in areas with only small grid capacity. The compact design of the SMR core unit allows for transportation by rail, trucks or barges to the planned reactor site. The small energy output also makes them fit to replace decommissioned coal-fired plants of which most units only produced 500 MWe or less (World Nuclear Association 2017d). The modularization of the reactor components would not only allow for line assembly in central manufacturing facilities but could also shorten the construction period at the reactor site (IAEA 2014; World Nuclear Association 2017d). These facts are supposed to lead to a lower upfront capital cost which should make the small nuclear power plants more affordable. The effect of mass fabrication is planned to be large enough to compensate for the *economy of scale* advantage that originally led to the increasing size of commercial nuclear power plants.

The effect of mass fabrication on the cost competitiveness of SMRs is not as straight forward as often claimed: first-of-a-kind units are always more expensive than later ones. The big question is how many units it will take before moderate construction costs are possible. Assuming a learning rate of first 10 % and later 5 % for the SMR production and an average correction factor for the economy of scale, it is shown that it will take several hundreds of SMRs before their energy production is cost competitive with respect to large nuclear power plants (Glaser, Ramana, et al. 2015). To get to this point, the number of ordered reactors must be sufficiently high. Furthermore, the construction cost per kilowatt of capacity increased rather than declined over the years even for large nuclear power plants (Lovering et al. 2016). The IAEA, which sees the SMRs' "*potential as options for enhancing the energy supply security*", lists the economic competitiveness as a challenge to SMRs deployment (IAEA 2017). At the current point, governmental subsidies are demanded by the vendors (Lyman 2013; Makhijani 2013). Nevertheless, the World Nuclear Association claims that with SMR development a shift away from government-led and funded R&D towards the private sector is taking place (World Nuclear Association 2017d).

One such case of governmental subsidies is the *SMR Licensing Technical Support (LTS) Program* started in 2012 by the United States Department of Energy (DoE). At the beginning it was planned to support two small, modular reactor design programs with a total grant of up to \$452,000,000 (DOE 2012). The first design awarded funding was the small light water reactor *mPower* from Babcock&Wilcox (B&W) with an energy output of 180 MWe. Since the program requires contribution of the private partners, there has been no funding provided since 2014 because of the reduced investments of the B&W Corporate (Mills 2012; Office of Nuclear Energy 2017). The second selected SMR is the *NuScale PowerModule* (NuScale Power 2013). It is also a light water reactor design and planned as 12 modules with a power output of 45 MWe each (ibid.). Key activities of the partnership include the final design of the reactor module until 2019 (Office of Nuclear Energy 2017). The LTS program set the focus to light water reactors, because imminent deployment was one objective.

When looking at the variety of internationally proposed reactor design, several fast small reactors are under development as well (IAEA 2014). The advantages proponents expect from large fast reactors also apply to small reactors. Besides, only fast reactors offer the possibility of extremely long core lifetimes up to several decades.

Advocates also assert the enhanced safety and security features of SMRs compared to large scale nuclear power plants (O'Meara 2013). In doing so, it is on the one hand argued that operation in countries with less experience in nuclear power is easily feasible. On the other hand, there is strong urge to reduce licensing requirements. As an illustration, the need for an on-site emergency

power supply and the size of the emergency planning zone is challenged by the vendors (Ramana and Mian 2014). Several of them claim that no diesel generators are needed because of the passive safety systems or their reactors. Passive safety systems rely on physical properties only. One example is natural circulation due to a heat gradient. According to their proponents, SMRs are safe enough to allow for a reduction of the emergency planning zone to the reactor area itself (Lyman 2013). It has to be seen in how far the effect of improved safety systems is leveraged by eased licensing guidelines.

The increase in nuclear power generation worldwide can solely be attributed to China (Schneider et al. 2016). Therefore, the possibility of new markets for nuclear energy by deploying SMRs in remote areas enthruses the industry. The option to incrementally increase the power output and therefore requiring a lower initial investment also addresses the needs of developing countries with only small financial resources (Kessides et al. 2012). The wide-spread deployment of SMRs might thus compensate for the declining market in the United States and Europe. In order to do so, implying that SMRs become an attractive choice for energy production, the number of deployed SMRs might grow to several hundreds. This would have serious effects on the current safeguard and non-proliferation regime. An assessment of proliferation risks of different SMR types was for example done in a publication by Glaser, Hopkins, et al. (2013). But especially for small fast reactors with extended core lifetime, information on these questions is scarce.

1.3.3 Partitioning and Transmutation

One application in which fast reactors are almost inevitable is the treatment of spent fuel with partitioning and transmutation (P&T). Highly radioactive spent fuel elements and waste from spent fuel reprocessing still pose a major challenge to the nuclear industry and a risk to mankind. Some isotopes in the radioactive waste have very long half-lives of up to several hundred thousand years. As of today, the best option to deal with the radioactive waste seems to be storage in deep underground repositories. Other approaches like transportation of the radioactive waste into space or dumping it in the ocean have been discarded a long time ago.

Not taking into account other potential risks such as proliferation, there is no absolute guarantee that safe containment can be ensured for such a long time. In the case of the long-term safety analysis of a deep geological repository in Germany one million years is the reference period (Reaktor-Sicherheitskommission and Strahlschutzkommission, Germany 2002). The siting of final repositories is not only a scientific but also a political challenge. Most countries that have been accumulating spent fuel are still at the very beginning of the process of exploring concepts and sides for a deep geological repository for their nuclear waste. Only in Finland and Sweden, the sites for the deep geological repositories are selected and detailed roadmaps for operation of the repositories exist (IPFM 2011; Gibney 2015). Some argue that other treatments such as P&T might be a better option, even though even proponents mention that a deep geological repository would still be necessary (Rubbia et al. 1995; Martínez-Val et al. 2008).

The Concept of P&T

Transmutation is the transformation of one isotope into another via different nuclear reactions such as decay, absorption or fission. In the context of nuclear waste treatment, it refers to the transformation of certain long-lived isotopes into stable isotopes or isotopes with a shorter half-life. The fraction of these isotopes in the high level waste is reduced by neutron irradiation in a nuclear reactor. It is argued that this would lead to a reduction of the radiological hazard of spent fuel, a reduction of the time for which safe containment in the deep geological repository must be ensured, and to a reduced heat load of the high level waste packages (Abderrahim, De Bruyn, et al. 2013). The idea of a transmutation fuel cycle has been discussed for several decades (Rubbia et al. 1995; NRC, Committee on Separations Technology and Transmutation Systems 1996; Bowman 1998). But

the implementation objectives have changed. Older publications usually mention the transmutation of minor actinides and long-lived fission products (Jameson et al. 1992; United States Department of Energy 1999; Kurata et al. 2002; IAEA 2004). This does not hold true for the implementation plans discussed today, e.g. by the European Union (Romero et al. 2007), France (CEA Nuclear Energy Division 2012), and Korea (NEA 2012a, p. 30). The focus lies solely on the transmutation (incineration) of minor actinides.

In order to transmute the minor actinides, the partitioning (separation) of the spent fuel in different waste streams is necessary. To reduce the initial heat the spent fuel is stored in interim storage. Long-lived fission products are not treated separately. They have to be stored in the deep geological repository. Uranium and the transuranium isotopes (plutonium and minor actinides) are used for the fabrication of new MOX fuel elements and can thus be used for energy generation. The minor actinides should be transmuted into short-lived or stable nuclides by nuclear reactions induced by the irradiation in the core.

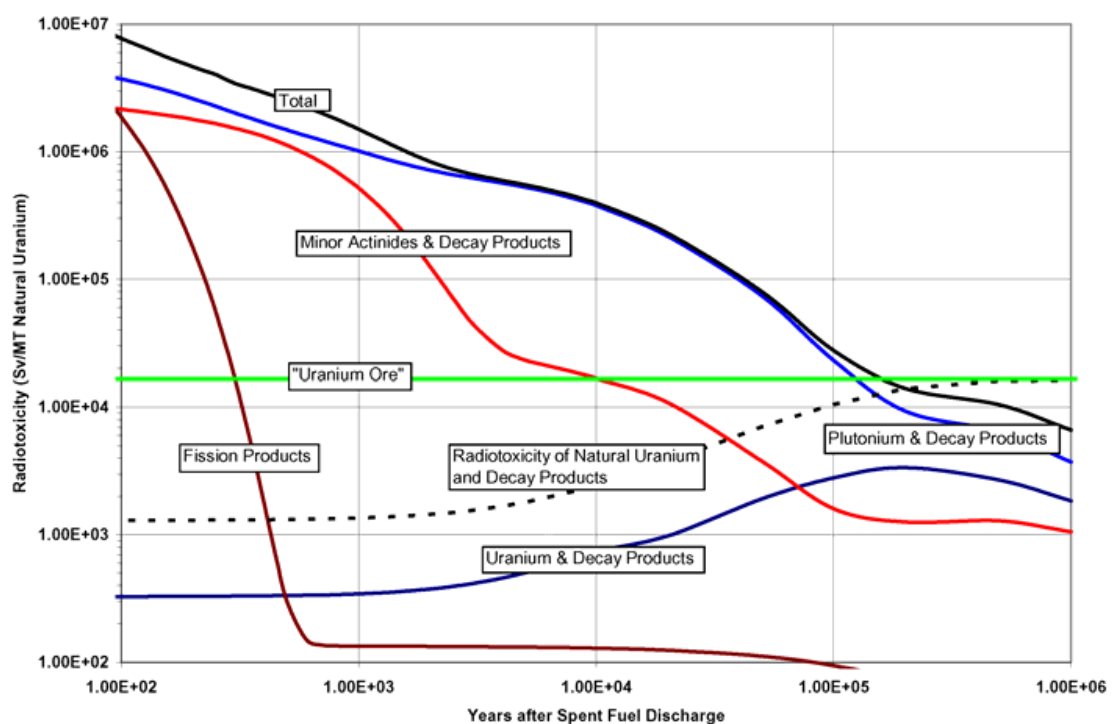


Figure 1.1.: Evolution of the ingestion radiotoxicity in spent fuel (NEA 2006, p. 9).

When arguing in favor of the transmutation of minor actinides, one figure is usually presented. It shows the evolution of the radiotoxicity for the different components of the spent fuel after discharge over time, see Figure 1.1. The main contributor to the radiotoxicity as defined in this figure are the plutonium isotopes. Especially in the first millenniums after discharge, the minor actinides and their decay products play a significant role. If all plutonium and minor actinide elements are removed from the spent fuel directly after discharge, radiotoxicity as defined here would decline quickly. In this case, the radiotoxicity of the spent fuel falls below the value of a typical natural uranium ore in less than 1000 years. The figure also shows the importance of uranium and its decay products, clearly among them radon. In detailed calculations for different repositories, the impact of radon is more visible (Svensk Kärnbränslehantering AB 2011, p. 657). However, two exemplary points criticizing Figure 1.1 are discussed in the following.

The first aspect is radiotoxicity of the uranium ore as a threshold value. In Figure 1.1, the radiotoxicity of a natural uranium ore is used as a safe reference value. The fact that it is naturally occurring does not necessarily imply that it is a safe environment for humans. According to

European regulations, the dose limit for public exposure is 1 mSv per year (Official Journal of the European Union 2013). Even taking into account that the nuclides must be released to the biosphere from the mine, this values is significantly lower.

The second aspect is the focus on transuranium elements. This calculation of the radiotoxicity, solely using the ingestion dose rates of the different nuclides, is a simplified case. It assumes that the complete high level waste as present in the deep geological repository is ingested. It is also assuming an intrusion scenario where human action brings the inventory to the surface. The consequences from such a scenario would be severe. But they would probably be quite localized and therefore easy to mitigate (IPFM 2015b, p. 108). The more likely scenario is that the nuclides are transported to the surface by natural processes. Considering the natural mobility of the different nuclides, the transuranium elements are not expected to dominate the radiotoxicity of the material mix that is transported. When the solubility and mobility of nuclides are taken into account, the long-lived fission products are the most relevant contributors to the dose rate. Section 7.6 explains this aspect in more detail.

Table 1.2.: Characteristics of important transuranium isotopes (Fanghänel et al. 2010).

Nuclide	Half-life years	Spont. Fission Rate 1/(s· g)	Specific Activity Bq/g	Specific Power W/g
Pu-238	87.7	$1.18 \cdot 10^3$	$6.33 \cdot 10^{11}$	0.567
Pu-239	$2.41 \cdot 10^4$	0.01	$2.3 \cdot 10^9$	$1.93 \cdot 10^{-3}$
Pu-240	$6.56 \cdot 10^3$	479	$8.4 \cdot 10^{10}$	$7.06 \cdot 10^{-3}$
Pu-241	14.3	$9.19 \cdot 10^{-4}$	$3.82 \cdot 10^{12}$	$3.28 \cdot 10^{-3}$
Pu-242	$3.75 \cdot 10^5$	805	$1.46 \cdot 10^8$	-
Am-241	432.7	0.505	$1.27 \cdot 10^{11}$	0.114
Am-242m	140	62	$3.87 \cdot 10^{11}$	$4.49 \cdot 10^{-3}$
Am-243	$7.37 \cdot 10^3$	0.27	$7.33 \cdot 10^9$	$6.43 \cdot 10^{-3}$
Cm-242	0.45	$7.47 \cdot 10^6$	$1.23 \cdot 10^{14}$	122
Cm-244	18.1	$4.0 \cdot 10^6$	$3.0 \cdot 10^{12}$	2.83

The fraction of transuranium elements must be increased in nuclear fuel for transmutation purposes. Since only a small fraction of these elements can be transmuted per irradiation cycle, the spent fuel also contains non-negligible amounts of those nuclides. Table 1.2 shows key parameters for the most important transuranium isotopes. They do not only influence reactor dynamics but also reprocessing and fuel fabrication. When investigating the long-term effect of a deep geological repository, the focus lies on nuclides with half-lives in the range of several 100,000 years. But when looking at the (spent) fuel, isotopes that have comparable short half-lives such as curium-242 must be taken into account as well. Especially their spontaneous fission rate is several orders of magnitude higher than the rate of other transuranium elements leading to high neutron radiation which must be handled. This will most likely be possible only using remote reprocessing and fuel fabrication including heavy shielding. Meanwhile, the high heat generation by some of the minor actinides requires appropriate cooling mechanisms.

Introducing a large fraction of transuranium elements in the fuel bears several problems in regard to safe reactor operation. These are, at least to some degree, the same problems associated with plutonium-based MOX fuel. Due to these difficulties, thermal reactors are often only licensed to fuel only one third of their core with MOX. The main effects are the reduced delayed neutron fraction and the deterioration of reactivity coefficients such as the Doppler coefficient. More than 99 % of the neutrons are released within the first 10^{-13} s after the actual fission. These neutrons are called prompt neutrons in distinction to the delayed neutrons that are released afterwards. Delayed neutrons have a lower average energy than prompt neutrons but also a smaller mean free

path due to the increased fission cross sections (United States Department of Energy 1993a, p. 134). If a reactor is prompt critical, the neutron population is self-sustained even without the delayed neutrons allowing for fast power excursions. To have a gracious time to regulate the neutron multiplication factor in the core for example by inserting control rods, it is desired that the reactor core only becomes critical taking into account the delayed neutrons. As an illustration, the fraction of delayed neutrons β is 0.0149 for uranium-238, but only 0.0022 for plutonium-239 and 0.0013 for americium-241 and curium-244 (Wallenius 2012).

Reactivity coefficients describe the reactor behavior caused by changes in the physical properties of the reactor. This could for example be a change in coolant temperature or pressure. Another example is the change in fuel temperature where the fuel temperature coefficient is defined as the change in reactivity per degree change in temperature. The fuel temperature coefficient is also called the Doppler coefficient, since the motion of the nuclides leads to broadening of the reaction resonances. With higher temperature, the nuclides move faster leading to wider resonance in which incoming neutrons can interact (United States Department of Energy 1993b, p. 50). The main reaction affected by Doppler broadening is absorption. It is shown that the introduction of americium to the fuel increases the Doppler feedback substantially (NEA 2005, p. 32). For the safety case of nuclear reactor systems, negative reactivity coefficients are essential. Negative coefficients describe a self-regulating system which is consequently less prone to criticality excursions that must be mitigated by other means.

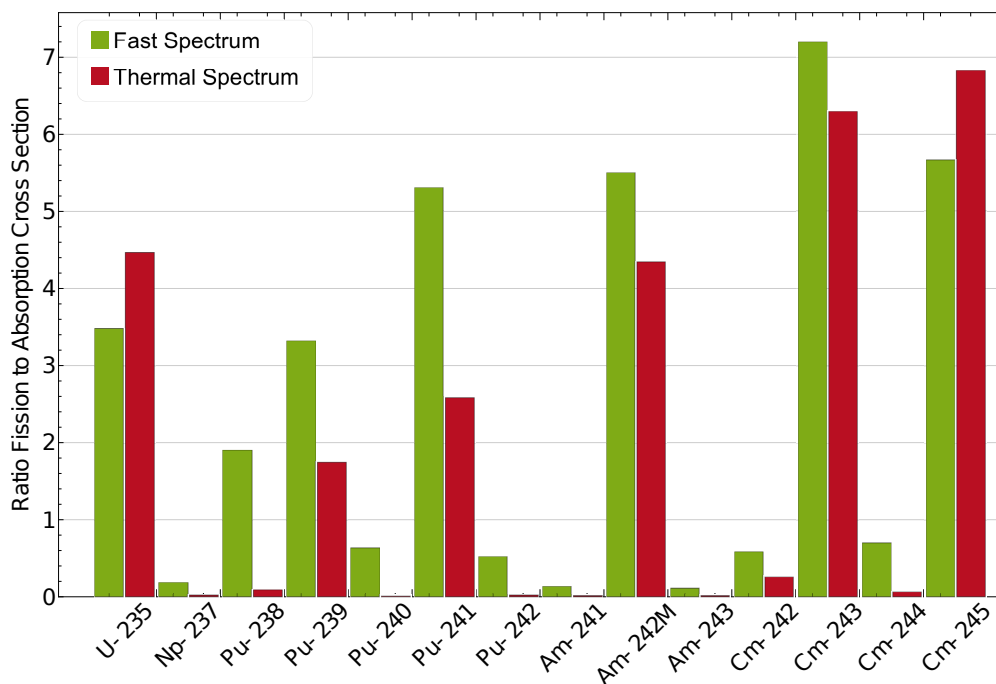


Figure 1.2.: Ratio of the fission and absorption cross section in a fast and in a thermal neutron spectrum for transuranium isotopes. Figures are taken from NEA (1999, p. 142)

The degree to which certain nuclides can be transmuted into stable or short-lived isotopes is, among others, determined by the microscopic cross section of fission and absorption reactions. For transmutation, a high fraction of nuclides should undergo fission instead of any other reaction. In Figure 1.2, the ratio of the fission to the absorption cross section for an average fast and thermal neutron spectrum is shown. In a fast spectrum, most transuranium isotopes are more likely to undergo fission instead of absorption. The energy resolved cross sections show that for minor actinides the incoming neutrons must have energies of 1 MeV or higher to induce more fission than absorption reactions. The need for a fast neutron spectrum becomes even more evident when

looking at the neutron consumption per fission. In a fast spectrum, more neutrons are released per fission. On average, the fission of a transuranium nuclide in a thermal neutron spectrum requires more neutrons than it produces.

The above mentioned points make it basically impossible to operate critical reactors with minor actinide rich fuel. This problem might be solved by the introduction of sub-critical reactors. They are advertised as a possibility to enable the safe operation of fast neutron spectrum reactor systems with fuel tailored to the objective of efficient minor actinide transmutation.

Accelerator-Driven Systems and the Double-Strata Fuel Cycle

A nuclear reactor is a system designed to sustain a nuclear chain reaction. In steady-state operation, the neutron-induced fission of isotopes produces enough additional neutrons for the neutron flux to remain constant. The reactor is operated in critical mode ($k_{eff} = 1$). The fission energy can be used for electricity production (or other applications such as saltwater desalination and district heating).

This is different in an accelerator-driven system (ADS). These systems typically consist of a particle accelerator, a spallation target and a sub-critical reactor core. The high energy protons from the particle accelerator hit the spallation target and produce neutrons there via spallation reactions. These neutrons are then multiplied in the fissile material of the sub-critical core (Rubbia et al. 1995; Abderrahim, De Bruyn, et al. 2013). The core itself does not contain enough fissile material to sustain a chain reaction. It mainly acts as an amplifier of the neutrons produced in the spallation target. The presence of external neutrons is essential to operate the reactor in continuous mode. Typical values for sub-criticality lie between $k_{eff} = 0.95$ and $k_{eff} = 0.99$.

The main safety advantage of a sub-critical core is that its dynamics are dominated by the external source neutrons and their behavior over time. Variations of the incoming proton beam influence the absolute number of produced neutrons entering the core. When the particle accelerator is turned off, the reactor shuts down. It depends on the margin to criticality to what extent the overall reactor behavior is dominated by the external source compared to the intrinsic behavior. The choice of the sub-criticality level is influenced by economic considerations: the lower the neutron multiplication factor of the core, the more external neutrons must be provided. This leads to an increase of the necessary beam power which is a significant cost factor.

As long as the core remains sub-critical, an exponential increase of the neutron population is impossible. Therefore, it is argued that several safety limitations regarding the fuel composition as discussed above and experienced in other reactor designs do not apply. Fuels with a high minor actinide fraction are possible. According to Mueller (2013), transmutation rates in an ADS could be up to ten times higher than in a critical reactor. The introduction of ADS into the fuel cycle increases the overall cost due to the higher complexity of the system compared to critical reactors. Consequently, in most scenarios using ADS for minor actinide transmutation, a double-strata fuel cycle is planned.

In a double-strata fuel cycle, there are two different reactor types with different objectives operated. The accelerator-driven systems are dedicated to the transmutation of minor actinides. In a second stratum, a fleet of critical reactors uses the plutonium from the ADS for energy generation. Depending on the design of the fuel cycle, it might even be necessary to use a fast reactor fleet. The irradiation of the plutonium in the ADS leads to a higher fraction of even isotopes that might be only fissionable in a fast neutron spectrum.

1.4 Research Synopsis

Fast reactors are currently not competitive in nuclear energy production due to several reasons. These include high costs for construction and operation as well as safety and security challenges. But fast reactors are essential for a closed fuel cycle. Countries with interest in such a fuel cycle

continue to advocate fast reactor use and promise possible applications for new and emerging fast nuclear reactor systems. A prominent example is the Russian fast breeder BN-800 that could be used for the disposition of excess weapon-grade plutonium. Small modular reactors with long core lifetimes could allow energy generation even in remote locations. Despite the fact that the treatment of nuclear waste in a partitioning and transmutation fuel cycle only exist on paper yet, enormous efforts are taken towards its possible realization. It is advertised as "*the solution to the nuclear waste problem*" (Mueller and Abderrahim 2010).

The discussion on possible advantages of fast nuclear reactor deployment is mostly dominated by different interest groups, including the industry, research institutes, and think tanks. For a comprehensive assessment of those promised applications, there is often missing information. The objective of this thesis is to fill some of the knowledge gaps for the three emerging fast reactor applications that are most widely discussed: the use of fast reactors for plutonium disposition, the energy generation in remote areas, and the treatment of high-level waste.

One important aspect is the proliferation risk of nuclear reactors. Even though the Russian BN-800 reactor could be used for plutonium disposition, it is operated using breeding blankets in which additional plutonium could be generated. Consequently, not only the plutonium inventory and composition in the core but also in the blankets will be analyzed. An analysis of the plutonium production characteristics is also done for the small, modular reactor. Furthermore, the possible consequences of SMR deployment for the non-proliferation regime must be taken into account when introducing and possibly spreading this technology worldwide.

The concept of partitioning and transmutation (P&T) is by far more complex than the first two examples. P&T requires a specialized fuel cycle and technologies not yet developed. Even though the available amount of literature is immense, many questions remain unanswered. Some of them might even challenge the feasibility and rational of the whole concept.

The first investigated issue is the influence of the fuel composition on reactor criticality and its possible implications on implementation scenarios. A second issue is to what extent the spent fuel elements and in consequence their handling would be comparable to typical thermal reactor spent fuel elements. As a last aspect, the meaningfulness of the radiotoxicity index is analyzed. The amount of remaining and newly produced long-lived fission products in P&T scenarios is calculated so that the concentration of long-lived fission products in a deep geological repository can be estimated.

The above mentioned questions are treated using simulations of exemplary reactor models. After the ambivalent experiences with nuclear technologies, it seems reasonable and necessary to assess emerging technologies already in an early design stage. This is especially true for Generation IV reactors and accelerator-driven systems (Liebert 2005). For prospective technology assessment, important aspects are the potential of the technology, the viability of the promised benefits, potential development risks, and possible future costs and consequences of actual deployment. In order to assess nuclear technology according to these objectives, it is unavoidable to also investigate its scientific-technological core (Liebert and J. C. Schmidt 2015). The results presented in this thesis will allow for a more comprehensive assessment of fast nuclear reactor technology.



2 Material Assessment & Non-Proliferation

It is inevitable to talk about nuclear material and its potential military use when discussing possible disadvantages of civil nuclear energy production. This chapter starts with an explanation of the occurrence of fissile material in the civil nuclear fuel cycle in section 2.1. The next section 2.2 describes the current non-proliferation regime. Then, after some general considerations about the potential proliferation risks in section 2.3, the concepts *Spent Fuel Standard* and *Figures of Merit* are introduced in sections 2.4 and 2.5.

2.1 Fissile Materials in the Nuclear Fuel Cycle

The civil and military uses of nuclear power cannot be separated from each other as easily as it is for example implied in the Treaty on the Non-Proliferation of Nuclear Weapons (NPT). Fissile material to manufacture nuclear weapons does not occur in nature but must be produced with the same facilities that are also part of the civil nuclear fuel cycle. The most common fissile materials are high enriched uranium (HEU) and plutonium.

Uranium contains about 0.7 % of the fissile uranium-235 isotope, 99.3 % uranium-238 and traces of uranium-234. Only the fission of uranium-235 results in enough additional neutrons to sustain a chain reaction at thermal neutron energies. To use uranium as fuel in typical light water reactors, enrichment of uranium-235 to 3 %-5 % is necessary (low enriched uranium, LEU). Isotopes of one element have the same chemical characteristics. Therefore, separation methods based on physical properties of the different isotopes must be applied. For uranium enrichment, the most common enrichment technology today uses centrifuges. In centrifuges spinning at extremely high speeds, the heavier uranium isotopes in uranium hexafluoride gas, UF_6 , concentrate slightly more toward the outer wall and can be extracted. Because of the small separation factor, the centrifuges must be installed in series (cascade). This procedure is used for enrichment to all desired levels up to high enriched uranium which contains more than 20 % uranium-235.

The capacity of an enrichment facility is given in Separative Work Units (SWU) per year. The SWU can be seen as a measure for the work to enrich to a certain percentage. It depends on several aspects such as the isotope concentrations of the feedstock, the output and the tailings. Most of the enrichment work is needed for the enrichment to very low uranium-235 fractions. Enriching natural uranium with a uranium-235 fraction of 0.7 % to 3.5 % requires twice as many SWUs as further enrichment from 3.5 % uranium-235 to 90 % uranium-235 (Makhijani et al. 2004).

Only traces of some plutonium isotopes occur in nature. Plutonium is produced in nuclear power reactors by neutron absorption of uranium-238, leading to uranium-239 which then decays into plutonium-239. Higher plutonium isotopes, such as plutonium-240 and plutonium-241, result mostly from later neutron absorption of plutonium-239. For the use in nuclear weapons, a low fraction of plutonium-240 is desired in the composition (cf. section 2.5). This could be reached for example by removing the fuel elements from the core after a short irradiation time to allow for less neutron absorption (Lovins 1980). In other reactor configurations, such as fast neutron spectrum or heavy water cooled reactors¹, the isotopic composition of the plutonium in the core changes. To prevent the use of these fissile materials for military purposes, detailed safeguard measures for nuclear materials have been developed. Depending on the material, the IAEA defines threshold values for each of its safeguard goals. These goals are the significant quantity for the amount of

¹ Heavy water is water that contains the hydrogen isotope deuterium in a larger fraction than naturally present. The Canadian CANDU nuclear reactors are based on heavy water as coolant and moderator.

the material, the time in which diversion is detected, and the detection and false alarm probability (IAEA 2001, p.24). One significant quantity is the *"amount of nuclear material for which the possibility of manufacturing a nuclear explosive device cannot be excluded"* (ibid., p. 23). In the case of uranium-235 contained in HEU for instance, the diversion of 25 kg should be detected within four weeks. The significant quantity for plutonium is 8 kg. The detection time depends on the mixture. The probability for false alarm and non-detection should be below 5 % in all cases.

One major obstacle in using the plutonium available in the spent fuel is the presence of fission and activation products. These isotopes are highly radioactive. If the plutonium is to be used in a nuclear weapon, it has to be separated from the rest of the material. This is a complicated endeavor and requires heavy shielding and remote handling because of the high radiation level. Considerable expertise and financial resources are needed. However, the same technology is needed for civil reprocessing of the spent fuel for later fabrication of MOX fuel elements or preparation for final storage. With the *"Atoms for Peace"* program initiated by U.S. president Eisenhower and the *"inalienable right (...) to develop research, production and use of nuclear energy for peaceful purposes"* as granted in Article IV of the NPT, these technologies are easily obtainable (United States Department of Energy 1996).

Operation of fast reactors that breed large amounts of plutonium only makes sense in a closed fuel cycle. The plutonium produced in the core is useless unless separated from the spent fuel and used for fabrication of fresh fuel elements. Consequently, at a certain point in the fuel cycle, separated, nuclear weapons usable material is present even if no military use is intended. Proliferation concerns are one reason why there is practically no fast breeder program ongoing in the United States (IPFM 2010, p. 105). The problem of prohibiting partners proliferation-prone technology which can be used for military purposes as well as for a closed fuel cycle was shown in the negotiations between the United States and South Korea. They lasted five years. With reference to Japan, South Korea wished to establish a national closed fuel cycle which contradicts the United States' non-proliferation policy. Under the agreement finally signed in 2015², South Korea is prohibited to develop and operate reprocessing technology such as pyro-processing and uranium enrichment facilities. But in principle, spent fuel can be shipped to the United States for reprocessing and then be re-imported to the country (Burnie 2015; Horner 2015).

2.2 The Existing Non-Proliferation Regime

Soon after the discovery of the fission process in 1938, the possible military application of the consequent energy release became evident. Huge efforts were undertaken in the Manhattan project that resulted in the bombing of Hiroshima and Nagasaki in August 1945. The extremely destructive power of nuclear weapons soon caused concern about proliferation. The United States hoped to remain the only state possessing nuclear weapons. But, with the first nuclear weapon test of the Soviet Union in 1949, this hope was scattered. In 1953, the United States started its *"Atoms for Peace"* program in an effort to control the further spreading of nuclear weapons. It offered assistance in research and development of nuclear power to all countries willing to waive the option of acquiring fissile material for nuclear weapons production. To reduce the risk of fissile material spreading, the idea of a central bank for nuclear materials was born (Jonter 2008, p. 15). Even though the international fuel bank was never established, from this idea the IAEA emerged. The IAEA's roots are still visible in its double purpose: on the one hand the agency shall promote civil nuclear energy, while on the other hand it is responsible for controlling technology and know-how in order to prevent the proliferation of nuclear weapons.

Nevertheless, several states still pursued the development of nuclear weapons. Sometimes motivated by the fear of countries already possessing nuclear weapons that they would lose their

² Agreement For Cooperation Between the Government of the Republic of Korea and the Government of the United States of America Concerning Peaceful Uses of Nuclear Energy, signed June 15, 2015.

superiority, sometimes by the horrible consequences of nuclear weapons, ways were searched to contain this trend. From 1958, Ireland proposed a treaty to prevent the dissemination of nuclear weapons. This draft can be considered the first version of the Treaty on the Non-proliferation of Nuclear Weapons (NPT), which entered into force in 1970 and was extended indefinitely in 1995. The NPT rests on three pillars: the non-proliferation of nuclear weapons, nuclear disarmament, and the promotion of the peaceful use of nuclear energy. The treaty establishes two classes of states, because it differentiates between Nuclear Weapon States (NWS) and Non-Nuclear Weapon States (NNWS). Only NWS have the right to possess nuclear weapons. NWS are all states that conducted a nuclear weapons test before 1967, namely China, France, the Soviet Union (now Russia), the United Kingdom, and the United States. While the NNWS commit themselves to not develop or acquire nuclear weapons, the five NWS are obliged to "*pursue negotiations in good faith on effective measures relating to (...) nuclear disarmament*" (Article VI of the NPT). Three other states — India, Israel, and Pakistan — never signed the treaty and later became de facto nuclear weapon states. The Democratic People's Republic of Korea withdrew from the NPT in 2003, which is possible within three months notice under Article X of the treaty (Nikitin 2012).

Whether the nuclear disarmament obligation is met by the NWS is subject to great controversy. This is one reason why a possible Nuclear Weapon Ban Treaty gained wide support among states. The ban treaty would provide a legal framework for the prohibition of nuclear weapons. Negotiations on such a treaty began in March 2017 and will continue in July 2017 (ican 2016). A draft treaty was submitted by the negotiations president in May 2018 (United Nations 2017).

2.3 General Considerations on Assessing Proliferation Risk

In order to assess the proliferation risk of a nuclear facility or the attractiveness of nuclear material, a variety of approaches can be used. The choice depends on the level of details that are analyzed as well as on the investigated scenarios. Three main classes of diversion of nuclear material can be considered (Committee on International Security and Arms Control 2000):

Host-nation breakout: In this case, the country legitimately holding the nuclear material chooses to divert it for military purposes. Consequently, expertise and technical capabilities gained from civil nuclear energy use can be assumed. The most likely objective would be the production of high yield nuclear weapons, thus leading to a preference for material that allows for easy and efficient fabrication. The country might either act openly, accepting international pressure, or clandestinely. In the second case, detection is more complicated, but a longer time period for completion is likely.

Theft by a non-hosting state: Probably with the help of an insider within a nuclear facility, material is diverted either clandestinely or using force. Afterwards, the material is transferred to the state that intends to use it for the fabrication of one or several nuclear weapons. Compared to the host-nation breakout, it can be assumed that the amount of involved material as well as the capabilities of the proliferator are lower, probably also resulting in a lower yield for the nuclear device.

Theft by a subnational group: In this case, no state actor is involved in the proliferation of nuclear material. Thus, detection of the material diversion would be a major concern. Requirements on the quality and quantity of the diverted nuclear material would be low. All nuclear devices that lead to a yield larger than a conventional weapon can be considered attractive³.

Sometimes, the second and the third scenario are summarized as "*unauthorized*" parties seeking access to nuclear weapons material (Hinton et al. 1996).

³ For certain purposes such as terroristic acts, even a radiation dispersion device (RDD) might be considered to be sufficient by the actors. RDDs use conventional explosives to spread radioactive material.

For every proliferator, the process of acquiring a nuclear weapon can be split into three distinct phases: the acquisition phase, the processing phase, and the utilization phase (Robel et al. 2013). In the first phase, the radiation emitted by the material and the net weight of the element are limiting parameters to a potential proliferator. Spent fuel elements for instance have a defined size and material inventory, affecting the transportation requirements and the total amount of elements that must be acquired to gain at least one significant quantity.

In the processing phase the form and concentration of the fissile material contained in the acquired material becomes relevant. The fissile material must be separated from the rest of the materials present.

In the final utilization phase, when the actual weapon is built, the bare critical mass of the gained material and its heat content are relevant for the weapon's design and the needed technical capabilities. The spontaneous fission neutrons source strength might also be important because the nuclear weapon might pre-ignite if the material is not compressed fast enough, requiring sophisticated technology.

Depending on the considered stage for material attractiveness assessment, the weighing of the factors is different. The spent fuel standard explained in section 2.4 considers nuclear material during the acquisition phase, while the Figures of Merit introduced in section 2.5 focus on the material after processing and separation in the utilization phase. Both approaches are explained in more detail in the following.

2.4 Spent Fuel Standard

After the end of the Cold War, the question arose how to deal with excess weapon-grade plutonium. In general, two different options are possible: either the plutonium is used to generate electricity or it is disposed of. In assessing different disposition options, one key criterion is the potential to recover the plutonium after disposition. The objective set was to make the recovery of the disposed weapon-grade plutonium as complicated as the recovery of the residual plutonium generated by civil nuclear power reactors. This plutonium is present in the spent fuel elements that also contain a high fraction of fission products. Therefore, they emit strong radiation.

If the plutonium was easier to access, it would still pose a security risk and safeguard problem. In contrast, it does not make sense either to put enormous efforts into going beyond the level of protection considered good enough for the civil plutonium. Thus, the term *Spent Fuel Standard* was shaped (Committee on International Security and Arms Control 1994). Going beyond the spent fuel standard is the long-term objective for the disposition of nuclear weapons material.

The spent fuel standard does not have exactly defined limits for the various parameters or barriers. Rather, it weighs different aspects such as, most importantly, the radiation field, but also the chemical dilution and the physical form of the material.

A high radiation field is the first barrier, since it forces the proliferator to have heavy shielding and remote operation in place for all parts of the process. In the original CISAC report on "*Management and Disposition of Excess Weapon Plutonium*", a reference value of 1 Sv/hr is mentioned (ibid., p. 164). This value is used by both the U.S. Nuclear Regulatory Commission (NRC) and the IAEA, as the radiation level above which the material can be considered to be self-protecting. Therefore, a lower level of safeguards is required. Already in 1994 it was stated that this value should be re-evaluated. An additional report by the National Academy of Sciences from the year 2000 states a value of 5 Sv/hr as a reference value. This value is derived from the radiation emitted from a ten year old canister (Committee on International Security and Arms Control 2000). The main contributor to the dose rate in the first decades after removal from the core is cesium-137 with a half life of about 30 years. Consequently, with intermediate cooling periods of up to 100 years before reprocessing and final storage, the radiation from the spent fuel elements declines considerably. The time frame, for which the radiation barrier is considered to be sufficiently high, differs depending

on the chosen dose rate. The spent fuel elements might well fall below the limit during their intermediate cooling period.

The chemical dilution of the material determines the difficulty for chemical separation of the fissile elements from the embedding matrix. The *Proliferation Vulnerability Red Team Report* evaluates the difficulty of the recovery of plutonium from various plutonium forms (Hinton et al. 1996, p. 43). Here, the complexity of recovery is referenced relative to spent LWR fuel. Only plutonium vitrified with either high level waste or pure cesium-137 is as complicated to extract as plutonium contained in spent fuel. Recovering plutonium from fresh fuel is much easier. Shielding and remote operation requirements are much lower, again showing the importance of the radiation barrier. The difficulty of recovering plutonium from pure plutonium/uranium-oxide powder or pellets is low.

After processing the spent fuel, the plutonium and other nuclear materials are separated. For further use, the material's physical properties are relevant. The bare critical mass and the isotopic composition of the material influence the possible weapon usability and design.

The different aspects, such as the radiation and the physical form of the material, together are supposed to result in end state conditions that leave the material as proliferation resistant as the spent fuel. These conditions depend heavily on the nuclear material itself, but also on the properties of the smallest plutonium containing item. In most cases this item is either a spent fuel element or a canister for disposition. As an illustration, the access to the nuclear weapons material in one item might be complicated to its radiation or size, and the total amount and the attractiveness of the nuclear material itself might also vary due to different circumstance, for example the previous irradiation period.

Usually, the greatest difficulties in reprocessing arise from the need of shielding and remote operation due to the high dose rates emitted by the spent fuel (Committee on International Security and Arms Control 1994). This is also shown by comparing the immobilization option and spent MOX fuel as means for excess plutonium disposition in terms of their compliance with the spent fuel standard: neither the difference in the isotopic composition nor the higher plutonium content in the MOX elements is a decisive factor (Kang et al. 2002). The focus on the radiation barrier does however not hold true when considering only the processed nuclear material, usually separated plutonium. Evaluation for several material compositions show that the dose rate is mostly inconsequential for the overall assessment of the material attractiveness (Bathke et al. 2009). The heat generation, the bare critical mass and, depending on the scenario, the spontaneous fission neutron rate are the most important parameters. They are explained in the following section.

2.5 Figures of Merit

For a long time, a central argument in the discussion on the non-proliferation of fissile material has been the unsuitability of reactor-grade plutonium for building a nuclear weapon. This conviction is mirrored by an early approach to the categorization of fissile material based on the plutonium-240 content in the composition (Pellaud 2002). Compositions with a plutonium-240 content of more than 30 % are called "*practically unusable*", because of the high spontaneous fission rate of this isotope. However, it has been confirmed by various sources that the possibility of building a nuclear device is not depending on the plutonium composition, even though there are compositions that allow for less advanced technological skills (Kankeleit et al. 1993; Committee on International Security and Arms Control 1994).

A more recent attempt to assess the attractiveness of materials that might be used in a nuclear weapon and are handled in forms separated from fission products is introduced in Bathke et al. (2009). Two formulas are derived that result in *Figures of Merit (FOMs)* and allow for quick assessment of material attractiveness.

The *FOMs* distinguish between a subnational group and a state actor. For the former, even a low quality device is considered to be an acceptable outcome. The difference between these two

adversaries is mirrored in the literature by introducing two terms: the proliferation resistance and the physical protection. The level of proliferation resistance is a measure for the obstacles a host states experiences when diverting nuclear material. The physical protection of a nuclear energy system refers to protection against theft and sabotage by subnational actors (Bathke 2009).

The most relevant factors in assessing the material attractiveness are the bare sphere critical mass, the heat generation rate, and the dose rate. The spontaneous neutron generation rate is an additional parameter that only matters when a significant military yield is required, but the actor lacks sophisticated weapons technology. Spontaneous fission neutrons might cause the pre-ignition of the nuclear weapon, leading to a drastically reduced yield. But even then, the yield is probably higher than of a conventional explosive and might thus satisfy the expectations of its owner. In this case, or when the actor is capable of a sophisticated weapon design to avoid pre-ignition, the spontaneous neutron fission rate does not have to be taken into account and the Figure of Merit can be calculated using the following equation

$$FOM_1 = 1 - \log_{10} \left(\frac{M}{800} + \frac{Mh}{4500} + \frac{M}{50} \left[\frac{D}{500} \right]^{\frac{1}{\log_{10}(2)}} \right), \quad (2.1)$$

where M is the bare critical mass in unpurified metal form in kg; h is the heat content in unpurified metal form in W/kg; and D is the dose rate of 20 % of M in a distance of 1 m in rad/h.

For all other cases, the spontaneous fission neutrons production rate S (in n/(s kg)) affects the Figure of Merit as well,

$$FOM_2 = 1 - \log_{10} \left(\frac{M}{800} + \frac{Mh}{4500} + \frac{MS}{6.8 \cdot 10^6} + \frac{M}{50} \left[\frac{D}{500} \right]^{\frac{1}{\log_{10}(2)}} \right). \quad (2.2)$$

For the definition of the above equations, certain threshold values were used (Bathke et al. 2009). For attractive nuclear weapons material, the following constraints apply:

- The mass should be lower than the critical mass of uranium with 20 % uranium-235 enrichment.
- The heat production should be lower than that of plutonium consisting of more than 80 % plutonium-238.
- The material should emit less than a self-protecting dose rate of 5 Sv/hr in one meter distance.
- The spontaneous fission neutron rate should be lower than that of reactor grade plutonium with a plutonium-240 content of more than 20 %.

Noteworthy is the limit of 5 Sv/hr for the dose rate originating from the material. Often, a value of only 1 Sv/hr is seen as the threshold above which the material is considered to be self-protecting. Self-protecting connotes that shielding and remote handling is necessary to protect potential adversaries (or workers) from the radiation hazard. This threshold value expects the proliferator unwilling to sacrifice his life. The higher value of 5 Sv/hr reflects the willingness of a potential actor to risk his life by exposure, assuming there is no additional shielding (Robel et al. 2013). The conservative approach by the $FOMs$ is also mirrored by the fact that no further distinction of the uranium enrichment is done. The United States Department of Energy differentiates between uranium with an uranium-235 fraction between 20 % and 50 % and above 50 %. Only the latter is assigned to be high-grade material with the corresponding higher attractiveness level (United States Department of Energy 2011).

Table 2.1 gives an overview of material attractiveness, weapon utility and corresponding Figures of Merit calculated according to equation 2.1 and equation 2.2. There is no absolute criterion for the attractiveness and usability of nuclear material. The attractiveness is only ranked qualitatively. A nuclear device can be built with low attractive material, even though this would require higher

Table 2.1.: Figures of Merit (*FOMs*) and their meaning. There is no threshold below which the material is considered unusable.

FOM	Weapons Utility	Attractiveness
> 2	Preferred	High
$1 - 2$	Attractive	Medium
$0 - 1$	Unattractive	Low
< 0	Unattractive	Very Low

efforts and entails a smaller chance of success. As a consequence, the Figures of Merit give a rather conservative assessment.



3 Theoretical Basis

For the assessment of core dynamics in different types of nuclear reactor systems it is essential to understand the physical basics laid out in the following chapter. The neutron flux in the core is described by the Boltzmann Equation in the critical and the sub-critical system. It is introduced in section 3.1. In a sub-critical reactor driven by external neutrons, the source efficiency condenses the importance of the source neutrons compared to the intrinsic neutrons produced in the core into one number, presented in section 3.2. Then, the Bateman Equations yielding the time-dependent evolution of the isotopic composition in the core are explained in section 3.3. In the case of an accelerator-driven system, the source neutrons are produced via spallation in a heavy metal target. Section 3.4 shows basics of the spallation reaction. Finally, the hazard imposed on humans by radiation is described in section 3.5.

3.1 Neutron Flux Distribution

A variety of particles is present in a nuclear reactor core. They move around, collide, and undergo spontaneous or induced reactions that might lead to the generation of new particles. Most important are the neutrons. A neutron can induce fission, undergo absorption, or be scattered leading to a change in energy and direction. Each neutron can be described by its position \vec{r} , its vectorial velocity $\vec{v} = v \cdot \vec{\Omega}$, and the time t . The absolute value of the velocity v depends on the energy $v = \sqrt{2E/m}$. Every neutron that induces a fission destroys a fissile isotope while at the same time it generates fission products and additional new neutrons and other particles, which in turn influence the neutron flux distribution in the core.

The neutron (or any other particle) behavior is given by the linear Boltzmann Transport Equation. Transport in this case means the process in which particles propagate through a system and interact with it. The conservation equation for the neutron density $n = n(\vec{r}, E, \vec{\Omega}, t)$ is

$$\frac{d}{dt} \int_V n(\vec{r}, E, \vec{\Omega}, t) dV' = \int_V \sum_i S_i dV'. \quad (3.1)$$

Wherein are S_i all neutron sources and sinks in the considered volume. The net neutron production in a respective volume equals the total change in the number of neutrons in the given volume.

The time dependent change of a field $\Psi(\vec{r}, t)$ in a given volume is the same as the change of the field within the volume and the net gain through the boundary of the volume. This is called the Reynolds Transport Theorem

$$\frac{d}{dt} \int_V \Psi(\vec{r}, t) dV' = \int_V \frac{\partial \Psi(\vec{r}, t)}{\partial t} dV' + \int_S \Psi(\vec{r}, t) \vec{v} d\vec{S}'. \quad (3.2)$$

Combining equation 3.1 and 3.2 and replacing Ψ with n yields

$$\int_V \frac{\partial}{\partial t} n(\vec{r}, E, \vec{\Omega}, t) dV' = - \int_S n(\vec{r}, E, \vec{\Omega}, t) \cdot \vec{v} d\vec{S}' + \int_V \sum_i S_i dV'. \quad (3.3)$$

Wherein is \vec{v} the velocity of the neutron density n . Using the Gauss's Divergence theorem

$$\int_S \vec{A} d\vec{S} = \int_V \nabla \vec{A} dV' \quad (3.4)$$

with $\vec{A} = n\vec{v}$, the change of the neutron density can be written as

$$\int_V \frac{\partial n}{\partial t} dV' = - \int_V \nabla n \vec{v} dV' + \int_V \sum_i S_i dV'. \quad (3.5)$$

This equation must hold true for all possible volumes, thus the integral can be canceled to get

$$\frac{\partial n}{\partial t} = -\nabla(n\vec{v}) + \sum_i S_i. \quad (3.6)$$

The neutron flux $\Phi(\vec{r}, E, \vec{\Omega}, t)$ is the neutron density times its absolute velocity, $v(E) \cdot n(\vec{r}, E, \vec{\Omega}, t)$. Inserting this in the above equation and using the multiplication rule for the derivation results in the Boltzmann Equation in its known form

$$\frac{1}{v} \frac{\partial \Phi}{\partial t} = -\vec{\Omega} \nabla \Phi + \sum_i S_i. \quad (3.7)$$

To express the neutron creation and loss process in the core more explicitly, the macroscopic cross section is useful. The microscopic cross section $\sigma_{i,R}(E)$ is the probability that an isotope i undergoes reaction R for an incoming neutron with the energy E . Its units are usually barn ($= 10^{-24}$ cm). It depends on the target isotope and the reaction. If the interaction of neutrons with a material is considered, the macroscopic cross section Σ

$$\Sigma_{i,R} = \sigma_{i,R} \rho_i \quad (3.8)$$

is often used, taking into account the isotope density ρ_i . The total macroscopic cross section Σ_t is the sum of the macroscopic cross section of all possible reactions. Leaving aside generally rare reactions, these are fission, capture and scattering. The inverse of the total macroscopic cross section is the mean free path of a particle in the material.

The change in the neutron density plus the net leakage out of the considered volume and the collision rate equal the in-scattering rate, the production of neutrons by fission, and possible source neutrons. These loss and gain terms written more explicitly results in the time-dependent neutron transport or linear Boltzmann Equation (Prinja et al. 2010, p. 449)

$$\begin{aligned} & \frac{1}{v} \frac{\partial}{\partial t} \Phi(\vec{r}, E, \vec{\Omega}, t) + \vec{\Omega} \cdot \nabla (\Phi(\vec{r}, E, \vec{\Omega}, t)) + \Sigma_t(\vec{r}, E) \Phi(\vec{r}, E, \vec{\Omega}, t) \\ &= \int_0^\infty \int_{4\pi} \Phi(\vec{r}, E', \vec{\Omega}', t) \Sigma_s(\vec{r}, E' \rightarrow E, \vec{\Omega}' \rightarrow \vec{\Omega}) d\vec{\Omega}' dE' \\ & \quad + \chi(E) \int_0^\infty \int_{4\pi} v \cdot \Phi(\vec{r}, E', \vec{\Omega}', t) \Sigma_f(E') d\vec{\Omega}' dE' \\ & \quad + Q(\vec{r}, E, T). \end{aligned} \quad (3.9)$$

Here, Σ_s is the macroscopic cross section for scattering and Σ_f the macroscopic cross section for fission. The factor $\chi(E)$ accounts for the energy spectrum of the neutrons generated by fission.

The average number of neutrons generated by one fission is assigned to be ν . The factor $Q(\vec{r}, E, T)$ describes an internal or boundary source. The term fission source is sometimes used in reactor problems. Even though called source, it then used to describe the neutrons produced by fission events in the considered volume. The fission source, unlike the external source, depends on the neutron flux distribution in the core. Equation 3.7 does not differentiate between prompt and delayed neutrons and is thus already an approximation of a steady-state problem.

In steady-state problems, the time derivative of the neutron flux is zero. If the fission source is modified by a factor k and there is no external source present, the equation yields

$$\begin{aligned} & \vec{\Omega} \cdot \nabla(\Phi(\vec{r}, E, \vec{\Omega}, t)) + \Sigma_t(\vec{r}, E)\Phi(\vec{r}, E, \vec{\Omega}, t) \\ &= \int_0^\infty \int_{4\pi} \Phi(\vec{r}, E', \vec{\Omega}', t) \Sigma_s(\vec{r}, E' \rightarrow E, \vec{\Omega}' \rightarrow \vec{\Omega}) d\vec{\Omega}' dE' \\ & \quad + \frac{\chi(E)}{k_{eff}} \int_0^\infty \int_{4\pi} \nu \cdot \Phi(\vec{r}, E', \vec{\Omega}', t) \Sigma_f(E') d\vec{\Omega}' dE'. \end{aligned} \quad (3.10)$$

This equation can also be expressed in matrix form with an accordingly defined production operator P and consumption or loss operator A (Bell et al. 1970). With the correction factor k and the flux vector $\vec{\Phi} = \Phi \cdot \vec{\Omega}$, a system where the gain and the loss rates are equal is described as

$$A \cdot \vec{\Phi} = \frac{1}{k} \cdot P \cdot \vec{\Phi}. \quad (3.11)$$

This equation obviously has the solution $\vec{\Phi} = 0$, but there also exist non-zero solutions for distinct k . The largest value of k with a non-zero solution for $\vec{\Phi}$ is called the criticality of the system. If $k = 1$, the production rate equals the loss rate and the system sustains a chain reaction. If $k < 1$, the losses dominate and the reactor is sub-critical. Fission dominates other reactions for $k > 1$. The criticality or neutron multiplication factor k is one of the most important parameters in describing a system. It is an intrinsic property and can be seen as the ratio of the number of fissions in any one generation to the number of fissions in the immediately preceding generation. Equation 3.11 only holds true if there are no external or boundary sources present in the system. The neutron multiplication factor k is labeled effective, k_{eff} , if the finite size of the reactor core is taken into account properly.

To establish steady-state condition in a sub-critical system, an external neutron source is required. Therefore, the differential equation is inhomogeneous and leads to other possible solutions Φ_{in} (NEA 2002, p. 138). Equation 3.11 then yields

$$A\vec{\Phi}_{in} = P\vec{\Phi}_{in} + S. \quad (3.12)$$

The neutron flux is fully determined by this equation. With declining source intensity, the inhomogeneous flux Φ_{in} converges toward Φ of the homogeneous system. Analogously to the balance equation 3.11, criticality can be defined as k_{src} for a system with an external source using

$$A \cdot \vec{\Phi}_{in} = \frac{1}{k_{src}} \cdot P \cdot \vec{\Phi}_{in}. \quad (3.13)$$

When integrating and thus determining the source neutron multiplication factor k_{src} as

$$k_{src} = \frac{\langle P \cdot \vec{\Phi}_{in} \rangle}{\langle P \cdot \vec{\Phi}_{in} \rangle + S}, \quad (3.14)$$

no distinction is made between the neutrons generated by fission and the neutrons coming from the external source. The integral over the phase volume is denoted by $\langle \rangle$.

The efficiency of source neutrons is an ambiguous figure in a sub-critical reactor. There are other definitions of k_{src} , for example linking it to the power level of the sub-critical system or the differentiation between source and fission neutrons (Gandini et al. 2002). As a result, changing reactor conditions might influence k_{src} differently depending on the definition.

3.2 Source Efficiency

The presence of a spallation target leads to a neutron heterogeneity in the core. Neutrons generated in the spallation target have a lower median energy when they react because they travel a longer way. At the same time, there is a high energy tail of neutrons coming from the spallation target. To understand the behavior of an accelerator-driven sub-critical reactor core, the importance of the source neutrons compared to the fission neutrons is relevant. The source importance or source efficiency Φ^* is defined as

$$\Phi^* = \frac{1 - k_{eff}}{k_{eff}} \cdot \frac{k_{src}}{1 - k_{src}} = \frac{P \cdot \Phi}{S} \quad (3.15)$$

and denotes the likelihood of multiplying for source neutrons compared to intrinsic fission neutrons. The definition of the source efficiency is only valid for sub-critical systems, $k_{eff} < 1$. The last term, the fraction of all produced neutrons $P \cdot \Phi$ to all source neutrons S can be rewritten to be $\nu \cdot N_f$ with the number of fissions per source neutron N_f . The inverse of the number of fissions per source neutron is the average number of source neutrons per fission Γ . It is used in the following relation

$$\frac{\Gamma}{\nu} \Phi^* = \frac{1 - k_{eff}}{k_{eff}} - 1, \quad (3.16)$$

which is particularly useful when experimentally identifying the source importance (NEA 2002, p. 139). The value of the source efficiency depends on different aspects, for example the ratio of the free mean path for the source neutrons compared to the size of the sub-critical core containing the fissile material. For $\Phi^* < 1$, the external neutrons are multiplying less than the intrinsic fission neutrons in the core. For $\Phi^* = 1$, the external source neutrons and the fission neutrons behave the same. A higher source efficiency is not targeted during operation because then the source neutrons multiply with a higher rate than the fission neutrons, implying a high level of sub-criticality in the core (IAEA 2015, p. 16).

The source efficiency affects several parameters for operating an accelerator-driven system. It directly relates to the proton beam current I needed for a certain power output P via

$$I = \frac{P}{Q_{fiss}} \cdot \frac{1 - k_{eff}}{k_{eff}} \cdot \frac{\nu}{\Phi^* \cdot Z}. \quad (3.17)$$

The average energy release per fission is denoted Q_{fiss} . The number of produced neutrons per incident proton $Z = n/p$ depends on the spallation target material, geometry and on the beam characteristics (Gandini et al. 2002).

There exist competing priorities regarding the source efficiency when designing a sub-critical reactor. From an energetic point of view, the criticality should be as close to one as possible leading to a low importance of source neutrons. As seen from equation 3.17, for k_{eff} converging toward one, the needed beam current for a given power out of the system declines. A small beam current requires only a small accelerator and reduces the costs of the overall system. From a safety point of view, the margin to criticality must be sufficiently high during maintenance and operation to

justify the possible waiving of control rods and similar systems that can add negative reactivity to the core. Additionally, a higher incident proton energy leads to a higher source efficiency because more neutrons are produced per incident proton. With a higher incident particle energy, the spallation neutrons will also yield higher energies increasing the damage done to the materials in the core (Mansani et al. 2012).

3.3 Material Depletion

The change of the material composition considered in a depletion calculation is described by the burn-up or Batemann Equations. For each isotope i , the time and spatial dependency of the total number density N is given by the following balance equation that yields the net number change summarizing the different gain and loss processes (Turinsky 2010, p.1244)

$$\begin{aligned} \frac{d}{dt}N^i(\vec{r}, t) = & \sum_{i \neq j} l^{ij} N^j(\vec{r}, t) - \lambda^i N^i(\vec{r}, t) \\ & + \sum_{i \neq j} \left[\int_0^\infty dE f^{ij}(E, t) \sigma_f^j(E, \vec{r}, t) \Phi(E, \vec{r}, t) \right] N^j(\vec{r}, t) \\ & - \left[\int_0^\infty dE \left(\sigma_f^i(E, \vec{r}, t) + \sum_{A \in AR} \sigma_A^i(E, \vec{r}, t) \right) \Phi(E, \vec{r}, t) \right] N^i(\vec{r}, t) \\ & + \sum_{A \in AR} \left[\int_0^\infty dE \sigma_A(A \rightarrow i)(E, \vec{r}, t) \Phi(E, \vec{r}, t) \right]. \end{aligned} \quad (3.18)$$

The first part describes the creation of new isotopes, summing over all other isotopes j that undergo radioactive disintegration resulting in the nuclide i with the probability l^{ij} . The second part simply expresses the loss due to radioactive decay, depending on the decay constant λ^i . Further nuclides are created by the fission of other isotopes j . The fraction f^{ij} denotes the likelihood of a fission of nuclide j resulting in nuclide i and σ_f^j the respective fission cross sections. These gains depend on the number density of the initial isotope N^j and the neutron flux Φ . The destruction rate of isotope i due to neutron induced processes (fission and radioactive neutron capture) is described by the next part, summing over all possible neutron absorption reactions AR . The last part describes the gain by neutron induced reactions other than fission that end in the considered nuclide i . Depending on the isotope, not all of the terms will appear.

These equations for all considered isotopes form a set of coupled, linear differential equations. Assuming a constant neutron flux, they can be written in matrix form

$$\frac{d\vec{N}(\vec{r}, t)}{dt} = A\vec{N}(\vec{r}, t). \quad (3.19)$$

The diagonal elements of the burn-up matrix A denote losses and the off-diagonal elements denote gains in the concentration of a certain nuclide. Usually, the spatial dependence of the Bateman Equations are suppressed by assuming that the material is homogeneously spread over the considered volume and that there is no movement of the material (Pusa 2013).

The neutron flux, as expressed by the Boltzmann Equation 3.7, appears in the Bateman Equations as well. Since it depends on the number density of the nuclides, all these equations form a complete, closed, and non-linear system of time dependent particle transport in the core. This set of equations is of course limited, as several aspects affecting reactor operations are not taken into account. As an example, the thermal expansion of the material or the Doppler broadening of cross section

resonance are not considered due to their small influence during planned operation (Haeck 2011). Their negligence might not necessarily hold true for all conditions. When looking at safety aspects, it is required to consider the behavior of the structural and cladding material. This is also inevitable when calculating accident scenarios.

The analytic solution of the Bateman and Boltzmann Equations is only possible for very simple (or simplified) problems. Consequently, in most cases nowadays, numerical methods are used. Even then, several assumptions still need to be made. The computational procedure used in this thesis is explained in detail in section 4.1 and 4.2.

3.4 Spallation Reaction

Spallation is a process that releases neutrons from the nucleus. Unlike fission and fusion, the spallation process is endothermic. It requires additional energy supplied by high-energy protons hitting the target. In a spallation reaction, the heavy target nucleus is fragmented into several parts. The nucleus usually emits several lighter fragments, such as light elements and neutrons. Since the number of resulting neutrons can easily be controlled by the beam current, spallation sources are well fitted for scientific purposes where high energy neutrons are needed. They also offers an option for the production of exotic elements. In the context of transmutation in an accelerator-driven system, the sub-critical core of the reactor surrounding the source multiplies the neutrons from the spallation reaction.

The high energy of the incoming particles is essential for the spallation reaction. Particle energies from several 100 MeV up to 1 GeV are planned for the operation of the future accelerator-driven system. In this energy range, the probability for transfer reactions decreases and nucleon-nucleon collisions dominate the reaction mechanism. The de Broglie wavelength of the incident particles lies in the order of 10^{-14} cm. This is smaller than the diameter of the target nucleus. Therefore, the treatment of the nucleons as almost free particles is justified. The interaction of the incoming proton with the target nucleus can therefore be described as a series of collisions with individual nucleons inside the nucleus. The whole spallation process can be divided into three different stages (Bauer 1998, p. 9).

The initial stage happens within the first 10^{-22} s, the time it takes the incident particle to travel across the nucleus. In doing so, some the energy of the incoming particle is transferred to the target nucleons. The nucleus is heated up. Some high-energy particles may already leave the nucleus. This step is called the intra-nuclear cascade. In this stage of the spallation process, the energy is only transferred to some nucleons along the pathway. In the following transition stage, lasting up to 10^{-18} s, the energy is spread more evenly throughout the nucleus via secondary collisions. Again, during this stage, individual nucleons can be ejected from the nucleus. The transition stage leaves the nucleus in a highly excited state. The last stage is the nuclear evaporation of single nucleons or even some lighter elements, such as helium and hydrogen (Musiol et al. 1988, p. 133). This is also called fragmentation of the nucleus. There is also a small probability of the highly excited nucleus to fission or capture additional neutrons. The composition of a heavy metal spallation target hence comprises mostly all elements, even though the majority in very low quantities.

The particle emitting from the original nucleus might trigger additional spallation reactions in surrounding nuclei. This is called the intra-nuclear cascade. The contribution of these secondary spallation reactions to the overall neutron gain depends on the geometry and density of the heavy metal target. The energy spectrum coming from a spallation source consists of a high energy tail up to the energy of the incoming proton. It has a peak at this energy because of total momentum transfer from the incoming particle.

When designing a neutron source using the spallation reaction, the neutron yield per incoming particle is a crucial parameter. It depends on the incident particle, its energy, and the target material and geometry. For a cylindrical lead target with 20 cm diameter and 60 cm height, functions to

describe the neutron yield in dependency of the energy of the particle $Y_p^m(E_p)$ are derived in Vassil'kov et al. (1990). They used previous and own experiments. For incoming protons with the energy E_p in GeV the equation yields

$$Y_p^m(E_p) = -8.2 + 29.3E_p^{0.75}. \quad (3.20)$$

For the range between 200 MeV and 1.5 GeV and for different target materials with 10 cm diameter and the same height as above the yield can also be calculated using

$$Y(E_p) = a(A + 20)(E_p - b). \quad (3.21)$$

Wherein is b a correction factor set to 0.12 GeV which basically defines a threshold below which spallation is negligible compared to other processes, such as ionization. This equation is applicable for different target materials with the atomic mass number A . The factor a is 0.1 for all heavy elements except for uranium-238 ($a = 0.19$). Using a uranium-238 target hence leads to a nearly doubled neutron yield compared to other targets (Bauer 1998).

The experiments from which the above equations are derived comprise only the target material. The spallation source in an accelerator-driven system is surrounded by the fissile and fertile materials of the fuel in its sub-critical reactor core. The neutrons emitted from the source can induce further reactions in the fissile material and might as well reenter the source volume and induce reactions there as well. In the simulation of a spallation source, the designated source particles are protons coming from the particle accelerator and not neutrons as common in reactor core calculations.

As a result, there exist different options how to define source neutrons which in turn influences the calculation of the source efficiency. Several of these options are based on a two step approach: in a first step, the spallation target is simulated and the produced neutrons with their energy, position, and direction are written into a separate file. This file is then used in a second step as an input for the simulation of the sub-critical reactor core. Possible approaches are for example described in Seltborg (2005).

The first and very simple approach is the target neutron leakage source. The geometry of the spallation target is the parameter defining which particles count as source neutrons in this computation method. As soon as a particle leaks out of the spallation target, its position, energy, and direction are saved for later calculations. When using this method, reentry of a neutron into the target material and its induction of further reactions there is not possible.

The second approach relies on the fact that the energy distribution of spallation neutrons is completely different from the energy of neutrons usually present in a reactor core. Characteristic is the high-energy tail of the distribution. During the simulation of the spallation and secondary processes, all neutrons that fall below a certain limit are not further transported. Their properties are written into the source file for the upcoming generation. The advantage is, that, unlike in a target neutron leakage source, no high energy particles are present in the second step of the simulation.

In a primary neutron source, the neutrons are attributed to two groups: the primary and the secondary neutrons. Primary neutrons originate from a spallation reaction which is induced by an incident proton. Secondary neutrons are generated by all kinds of reactions. In a two-step computational process, this implies that only the properties of neutrons coming from a proton induced spallation reaction are recorded. The simulation of the secondary neutrons takes place in the second part of the simulation.

When using current computer simulation programs, it is usually not necessary to split the calculation in two parts. Consequently, the differentiation between the different implementation methods of a spallation source lost its importance and is only relevant to very specialized questions that are not targeted in this thesis. Section 4.3 explains the approach taken for the modeling.

3.5 Interaction of Radiation and Tissue

The effect of radiation on humans is based on the interaction of particles with tissue. It mainly depends on the energy deposition per mass unit (Krieger 2012). The energy dose D is thus defined as the absorbed energy dE from ionizing radiation per mass dm

$$D = \frac{dE}{dm}. \quad (3.22)$$

For energy deposition in a material, the energy of the secondary electrons produced by ionization of the material is the most relevant contribution. Since this energy depends on the ionizing energy of the nuclides present in the material, the energy dose depends on the absorbing material. The unit of the energy dose is Joule per Kilogram and has the unit Gray (Gy). The older unit *rad* originates from the abbreviation for *radiation absorbed dose*.

Table 3.1.: Important dosimetric quantities.

Name	Definition	Unit	Old Unit
Activity	Number of radioactive transformations per time unit	Becquerel (1/s)	Curie
Energy Dose	Absorbed energy per mass unit	Gray Gy (J/kg)	rad
Radiation Weighting Factor	Weighting of particle type and energy	-	-
Equivalent Dose	Energy dose multiplied by particle weighting factors	Sievert	rem
Effective Dose	Equivalent dose multiplied by tissue weighting factors	Sievert	rem

Depending on the incoming particles and their energy, the imposed harm differs. The equivalent dose H_T is the product of the energy dose and the radiation weighting factor w_R depending on particle type and energy of the radiation. For gamma and beta radiation, the quality factor is always one, independent of energy. For neutrons, it ranges between two and twenty-three (ICRP 2010, p. 34). The unit of the equivalent dose is Sievert, where one Sievert equals one Joule per Kilogram. Depending on the exposed organ, the same equivalent dose can have different effects. This fact is covered by the introduction of tissue weighting factors for the respective organs. The effective Dose E is the sum over all organ absorbed equivalent doses H_T times the respective tissue weighting factors w_T . The gonads have the highest weighting factor of 0.20.

The activity of the material, an intrinsic property that describes the number of radioactive transformations per time unit, defines radiation emitted from a material and thus the absolute dose rate. It is expressed in Becquerel or one disintegration per second. The old unit Curie equals $3.7 \cdot 10^{10}$ Becquerel. Table 3.1 lists the different quantities relevant for dose rate calculations and their units.

As can already be seen from the introduction above, the dose rate someone is exposed to not only depend on the emitting material, but also on the person itself and its position in relation to the source. Hence, for practical purposes operational and personal equivalent doses are introduced. The operational quantities, such as the ambient dose equivalent, can be calculated easily and are a conservative upper limit of the actual effective dose a person is exposed to at a certain point relative to the radiation source. In radiation protection, compliance with dose limits is expressed in terms of personal protection quantities, but it is demonstrated by the operational quantity for external radiation. The ambient dose equivalent $H^*(10)$ is designed for area monitoring "and continues

to provide a reasonable assessment of the effective dose [...] for photons" (ibid., p. 16). It is based on the radiation field measured at a certain point in space which is then expanded into an aligned field covering the whole area. The ambient dose equivalent is the dose produced in "*the ICRU sphere at depth of 10 mm on the radius opposing the direction of the aligned field*" (ibid., p. 41). The ICRU sphere consists of tissue equivalent material with a density of 1 g/cm^3 and has a diameter of 30 cm. In most cases, this construct is a good approximation of the human body (ibid., p. 41). The introduction of the ICRU sphere greatly simplifies the calculation of dose conversion coefficients. The dose conversion coefficients are the link between the physical description of the radiation and the measurement of the radiation dose. They allow easy transformation of a measured value, the fluency, into a figure that represents the actual risks to humans. The dose conversion factors are calculated using detailed models of the human body and are tabled for various different exposure situations, for example by *the International Commission on Radiological Protection* (ICRP 1996). The dose conversion coefficients depend on the incoming particles and their energy, but also on the exposed tissue. The coefficients are controversially discussed, most notably for low energies.



4 Simulation Methods

Knowing the theoretical basics of neutron transport does not help in describing the neutron flux in most reactor systems. Due to their complexity, numerical methods must be used.

Some fundamentals on the calculation of neutron populations using Monte-Carlo Methods and the program MCNPX¹ are explained in section 4.1. The resulting neutron flux can then be used in a more complex program system for depletion calculations, using either MCMATH or VESTA² described in section 4.2. MCMATH was developed by the IANUS group³, providing free access and modifying options. VESTA is distributed by the Nuclear Energy Agency (NEA).

For later analysis of the spallation reaction, it is essential to calculate the neutron yield from the incoming particles. These values cannot be directly derived from the MCNPX output file. Their derivation and the modeling of the spallation source itself in MCNPX is explained in section 4.3. The chapter concludes with an introduction to dose rate calculations using MCNPX in section 4.4.

4.1 Monte Carlo Calculation of the Neutron Flux

The determination of the neutron flux as described by equation 3.7 is essential for the analysis of reactor dynamics. An analytical solution is only possible for very easy or simplified cases. Therefore, numerical methods, such as the Monte-Carlo algorithm which is based on random number generation, are used. To mirror the actual conditions in the core, the tracks of a sufficiently high number of particles, usually neutrons, are followed. For each of these particles, its position, velocity, and possible reactions are sampled using appropriate probability functions. These functions depend on physical properties, such as cross sections, energies and densities, that affect the considered reaction. If new particles are produced during a reaction, their tracks are followed as well. To account for changes in traveling direction, elastic scattering is also modeled. Depending on the problem and the desired output, various options can be set, determining for example which particles are being tracked.

In this thesis, the Monte Carlo neutron transport program MCNPX is used. For adequate modeling, the problem geometry is described using different cells defined by bounding surfaces. Cells can be filled with material for which at least isotopic composition and density must be defined in the input file. The desired output is defined using so-called tallies. Various tallies tracking current, flux or energy disposition for different particles can be chosen and modified.

In an MCNPX simulation of a reactor core, only a fraction of the actual neutron population is sampled. From this fraction, the neutron flux and other related parameters can be derived. The Boltzmann equation is not used. For the approximation of infinite neutron histories, the analytical and the numerical result will be the same. As a rule of thumb, the more particles are tracked, the more precise the results will be. Several options are also available within the program to obtain statistically more significant results.

Beside the neutron flux, MCNPX allows the calculation of the neutron multiplication factor or criticality of a system. It is defined as the number of neutrons in one generation compared to the number of neutrons in the previous generation. For reactor operation, an almost constant number of neutrons is desired. Even with the newest MCNP Version 6, it is not possible to combine

¹ Monte Carlo N-Particle eXtended, Version 2.7.a (Pelowitz 2011). The newest version, MCNP 6, is not used because the older versions provide all necessary options and are running more stable.

² VESTA depletion code, Version 2.1, Nuclear Energy Agency Data Bank, NEA-1856/02, 2013.

³ Interdisziplinäre Arbeitsgruppe Naturwissenschaft, Technik und Sicherheit, Technische Universität Darmstadt.

criticality calculations with the simulation of a spallation source. Therefore, for the sub-critical system, additional calculations for the determination of the multiplication factor were necessary.

4.2 Depletion Calculation

As for the Boltzmann Equation, the set of burn-up equations (3.18) can only be solved analytically for simple problems. For more complex geometries and material compositions, iterative approaches based on numerical methods are used. The general procedure is explained in the following and afterward, the two applied programs, VESTA and MCMATH, are described in more detail.

4.2.1 Solution Approach for Depletion Calculations

To solve the set of equations describing the neutron population in the core, the problem is discretized in time and space. The space dependency of equation 3.18 is removed by assuming a spatially constant neutron flux and concentration of certain isotopes for certain volumes within the problem. This calculated neutron flux is set to be constant during the following time step. In doing so, the equations form a set of linear first order differential equations with constant coefficients that can be solved. The change in concentration for each time step is then determined depending on reaction cross sections and decay constant for each considered nuclide. With the new material composition, a new neutron flux is calculated which is then used for a subsequent time step. This iteration process continues until the whole period that should be analyzed is covered. Information connected to the isotopic concentration of the fuel can be derived from the output files. Beside the obvious material composition, they might also include the decay heat, the calculated effective cross sections or the activity of the spent fuel.

For the accuracy of the results, the choice of time steps and burn cells is crucial. The assumption of a constant neutron flux will not hold true neither in space nor in time, because every change in isotopic composition also influences the neutron flux. The time steps should be chosen in order to keep changes in the neutron flux as small as possible between subsequent time steps, at best not exceeding few percent. As an illustration, for a light water reactors the effect of xenon poisoning must be taken into account by adding a small time step at low burn-up to allow for xenon-135 with a half-life of nine hours to build-up to equilibrium concentration. The material in the burn cells should be as homogeneously spread as possible.

Meanwhile, splitting the calculation period into too many time steps might neglect the effect of delayed gammas and, more importantly, proportionally increases computing time. There are similar issues concerning burn cells: the more cells are defined for which the neutron flux is calculated separately, the better is the varying neutron flux distribution in the core mirrored. At the same time model complexity and computing time are increased.

There are several possibilities to improve the results with only a small penalty on computing time. One example is the predictor corrector approach, in which the neutron flux calculated at the end of one time step for the next time step is once again used to deplete the material for a second time. For the actual nuclide concentration, an average value from both depletion calculations is taken. Another option that can be considered is the reduction of the number of nuclides for which the Bateman Equations are actually solved. Typically, the neutron flux is dominated by merely a handful of isotopes. Deciding which isotopes must be treated requires good knowledge of the relevant reactions in the core.

Naturally, the above procedure does not allow for the analysis of rapidly changing conditions, such as transient calculations. Also, changes in core geometry are only possible to a very limited scale. For safety analysis including possible core deformations, other modelling tools are needed.

4.2.2 The Depletion Codes MCMATH and VESTA

There are different code systems that allow the approximation of the solution of the burn-up equations in the previously described manner. For this work, the code VESTA is used in most cases. It was developed by the French Institute for Radiological Protection and Nuclear Safety (IRSN) and is still maintained. In the long term, VESTA is planned to be used as a generic code that can couple an arbitrary Monte Carlo transportation code to any desired depletion code. With the current version of VESTA, any MCNP(X) version can be used for neutron transport. For depletion calculations, either the build-in PHOENIX module or the depletion code ORIGEN-2.2⁴ can be selected (Haeck 2008).

The ORIGEN-2.2 depletion code was originally developed in the 1980s and has several limitations, such as the small memory due to the age of the code. To overcome these limitations, the PHOENIX depletion module is under development at IRSN. Unlike ORIGEN-2.2, PHOENIX can choose between three different methods to solve the transition matrix determined by the Bateman Equations for the problem. One obstacle in solving the matrix exponential is the wide range of entries. To ease the numerical problems associated with this, the very short-lived isotopes are treated separately in the PHOENIX module (Haeck 2011).

A second option to perform depletion calculations is the MCMATH code which was developed in the IANUS working group by Glaser (1998), Pistner (1998), Pistner (2006), Kütt (2007), Englert (2009), and Kütt (2011). It is written in Mathematica⁵ and relies on MCNPX 2.7 for the determination of the neutron flux. The depletion module is included in Mathematica. MCMATH allows for a better control of the different parameters, but it is not applicable to problems where material is shuffled within the reactor core.

One major difference between the two code systems is the determination of the effective cross sections for the depletion step. The effective cross sections Σ needed for the depletion step is given by an integral of the form

$$\sigma_{eff} = \frac{\int_0^\infty dE \sigma(E, t) \Phi(E, t)}{\int_0^\infty dE \Phi(E, t)}. \quad (4.1)$$

This integral can directly be calculated in MCNPX using the average flux in one cell. This approach is named *one-group* binning of the energy, because only one cross section for all energies is provided as MCNPX output. MCMATH uses this method. It can be seen as the convolution of the energy distribution and the cross section over the total energy range. VESTA is based on the *multi-group* binning approach: the integral is converted into a sum over several small energy ranges. For each energy bin, the energy and the microscopic cross sections are assumed to be constant. Consequently, instead of a quasi-continuous neutron flux, only a fine multi-group spectrum of the neutron flux has to be calculated by MCNPX. This is then used by VESTA to calculate the reaction rates using implemented multi-group cross section data. The default structure in VESTA consists of 43,000 energy bins but can be changed to the user's preference in accordance with the problem's requirements. It is for example possible to account for exotic resonance regions if necessary.

Another difference between the two systems is the determination of the neutron flux used for the depletion step. In MCMATH, the neutron flux for the subsequent time steps is calculated using the isotopic composition at the end of the previous time step. For better results, after the first round of calculations called the *direct run*, a second run with twice the time steps is performed. The cross sections for the *center calculations* are determined via linear interpolation of the values from the first run. In doing so, no new Monte-Carlo calculations are necessary. The same procedure

⁴ ORIGEN-2.2, Isotope Generation and Depletion Code Matrix Exponential Method, Nuclear Energy Agency Data Bank, CCC-0371/17, 2002.

⁵ Wolfram Mathematica, Version 8.0.1.

can be followed by VESTA, which it is called the predictor-corrector approach there. Using VESTA, other methods to improve the result for the neutron flux are also possible. Beside the default predictor-corrector treatment, there are also options that often require additional flux calculations using interpolated reaction rates.

VESTA and MCMATH have different concepts in regard to the definition of burn cells: in MCMATH discrete volumes filled with any material are defined as burn cells. This material can be removed from the core and continues decaying but cannot be inserted into the core at another position. In VESTA, burn materials are defined. Every cell in which this material is used in MCNP is then part of a burn cell. The burn materials can be removed from the core or placed at another position. Limited changes in the geometry are explicitly possible in VESTA. In MCMATH, additional burn cells must be defined where the material is replaced accordingly, for example coolant instead of absorbers.

4.3 Spallation Source

The spallation source is an essential part for the continuous operation of a sub-critical reactor. In the following, the options for the simulation of spallation sources in MCNPX are described and the procedure to calculate the source efficiency from the MCNPX output is explained.

4.3.1 Implementation in MCNPX

In the old MCNP versions, only neutron transport could be performed and energy ranges were restricted to ranges for which tabled cross sections were available. With the merge of the capabilities of the LAHET 2.8 program and MCNP-4B into MCNPX, more applications became possible. LAHET allows particle transport also for higher energies using different theoretical models. Since then, MCNPX is capable of simulating all particles and energies (Pelowitz 2011). When no tabled cross sections are present, which often is the case only up to 20 MeV, theoretical models to determine the reactions rates are used. The user can choose between several physics models.

For the implementation of the spallation source in the computer model, the example in the MCNPX User's Manual (*ibid.*, p. 373ff) comparing the different physics options is used as a reference for the resulting neutron production per incoming proton. In the base case, protons, neutrons and charged pions are transported. LAHET physics are used when no cross section data is present. The nucleon and pion interactions are also simulated using LAHET physics with the Bertini model based on the intra-nuclear cascade description of spallation processes. It is the most simplified model using only three different zones for the description of the charge in the nucleus. The CEM03 code increases this number to seven and the ISABEL code to 16 zones. For these different available physics models, the resulting neutron yield and computing time are tabled. Furthermore, one calculation also transporting light ions using the ISABEL INC model was documented (*ibid.*). It is shown that for the neutron production in a spallation target, the transport of protons, neutrons and charged pions is sufficient. The resulting values for the neutron yield n/p vary only slightly depending on the physics model.

It is recommended in the MCNPX User's manual that the user tries the different options to decide which model is appropriate for the considered problem. Consequently, several calculations for the case of a spallation source in the center of a sub-critical reactor system were performed. The calculated values for n/p show only small variations and are consistent with published figures for the case of a spallation source (Şarer et al. 2013). Yet, because the CEM03 code is widely recommended to model the actual physics best, it was used for production calculations. Additionally, to account for higher energies than commonly present in reactor core calculations, the cut-off energy for neutrons protons was increased from 100 MeV to 1000 MeV.

The depletion code VESTA allows not only criticality sources in the Monte Carlo module as input for its depletion calculation, but all possible sources. Therefore, the spallation source could be simulated during burn-up and the influence of the high-energy tail of the spallation neutrons is represented in the material compositions derived from the simulation. But even with the newest MCNPX Version, the neutron multiplication factor can only be calculated with a specialized criticality source. Consequently, separate calculations for the criticality of the system were conducted at the beginning of life with fresh fuel and also with partly burnt spent fuel taken from the depletion calculation.

4.3.2 Calculation of the Source Efficiency

For the calculation of the source efficiency, it is necessary to determine the neutron yield n/p for the given problem. As already discussed, there are various ways to define a source neutron in a more complex geometry than a simple spallation target. In the MCNPX manual, two ways to calculate the neutron yield are described for a simple geometry (Pelowitz 2011). All necessary information is by default printed in the MCNPX output files.

The problem summary in the output file lists neutron creation and loss figures for elastic and inelastic nuclear reactions, denoted nuclear interactions and (n, xn) reactions⁶. All figures are given per source particle and averaged over the whole computer model. For the case of the simulation of a proton beam on a target, the source particles are the incoming protons and the problem only consists of the spallation target. The neutrons yield can then be calculated as

$$\frac{n}{p} = \text{net nuclear interaction} + \text{net } (n, xn) + \text{tabular sampling.} \quad (4.2)$$

Tabular sampling herein accounts for the energy region where no cross sections are provided and only models are used. For the case of a sole spallation source, a simplified approach can be taken: since the only loss mechanisms for neutrons are escape and capture, these two values can be simply added up for the net neutron production. This does not hold true anymore when fissile material is present around the core. In this case, the loss and capture figures comprise fission reactions as well. Consequently, for the analysis of an accelerator-driven system, equation 4.2 is applied. It is simplified that the fission reactions occur in the sub-critical core. The nuclear interaction and (n, xn) reactions occur in the spallation target. Several preliminary calculations have shown the viability of this approach. Moreover, the consideration of fission figures in the shorter *loss and creation* method yields the same results as equation 4.2.

Theoretically, even more reactions and factors could be taken into account. For instance, the problem summary also lists creation due to delayed fission separately. Its relative (per source particle) appearance in the core is considerably smaller than the figure for prompt fission. The change on n/p is affected more by the position of the spallation target in the core than by the less likely reactions in the core. These are neglected in the determination of its value.

For the calculation of the source efficiency according to equation 3.15, additional calculations for the determination of the multiplication factor k_{eff} were performed. The average neutron yield per fission was set to 2.95 and the number of fissions per source neutron can be derived from the number of fission per source particle as listed in the MCNPX output file and the neutron yield n/p . The resulting values for the source efficiency can be used in a second step to estimate the beam power for a given power output and criticality of the system. According to definition 3.17, the beam power depends on the source efficiency and the neutron yield. If these two factors are explicitly inserted, some of the dependencies cancel each other out. The beam current then only depends

⁶ The from (n, xn) denotes the interaction of an incoming neutron with the target resulting in the production of x neutrons: $A + n \rightarrow A + xn$. The number of protons in the target nuclei remains the same.

on the neutron loss per fission as provided in the MCNPX output file and constant parameters for the considered problem. This includes the average energy yield per fission Q_{fiss} and the power of the reactor system. The equation can thus be simplified for the considered reactor system with 100 MWth as

$$I = 0.5A \cdot \frac{1}{\text{loss to fission}}. \quad (4.3)$$

It yields the beam current I in Ampere in dependence of one single figure from the computational output.

4.4 Dose Rate Calculations

All dose rate calculations were performed using MCNPX 2.7 transporting only photons since other particles are not relevant to the result. To allow for comparability, for all spent fuel elements the ambient dose rate in one meter distance from the active zone is estimated.

The source photons were produced using internal data from MCNPX. The `par=sp` parameter in the source definition produces decay gammas with energies according to the possible decay lines of all radioactive isotopes in the considered material. A point detector (F5 in MCNPX) tallies the fluence at a certain point in space and thus reflects the definition of the ambient dose best: it is calculated using the fluence at a certain point under the assumption that it is expanded into an aligned field. Since the fuel elements are symmetric, a ring detector can be used which reduces computational time due to a higher number of particle scoring to the tally.

In general, it is also possible to estimate dose rates using a different tally that tracks the fluence through a surface (F2 in MCNPX). Compared to the F5 tallies, fewer total histories are necessary to get the same accuracy of the result. For the distance of 1 and 2 meters from the surface, the photon fluence has been tallied using F2 flux and F5 point detector tallies. The results are shown in Table 4.1. The surface of the F2 tallies is either set to a known area (limited) or to an infinite cylinder. For longer distances, where the radiation field is near parallel, the results of the different tallies converge. This is not yet true for the distance of 1 meter. Moreover, the choice of the considered surface for normalization of the results is somewhat arbitrary. Therefore, in the dose rate calculations, the gamma spectrum is always tallied using a ring detector. This is consistent with the methods used by others for calculations of the ambient dose rate (Ward 2009; Traub 2010).

Table 4.1.: Different MCNPX Tally outputs in arbitrary units for comparison in dose rate calculations.

	1 m	2 m
F2 limited	3.30	1.35
F2 unlimited	4.06	1.32
F5	4.36	1.40

MCNPX provides the option to directly use fluence-to-dose conversion coefficients for the transformation of the fluence into dose rates. To allow for an easier comparison of different conversion coefficients, these are, however, not used. Instead, the tally is divided into 25 energy bins according to the energy bins used for the fluence-to-dose conversion coefficients. Dose rates were then externally calculated by multiplication of the fluence with the conversion factors for ambient dose rates as given in ICRP (1996, p. 179, Table A.21). The values are listed in Table 4.2. Up to this point, the results are given per source particle. For the special case of a spontaneous photons source, the MCNPX output provides the user with the activity of the source material using the

Table 44 option. This figure can then be used for the normalization of the dose rates to Sievert per hour and not per source particle.

Table 4.2.: Photon dose conversion coefficients as used for the calculation of the gamma dose rates. Values are taken from ICRP (1996, p. 179).

Energy in MeV	Conversion Coefficient in Sv/cm ³	Energy in MeV	Conversion Coefficient in Sv/cm ³
0.01	$6.1 \cdot 10^{-14}$	0.5	$2.93 \cdot 10^{-12}$
0.015	$8.3 \cdot 10^{-13}$	0.6	$3.44 \cdot 10^{-12}$
0.02	$1.05 \cdot 10^{-12}$	0.8	$4.38 \cdot 10^{-12}$
0.03	$8.1 \cdot 10^{-13}$	1.	$5.2 \cdot 10^{-12}$
0.04	$6.4 \cdot 10^{-13}$	1.5	$6.9 \cdot 10^{-12}$
0.05	$5.5 \cdot 10^{-13}$	2.	$8.6 \cdot 10^{-12}$
0.06	$5.1 \cdot 10^{-13}$	3.	$1.11 \cdot 10^{-11}$
0.08	$5.3 \cdot 10^{-13}$	4.	$1.34 \cdot 10^{-11}$
0.1	$6.1 \cdot 10^{-13}$	5.	$1.55 \cdot 10^{-11}$
0.15	$8.9 \cdot 10^{-13}$	6.	$1.76 \cdot 10^{-11}$
0.2	$1.20 \cdot 10^{-12}$	8.	$2.16 \cdot 10^{-11}$
0.3	$1.80 \cdot 10^{-12}$	10.	$2.56 \cdot 10^{-11}$
0.4	$2.38 \cdot 10^{-12}$		



5 Plutonium Breeding and Disposition in the Russian Fast Reactor BN-800

The Russian fast breeder BN-800 is designed to meet various objectives, among others the disposition of excess weapon-grade plutonium. This chapter investigates the feasibility of this concept and has a look at the proliferation risks posed by the reactor design. After a brief history of fast reactor development in Russia in section 5.1, the reactor model is introduced in section 5.2. The possibility of plutonium disposition in the core and an assessment of the resulting material in the core and blanket elements is evaluated in section 5.3. Section 5.4 summarizes the results of the depletion and dose rate calculations.

5.1 History of Russian Fast Reactors

Russia is a prominent example among countries using nuclear energy for the long history of fast breeder reactors. Expecting a future uranium shortage, already in 1949 a fast breeder development program was launched (Cochran 2010). At the dawn of nuclear energy production in the 1950s and 1960s, the Soviet Union undertook enormous efforts to close the nuclear fuel cycle, using sodium-cooled reactors. Meanwhile, it fostered research and development of nuclear propulsion systems. The use of lead-bismuth cooled nuclear reactors in her submarine fleet helped to build expertise in designing and operating metal cooled reactors.

The BN-350 was the first prototype of a series of sodium-cooled fast breeder reactors¹. It was built at Mangyshlack Atomic Energy Combine — now located in Kazakhstan — and was operating between 1972 and 1999 (Cochran 2010, p. 64; Nuclear Energy International Magazine 2017). Its successor, the BN-600 reactor, became operational in 1980 at the Beloyarsk nuclear power plant site. For a long time, it was the only commercially operated fast reactor worldwide. Nearly immediately after the BN-600 start-up, the construction of the improved and scaled-up BN-800 started. Already not economically competitive to the light water and graphite moderated thermal reactor fleet, the Chernobyl accident in 1986 stalled construction due to a lack of funding (Cochran 2010).

About 20 years later, the construction license of the BN-800 was renewed in 1997 (Rosatom 2017). Russia aims to increase the share of nuclear power in her overall energy production while again at the same time planning to replace her thermal reactors by fast reactors in a closed nuclear fuel cycle (IAEA 2012a, p. 777). As of today, only Russia is committed to the commercial use of fast reactors (World Nuclear News 2010). The BN-800 is considered to play an important role in the development of key technologies necessary and the demonstration the feasibility of the concept. It is noteworthy that in a next step the transmutation of minor actinides is also planned (Rosatom 2017).

The BN-800 reached first criticality in June 2014 and was connected to the grid more than one and a half years later in December 2015 (Burnie 2015). Despite its very short operation history, the BN-800 already won the Top Plant 2016 award in the nuclear generation category by the industry (Rosatom 2017). It is designed to use MOX fuel containing excess weapon-grade plutonium. But the new MOX fuel fabrication facility (MFFF) only became operational at Russia's Mining and Chemical Combine (MCC) Complex in Zheleznogorsk at the end of 2014 and was formally commissioned in September 2015 (Burnie 2015). The facility is designed to produce 400 fuel elements consisting of

¹ The BN series for *Bystrye Neitrony* — fast neutrons. The number assigns electrical output.

pelleted MOX fuel. Fuel fabrication from any isotopic composition of plutonium will be possible (World Nuclear Association 2017b). Due to the delay in operation of the MCC Zheleznogorsk MOX fuel fabrication facility, the initial core loading of the BN-800 contained fuel from different sources and in different forms. Besides the 102 fuel elements made from high enriched uranium, the core was filled with MOX fuel partly as pellets and partly in vibrocompacted form (Burnie 2015).

The original motivation of modeling the BN-800 core was the evaluation of the procedure for plutonium disposition as agreed-upon in the Plutonium Management and Disposition Agreement (PMDA) (Governments of the United States and Russia 2000; Governments of the United States and Russia 2010). This agreement was signed by the United States and the Russian Federation to dispose of 30 tons each of the excess weapon-grade plutonium. The thesis's objective was to show the feasibility of plutonium disposition in a fast reactor by this example. In October 2016, the implementation of the PMDA was suspended. Yet, Russia might still proceed with the disposition of her excess weapon-grade plutonium. She is however free not to implement certain elements of the agreement that might impede her efforts to close the nuclear fuel cycle. These could be for example the restrictions on reprocessing of blanket elements (IPFM Blog 2016). The PMDA as it was implemented before the suspension is used as an exemplary model on how the disposition of plutonium could be done².

Meanwhile, the BN-800 might be the first commercial fast reactor to be exported to other countries. Russia's Atomstroy Export, the China Institute of Atomic Energy (CIAE), and the Chinese Nuclear Energy Industry Company (CNEIC) agreed on pre-project and design works for two commercial nuclear power reactors based on the BN-800 in 2010 (World Nuclear News 2010). Due to a disagreement over the price and unnamed political reasons, the purchase was postponed in 2012 (IPFM Blog 2012). With the possible export of the reactor design to other countries, the nuclear material produced in the BN-800 becomes more relevant. It can be assumed that Russia has no objective in producing additional weapon-grade plutonium. And if they had, being a nuclear weapon state, they would not have to mask it within their civil energy production. This might be different for a state wanting to gain a possible pathway to acquire nuclear weapons or at least access to nuclear weapons material.

5.2 BN-800 Reactor Simulation Model

The BN-800 is a sodium-cooled fast reactor with a thermal power output of 2100 MW_{th}, corresponding to roughly 800 MW_e. For the simulations, the reactor is modeled according to the Fast Reactor Database of the IAEA (2006). It can be seen as an example for either plutonium disposition in the core, or more general, for the possibility of breeding nuclear weapons material in a fast reactor.

5.2.1 Description of the Reactor Design

The BN-800 consists of 565 hexagonal fuel elements that are split into three different zones that vary in regard to their plutonium content. Each of the zones is further split into three batches for refueling. In the sketch of the core model, Figure 5.1, the zones are colored in a red, green, or blue color scheme. At the periphery of the core, 90 breeding elements can be inserted. The design further foresees axial blankets placed below the active region, but none above. The core is surrounded by a ring of steel reflector elements and contains 30 control and safety rods. These have been assumed to be withdrawn for the depletion calculations during which the total neutron flux is normalized according to the overall reactor power. Table 5.1 summarizes key core values. More information on the design of the single fuel and blanket elements is given in Table 5.2. For simulation, the fuel elements were treated as homogeneous material mixtures.

² The calculations on the BN-800 presented in this thesis were finished before the suspension of the agreement.

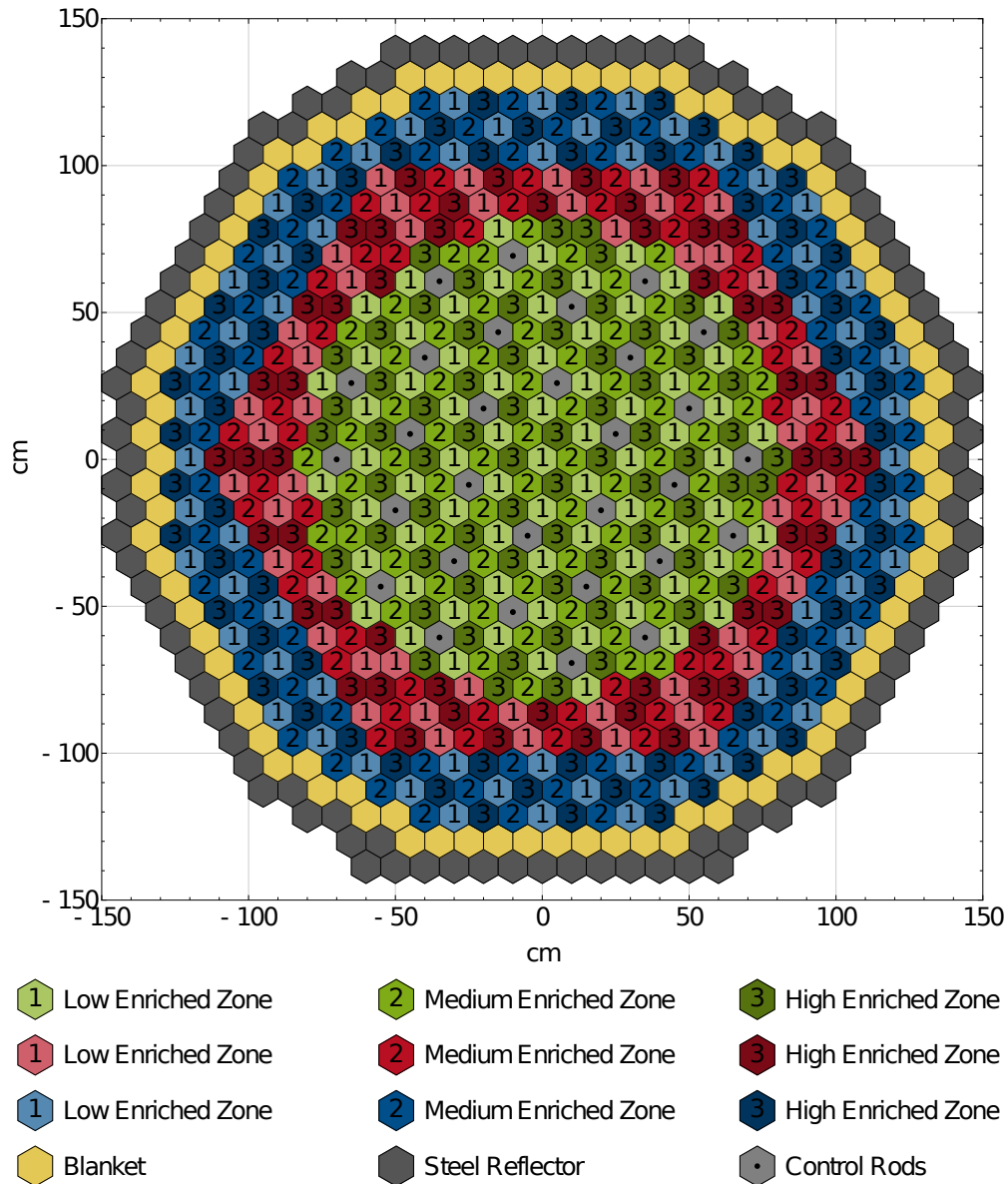


Figure 5.1.: Cross section of the BN-800 reactor model. The core contains three different fuel zones split into three batches each. The active zone is surrounded by a ring of blanket elements. There are 30 control and safety rods present.

Table 5.1.: Core and element design data for the BN-800 core model. All values from IAEA (2006).

Parameter	Unit	Value
Total Thermal Power	MW	2100
Number of Fuel Elements		211+156+198
Number of Blanket Elements		90
Number of Control Elements		30
Fuel Element Pitch	cm	10
Can Thickness	cm	0.275
Active Core Height	cm	88
Height of Lower Axial Blanket	cm	35

Table 5.2.: Geometric dimensions of the fuel and blanket elements in the BN-800 core (IAEA 2006).

Parameter	Unit	Fuel	Blanket
Number of Pins per Element		127	37
Outer Pin Diameter	cm	0.66	1.4
Cladding Thickness	cm	0.04	0.04

The coolant density ρ_{Na} can be calculated using equation

$$\rho_{Na} = 950.0483 - 0.2298T - 14.6045 \cdot 10^{-6}T^2 + 5.6377 \cdot 10^{-9}T^3. \quad (5.1)$$

It results in the density in kg/m^3 depending on the temperature T in $^{\circ}\text{C}$ (Rouault 2010, p. 2354). An average coolant temperature of 450°C is assumed. For structure, cladding and reflector material, stainless steel ChS-68 is selected (IAEA 2012c). Material composition was chosen according to Porollo et al. (2009). Table 5.3 lists the original materials and their densities for the derivation of the homogeneous materials.

Table 5.3.: Selected material properties used in the BN-800 core model.

	Material	Density in g/cm	Reference
Fuel	MOX	8.60	(IAEA 2006, p. 57)
Blanket	Uranium Dioxide	9.70	(IAEA 2006, p. 59)
Cladding, Structure	ChS-68 Steel	7.75	(IAEA 2012a, p. 525)
Coolant	Sodium	0.84	(IAEA 2006, p. 15)

For the MOX fuel and the blanket material, the "*smear density of fuel with fuel assumed to occupy whole space inside the cladding tube*" is tabled (IAEA 2006, p. 57, p. 59). In the original reactor design, MOX fuel using reactor-grade plutonium is planned. Table 5.4 shows the exemplary isotopic compositions for weapon- and reactor-grade plutonium used for the model. The reactor-grade composition originates from fuel with low burn-up of about 30 MWd/kgHM. During the design phase of the BN-800 this was a common burn-up in commercial light water reactors. The exact composition of Russian excess weapon-grade plutonium is not known but it is assumed that the content of plutonium-239 is higher than in the given vector. According to the PMDA, Russia is allowed to blend down her original weapon-grade plutonium to reduce the fraction of plutonium-239.

Table 5.4.: Isotopic composition of weapon-grade and reactor-grade plutonium. Reactor-grade plutonium as given in NEA (1995, p. 77) and weapon-grade plutonium as given in Holdren et al. (1995, p. 45).

	Pu-238	Pu-239	Pu-240	Pu-241	Pu-242
Reactor-grade Plutonium	1.80	59.00	23.00	12.20	4.00
Weapon-grade Plutonium	0.01	93.80	5.80	0.13	0.02

There are three different zones in the reactor: the inner zone consisting of 211 fuel elements with a plutonium fraction of 19.3 %, the intermediate zone consisting of 156 fuel elements with a plutonium fraction of 21.9 % and the outer zone consisting of 198 elements and containing 24.5 % plutonium. In the following, the zones are labeled low, medium, and high enriched zone (LEZ, MEZ, HEZ). The plutonium content is not published explicitly in the IAEA database, but rather an

enrichment defined as the mass of the fissile isotopes divided by the mass of the fertile and fissile isotopes. The published values of 19.5 %, 22.1 %, and 24.7 % enrichment include uranium-235 in the fissile mass. Using the figures given for the total uranium-235 and uranium-238 inventory, it was derived that depleted uranium with 0.3 % uranium-235 is used for the design and thus the above values for the plutonium enrichment could be calculated.

For the analysis concerning the PMDA, the reactor-grade plutonium in the fuel is replaced by weapon-grade plutonium. To keep core characteristics as similar as possible to the already developed model, the plutonium fraction in the fuel is decreased. The resulting average fission cross section of the weapon-grade plutonium is set to be roughly the same as for the reactor-grade plutonium. The plutonium fraction in the different zones is thereby calculated to be 17.8 %, 20.2 % and 22.7 % respectively. This adjustment in the plutonium enrichment also leads to changes in the neutron economy in the core, but they are considered to have only small effects on reactor dynamics. Further, several other options to adjust for the different plutonium vectors can be imagined. This includes the final number of MOX elements, the possible introduction of uranium fuel elements or other plutonium fractions in the fuel.

The axial blankets follow the same geometry as the fuel elements, whereas for the radial elements a special structure applies (cf. Table 5.2). As blanket material, depleted uranium dioxide is used. If no blankets are present, the elements are filled with sodium. This replacement leads to only minor changes in reactivity and the average burn-up of the fuel elements. The temperature is set to 600 Kelvin, except for the fuel and breeding elements with an assumed temperature of 1200 Kelvin.

5.2.2 Simulation Parameters

For the depletion calculation, a reactor power of 2100 MWth and a cycle length of 420 full power days (FPD) for every fuel element is modeled. Every 140 FPD, one third of the fuel elements from each zone is replaced. The different batches³ are labeled from one to three in Figure 5.1, according to the period after which they are replaced by a fresh fuel element. The axial blankets are replaced every 420 FPD, together with the fuel elements. The radial blanket elements have a longer irradiation time and remain in the periphery of the core for 840 FPD.

Since the simulation starts with a core completely filled with fresh fuel, more than three cycles are simulated for the core to reach equilibrium operation mode⁴. For the evaluation, fuel elements are taken into consideration from the cycle when each batch has been refueled at least twice. To shorten the simulation time, the first radial blanket batch was already replaced after 420 days.

The IAEA fast reactor database lists an average burn-up of 66 MWd/kgHM (ibid., p. 41). Since one of the requirements set by the PMDA is the fulfilling of certain radiation barrier by the spent fuel elements, in the agreement different minimal burn-ups are defined. Those must be reached before the elements can be removed from the core. During the commissioning period, lower values are allowed. Additional to the values for one single element, also average batch values are stated. In the agreement, the burn-ups are given in percent of heavy metal atoms that are fissioned. Table 5.5 gives the published values and those translated into MWd/kgHM. Depletion calculations were performed using MCMATH.

³ One batch are all elements discharged at the same time. It contains elements from all fuel zones.

⁴ At BOL, the core is only fueled with fresh fuel elements, resulting in a higher criticality. Consecutively, the batches are replaced by fresh elements until the equilibrium operation mode is reached. The first batch reaches only one third of the targeted burn-up, the second batch already two thirds. Not even the first batch reaching full burn-up shows equilibrium behavior since it was exposed to higher neutrons fluxes at BOL. Only when elements from the same position show the same burn-up and composition after removal from the core, equilibrium mode is reached.

Table 5.5.: Minimum burn-up values as agreed-upon in the Plutonium Management and Disposition Agreement.

	HM atoms fissioned	
	% HM	MWd/kg HM
Fuel Element, Commissioning Period	3.9	36.4
Fuel Element, Main Operation	4.5	42.1
Batch, Commissioning Period	5.0	46.7
Batch, Main Operation	6.0	56.1

5.3 Results of the BN-800 Simulation

The evaluation of the depletion calculations presented in this chapter focuses on three different aspects. First, the evaluation of the plutonium vector in the fuel elements is analyzed. In a second step, the plutonium production in the blanket elements is investigated. Then, the gamma dose rates are evaluated for all elements after different cooling periods.

5.3.1 Evolution of the Plutonium Vector

When disposing of weapon-grade plutonium by burning it in a nuclear reactor, there are two objectives: one is the reduction of the fissile isotope plutonium-239, the other is the build-up of fission products to form a radiation shield. In Figure 5.2, the evolution of the plutonium-239 fraction for single elements from each enrichment zone and the batch average are shown. Since the core is designed to be operated with blankets, analysis is conducted in the presence of blanket elements. For easier comparison with the minimum burn-up values (cf. Table 5.5), the fractions are plotted against burn-up in MWd/kgHM. Different elements experience different burn-ups during the same irradiation period because they are exposed to different neutron fluxes depending on their position in the core.

All elements start with a plutonium-239 fraction of almost 94 % as fixed by the original composition of the weapon-grade plutonium. During the irradiation for 420 FPD, the fraction drops to about 88 % for the elements from the zone high enriched in plutonium. Elements from LEZ experience the highest burn-up and their plutonium-239 fraction falls below 83 %. While not fulfilling the common definition of weapon-grade plutonium with a plutonium-239 fraction of more than 90 %, the spent fuel still contains significantly less plutonium-240 than average spent fuel from light water reactors ($\approx 60\%$, cf. Table 5.4). When operating the reactor with fuel cycles equaling 420 FPD, the minimum agreed-upon burn-up values are met. In Figure 5.2, only the limits for normal operation are plotted. During commissioning, even lower values are acceptable leading to even higher fractions of plutonium-239 in the spent fuel.

The batch average and the minimum agreed-upon burn-up for one batch during operation are also shown, because spent fuel elements from all three zones are usually removed during one reload of the reactor core and are most likely reprocessed together. The batch average is formally fulfilling the requirements set by the PMDA. But compared to spent light water reactor fuel, it contains plutonium with an isotopic composition relatively close to weapon-grade plutonium.

The breeding ratios for the reactor based on production and destruction of the four most important fissile isotopes in the fuel (uranium-233, uranium-235, plutonium-239, and plutonium-241) are always lower than one. Therefore, they fulfill the requirement set by the PMDA. This requirement is met by reactor configurations with and without blankets.

Table 5.6 denotes the mass balance for all plutonium isotopes and the fissile plutonium isotopes. A load factor of 0.8 is assumed. Considering all plutonium isotopes, the annual balance of

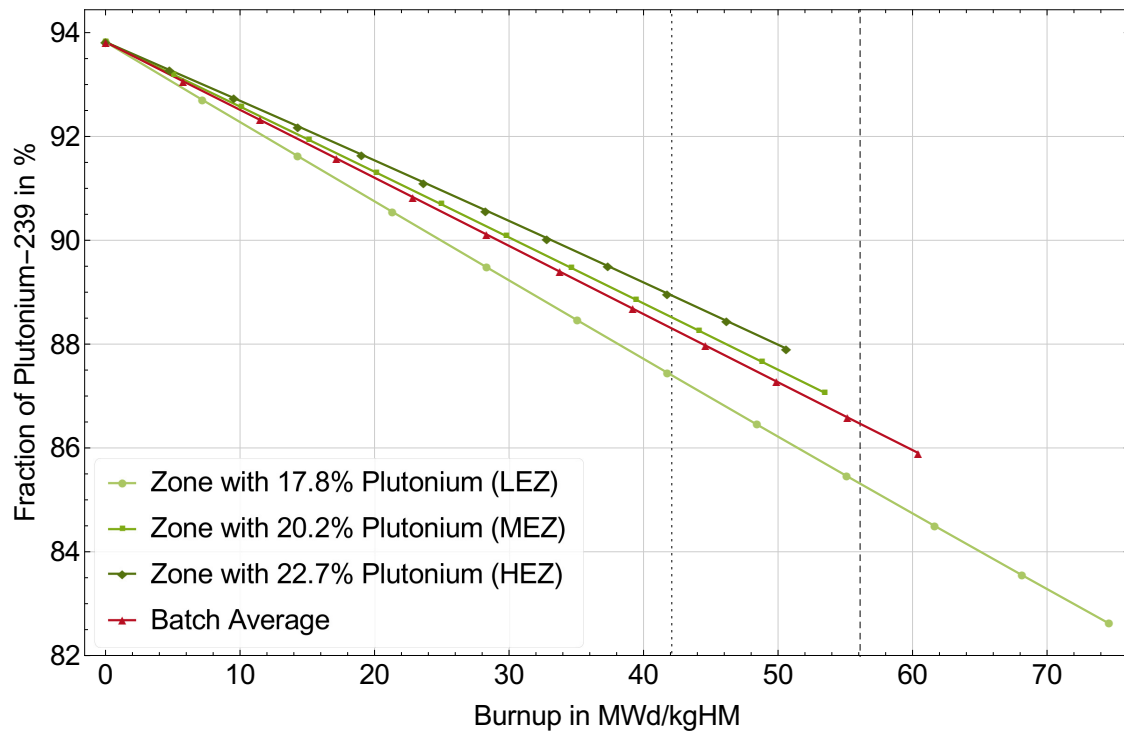


Figure 5.2.: Evolution of the plutonium-239 fraction for elements from different zones and batch average against burn-up. The minimum agreed-upon burn-up values for batch (dashed) and single elements (dotted) during the operation period are plotted as well.

plutonium is 25 kg. With blankets, the BN-800 thus is a net plutonium producer. This contraction to the calculated breeding ratios below one can be explained by the fact that only fissile isotopes are considered in the calculation of the breeding ratios. Nearly 100 kg of plutonium-239 or plutonium-241 are either fissioned or transmuted into other isotopes annually. More details on these results including an analysis of the time-dependent breeding ratios are given in Kütt et al. (2014). The ratio of plutonium-240 to plutonium-239 is 0.17 at EOL which is higher than the fraction stated in the PMDA and matches reported figures (Plutonium Disposition Working Group 2014, p. 114).

Table 5.6.: Annual plutonium throughput in the core for all plutonium isotopes and the fissile plutonium isotopes only (only plutonium-239 and plutonium-240 are used for the calculation of the breeding ratio).

	Core				Blankets		Total Balance
	Start-up	Reload	Removal	Balance	Radial	Axial	
Pu	2,572 kg	1,788 kg	1,652 kg	-136 kg	83.4 kg	78.0 kg	25 kg
Pu _{fiss}	2,421 kg	1,683 kg	1,438 kg	-245 kg	78.4 kg	76.1 kg	-91 kg

5.3.2 Plutonium Breeding in the Blankets

The BN-800 is originally designed as a breeder reactor. Only for the disposition of excess weapon-grade plutonium, it was agreed-upon in the PMDA to set its breeding ratio below one. Nevertheless, breeding blankets are present. Unlike the axial blankets, which are connected to the fuel elements, the radial blanket elements can be loaded and removed from the core independently from the fuel

reloading strategy. The plutonium breeding can thus be enhanced without a penalty on reactor operation.

The evolution of the plutonium content and the build-up of fission products in the radial blankets over the irradiation time in the core is shown in Figure 5.3. It takes only about 200 FPD for the plutonium concentration to reach 1 % of the blanket material. After 420 FPD, the concentration is doubled. After 840 FPD (EOL), the blanket elements contain nearly 4 % plutonium. Even after such a long irradiation period, the plutonium still comprises mainly plutonium-239 due to the reduced neutron flux in the core periphery where the blankets are positioned.

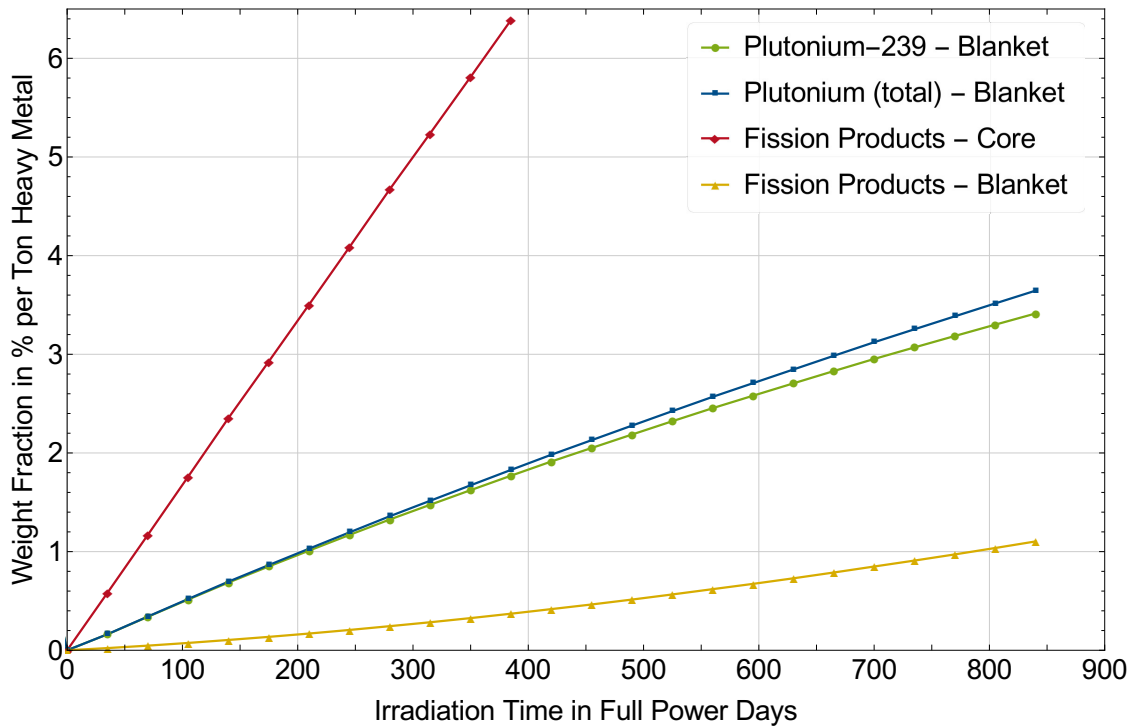


Figure 5.3.: Plutonium and fission product build-up in the radial breeding blanket. Fission product concentration is also given for a fuel element, but only plotted up to 390 FPD.

When considering the attractiveness of the material bred in the blankets, the build-up of fission products is of major relevance. Hence, the fraction of fission products in the core and blanket elements also is plotted in Figure 5.3. After 840 FPD, the concentration of fission products in the blanket is only slightly higher than 1 %, whereas for the core at only half the irradiation time the fraction reaches almost 7 %. The most important contributor to the dose rates in the first years after discharge is cesium-137. After a full irradiation of 840 FPD, the cesium activity in the blankets is only $1.26 \cdot 10^{12}$ Bq/kgHM while for the core elements at EOL the cesium-137 concentration is $8.0 \cdot 10^{12}$ Bq/kgHM. The radiological barrier as an obstacle to reprocessing of the spent fuel and blanket elements is further analyzed in the following section.

Only one row of breeding elements as in the BN-800 reactor is a comparably small breeding zone. But several significant quantities of plutonium are bred there, even when the reactor is operated with a breeding ratio below one. Additionally, there are axial blankets placed below the fuel region in the core. These elements are assumed to be replaced according to the fuel cycling scheme. Therefore, their plutonium content only adds up to an average of 1.57 % at EOL (420 FPD). The concentration of fission products is only 0.23 % in the axial blanket and at the same time the plutonium-239 fraction is higher than 97 %. Isotopic vectors for both blankets separately and mixed with spent fuel can be found in Kütt et al. (2014).

5.3.3 Dose Rates from Spent Fuel Elements

In the Plutonium Management and Disposition Agreement, one condition defining disposed of plutonium is the gamma dose rate emitted by the spent fuel elements. It is stated in the Annex on Technical Specifications, Section II (Governments of the United States and Russia 2010):

"Disposition plutonium shall be considered disposed if the spent plutonium fuel resulting from irradiation in the BN-600 and BN-800 reactors meets the four criteria below.

[...]

4. The radiation level from each spent plutonium fuel assembly is such that it will become no less than 1 Sievert per hour one meter from the accessible surface at the centerline of the assembly 30 years after irradiation has been completed."

Gamma dose rate calculations were carried out for fuel elements from the different zones in the reactor core to check whether they meet this requirement. Additional calculations were performed for the radial blanket elements. Although the dose rate from these elements is not covered in the PMDA, they are an important factor in assessing the material attractiveness of the plutonium produced in the blankets. The values for material composition and fuel geometry were directly taken from the previous burn-up calculations, resulting in one homogeneous hexagon surrounded by air as input for the dose rate calculations (Frieß and Kütt 2016; Frieß and Kütt forthcoming 2017). For fuel elements comprising so many fuel pins, the difference in the resulting dose rates can be neglected (Trumbull et al. 2005). Only for elements comprising only a small number of fuel pins self-shielding should be simulated using a heterogeneous geometry model.

Table 5.7.: Plutonium content and ambient gamma dose rates for different elements 30 years after discharge from the core. The radial blankets were irradiated for more than 840 FPD compared to 420 FPD for the other elements.

	LEZ	MEZ	HEZ	Axial Blanket	Radial Blanket
Pu per Fuel Element	3.79 kg	4.28 kg	4.76 kg	0.14 kg	3.02 kg
Pu Fraction	17 %	19 %	21 %	1.6 %	3.8 %
Dose Rate	2.15 Sv/hr	1.58 Sv/hr	1.55 Sv/hr	<0.02 Sv/hr	0.13 Sv/hr

Table 5.7 shows the gamma dose rates, the plutonium content, and the plutonium fraction for fuel and blanket elements. In accordance with the PMDA, the cooling period is 30 years after discharge from the core. Naturally, the plutonium fraction is higher for the driver fuel elements which contain plutonium from the beginning onwards. All fuel elements are in compliance with the dose rate requirement, emitting more than 1 Sv/hr 30 years after discharge. Elements from the zone with the highest plutonium fraction emit the lowest dose rates. The elements from that zone are placed in the periphery of the core where the neutron flux is lowest and thus the lowest number of fissions takes place.

Accordingly, the dose rates from the axial blankets are the lowest for elements from the outer fuel zone. The axial blankets could be separated from the fuel elements and would result in an attractive source material for the separation of weapon-grade plutonium. The dose rates from the axial blankets fall below the self-protecting limit of 1 Sv/hr practically immediately after discharge. After 30 years, one element emits less than 0.02 Sv/hr. As long as not separated from the fuel, the dose rate is dominated by the fission products in the fuel. Due to their small volume, each axial blanket contains only 140 g of plutonium.

The dose rates from the radial blanket elements are higher: after 30 years, they emit 0.13 Sv/hr, if irradiated for 980 FPD before discharge. The longer irradiation leads to a higher plutonium

fraction. Each radial blanket element comprises slightly more than 3 kg of plutonium. After the full irradiation period these elements contain 240 kg of weapon-grade plutonium in total. Using the significant quantity of 8 kg as a reference value, enough material to produce about 30 nuclear weapons is present in the blanket elements. Or conversely, only three of them must be diverted to acquire enough fissile material for one nuclear weapon.

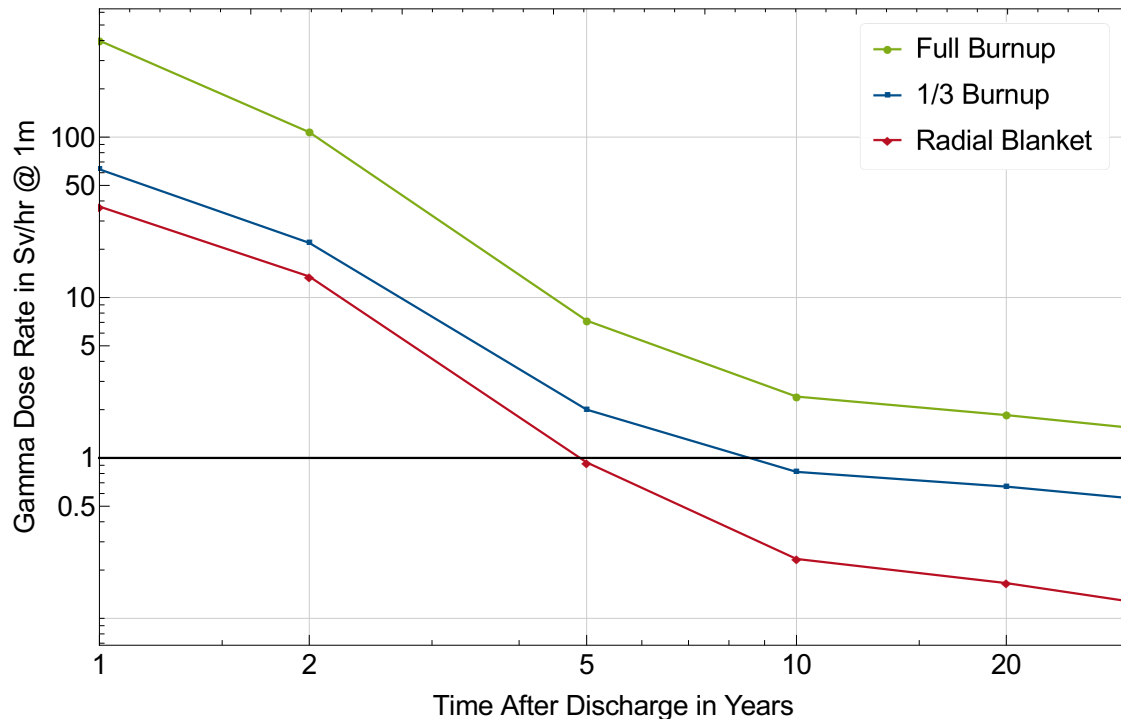


Figure 5.4.: Dose rates for fuel and radial blanket elements after different cooling periods. Only with full burn-up the radiation barrier is still working after 30 years of cooling. The dose rates from the radial blanket elements fall below 1 Sv/hr after only five years of cooling.

Figure 5.4 shows the influence of the cooling period on the gamma dose rate. In the first years after removal from the core, the dose rate is high but declines rapidly. During this time, many short-lived fission products contributing to the gamma dose rate decay. Dose rates from fuel elements that were exposed to the full irradiation time never fall below the limit of 1 Sv/hr. No values were calculated for longer cooling periods, as they would clearly continue to decrease. The radial blanket elements emit less than 1 Sv/hr after a five year cooling period. If a possible proliferator is willing to risk personal injury when acquiring nuclear material, after even shorter cooling periods the blanket elements cannot be considered to be self-protecting anymore. No figures for the axial blankets are given, since their dose rate is mostly equal to the rate from the spent fuel elements.

Even though no early removal of fuel elements from the core is planned, this might be necessary due to e.g. mechanical failure or other safety reasons. In Figure 5.5, the effects of a shortened irradiation time on the resulting dose rates are illustrated. The periods were selected according to typical refueling intervals of the BN-800, when the reactor is shut down and one third of the fuel elements are replaced by fresh fuel elements. After only one third of the scheduled irradiation time of 420 FPD, no elements fulfill the requirement of emitting a dose rate of more than 1 Sv/hr. After two thirds (280 FPD), the elements with medium and high fraction of plutonium barely stay above the limit, whereas fuel from the inner zone containing low enriched uranium already emits more than 1.5 Sv/hr. Removing fuel elements before reaching fuel burn-up reduces the cooling periods and eases handling of the spent fuel elements.

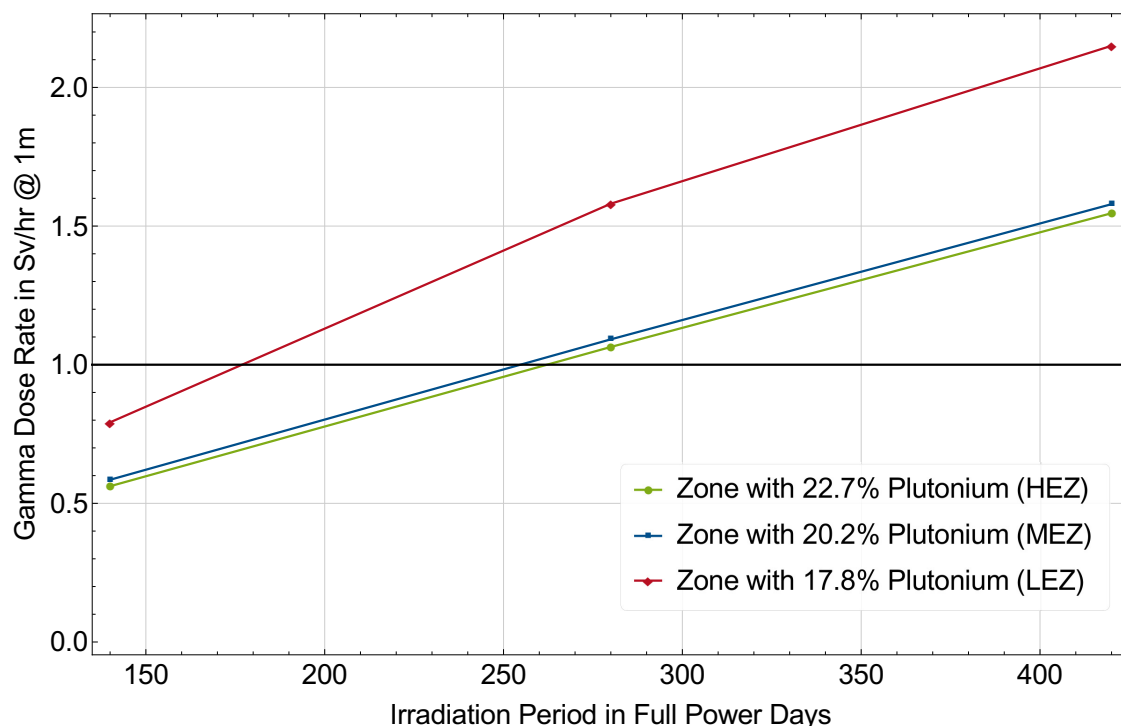


Figure 5.5.: Dose rates after different irradiation periods in the core for one exemplary fuel element from each zone. With only one third of the agreed-upon burn-up, the fuel elements emit less than 1 Sv/hr after a 30 year cooling period.

5.4 Summary

The Russian fast breeder reactor BN-800 was one option for Russia to fulfill her obligations under the PMDA to render 30 tons of its excess weapon-grade plutonium unusable. Even though the agreement has been suspended only recently, the BN-800 is still a viable example for the disposition of weapon-grade plutonium in fast reactors. At the same time, it brings with it the typical breeder characteristic of producing additional weapon-grade plutonium.

Depletion calculations show that the isotopic composition of the weapon-grade plutonium shifts toward reactor-grade plutonium. After the planned irradiation time the fraction of plutonium-239 is still considerably higher than in reactor-grade plutonium. It comprises about 80 % compared to roughly 60 %. The annual plutonium balance is close to zero, even though the reactor is operated with a breeding ratio well below one. This ostensible contraction can be explained by the fact that only the build-up of fissile isotopes contributes to the breeding ratio. To have a true plutonium burner configuration, the breeding blankets would need to be removed from the core as considerable amounts of plutonium are produced within them.

One condition to consider the excess weapon-grade plutonium to be disposed is the radiation barrier. After a cooling period of 30 years, the emitted gamma dose rate should be higher than 1 Sv/hr in one meter distance. This requisite is fulfilled by all fuel elements present in the core for the scheduled irradiation time of 420 FPD. It is not fulfilled for shorter irradiation periods and never for the blanket elements. Chapter 8 discusses possible implications in more detail.



6 Plutonium Production in Small, Fast Reactors

This chapter investigates the proliferation risk of nuclear batteries, one special type of small, modular reactors (SMRs) with a very low energy output. Their characteristics are explained in section 6.1. A generic computer model to perform burn-up calculations is set up in section 6.2. It is based on the Toshiba 4S reactor. The changing isotope composition in the core and the attractiveness of the generated fissile material using Bathke's Figures of Merit and the gamma dose rate emitted by the spent fuel elements is assessed in section 6.3. Section 6.4 summarizes the results.

6.1 Nuclear Batteries – The Smallest Nuclear Reactors

Some small modular reactors are designed to have core lifetimes of several decades. The core remains sealed during the complete lifetime. These reactors are called nuclear batteries because of the anticipated ease of deployment. The fuel or even the already sealed core is delivered to a reactor site. After the lifetime, the spent fuel is either removed from the core on-site using special equipment or the complete core is transported back to a central reprocessing facility. Nuclear batteries have a very small power output and require reduced on-site handling and maintenance. Hence they might exploit new markets for nuclear power plants. The small power output is designed to meet the demand in remote locations with only a small electricity grid. The possible deployment in these locations or in countries that lack experience in regulating and operating nuclear power plants rises security concerns. Proponents answer them by referring to the sealed core and the virtually absent access to the (spent) fuel.

As a demonstration for this reactor type, the Toshiba "*Super-Safe, Small, and Simple*" reactor (4S) is chosen. It is a small sodium-cooled fast reactor using metal fuel with an energy output of either 10 MWe or 50 MWe. It is developed for energy production, but can also incorporate seawater desalination and hydrogen and oxygen production systems (Tsuboi et al. 2012; IAEA 2016). For the 10 MWe output core, the reactor is designed to have a 30 year lifetime, whereas for the larger energy output the core lifetime is only ten years. Deployment is mainly envisioned in remote areas, such as small cities and mining sites. Just as most other innovative reactor designs, the Toshiba 4S has not gone beyond design stage yet. However, it is still considered to be deployable in the near future (Subki 2016).

Licensing activities for the 4S design were initiated with the U.S. Nuclear Regulatory Commission (U.S. NRC) in 2007. A demonstration plant was planned for Galena, Alaska. Apparently, the project has been stalled due to high installation and operating costs (Holdmann 2011, p. 13). Nevertheless, Toshiba continued to submit technical reports on the 4S to the U.S. NRC at least until 2013 (Toshiba 2013). In the same year, The Daily Yomiuri announced that Toshiba is developing a small reactor to be deployed in oil sand mining. The article further stated that Toshiba is awaiting results from the design approval procedure underway with the U.S. NRC (The Yomiuri Shimibun 2013). Since then, not much has been heard of the project, but it does not seem to have been shut down completely (Wilson 2016).

One key feature of the 4S is its long core lifetime of 30 years and the absence of any refueling or shuffling of fuel elements during this period. The core is supposed to remain sealed during operation. To achieve this long core lifetime, it is necessary to use fuel with a higher uranium

enrichment than typical for modern light water reactors: the core is fueled with uranium enriched close to the limit of 20 % (United States Department of Energy 2014). Above 20 % enrichment, stronger safeguards would be required and it is common understanding to not use uranium that high enriched to reduce the proliferation risk.

The fuel is transported to the reactor site at begin of life (BOL) and loaded into the core which is then sealed. At the end of life (EOL), there is some in-vessel cooling needed before the spent fuel can be removed by a special handling machine and transported to a central (re)processing facility (Tsuboi et al. 2012). This machine is supposed to be used for several reactor sites and is thus not permanently installed. It is not clear yet who would be the owner and operator of such machines and reprocessing facilities. Possible options are states, private companies, or international organizations such as the IAEA.

Especially when deploying a high number of SMRs, states might argue for their own equipment for refueling and reprocessing of the spent fuel. This opens the door for wide spread facilities that allow handling of items emitting strong radiation.

Many arguments in favor of the security of nuclear batteries depend on the sealing of the core to prevent unauthorized access to the nuclear material. Potential diversion is supposedly only possible to occur during refueling. This argument implicitly assumes that the integrity of the seal can be assured at all times and that for the host state an open breakout scenario is no alternative. At the same time, the wide spread of SMRs will challenge the current safeguard regime. The number of reactor sites that should be inspected would increase, and at least some of them would be sited at locations that are complicated and time-consuming to reach. It has yet to be seen, to what extent remote sensing and video monitoring, as currently under development, will be able to replace on-site inspection.

At the same time, the nuclear industry argues for less strict requirements regarding safety and security aspects for SMRs. Up to 80 % reduction in security staff is argued to be feasible, but details are not provided (Azad 2012; Lyman 2013; Ramana, Hopkins, et al. 2013). In the case of a possible deployment of the Toshiba 4S in Galena, Alaska, only four security and eight plant employees were foreseen (Bergmann et al. 2009). The fact that SMRs are likely to be placed in newcomer states with only low experience in reactor operation does not strengthen the overall security case. Weak state authorities could ease unauthorized access to nuclear material.

To assess the proliferation resistance of nuclear reactors, many aspects should be considered. In the case of the Toshiba 4S, the fact that the fuel is already enriched to nearly 20 % uranium-235 significantly reduces time and costs to produce high enriched uranium for a nuclear weapon. In particular, if the hosting country already has, even limited, enrichment capabilities the uranium is an attractive proliferation pathway. For nuclear batteries, like for most SMRs, a closed fuel cycle is envisioned in the long-term perspective. Consequently, the front and back end facilities of the fuel cycle are equally important to address.

Nonetheless, this thesis focuses on the plutonium produced in the core of a small, fast reactor. The total amount and its quality is assessed using a computer model based on the Toshiba 4S. Difficulties in processing the nuclear material are estimated calculating dose rates for the spent fuel elements. This allows an assessment of the latent proliferation risk of the special SMR type nuclear battery. How attractive is this reactor type for a state actor that would like to have at least the option to acquire nuclear weapons material?

6.2 SMR Reactor Simulation Model

A computer model of an exemplary nuclear battery is set up to perform burn-up calculations. As a starting point, the fast, small Toshiba 4S is taken. The reactor model and necessary assumptions are described in the following section. Afterwards, the simulations parameters are introduced.

6.2.1 Description of the Reactor Design

A core model of a small fast reactor was set up for depletion calculations. As far as possible, publicly available technical data for the Toshiba 4S reactor was used. This reactor has an exceptional long lifetime of 30 years without refueling and reshuffling of fuel elements and an electric output of either 10 MWe or 50 MWe (IAEA 2007, p. 395-419; Yacout 2008; Tsuboi et al. 2012). Since the main applications are seen in the smaller version, for the model this version of the reactor with an output of 10 MWe was used. The reactor core would be factory-built, transported to the site, and installed in an underground reactor building. Primary components, such as the heat exchanger, the electromagnetic pumps and the reflector, are located inside the reactor vessel. This setup is referred to as an integral or pool type reactor and is common among SMRs.

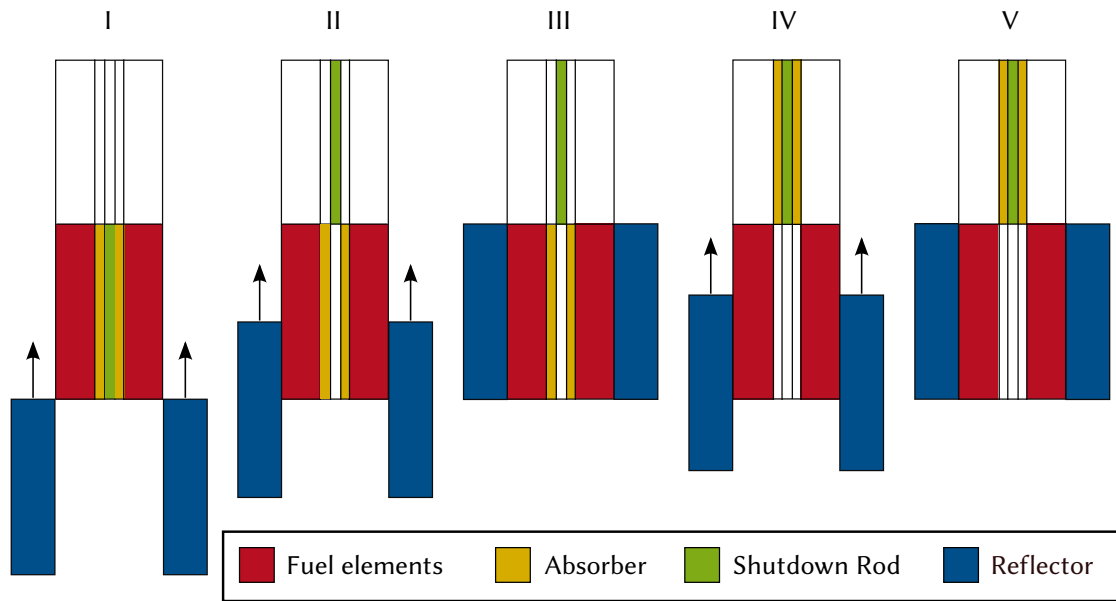


Figure 6.1.: Movement of the reflector surrounding the reactor core. Before start-up, the reflector is placed below the core. The absorber and shutdown rods are inserted (I). To reach criticality, it is moved upwards (II) and then continues its movement up to the top of the active zone (III). After 15 years, the absorber is withdrawn and the reflector falls back to a lower position (IV). From there it starts its second cycle of upward motion (V).

The long core lifetime is possible due to an adjustable, annular reflector that surrounds the core only partially and a fixed hafnium absorber in the middle of the core. Figure 6.1 shows the different configurations in detail. Before operation, the reflector is placed below the core and the shutdown rod and hafnium absorber are inserted for a sufficient margin to criticality. To start reactor operation, the reflector is lifted to approximately 100 cm and the shutdown rod is withdrawn. At this position, enough neutrons are reflected back into the core that a chain reaction can be sustained. For the following 15 years, the reflector moves continuously upwards, always covering new regions of the core. This is equivalent to adding fresh fuel to the active zone of the core. Since sodium is also a rather good neutron reflector, the volume above the reflecting steel region is filled with inert gas. This prevents that too many neutrons are reflected back into the zone which is not yet due to be burned. With a reflector top position at 175 cm, the replacement of the gas with sodium leads to a small increase in criticality from $k_{eff} = 1.028$ to $k_{eff} = 1.032$.

Hafnium as a neutron poison is particularly qualified for the use in a nuclear battery since the absorption of one neutron leads to the production of another neutron absorbing isotope. This chain continues for five reactions, thus enabling the absorber to work for 15 years (United States

Department of Energy 1993b). Afterwards, the absorber is withdrawn, the reflector falls back to the position where the reactor core barely reaches criticality and starts its second cycle of upward motion.

Originally not planned as a breeder reactor, there are considerations to modify the Toshiba 4S in a way that allows for breeding (Chihara 2010). The main change would be the enlargement of the core diameter to enable the placement of breeding blankets inside the reflector. In the lead-cooled variant of the 4S designed by the Japanese Central Research Institute of Electric Power Industry (4S-LMR for liquid metal reactor) the core diameter is already larger compared to the sodium cooled design (IAEA 2007). In this thesis, the breeder design variant is not further considered. The introduction of breeding blankets would of course lead to an increased plutonium production in the core.

Table 6.1.: Core and element design data for the small, fast reactor model.

Parameter	Unit	Value	Reference
Total Thermal Power	MW	30	(Tsuboi et al. 2012)
Enrichment of Uranium-235 @ BOL	wt%	17.0/19.9	(U.S. DoE 2014)
Total Number of Fuel Elements		18	(Tsuboi et al. 2012)
Fuel Pins per Element		169	(Tsuboi et al. 2012)
Fuel Element Pitch	cm	20.6	(IAEA 2007)
Active Core Height	cm	250	(Tsuboi et al. 2012)
Fuel Pin Diameter	cm	1.4	(Yacout 2008)
Cladding Thickness	cm	0.11	(Yacout 2008)
Pin Pitch (Center to Center)	cm	1.51	(Yacout 2008)
Element Pitch (Center to Center)	cm	0.25	(Yacout 2008)
Duct to Duct Gap	cm	0.22	(Yacout 2008)

In Figure 6.2, cross and vertical section of the reactor core are depicted. The core consists of 19 fuel elements. The central element contains the hafnium absorber and the space for the (emergency) shutdown rod. Uranium-zirconium alloy with 10 wt% zirconium is used as fuel¹. The six outermost fuel elements have a higher uranium enrichment of 19.9 % uranium-235, whereas the inner twelve elements contain only 17 % uranium-235 in their uranium fraction (Kilaru et al. 2010; NRC 2012). The inner and outer fuel elements have the same geometry. Each assembly consists of 169 fuel pins. It is surrounded by an HT9-steel duct and completely submerged in sodium. The total heavy metal inventory is 9.24 tons.

The vertical section shows that only the lower part of the fuel pins is filled with fuel. The rather high space for fission gases is needed due to the long core lifetime and the subsequent production of fission gases. The fuel pins are surrounded either by the reflecting region or by gas tanks filled with helium. Geometric dimensions for the computer model are summarized in Table 6.1.

The materials and densities as implemented in the model and their respective source are listed in Table 6.2. Isotopic compositions were derived from the Janis data base (NEA 2012b). The temperature gradient in the core is modeled using temperatures of 600 K and 900 K. For these temperatures, cross section data is readily available in VESTA. The outer steel cladding and the inlet sodium have a temperature of 600 K, while the rest of the core is considered to have 900 K. Temperature differences lead to different coolant densities, which are calculated using equation 5.1. In the following calculations a mean value for the sodium density of 0.85 g/cm³ is used, since it is shown that the influence on k_{eff} is negligible compared to calculations with different coolant

¹ Fractions can either be given in weight percent or atom percent. The more the composites differ in weight, the higher is the difference between the two values.

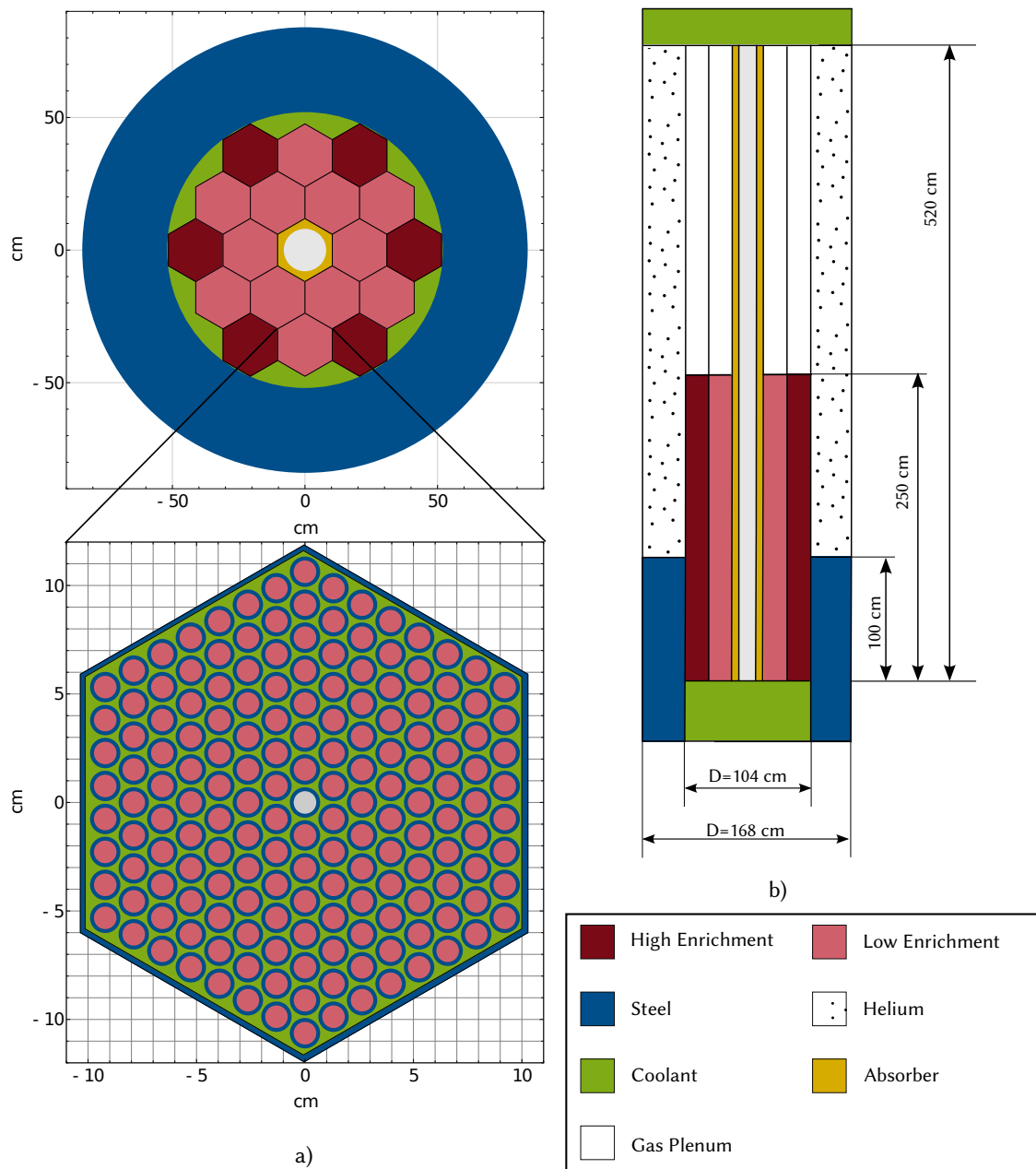


Figure 6.2.: Core layout of the small, modular reactor. (a) shows the cross section of the reactor with all 19 fuel elements and the surrounding steel reflector. One fuel element is shown as a close-up, depicting all 169 fuel pins. The inner assembly contains the hafnium absorber and the shutdown rod. The vertical section of the reactor core in (b) depicts the end of the reflecting region at 100 cm and the above placed helium tanks. The figure is adopted from Frieß, Kütt, and Englert (2015).

densities ($\Delta k \approx 0.00025$). The density of the HT9-steel is estimated using the thermal expansion coefficient of steel.

Table 6.2.: Selected material properties as used in the SMR core model.

	Material	Density in g/cm ³	Reference
Coolant	Sodium	0.87/0.83	(Rouault 2010)
Fuel	U-Zr-alloy	15.9	(Yacout 2008)
Cladding, Structure	HT9-Steel	7.8	(Brewer 2009)
Reflector	Stainless Steel	7.92	(Brewer 2009)
Absorber	Hafnium	13.31	(Tsuboi et al. 2012)
Gas	Helium	$1.8 \cdot 10^{-5}$	(Tsuboi et al. 2012)
Shutdown rod	B ₄ C	2.51	(Brewer 2009)

This model is used for all following calculations on the small modular reactor and was extensively described and validated in Fassnacht (2013).

6.2.2 Simulation Parameters

Beside the geometric model, additional data must be provided for the depletion calculation. Most important are the reflector movement and simulated time periods. The core lifetime is set to 30 years, split into time steps of one year each. Comparison runs with shorter steps and therefore more steps in total have shown no significant effect on the material compositions. In fast reactors, there is only minor xenon production, hence no shorter time step of approximately five days at BOL is necessary.

At the EOL, several depletion steps with increasing length were added. During these steps, power output of the reactor is set to zero and only natural decay is calculated. The material to calculate the dose rates from the spent fuel elements after different cooling periods can thus be easily extracted from the output files.

The core was split into ten different burn-up regions for the burn-up calculations. For each of these regions, neutron flux and material composition are constant during one depletion step. Two zones based on the fuel enrichment were defined in radial direction. To properly account for the changing reflector position and resultantly on the highly variable conditions in the different height layers of the core, each of the two radial zones has been further split into five different axial zones.

Preliminary calculations of the criticality in dependency of the reflector position show that criticality is reached when the top of the reflecting region is placed around 120 cm height. After 15 years, when the fixed hafnium absorber is withdrawn, the emerging volume is filled with sodium. The reflector falls back to a position of 157 cm. The higher position in comparison to the initial criticality position is indicated by a figure depicted in IAEA (2007). It seems reasonable because the fuel is already burnt to some degree. The reflector then moves up to its final position at 250 cm with constant velocity, even though the same figure indicates that the constant velocity assumption does not hold true. No more data on this issue could be found in the open literature.

For the simulation, the burn-up code VESTA as described in section 4.2 is used. Cross section data comes from the Joint Evaluated Fission and Fusion Data JEFF-3.1. The power output is set to 30 MWth and assumed to be constant during the complete simulation time.

6.3 Results of the SMR Simulation

Criticality of the Toshiba 4S reactor for various core configurations, e.g. with and without reflector and/or control rod, was already presented in Fassnacht (2013). Consequently, in the following

only the evolution of the neutron flux and the criticality in dependence of the reflector position are shown. The ultimate objective of the simulation is the assessment of the material attractiveness in regard to its use as nuclear weapons material. It is analyzed based on the isotopic compositions derived from the burn-up calculations.

6.3.1 Neutron Flux and Criticality

A key concept of the nuclear battery is the moving reflector. Covering only parts of the core leads to an axial neutron flux distribution that is distinct from standard nuclear power plants. At the same time, the flux distribution obviously changes more significantly during the core lifetime.

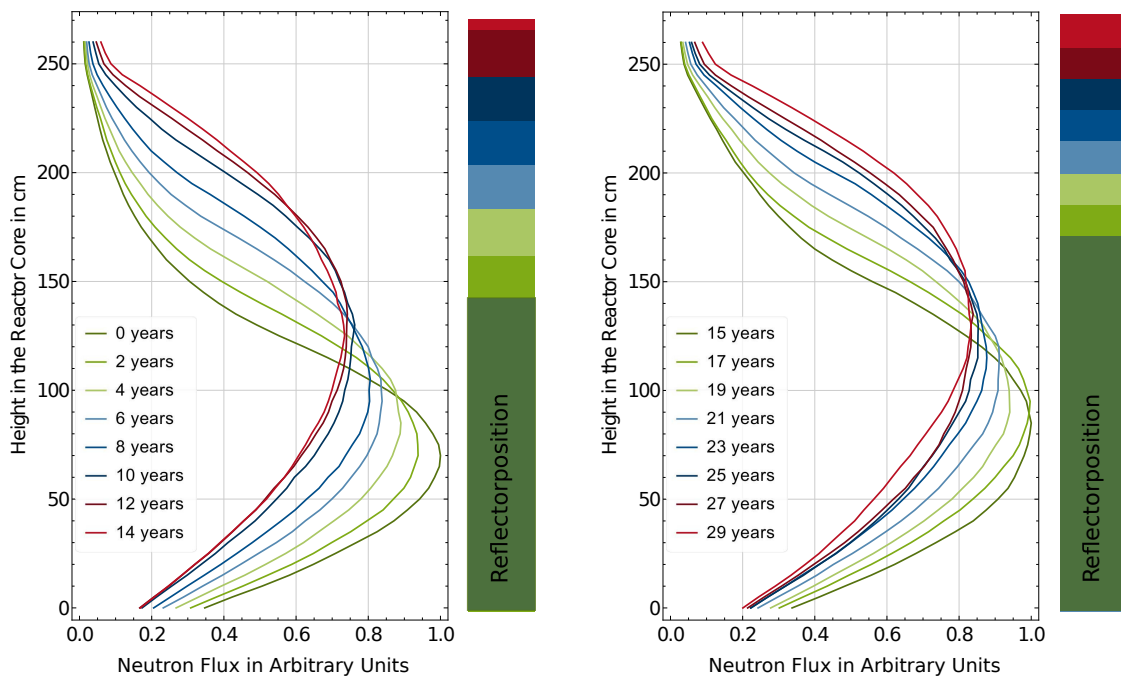


Figure 6.3.: Neutron flux distribution in axial direction in dependence from the reflector position. With increasing burn-up and subsequent higher volume fraction of the core contributing to the active zone, the profile flattens.

Figure 6.3 shows this effect. The neutron flux in axial direction is plotted in arbitrary units for different reflector positions. For easier understanding, the plot is split into two separate figures, each covering 15 years. The flux is highest in the volume surrounded by the reflecting region and declines toward the top and bottom end of the reactor. With the reflector moving upward, the flux profile flattens and a greater fraction of the reactor contributes to the power generation. For the depletion calculations, the thermal power output is set to the constant value of 30 MW. The neutron flux is normalized to cause a sufficiently high number of fission to produce the target thermal power. As a result, the area under the graphs showing the neutron flux is not supposed to be constant during the lifetime of the reactor core.

The flux profile in general is more flattened in the axial direction in the second half of the reactor operation time. To account for the irradiated fuel, the reflector top already starts at a higher position and the active volume is increased. The higher position of the reflector top after the first 15 years of operation is also seen in Figure 6.4. It depicts the criticality and the reflector position over the lifetime of the core. The reflector top starts at 157 cm for its second movement upwards. This value is chosen to match Figure XIV-5 in IAEA (2007, p. 403). There it is also stated, that the reflector moves in order to keep neutron multiplication factor in the core as constant as possible.

For the simulation, however, a constant velocity is assumed. For the second half of the lifetime, this results in nearly constant k_{eff} . It seems that the starting position of 157 cm was chosen too high. After the withdrawal of the absorber, a lower reflector position would have been sufficient to reach criticality. The leap in criticality is of only minor concern, because for the depletion calculations the neutron flux is scaled according to the predefined power output. This not true for safety calculations, because they must include for example change in coolant temperature or density which is directly connected to the actual number of fissions in the core. In general, the reactor model shows the expected behavior. It can thus be used for assessment of the material build-up in a small fast reactor as done in the following section.

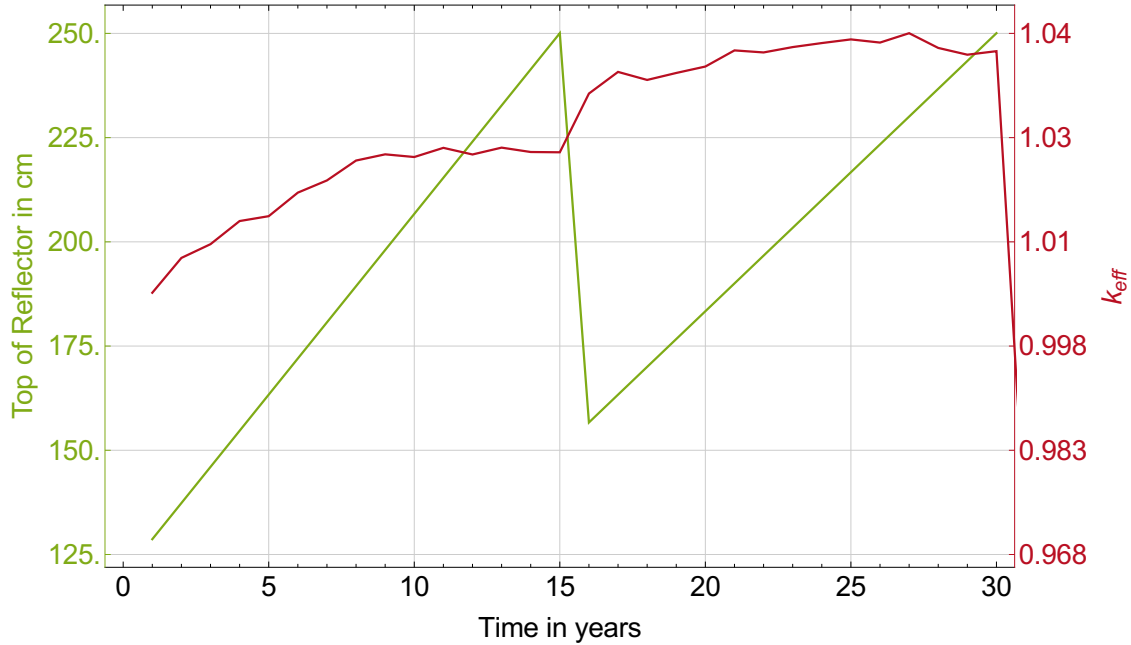


Figure 6.4.: Criticality and reflector position during 30 years of operation time. Due to the simulation method, the quasi instantaneous fall of the reflector for the second 15 years and at EOL is not plotted correctly. For the same reason, the value for k_{eff} at EOL is missing.

6.3.2 Material Attractiveness

The core of the Toshiba 4S contains uranium that can just barely be considered to be low enriched uranium. Nevertheless, this thesis focuses on the plutonium production in the core. The plutonium production is one crucial factor for the assessment of the proliferation risk. Different criteria are of interest. First, the overall build-up of plutonium in the core and its isotopic composition are analyzed. Beside the suitability of the material for nuclear weapons, for a possible proliferator the complications associated with its handling are of interest. This includes the overall material that has to be diverted to gain at least one significant quantity as well as the obstacles associated with handling and processing the material. These aspects are mirrored by the plutonium content per fuel assembly, the dose rate emitted by one fuel assembly, and the Figures of Merit. The Figures of Merit are a condensed value for material attractiveness assuming access to processing facilities.

The continuous increase in plutonium and fission products concentration in the reactor core is shown in Figure 6.5. Clearly, all values start at zero, but increase almost linearly until the target burn-up at EOL of about 35 MWd/kgHM is reached. The fission product inventory accumulates up to 40 kg per ton heavy metal at EOL. For the plot, the amount of the cladding material zirconium is

subtracted from the total zirconium inventory because the zirconium alloy cladding is naturally present in the core from the beginning.

At EOL, the net plutonium content is about 18 kg per ton heavy metal. It consists mainly of plutonium-239. The plutonium content in a typical light water reactor with a comparable burn-up of 40 MWd/kgHM is about 9 kg per ton heavy metal, but with a far lower plutonium-239 fraction (Albright et al. 1993, p. 76). In a thermal reactor, neutron absorption is more likely to lead to a larger fraction of higher plutonium isotopes, such as plutonium-240. For comparison: irradiation times should not exceed eight months for acquisition of material with a plutonium-239 fraction of more than 90 % from a light water reactor. The net plutonium content would be only about 2 kg per ton heavy metal inventory after this irradiation time (Gilinsky et al. 2004).

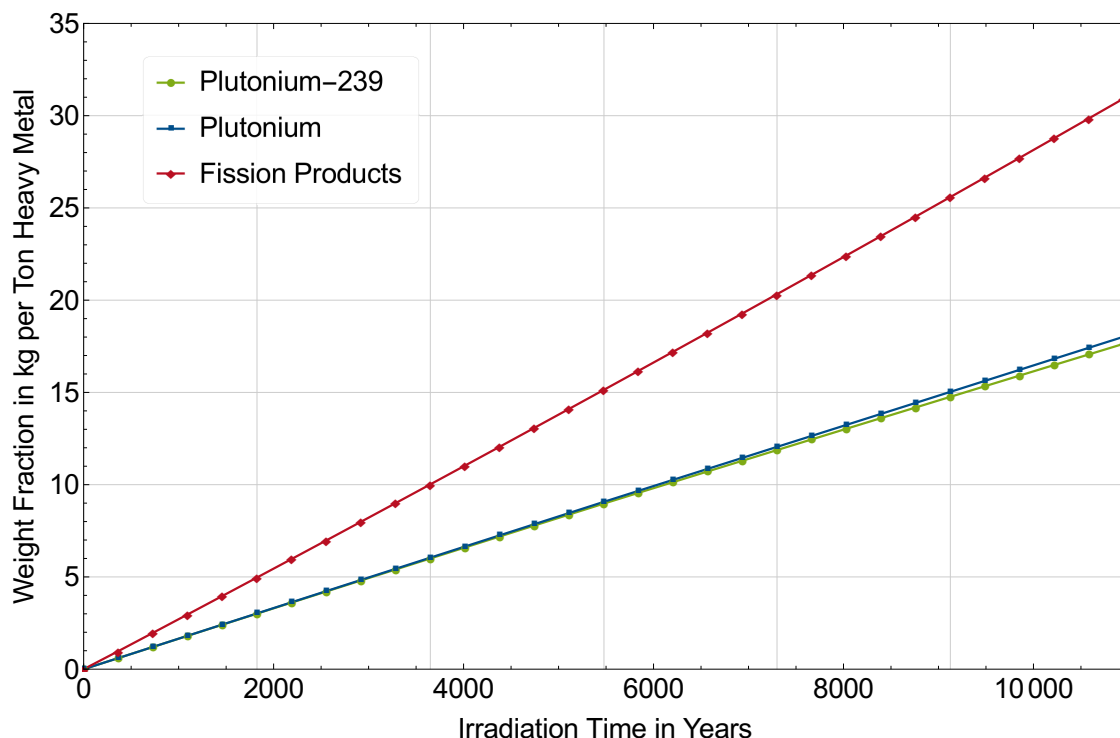


Figure 6.5.: Weight fraction of plutonium-239, the overall plutonium vector, and fission products in the reactor core. At EOL, the net plutonium content per ton heavy metal is about twice as high as in a light water reactor and comprises almost exclusively plutonium-239.

The evolution of the plutonium vector and the total plutonium content in the core is shown in Table 6.3 for selected irradiation times. It takes only two years for the core to produce one significant quantity of plutonium. The plutonium is super-grade at all times. It contains a plutonium-239 fraction of more than 97 %, even though with decreasing fraction.

After 30 years, the core contains about 160 kg plutonium. This value is comparable to a published value of 150 kg for the Toshiba 4S (IAEA 2007). In general, there is hardly any comprehensive information on the plutonium vector in the core. The calculations presented here show that after the full operation time, one fuel assembly alone contains more than one significant quantity of super-grade plutonium. Hence, the diversion of one fuel element during refueling would be sufficient for a potential adversary to acquire enough nuclear material for one nuclear weapon.

The dose rate emitted from the spent fuel elements is a main barrier to acquire the fissile material after discharge from the core. Figure 6.6 shows the gamma dose rates for different irradiation times and cooling periods.

The values differ from the values published in Frieß, Kütt, and Englert (2015) due to corrections in the calculation method. In the original analysis, a combination of F2 tallies measuring the flux

Table 6.3.: The plutonium content and the isotopic composition of the total plutonium vector in weight percent.

	Pu-238	Pu-239	Pu-240	Pu-241	Pu-241	Pu content
2 years	0.01	99.83	0.16	<0.005	<0.005	11 kg
15 years	0.04	98.97	0.99	0.01	<0.005	82 kg
30 years	0.09	97.91	1.97	0.02	<0.005	159 kg

through a surface was used for assessing the gamma flux in one meter distance from the surface of the fuel elements. For normalization of the values it has been falsely assumed, that MCNPX returns the average and not the cumulative value for a combination of F2 tallies. Therefore, the calculated values for the dose rates are too low. The revised values use F5 tallies as explained in section 4.4. All isotopes from the VESTA output files and not only the selection forwarded by VESTA to the MCNP input files are used for the spent fuel composition.

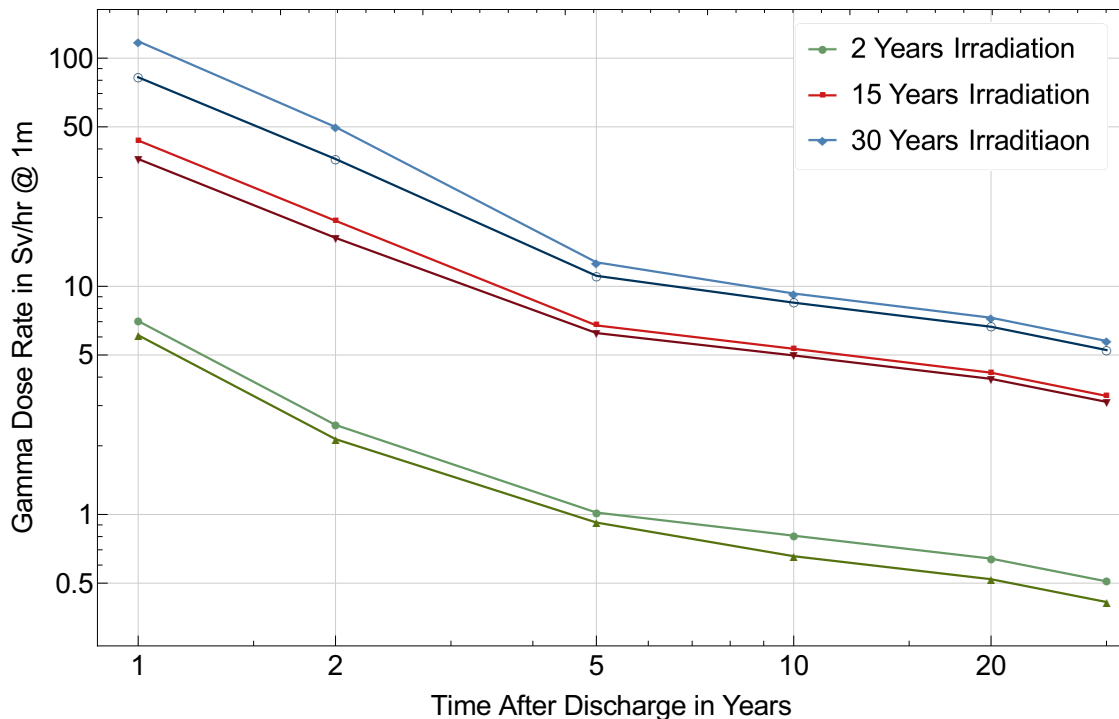


Figure 6.6.: Ambient dose rates at one meter distance emitted by spent fuel elements in dependence of the cooling period. Fuel elements with the full irradiation time of 30 years emit the highest dose rates while fuel elements removed after only two years show the lowest values. Elements from the outer fuel zone containing more uranium-235 are shown in the darker color.

The elements from the inner zone of the reactor contain more fission products than the elements from the periphery due to the higher neutron flux. Consequently, the dose rates from the inner elements are always higher than from the outer elements. The difference is very small compared to the influence of the irradiation time on the dose rate. In the first few years after removal, the dose rate declines rapidly. If the fuel elements are irradiated in the core for only two years, it takes the ambient dose rate about five years to decline to a value of 1 Sv/hr. Below this value, the elements cannot be considered to be self-protecting anymore. This lies within the range of on-site cooling of spent fuel elements as done for elements from conventional nuclear power reactors. Since more

fission products are generated for longer irradiation times, the fuel elements remaining for 15 or 30 years in the core fulfill the limit usually seen as a part of the spent fuel standard. They emit more than 1 Sv/hr 30 after discharge from the reactor core.

Table 6.4.: Relevant parameters of one fuel element with 17 % uranium-235 enrichment that are connected to material attractiveness.

Time	Pu Content kg	Dose Rate Sv/hr	FOM_1 -	FOM_2 -
2 years, 5 year cooling	0.6	1.0	2.8	2.7
2 years, 30 year cooling		0.5		
15 years, 5 year cooling	4.6	19	2.8	2.5
15 years, 30 year cooling		3.3		
30 years, 5 year cooling	8.8	50	2.7	2.3
30 years, 30 year cooling		5.8		

Table 6.4 summarizes dose rates and other relevant parameters to assess the material produced in one fuel element. After 30 years of cooling, even the elements irradiated for the full time show dose rates close to the limit of 5 Sv/hr. This higher limits apply for the case of an proliferator who is willing to sacrifice his life. It should be noted that only one fuel element contains enough highly attractive weapons material for one warhead then.

While the dose rates from spent fuel elements are only relevant as long as the material has not been processed, the Figures of Merit focus on the transuranium elements that could have been extracted from the original spent fuel. Due to the long half-lives of the transuranium elements, the $FOMs$ do not change over the considered time period. The values for the exemplary fuel element are given in Table 6.4. According to this classification, the material has to be considered to be highly attractive ($FOMs$ greater than two) for all conditions. The neutrons from spontaneous fission do not influence the attractiveness. Even for an adversary lacking the capability to cope with possible pre-ignition of its nuclear device, the material remains highly attractive.

6.4 Summary

Small modular reactors with a long core lifetime, also called nuclear batteries, are claimed to be more proliferation resistant than thermal SMRs based on LWR technology. In the previous sections, an exemplary model of such a reactor based on the Toshiba 4S is set up to analyze the attractiveness of the nuclear material produced in the core. This reactor has an energy output of 10 MWe and the core is planned to remain sealed for the total core lifetime of 30 years.

The burn-up calculations show a plutonium production rate of more than 5 kg per year. At EOL, each of the fuel elements contains more than one significant quantity (8 kg) of plutonium. The net plutonium content is about 18 kg per ton heavy metal inventory, roughly twice the amount of the content in light water reactors at a comparable burn-up of 40 MWd/kgHM.

Unlike the plutonium contained in typical spent fuel from light water reactors, the isotopic composition consists almost exclusively of plutonium-239. The perfect usability of that nuclear material for building a nuclear device is also mirrored by the calculated Figures of Merit that assign the material to be highly attractive. The main obstacle for reprocessing are the dose rates of the spent fuel elements. In most cases, the gamma dose rates are high enough to qualify the elements to be called self-protecting. Potential implications are discussed in more detail in chapter 8.



7 Partitioning and Transmutation Fuel Cycle

The incineration of minor actinides in fast reactors to get less radiotoxic high level waste finally sent into the deep geological repository is seen as one option to solve the nuclear waste problem. Looking at this endeavor more closely, several discrepancies and open questions arise: Can the same plutonium be used for several cycles of irradiation? How do the characteristics of spent P&T-fuel elements behave compared to light water reactor spent fuel elements? Besides these and other technological questions, what about possible production of nuclear weapons material? And if all these problems can be actually solved, does the transmutation of only minor actinides really have the claimed positive effects? The latter concerns in particular the generation of long-lived fission products.

The objective of this chapter is to address at least some of these questions. Exemplary fast reactor systems are modeled to analyze the potential of minor actinide transmutation. Since the underlying concept, namely the fission of fissile material in a neutron spectrum, is obvious, other aspects were investigated more closely.

A short introduction into the history of partitioning and transmutation in Europe is presented in section 7.1. The geometric computer models of the two different accelerator-driven systems, MYRRHA and EFIT, that were set up for computer simulation are described in section 7.2.

Since for the most part the EFIT reactor is in the early design stage, information on the reactor and how it is supposed to be operated is scarce. With the data available, it did not seem suitable to perform burn-up calculations. Thus, this type of calculation was only conducted for the MYRRHA reactor for which more design information is available. The behavior of some EFIT-like fuel elements was simulated irradiating them at special positions in the MYRRHA core. The evolution of the isotopic composition within these fuel elements over the time is derived. From that, statements on the possible transmutation and the build-up of fission products in a potential EFIT environment can be made. To show the viability of this approach, the neutron flux distribution in both the freshly fueled EFIT core and the MYRRHA core are compared to each other in section 7.3. Some other validation calculations for the computer models are also discussed there.

The following sections grant a closer look at three specific aspects of a potential partitioning and transmutation fuel cycle. The first one is the impact of different fuel compositions on the criticality of the system: using actinides from spent fuel elements for fuel fabrication impacts the criticality of the fresh fuel. Until now, plutonium from spent fuel was mostly used a second time in MOX fuel. Section 7.4 shows the effect of different irradiation histories on the neutron multiplication factor. When possible fuel cycle implementations are discussed, it is often quietly assumed that the spent P&T-fuel elements show the same characteristics as conventional spent light water reactor fuel elements. Therefore, the activity, the residual heat, and the gamma dose rates for spent P&T-fuel elements are calculated in section 7.5.

Finally, the benefit of the sole transmutation of minor actinides is challenged by looking at the generation of long-lived isotopes. Certain long-lived fission products are responsible for most of the dose rate originating from deep geological repositories. Their build-up is discussed in section 7.6. Section 7.7 concludes the chapter with a summary of the results.

The proliferation risk associated with a P&T fuel cycle is not discussed in greater detail in this thesis. The risk of closed fuel cycles is well known (Hartigan et al. 2015; IPFM 2015b). Moreover, it speaks volumes that calculations showing the possible plutonium production in the MYRRHA core are classified (Rossa 2011).

7.1 The History of Accelerator-Driven Systems in Europe

The idea of an accelerator-driven system to incinerate some of the nuclides contained in nuclear waste became prominent in Europe in the mid-1990s (Rubbia et al. 1995). Within its 5th and 6th Framework Programme, the European Union gave funding for the basic design of a lead-bismuth cooled accelerator-driven system starting in 1998. The result was the eXperimentaL-ADS (XT-ADS) design with a power output of 57 MWth (Bruyn et al. 2013). Based on this reactor model, in the 7th Framework Programme a central design team for a Fast Spectrum Transmutation Experimental Facility (FASTEF) was established (Di Maria et al. 2012). The leading efforts were taken by the Belgian Nuclear Research Center SCK·CEN. Belgium had been working on their own design of a multipurpose R&D facility for more than ten years by then (Abderrahim, Kupschus, et al. 2001). The Multi-purpose hYbrid Research Reactor for High-tech Applications (MYRRHA) is the Belgian research reactor currently under development (Abderrahim 2013). MYRRHA is called a hybrid reactor because critical and sub-critical core layouts exist. The reactor system is supposed to be operated in both configurations. Its predecessor was the ADONIS project which was the first project researching the coupling of accelerator, spallation target, and sub-critical core (ibid.). MYRRHA is planned to fit into the European strategy to develop an accelerator-driven system demonstration facility as a proof of concept of a sub-critical system driven by a spallation source in the middle of the core.

Consequently, the MYRRHA and FASTEF design projects are tightly connected to each other. The FASTEF core is equivalent to the MYRRHA sub-critical core configuration at a power level of 100 MWth. Yet, first loadings of MYRRHA will not be able to operate at such a high level due to lacking materials that qualify for the high temperatures (Sarotto 2012).

In 2013, developers still claimed that operation of the MYRRHA facility could be starting in 2024 (Bruyn et al. 2013; Sarotto et al. 2013). By now, the project seems stalled. The official homepage still states that construction is planned for the period 2017-2021 (SCK-CEN 2017). The same homepage also states that MYRRHA is designed to replace the old research reactor BR2 which has been in operation since 1962. In 2016, the Ministerial Statement of Belgium at the *IAEA International Conference on Nuclear Security: Commitments and Actions* stressed its efforts toward the conversion of the BR2 to low enriched uranium fuel (Belgium 2016a). This conversion requires efforts that do not indicate that the BR2 reactor will be replaced any time soon. In its general statement at the NPT Preparatory Committee 2017, Belgium, however, noted that for the MYRRHA design, "*particular attention [...] given to the transmutation of long-lived radioactive waste*" (Belgium 2016b).

It is claimed that the Lead-Cooled European Facility for Industrial-Scale Transmutation (EFIT) is the first design for an accelerator-driven system that has been designed up to a rather detailed engineering level (Mansani et al. 2012). Nevertheless, there are still several design choices to be made. Deployment is foreseen somewhere around 2040. There are still major uncertainties that have to be resolved, for example the large dimension of the spallation source, leading to very low source efficiencies (Artioli et al. 2007). Since the design of the EFIT reactor is supposed to be based on the experience gained by the operation of MYRRHA/FASTEF core, it seems most likely that its design, building and operation schedules will be postponed as well.

EFIT is developed in the frame of the European EUROTRANS¹ Integral Project in the 6th Framework Programme (Mansani et al. 2012). From 2006 to 2008, the European Union founded a project now called the Partitioning and Transmutation European Roadmap for Sustainable Nuclear Energy (PATEROS) (Martínez-Val et al. 2008). It "*was aimed at establishing a European Vision for the Deployment of Partitioning and Transmutation of Nuclear Waste, up to the level of industrial implementation*" (ibid., p. 2). Unlike France, which sees its future ASTRID breeder reactor as the reference system for the treatment of radioactive waste (CEA Nuclear Energy Division 2012), the

¹ EUROTRANS stands for EUROpean Research Programme for the TRANSmutation of nuclear waste.

EU's plans on minor actinide transmutation focus on accelerator-driven systems. In the PATEROS studies, the EFIT reactor is used as the reference accelerator-driven system.

During PATEROS, possible scenarios for the implementation of a P&T fuel cycle were analyzed. All scenarios are based on different groups of countries:

- Group A countries only want to manage their spent fuel because they are in a stagnant or phase-out scenario.
- Group B countries continue to use nuclear energy and want to optimize its use of plutonium.

Only scenarios using accelerator-driven systems are relevant for this thesis. These scenarios differ in regard to the use of the plutonium coming from the transmutation facilities: it is either immediately used in a LWR fleet or stored until the capacity of the fast reactor fleet is sufficiently high (Salvatores et al. 2008). Only regional implementations of a P&T fuel cycle were considered within the frame of PATEROS. In this context, regional means that there exist specialized ADS facilities for the transmutation of the minor actinides coming from the spent fuel from Group A and Group B countries. All facilities associated with transmutation, such as the ADS, the reprocessing and fuel fabrication facilities, are shared between the partner states. As a contrast, in a national scenario all facilities are operated by one state without international partnerships. The objectives of a regional P&T scenario are, among others, the decrease of the spent fuel stock within a century for the group A countries and the stabilization of the minor actinide inventory for the group B countries. It is noteworthy that only France is considered to be a Group B country in the PATEROS regional scenario studies (ibid, p. 11).

The EFIT and the MYRRHA reactor core are used in this thesis to assess selected aspects of a partitioning and transmutation fuel cycle. This does not mean that there are no other R&D efforts in regard to transmutation of nuclear waste underway. Research is for example conducted in France, China, or Japan (IAEA 2015; IPFM 2015a).

7.2 Accelerator-Driven System Reactor Models

To simulate the neutronic behavior in the reactor core and perform burn-up calculations to assess the material composition, detailed computer models have to be set up. Information for modeling is taken from the open literature when possible. Because the reactors have not been built yet, there often exists contradictory information on certain aspects. Thus, strictly speaking, neither the MYRRHA reactor nor the EFIT reactor are modeled but generic accelerator-driven systems based on the MYRRHA and EFIT design. Where data was missing or unclear, estimations and assumptions had to be made to fill the gaps.

7.2.1 The MYRRHA Reactor Model

Since MYRRHA is designed to operate both in critical and sub-critical configurations, both layouts were set up. The main difference between the two configurations is the plutonium enrichment in the fuel and the total number of fuel elements in the reactor: while for the fuel in the critical core a plutonium content of 34.5% is planned, the fuel contains a maximum of 30 % plutonium in the sub-critical core configuration. The critical core consists of 69 fuel elements in equilibrium state, with six control rods at the periphery. For the sub-critical core configuration, the control rods are planned to be moved further outwards and they would only be used during the refueling process. The sub-critical core contains between 58 and 72 fuel elements (Sarotto et al. 2013).

At an early stage of a new computer model, there are usually several flaws that must be corrected. To do so, the criticality and neutrons flux of the critical core were calculated. The criticality and the criticality worth of the control rods are in good accordance with expected values for a

typical reactor. The energy spectrum of the neutron flux shows the distribution expected in a fast reactor core. The critical layout could also be used for transmutation, but with the limitations mentioned in section 1.3: only a small fraction of minor actinides in the fuel is possible due to safety considerations. Thus the focus of this thesis is set to the sub-critical core, whose layout is described in the following.

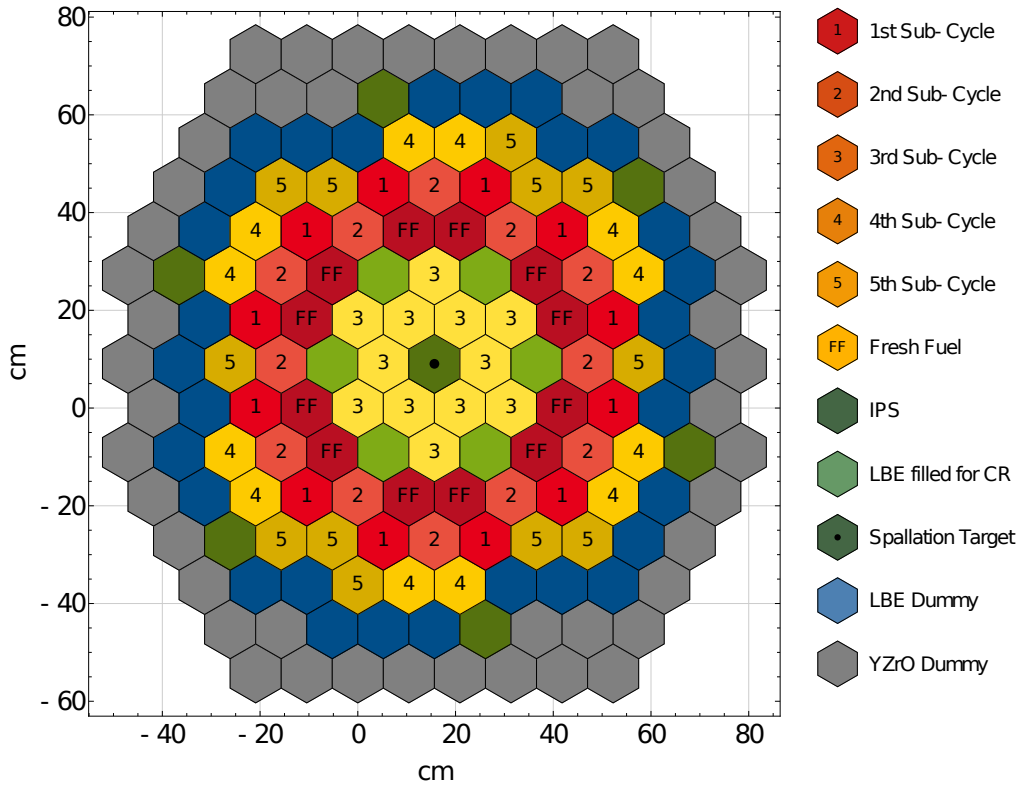


Figure 7.1.: Core layout of the MYRRHA core for the equilibrium sub-cycle. Control rods (CR) are not inserted but filled with coolant. The in-pile test sections (IPS) are filled with either coolant or EFIT-like fuel elements.

At begin of life (BOL), the sub-critical core consists of only 58 fuel elements to account for the higher reactivity of a core completely filled with fresh fuel. This number will subsequently be increased until the reactor reaches equilibrium mode with 72 fuel elements. Figure 7.1 depicts a cross section of the MYRRHA ADS equilibrium core model.

There are six different fuel zones in the core which designate the different batches. After each sub-cycle of 90 days, elements from the outer perimeter of the core that have been irradiated for a full cycle are removed from the core (depicted as '5' in Figure 7.1). All other elements are shuffled to the fuel zone with the next higher number. The then freed positions are filled with fresh fuel elements ('FF' in Figure 7.1) and the other elements are shuffled to the next fuel zone. After one complete cycle consisting of six sub-cycles, all fuel elements are replaced by fresh fuel elements. One cycle subsequently consists of 540 full power days (FPD) or 840 days including shutdown periods. Unlike at BOL, where all elements comprise fresh fuel, at begin of cycle (BOC), only one batch contains fresh fuel. Plutonium enrichment and fuel composition is the same for all batches when they are loaded into the core (Sarotto et al. 2013).

The six in-pile test sections (IPS) planned in the center of the MYRRHA core can be used for various experiments. Otherwise, they are filled with coolant. For the depletion calculations, only two IPS are replaced by the transmutation fuel elements. Their insertion into the core adds too much positive reactivity to replace all six IPS, with all IPS filled the core would be critical. In the transmutation fuel element, a fuel pin design is used as envisioned for the European Industrial

Sized Transmutation Facility (EFIT) and described in the following section. The number of pins per fuel element was reduced to fit into the smaller assembly geometry of the model based on the MYRRHA geometry. These elements are called EFIT-like fuel elements in the following.

The core is surrounded by dummy elements filled with lead-bismuth eutectic (LBE) and reflector elements consisting of yttrium-stabilized zirconium (YZrO). Reflector elements help to flatten the power profile and thus to increase the total power without raising the maximum power (United States Department of Energy 1993b, p. 118). In the sub-critical core configuration, the control rods (CR) function as six absorbing devices that can be inserted in case of refueling to ensure a sufficiently high level of negative reactivity. When not in use, these elements are filled with coolant as well.

Table 7.1.: Geometric dimensions of the MYRRHA computer model. The number of fuel elements is given at BOL and BOC. The center pin in each assembly is a structure pin. The values are taken from Sarotto (2012) and Sarotto et al. (2013).

Parameter	Unit	Value
Number of Fuel Elements	-	58/72
Number of Fuel Pins per Element	-	126+1
Radius of Fuel Pin	cm	0.271
Active Height	cm	60
Cladding Thickness	cm	0.045
Fuel Assembly Pitch	cm	10.45
Can Thickness	cm	0.2
Can Inner Diameter	cm	9.755

Each MYRRHA fuel element consists of 126 fuel pins and one structure pin. The active height of the core is 60 cm. The exact geometric dimensions are listed in Table 7.1. The zones above and below the active zone consist of a steel cap, a helium plenum to account for fission gases, and a reflector. The center assembly hosts the spallation target. The discussion in the literature is unspecific on whether to use a design with or without a window. Since this choice mostly influences material stress, a simple windowless design was implemented in the model.

The spallation source consists of a proton beam with 600 MeV energy and a maximum beam intensity of 4 mA. The beam has a "*donut-shaped*" footprint on the spallation target. The inner and outer diameter are 5 cm and 10 cm (Mansani et al. 2012; SCK-CEN 2016). Sweeping of the beam on the target was not modeled since material stress limits in the spallation target or elsewhere in the reactor core are beyond the scope of this work. The exact position of the spallation target could not be found in the literature. Only rather general statements are published on the fact that the position of the target is optimized in order to achieve the highest possible neutron yield. A set of calculations with different target positions was performed to optimize the position in the model (see section 7.3.2). From this set of calculations, the optimum position for the top of the spallation target was estimated to be 20 cm below the upper end of the active region in the core.

Lead-bismuth eutectic (LBE) is used as coolant and target material. The chemical activity of LBE is lower than that of sodium while at the same time the neutron spectrum is harder in an LBE cooled core. This benefits the transmutation of minor actinides (Tsujimoto et al. 2004). Disadvantages are the generation of polonium and, as for all liquid metal coolants, the opaqueness of the material. The opaqueness impedes easy assessment of the conditions in the core, for example during refueling.

The coolant inlet and outlet temperature is referenced as 270 °C and 410 °C respectively (Leysen 2012; Abderrahim 2013). This results in an average coolant temperature of 340 °C. According

Table 7.2.: Selected material properties used in the MYRRHA model. The temperatures are listed as chosen for the simulation.

	Material	Density in g/cm ³	Temperature
MOX	(U-PU)O ₂	10.27 g/cm ³ (96%TD)	1500 K
Transmutation Fuel	(Pu-MA)MgO	6.27 g/cm ³ (95%TD)	1500 K
Spallation Target	LBE	10.3 g/cm ³	600 K
Coolant	LBE	10.3 g/cm ³	600 K
Structure	SS T-91	7.66 g/cm ³	600 K
Absorber Material	B ₄ C (90% enrich.)	2.52 g/cm ³	600 K
Reflector	YZrO	6.05 g/cm ³	600 K
Gas Plenum	He	0.000325 g/cm ³	600 K

to Stankus et al. (2008), the density function for LBE in dependence of temperature T in Kelvin yields

$$\rho_{LBE}(T) = (11136.77 - 1.69728T + 0.45496T^2 + 0.12290 \cdot 10^{-6}T^3) \text{ kg/m}^3. \quad (7.1)$$

With the average coolant temperatures in the MYRRHA reactor, the density for the LBE coolant is 10.3 g/cm³. Table 7.2 lists the materials, densities and simulation temperatures for all materials except the fuel. Lead-bismuth eutectic consists of 44.5 wt% lead and 55.5 wt% bismuth (Sobolev and Benamati 2007).

Different references list different steels for the cladding of the fuel pins, structure, and other parts of the reactor core. This is because existing steels are not able to endure the harsh conditions in the core for the complete planned irradiation period of three years. The limiting factor is the exposure to the high energy neutron flux in a fast neutron spectrum. More enduring steels are still under development. Some references list the to planned materials while others list the currently available materials. Improved steel characteristics include higher resistance to embrittlement, clad corrosion, erosion, and oxide precipitations.

In the model, ferritic martensitic steel T-91 (also referred to as stainless steel t-91, or T91) is used for all steel parts. This follows the recommendation of the NEA report on fuels and materials for transmutation for cladding materials in LBE-cooled reactors (NEA 2005, p. 124). The material composition is derived from Auger et al. (2004). The density at room temperature (20°C) is 7.76 g/cm³ and the thermal expansion coefficients for T-91² are given in ThyssenKrupp Materials (2011). Accordingly, the steel density at coolant temperature is estimated to be 7.66 g/cm³. The cladding surface temperature is still a design problem in the MYRRHA reactor, since the cladding materials to achieve full power output of 100 MWth are not sufficiently developed yet. In the simulation, all temperatures except for the fuel are set to 600 K. For this temperature, reaction cross sections are tabled in the used JEFF-3.1 cross section libraries³. The same holds true for 1500 K cross section used for the fuel.

For the absorber rods, boron carbide with an enrichment of 90% boron-11 is used (Bruyn 2012; Sarotto et al. 2013). The density is set to 2.52 g/cm³ and it is assumed to be temperature independent in the considered range (AZOM 2015). Natural helium has a density of 0.000325 g/cm³ (Uyttenhove et al. 2011; McCarty 1972, p. 61). The reflector elements have the same geometry as the fuel elements, but they are filled with yttrium stabilized zirconium pellets instead of fuel pellets

² The linear thermal expansion coefficient in 10⁻⁶ per Kelvin is 12.9 between 20°C and 300°C and 13.5 between 20°C and 400°C. The density is calculated using the value for 300°C.

³ Joint Evaluated Fission and Fusion File Library, Nuclear Energy Agency. If cross sections at other temperatures are required by the input file, MCNPX interpolates the appropriate cross sections from the tabled values. Consequently, giving exact temperature in the input file leads to errors in the cross sections as well.

(Sobolev 2005; Abderrahim 2013). This material consists of $\text{ZrO}_2 + 3\%\text{Y}_2\text{O}_3$ and is commercially available (Schlichting et al. 2001). The density for the sintered material is 6.05 g/cm^3 (Tosoh Corp 2017).

For MYRRHA, the operation is planned using conventional mixed-oxide (MOX) fuel with natural uranium. The plutonium vector is derived from a pressurized water reactor at a burn-up of 45 MW/kgHM and after a cooling period of 50 years. For the simulations, a standardized reactor-grade plutonium vector as given in Table 5.4 is used. It is based on the composition in NEA (1995, p. 77). Many countries think about the double-strata approach (cf. section 1.3) to deal with their legacy of nuclear energy production, the radioactive waste. Hence, it is reasonable to use a plutonium vector as present in today's accumulated spent fuel with a comparably low burn-up. To account for the time since discharge and the subsequent generation of americium, a certain amount of americium-241 that is produced by beta decay of plutonium-241 (half-life = 14.3 years) is added to the composition (Sarotto et al. 2013).

The plutonium and americium content was set to 30 % combined for the sub-critical core configuration, whereas for the critical core the enrichment in plutonium and americium is 34 %. Fuel temperature is 1470 K (Sarotto 2012). The theoretical density of MOX fuel at a temperature T (in Kelvin) and the plutonium fraction y can be calculated as follows (Uffelen et al. 2010, p. 10; IAEA 2008, p. 25):

$$\rho_{\text{mox}}(T, y) = \rho_{\text{mox}}(273 \text{ K}, y) (L(273 \text{ K})/L(T))^3, \quad (7.2)$$

using the thermal expansion coefficient

$$L(T) = L(273 \text{ K}) (0.99672 + 1.179 \cdot 10^{-5} T - 2.429 \cdot 10^{-9} T^2 + 1.219 \cdot 10^{-12} T^3) \quad (7.3)$$

for a temperature between 923 K and 3110 K and the density at room temperature of

$$\rho_{\text{mox}}(273 \text{ K}, y) = (10.963 + 0.497y). \quad (7.4)$$

The smeared density was set to 0.96 of the theoretical density⁴. This is a rather high value but lies within the limits of a typical fast reactor system (Popov et al. 2000). The equation yields a fuel density of 10.27 g/cm^3 .

The chosen value for the smeared density contradicts the published information that the MYRRHA fuel pins are designed to be very similar to the (Super)Phénix fuel pins to ease the fuel qualification process (Sobolev 2005; Sarotto et al. 2013). For the Phénix and Superphénix fuel pins, a smeared density of only 82 % and 88 % of the theoretical density is reported in Rouault (2010) and IAEA (2006, p. 57). The density supposed to be used in MYRRHA cannot be deduced from publicly available information, maybe due to the unfinished design of the reactor core. The statement that even with a density of 10.55 g/cm^3 , the criticality of the MYRRHA core is still too low can be found in Sobolev (2005). There are also suggestions to increase the plutonium content at least for the critical core layout due to its comparably low criticality in Sarotto et al. (2013).

The maximum fuel temperature is 1473 K (ibid.). Since the depletion code VESTA requires exact matching of the temperatures of the burn materials and available cross sections, the temperature was set to 1500 K.

To efficiently transmute minor actinides homogeneously spread in the fuel, it is inevitable to increase their content in the initial composition⁵. For the MYRRHA reactor, no operation using

⁴ In the sintering process of fuel pellet fabrication, it is not possible to reach 100% of the theoretical density. There is always some porosity in the material. This is also necessary to allow some space for the fission products which are not as dense as the heavy metal fuel.

⁵ There is also the possibility to use heterogeneous recycling. In this case, there are special elements containing only the minor actinides placed in the periphery of the core. Heterogeneous recycling requires additional driver

Table 7.3.: The minor actinide vector used in the simulation for MOX and P&T-fuel (EFIT-like fuel) in weight percent. Plutonium is originating from spent LWR fuel. For P&T-fuel, the uranium matrix is replaced by an inert MgO matrix.

Isotope	Conventional MOX	P&T-Fuel
Plutonium-238	1.77	1.73
Plutonium-239	58.04	21.34
Plutonium-240	22.63	15.63
Plutonium-241	12.00	1.75
Plutonium-242	3.94	5.38
Plutonium-244	-	$4.5 \cdot 10^{-4}$
Americium-241	1.62	40.93
Americium-242m	-	0.14
Americium-243	-	8.63
Neptunium-237	-	2.1
Curium-243	-	0.04
Curium-244	-	1.61
Curium-245	-	0.61
Curium-246	-	0.05
Curium-247	-	$1.05 \cdot 10^{-5}$

minor actinide rich fuel is planned. To analyze possible transmutation, the fuel composition proposed for the European Industrial Sized Transmutation Facility (EFIT) is used in the IPS of the MYRRHA model (Mansani et al. 2012; Artioli et al. 2007). Table 7.3 shows the isotopic composition. To avoid further plutonium breeding from uranium, magnesium oxide instead of uranium is used as a matrix almost inert to the neutron flux in the core. The fuel pin is described in more detail in the following section. The number of fuel pins per fuel assembly had to be reduced to fit into the MYRRHA fuel assembly geometry. The fraction of plutonium and all transuranium elements is set to 0.457 (Sarotto et al. 2013). During the whole chapter, EFIT-like fuel elements refers to elements with a reduced number of pins to fit into the MYRRHA geometry. For calculations, such as the decay heat and the gamma dose rates, the original EFIT fuel element geometry is filled with the spent fuel from the EFIT-like fuel elements. These elements are then called EFIT fuel elements.

7.2.2 The EFIT Reactor Model

The EFIT reactor is planned as a pool-type accelerator-driven system with an energy output of about 400 MWth (Mansani et al. 2012). An 800 MeV proton beam provided by the linear accelerator hits on a windowless lead target. Figure 7.2 shows the core layout of the used computer model. The core consists of three different fuel zones that are surrounded by reflector elements filled with yttrium-stabilized zirconium (YZrO).

Table 7.4 summarizes the geometric dimensions. The fuel elements in the inner and intermediate zone have the same geometric measures. For the outer zone, the radius of the fuel pins is increased to allow for more fissile material in the outer region of the core and thus enable a flattening of the power profile.

To avoid additional plutonium breeding from uranium, *inert matrix fuels* (IMF) are used: the fissile material is placed in a matrix material which does not interact with neutrons. There exist

fuel elements. ADS concepts, however, allow homogeneous recycling where the minor actinides are mixed into the normal fuel matrix.

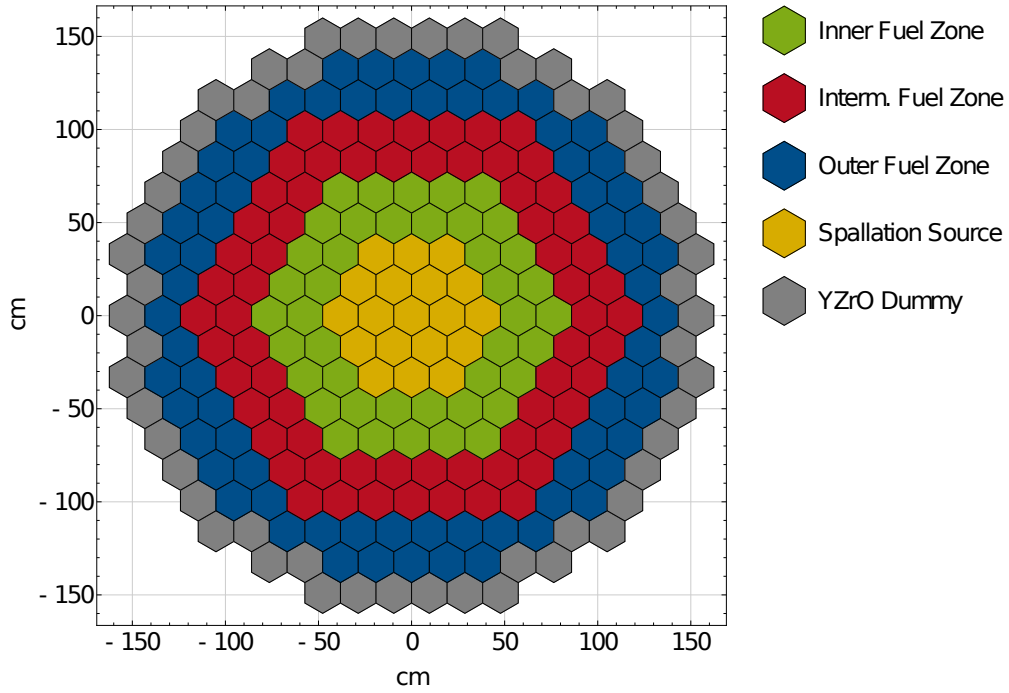


Figure 7.2.: Core layout of the EFIT ADS core for equilibrium sub-cycle. The inner 19 fuel elements contain the spallation source. No control rod elements are foreseen.

different options for the host matrix, the most promising are the so-called CerCer (magnesium oxide) and CerMet (molybdenum oxide) fuels. Since for CerMet fuels only molybdenum-92 is used, reprocessing of the spent fuel elements must include the complicated isotopic separation of molybdenum-92. Therefore, in the model the magnesium oxide matrix (MgO) is used. It was shown that the choice of the fuel type (oxide, metal, nitride, and carbide) has only limited effects on the transmutation efficiency of minor actinides. The most important parameter for efficient transmutation is the hardness of the neutron spectrum (Fazio 2007).

Table 7.3 gives the exact composition of the plutonium and minor actinide vector used in the design. They originate from LWR fuel consisting of 10 % spent MOX fuel and 90 % spent UO_2 fuel with a burn-up of 45 MWd/kgHM. The plutonium is extracted after a 15 year cooling period and the minor actinides after a 30 year cooling period (Artioli et al. 2007).

In accelerator-driven systems, the generation of one neutron is more expensive than in a critical reactor. As a result, the neutrons in the ADS should be solely used for the fissioning of minor actinides instead for the fissioning of plutonium. For one TWh of energy, roughly 42 kg of isotopes must be fissioned⁶. The objective of only fissioning minor actinides and no plutonium isotopes is usually called the *42-0 concept*.

When looking at the reaction rates in the core, the ratio of plutonium and minor actinides determines to what extent the objective of only fissioning minor actinides can be reached. The amount of fissioned plutonium per second Pu_{fiss} depends on the fission cross section σ_F^{Pu} , the neutron flux Φ , and the total amount of plutonium initially present in the core M_{Pu} and is given by

$$Pu_{fiss} = \Phi \cdot \sigma_F^{Pu} \cdot M_{Pu}. \quad (7.5)$$

⁶ An average value of energy released per fission is 200 MeV, equaling $3.204 \cdot 10^{-11}$ J. To produce one TWh of energy, therefore $1.123 \cdot 10^{26}$ isotopes must be fissioned. Assuming an average mass of fissioned isotopes of 240 atomic mass units, this equals 42 kg. The number 42 is also calculated to be the ultimate answer to life, the universe, and everything (Adams 1979).

Table 7.4.: Geometric dimensions of the EFIT core model (Mansani et al. 2012). In the outer zone, the diameter of the fuel pins is increased and the pin pitch reduced.

Parameter	Unit	All Zones		
Active Height	cm	60		
Fuel Assembly Pitch	cm	19.1		
Can Thickness	cm	0.3		
Can Inner Diameter	cm	17.8		
		Inner Zone	Interm. Zone	Outer Zone
Number of Fuel Elements	-	42	66	72
Number of Fuel Pins per Element	-	168+1	168+1	168+1
Radius of Fuel Pin	cm	0.36	0.36	0.4
Cladding Thickness	cm	0.045	0.045	0.06
Pin Pitch	cm	1.363	1.363	1.354

The average fission cross section is determined by the isotopic composition of the fuel. Analogously, the amount of fissioned minor actinides per second can be described by

$$MA_{fiss} = \Phi \cdot \sigma_F^{MA} M_{MA}. \quad (7.6)$$

For a simplified analysis, all reactions except fission, most likely neutron absorption and α -decay, are grouped together as being *other* reactions. Only a fissioned minor actinide is transmuted. Further, only plutonium reactions resulting in minor actinides and vice versa are taken into account. The equations for the produced minor actinides MA_{other} and plutonium Pu_{other} are

$$MA_{other} = \Phi \cdot \sigma_{other}^{Pu} M_{Pu} \quad (7.7)$$

$$Pu_{other} = \Phi \cdot \sigma_{other}^{MA} M_{MA}. \quad (7.8)$$

$$(7.9)$$

The total amount of fissioned material $M_{fiss} = Pu_{fiss} + MA_{fiss}$ is fixed for a given power generation. In the *42-0 concept*, the net balance for plutonium should be zero. The amount of fissioned plutonium must thus equal the net plutonium production by all other reactions in the core: $Pu_{fiss} = -Pu_{other} + MA_{other}$. The neutron flux cancels from the equation yielding the fraction of plutonium and minor actinides to be

$$\frac{M_{pu}}{M_{MA}} = \frac{\sigma_{other}^{MA}}{\sigma_{other}^{Pu} + \sigma_F^{Pu}}, \quad (7.10)$$

providing the wanted fuel composition for the concept.

Reality is a bit more complex, of course. The cross sections depend on the neutron flux which in turn depends on isotopic composition of the fuel. The composition changes over time leading to new cross sections and a different neutron flux. Therefore, several iteration steps are needed to derive the optimum fraction in the fuel from equation 7.10. For the EFIT reactor, the (preliminary) result yields a plutonium fraction of 45.7 % as a part of all transuranium elements in the fuel (Chen, Rineiski, Maschek, et al. 2011).

To keep the conditions in the reactor as uniformly as possible, a flattened power profile is desired. This is usually done by increasing the fissile material content in the fuel elements at the periphery

of the core. This is not possible in the EFIT core with the optimum transmutation efficiency as the main objective. Meanwhile, allowable peak factors for the EFIT core are quite low (at most 1.2), since CerCer fuels have lower melting points than MOX fuels used in LWR (Maschek et al. 2008). Additionally, the coolant outlet temperature is higher for metal cooled reactors (about 480°C) than for water cooled reactors. The fraction of the MgO matrix is also limited by the thermal conductivity and cannot fall below 50 %. Hence, the only way to flatten the power profile is to position more fuel in the outer zone of the core which is done by increasing the pin diameter. The inner zone consists of 42 fuel elements, the intermediate of 66 fuel elements and the outer zone of 72 fuel elements (Mansani et al. 2012). The active height is 90 cm.

The theoretical density of CerCer fuel is 6.6 g/cm³ at a temperature of 1270 K (Eriksson et al. 2005; Maschek et al. 2008). With a bulk density of 0.95 of the theoretical value, the density of the EFIT P&T-fuel can be calculated to be 6.27 g/cm³. EFIT is supposed to be cooled with pure lead. Its density is set to be 10.52 g/cm³ for modeling. This value was calculated using the equation given in Cinotti et al. (2010, p. 2784) by taking into consideration the average inlet and outlet temperatures of 400°C and 480°C, respectively (Barbensi et al. 2007). Usually there is some oxygen dissolved in the coolant to form a protection layer on the surface of the cladding. It is not modeled, because it does not influence neutronic calculations.

For structure elements, stainless steel T-91 is assumed in the computer model. Values from the MYRRHA core model are used if no explicitly stated figures describing the EFIT core could be found in the literature.

The spallation source of the EFIT reactor is still in a very early design stage and only little information is available. In the current design, the inner 19 fuel elements contain the spallation source (Sobolev, Uyttenhofe, et al. 2010; Uyttenhofe 2016). They have not been modeled specifically but filled with coolant. With the EFIT core model, the attention lies on criticality calculations for different plutonium vectors here. For this type of calculations, the contribution of the spallation source can be neglected. Additionally, it seems unlikely that a design comprising such a large spallation source will actually be built since it would greatly raise costs.

7.2.3 Simulation Parameters

Burn-up calculations were only conducted for the MYRRHA reactor system due to a lack of information on the spallation source and the planned operation modus for the EFIT reactor core. The total power output of the MYRRHA core is constant at 100 MWth. The simulation starts with the equilibrium number of fuel elements. Two of the six in-pile test sections are filled with EFIT-like fuel elements. These elements are later taken for the analysis of the material composition taking place in P&T-fuel elements with a high fraction of minor actinides. Only two of the six IPS were filled with P&T-fuel elements since they add too much positive reactivity.

One sub-cycle in the MYRRHA reactor lasts 90 full power days (FPD) and is followed by a 30 day maintenance (shutdown) period. During this interval, the fuel elements are moved to the next fuel zone as depicted in Figure 7.1. The 90 irradiation days are split into three burn steps for higher accuracy. Every third sub-cycle there is a longer maintenance period of 90 days. One cycle lasts 840 days equivalent to 540 FPD. Burn-up of the elements is about 46 MWd/kgHM at discharge from the reactor core. For fast reactors there is no need to have a shorter time step of five days at the beginning of life to account for xenon poisoning. The simulation is run for six cycles to allow the system to reach an equilibrium state.

For the EFIT-like fuel elements in the IPS of the MYRRHA core, the irradiation time was set to be 1080 FPD or 4 cycles of the MOX fuel in the MYRRHA core. This equals roughly the planned three years for the irradiation time in the EFIT reactor core (Artioli et al. 2007). In doing so, during the simulation no separate time steps had to be defined for the EFIT-like fuel elements. The simulation was run for 840 FPD to reach equilibrium conditions. Then, in addition to the scheduled reshuffling

of MOX fuel elements, fresh P&T-fuel was inserted. This was irradiated for the full time period of 1080 FPD before it was discharged and its material used for analysis. The material composition is tracked at each time step during burn-up calculations. A long irradiation time hence also allows assessment of material that had (hypothetically) been removed from the core after a shorter time. To allow for easier evaluation of the influence of cooling periods after discharge of the irradiated P&T-fuel, at the end of depletion calculation several decay steps with increasing length were added to the simulation. These cover the first 100 years after discharge from the core with increasing step length.

Depletion calculations for the MYRRHA core filled with two EFIT-like fuel elements in the IPS were performed using VESTA 2.1 and MCNPX 2.7. For cross section libraries, the JEFF-3.1 data is used (NEA 2012b). The most recent version of JEFF, version 3.2, is not available in VESTA yet.

7.3 Model Verification

The generic computer model could only be set up filling incomplete information in the literature with assumptions based on other reactor models. Consequently, it is useful to perform calculations to verify the viability of the model. One of the first and easiest things is the evaluation of the criticality. Fortunately, this does not depend on the spallation source at all and could thus be done for the MYRRHA and EFIT core for various configurations using fresh fuel elements.

It is often implicitly assumed that the neutron flux distribution in the IPS of the MYRRHA core can be compared to the neutron flux in the EFIT core. To verify this assumption, the neutron flux in both cores is analyzed at different positions.

Based on the depletion calculation for the MYRRHA reactor, source efficiencies and beam currents over one sub-cycle are calculated. The content of the transuranium nuclides in the P&T-fuel elements in dependence on irradiation period in the IPS is analyzed. It is shown that the objective of mainly fissioning minor actinides, the *42-0 concept*, is fulfilled pretty well.

7.3.1 Criticality of the Reactor Cores

For the MYRRHA sub-critical reactor, two core configuration are published: one comprising 58 fuel elements (BOL configuration) and one comprising 72 fuel elements (BOC configuration). For both layouts, k_{eff} is calculated for a core filled with fresh MOX fuel elements. Table 7.5 presents the results. At BOL, k_{eff} is very low with only 0.93. Of course it would be possible to run the sub-critical reactor at such a low level but this would need a comparably high energy proton beam to provide sufficient neutrons in the core. The low value matches the statements in the literature that the criticality of the MYRRHA core might be too low for efficient operation (Sobolev 2005; Sarotto et al. 2013).

Compared to the critical layout of the MYRRHA reactor, for the sub-critical configuration six control rods are placed in the periphery of the core. They will only be inserted during refueling to enlarge the margin to criticality. The resulting values for k_{eff} show that the insertion of the control rods is about 0.03 worth in negative reactivity. The low value can be assigned to the position at the periphery where the neutron flux is low and the small number of only six control rods. It also mirrors the fact that in an accelerator-driven system, the main safety guarantee for prohibiting criticality excursions is the regulation of the proton beam and not the insertion of control rods.

The main objective of this chapter is to assess possible consequences of minor actinide transmutation in the sub-critical core and to evaluate possible impacts of P&T-fuel on reactor operation and the overall fuel cycle. Therefore, it is assumed that two EFIT-like fuel elements containing P&T-fuel are inserted into the IPS of the MYRRHA reactor. For this configuration, simulation results of k_{eff} are shown in Table 7.5 as well. It can be seen that the two EFIT-like fuel elements add about 0.01

Table 7.5.: Neutron multiplication factor k_{eff} for the MYRRHA sub-critical core at begin of life (BOL) and begin of cycle (BOC). At BOL the core consists of 58 fuel elements. The number is increased to 72 for equilibrium operation, denoted BOC.

	Basic	with Control Rods	with 2 EFIT-like IPS
BOL	0.930	0.903	0.940
BOC	0.995	0.964	1.004

worth of reactivity to the core. In the BOC configuration, the core even becomes critical with only two former coolant filled IPS dummies being replaced EFIT-like fuel elements due to the higher number of MOX fuel elements. This leads to some obstacles for the depletion calculations. Using the spallation process for generation of source particles in MCNPX in a critical core results in a infinite calculation, since for each source neutron even more neutrons are produced.

As a result, for the depletion calculation including the EFIT-like elements, the simulation could not be started with the full number of fresh MOX fuel elements (Frieß and Liebert 2015). Hence, the IPS were filled with EFIT-like fuel elements only after the first depletion steps had already been performed. The criticality of the whole system had declined to a level where the insertion of the EFIT-like fuel elements did not result in a critical core anymore.

In the EFIT core design, no control or safety rods are planned and only one core configuration is published. For this core layout, k_{eff} is calculated to be 0.960. This lies within the range as suggested by Mansani et al. (2012) for normal operation. For refueling, the margin to criticality is enlarged by absorbers that are to be positioned in some of the 252 dummy elements surrounding the core. These elements are not explicitly modeled due to a lack of information and insignificance to core dynamics during operation.

7.3.2 Position of the Spallation Source in the Core

Under the harsh conditions present in the core, the actual geometry of the spallation source has great impact on its performance. Until now, spallation sources have in general only been used for neutron generation for research purposes, but not as an external source inside a sub-critical reactor core. Hence, looking at the literature on the spallation source to be positioned in the MYRRHA reactor, differing, partly even contradictory information can be found. This probably also caused by the ongoing design process. For example, the spallation source occupies either one or three fuel elements (Palazzo et al. 2013; Sarotto et al. 2013). In the older design studies, a windowless design was planned (Abderrahim, Kupschus, et al. 2001; Guertin et al. 2011), while the current design seems to employ a window beam as well (Abderrahim 2013). Also, the position of the spallation source is not given precisely, only as being centrally placed in the active region of the core (Tichelen et al. 2001).

To optimize the position of the spallation source in the core, several calculations with the top of the spallation source at different heights in the reactor core were conducted. From the MCNP output, the neutron production per source particle and the number of neutrons lost to fission per source particle can be derived. Figure 7.3 plots the values normalized to their maximum value each. The number of neutrons that induces fission reactions (called *loss to fission* in MCNPX output) is highest when the spallation target ends at 106 cm. The neutron creation per source proton n/p has a maximum value when the target ends at 112 cm. The values for n/p are derived from the MCNPX output as described in section 4.3.2. The active length of the MYRRHA core ranges from 66 cm to 126 cm. Thus, the spallation source ending at 106 cm is equivalent to it ending 20 cm below the upper end of the active zone.

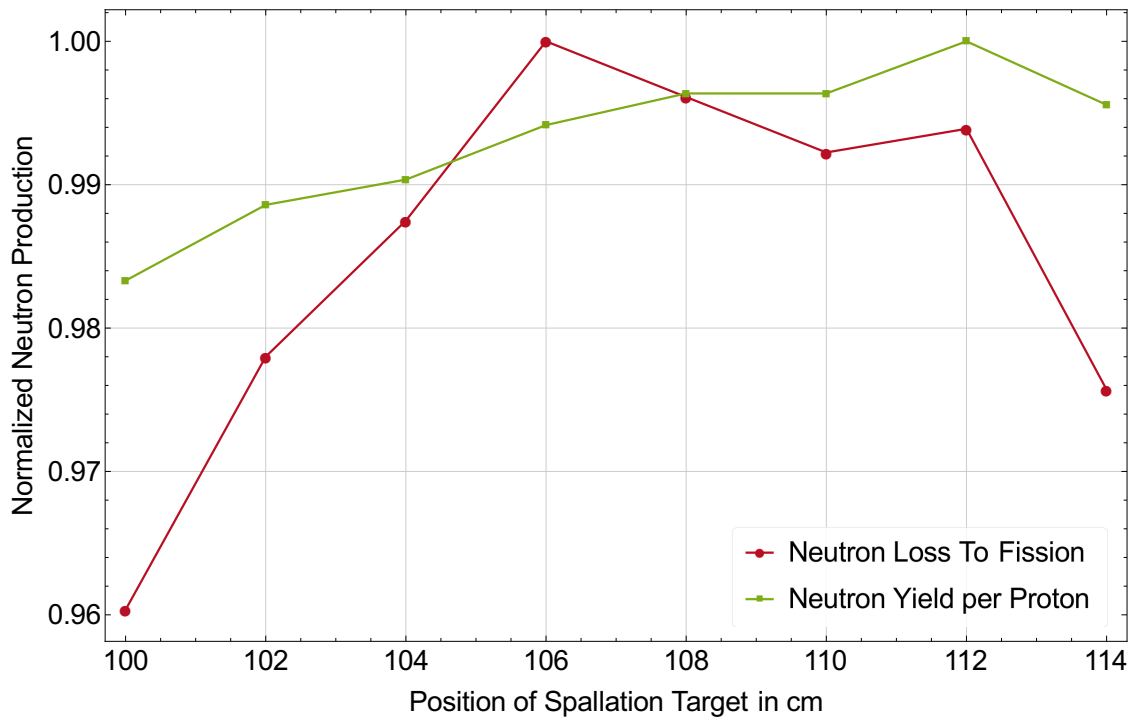


Figure 7.3.: The number of induced fissions and produced neutrons per source proton. Values are normalized to their respective maximum levels.

The difference can be explained by the varying reactions that are taken into account when calculating the figures. For n/p, the geometry of the spallation source, or, more exact, its length comes into play: the higher the target, the more neutrons can be produced in the volume. Reactions taking place in the core only play a negligible role. This, of course, does not hold true for the number of fissions induced by the spallation neutrons. Only in the core a significant amount of fissile material is present that can be fissioned. If the middle of the spallation source is positioned too close to the end of the active length, many neutrons are lost due to leakage and hence cannot induce further reactions. Consequently, the number of neutrons lost to fission is higher for a more centralized position. For the operation of a sub-critical target core the number of induced fissions is more important, the position of the top of the spallation target was set to 106 cm.

7.3.3 Neutron Flux in the Reactor Cores

For the evaluation of the fuel composition over burn-up in the future EFIT reactor, an approach already made by others was taken: two EFIT-like fuel elements are placed in the MYRRHA in-pile test sections (IPS) (Sarotto et al. 2013). But this approach implies that the neutron fluxes in the in-pile test sections of the MYRRHA reactor core can be compared to the fluxes in the future EFIT reactor. This assumption is tested simulating the MYRRHA and the EFIT core with fresh fuel and no spallation source present. For both cores, the same number of source particles is used.

The neutron flux distribution is calculated at different positions in each core. The results are plotted in arbitrary units in Figure 7.4. The energy range was chosen according to preliminary calculations of the neutrons spectrum in the core. For the EFIT core, the relative neutron flux is depicted for one exemplary fuel element from the inner, the intermediate and the outer core zone. As expected, the value is lowest in the outermost core zone. The behavior of the flux is quite similar for all three graphs in the medium energy range. For high and low energies, the statistical variation of the flux is much higher due to the lower number of scores per energy bin.

Looking at the neutron flux from the EFIT-like fuel element⁷ in the IPS section MYRRHA reactor, the same behavior of the energy distribution can be seen, but the normalized flux is about one magnitude higher than in the EFIT reactor. The neutron flux in the MOX element also shows one important difference: the dip at around 90 keV is missing. In the EFIT fuel elements, it is caused by the inert magnesium matrix. Magnesium-24, comprising nearly 80 % of natural magnesium, has a neutron absorption resonance at 83 keV⁸.

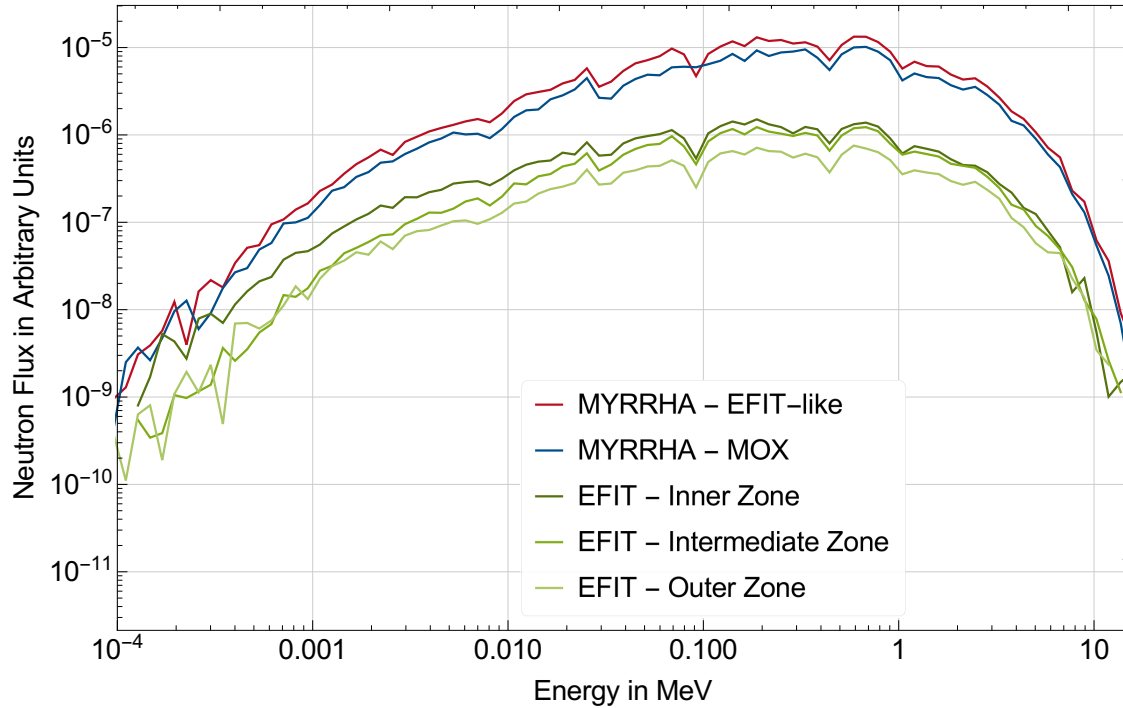


Figure 7.4.: The neutron flux distribution in the EFIT and MYRRHA sub-critical cores. The position of the elements in the EFIT core affects the absolute flux they are exposed to. For the MYRRHA reactor, the neutron flux distribution for one EFIT-like and one MOX fuel element is plotted. The MOX fuel does not show the characteristic dip at around 90 keV like the magnesium oxide matrix fuels. Absolute values depend on the actual power density in the reactor core.

There are different reasons why the flux curves for the two reactor cores differ so much. On the one hand, the different fuel compositions in the total core result in different probabilities for certain reactions. In the P&T-fuel present in the MYRRHA IPS and the EFIT elements (high content of plutonium and minor actinides), the probability of capture per source neutron is doubled compared to the MOX fuel elements. On the other hand, less neutrons introduce fission reactions (about 10 % less reactions per source particle in the Monte Carlo simulation).

This is also mirrored by the different criticality levels of the reactor cores. At EOL with fresh fuel, k_{eff} for EFIT is only at 0.96 while for MYRRHA k_{eff} (in BOC configuration, which is used in equilibrium operation) it is nearly one (0.99). The different values connotate indirectly the number of fissions that is induced per source neutron. Thus, starting the same number of particles does not equal the same number of fissions which also explains the lower level of the flux in the EFIT reactor. For EFIT an extremely low source efficiency of only 0.52 is published in Artioli et al. (2007). Therefore, a high proton beam is needed to achieve the targeted power output. To allow for a

⁷ EFIT-like fuel elements have a reduced number of fuel pins to fit into the MYRRHA fuel element geometry.

⁸ It seems strange that the *inert* matrix magnesium has such a strong influence on the neutron spectrum. To verify the statement, several calculations of the neutron flux distribution with different fuel compositions were performed.

smaller particle accelerator and a more economic operation of the reactor, it is quite likely that in the ongoing design process efforts will be taken to increase the source efficiency. For the MYRRHA core in BOC configuration, the calculation of the source efficiency results in a value of 0.97. For a given energy output equal to a certain number of fissions in the fuel, significantly fewer neutrons from the spallation source are needed.

The fact that the absolute magnitude of the neutron fluxes differs to such a high degree complicates the translation of the fuel element exposure from the MYRRHA IPS to the future EFIT core as for example done in Sarotto et al. (2013). Figures depending on the absolute neutron flux the material is exposed to must be carefully analyzed to ensure commensuration. In the following, this will be either done by evaluating the material after a range of irradiation times or, if possible, by using reference values that are mostly independent of the absolute value of the neutron flux.

7.3.4 Source Efficiency

One figure usually easily obtained from the burn-up calculations is the criticality of the system over burn-up. This does not hold true for a sub-critical system driven by a spallation source. Even the newest version of MCNPX (MCNP6) is not capable of doing criticality calculations while at the same time external neutrons, e.g. by a spallation source, are produced and tracked. The importance of the source neutrons increases with decreasing criticality over burn-up (reactivity swing). To keep the same power level during one sub-cycle, it is possible to increase the beam current. To calculate the source efficiency and the beam current, the knowledge of the effective multiplication factor k_{eff} is required. Consequently, for one sub-cycle during equilibrium operation of the MYRRHA reactor explicit criticality calculations were performed.

One sub-cycle consists of 90 days of irradiation and a subsequent 30 day maintenance period. Corresponding to the time steps in the burn-up calculation, the criticality, source efficiency, and beam current were calculated every 30 days, beginning at BOC. Table 7.6 shows the results. The reactivity swing over burn-up can be clearly seen. Criticality of the core increases again with the insertion of fresh fuel. All criticality values lie in the range between 0.95 and 0.97 as desired for safe reactor operation.

Directly connected to the neutron multiplication in the core is the source efficiency ϕ^* as described in section 4.3.2. The source efficiency denotes the importance of the external supplied neutrons compared to the neutrons produced in the core. It can be calculated using equation 3.15. By definition it is only usefully described in a sub-critical reactor where an external neutron source is present. For the MYRRHA reactor core, the calculated values range from 1.19 to 1.28 at the end of the sub-cycle. With decreasing intrinsic reactivity of the core due to burn-up the external source neutrons become more important for core dynamics. For comparison, a source efficiency of 1.08, calculated at BOL with $k_{eff} = 0.995$, is given in IAEA (2015, p. 45).

Table 7.6.: Evolution of the effective multiplication factor k_{eff} , the source efficiency and the beam current over one arbitrary sub-cycle in equilibrium mode of the MYRRHA reactor model.

	k_{eff}	Source Efficiency ϕ^*	Beam Current I
0	0.971	1.19	2.21 mA
+30 Days	0.964	1.24	2.65 mA
+60 Days	0.959	1.24	3.10 mA
+90 Days	0.954	1.28	3.43 mA
+120 Days	0.971	1.19	2.23 mA

The proton current supplied by the particle accelerator is used to balance the reactivity swing during reactor operation. The neutron production is proportional to the beam current on the

spallation target. The beam current I in particles per second is calculated using equation 3.17. Hereby, average values of 2.95 for the number of released neutron per fission and 200 MeV for the released energy per fission are taken. As also shown in Table 7.6, the resulting beam currents range between 2.21 mA and 3.43 mA. For the MYRRHA core, the planned maximum current is 4 mA.

7.3.5 Transmutation of Minor Actinides and Plutonium

The transmutation rate of transuranium elements in the EFIT-like fuel elements placed in the in-pile test sections in the MYRRHA reactor is evaluated to further check the computer models. The focus lies on the question to what extent the *42-0 concept* is already reached, using the preliminary fuel element design as already described.

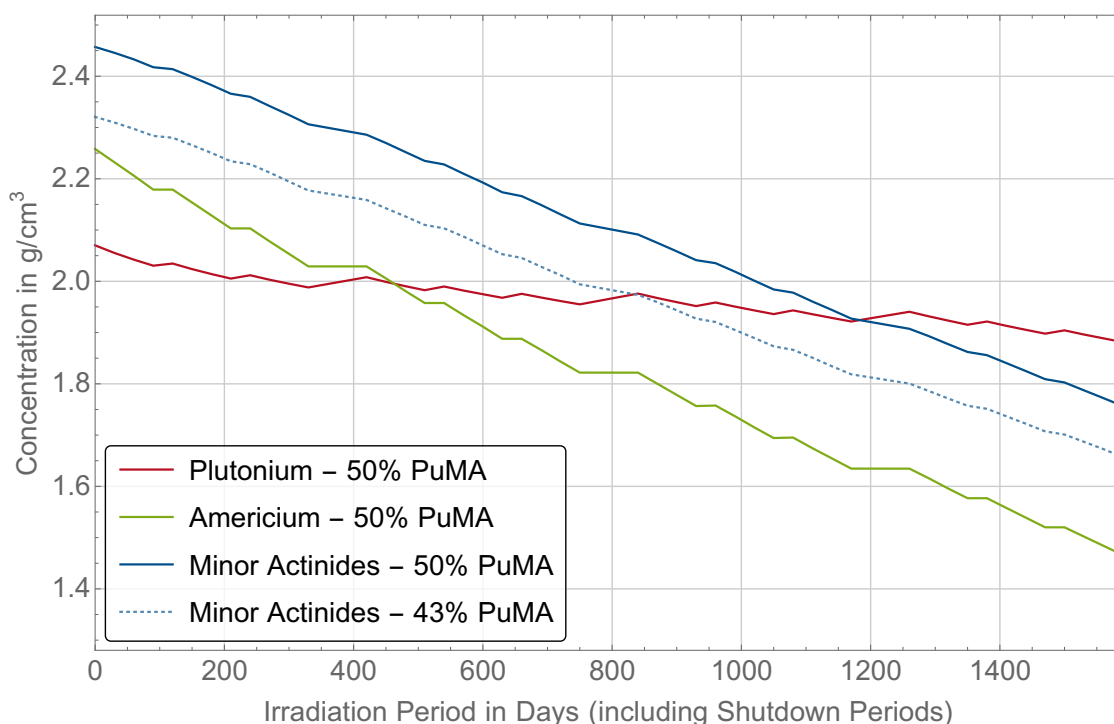


Figure 7.5.: Reduction of plutonium, americium and all minor actinides in an exemplary EFIT-like fuel element containing 50 % fissile isotopes (PuMA) and irradiated in the MYRRHA reactor. The reduction of the minor actinide content in an element with only 43 % fissile isotopes is also given. The periods with nearly constant concentrations show the maintenance intervals.

Figure 7.5 shows the development of the plutonium and minor actinide (PuMA) content in an EFIT-like fuel element with a 50 % fraction of transuranium elements over the whole irradiation cycle of 3 years or 1080 full power days (FPD). Only the three most important isotopes neptunium, americium, and curium are considered for the sum of minor actinides. From the other minor actinides, only traces can be found in the fuel. The results of the calculation lasting for 1590 days⁹ are depicted in Figure 7.5. They mirror an up to now unrealistic situation. With current technology, an irradiation period that long is not achievable due to lacking material endurance. This is one reason why case studies often only assume irradiation periods of 320 FPD.

A zero net balance for plutonium is not reached, the plutonium concentration in the fuel drops by roughly 10 %. The main part of the energy production occurs by the fission of minor actinides.

⁹ Four cycles of 420 days minus the last maintenance period of 90 days.

More optimization on the composition of the fuel elements could probably lead to even better results. Since americium is the main contributor to the minor actinides, its content is plotted separately. Looking at the values at BOL and EOL and comparing them to the concentration of the total of the minor actinides, it can be seen that the americium content alone decreases faster than the sum of all minor actinides. This is due to the build-up of curium in the reactor, which poses severe challenges to reprocessing and fuel fabrication.

Table 7.7.: Transmutation efficiency per irradiation time in FPD for minor actinides and all transuranium isotopes. (1080 FPD is roughly equivalent to 3 years.)

	270 days	540 days	810 days	1080 days
Only Minor Actinides	0.07	0.15	0.22	0.29
All Transuranium Elements	0.05	0.10	0.15	0.20

Several aspects determine the overall efficiency of the complete transmutation fuel cycle. When looking at the efficiency in regard to transmutation¹⁰, this includes for example the possible separation efficiency during reprocessing of the spent P&T-fuel, the targeted amount of minor actinides that go into the deep geological repository, and the transmutation efficiency per irradiation period in the reactor core η_T .

This transmutation efficiency per reactor cycle can be defined as

$$\eta_T = 1 - \frac{M_{EOL}}{M_{BOL}}. \quad (7.11)$$

using the final and the initial mass of the considered isotopes M_{EOL} and M_{BOL} . In a system with a higher transmutation efficiency, more isotopes are destroyed (=fissioned) than in a system with a lower transmutation efficiency. Unlike for the calculation of the breeding ratios in a reactor core, the ratio of the masses present and not the reaction ratios are going into the equation. A high transmutation efficiency results in fewer needed irradiation periods to reach the desired reduction of the original inventory. It is calculated for the EFIT-like fuel elements in the IPS of MYRRHA in the following.

Depending on the considered scenario, transmutation of either only minor actinides or all transuranium elements (PuMA) is planned. Table 7.7 lists the efficiencies for these two isotope groups after different irradiation times in the core. For all transuranium elements, the values are lower than for minor actinides due to the increased reference mass present in the core. Therefore, more cycles will be needed if there is no fast reactor fleet present to use the excess plutonium for energy production. If transmutation of all transuranium elements is planned, it might however be possible to modify the fuel in a way to improve performance (Renn 2013, p. 98).

A maximum lifetime in the core of 1080 FPD is assumed, but the transmutation efficiency was also calculated after each additional 270 FPD. With longer irradiation times, the efficiency increases linearly. This does not depict the situation in the core exactly, since with a decreasing number of isotopes to be fissioned, the transmutation efficiency declines as well. The change is too small to show off in the above figures. One limiting factor for the possible irradiation period in the core is the endurance of the cladding and structure material in the hard neutron spectrum in a lead-bismuth cooled core, leading to currently definitely less than 1080 FPD of irradiation.

Even assuming this challenge can be solved and there are only small losses during reprocessing and fuel fabrication, at least four irradiation periods are needed to fall below an exemplary final minor actinide inventory of 5 % of the initial inventory. This estimations considers a quasi indefinite reservoir of minor actinides, thus the same reduction takes place in each irradiation cycle. If only

¹⁰ Further possible aspects are power generation, economics, resource utilization, number of facilities, and others.

irradiation periods of 540 FPD or even 270 FPD are possible, the number of needed cycles increases drastically because of the low transmutation efficiencies. The calculated values (cf. Table 7.7) match the transmutation efficiencies of about 10 % per irradiation cycle which are given in the literature as being realistic using current technology (cf. (ibid., p. 92)). Consequently, about ten irradiation periods for an overall transmutation scheme seems to be a reasonable estimate using only current materials and not relaying on future development.

The number of needed transmutation cycles affirms the importance of the partitioning efficiency for a partitioning and transmutation fuel cycle. Even admitted by advocates of P&T, the partitioning efficiency is one possible game changer for the technology. For reasonable results, it should be at least 99.9 % for minor actinides, if not higher. Only then, the losses add up to a small enough fraction of the total inventory (assuming ten cycles with 99.9 % partitioning efficiency results in a loss of 1 %). With current technology, separation factors in that range are at best available on laboratory scale. One facility for handling minor actinide fuel was developed – with limited allowed masses of 150 g of americium-241 and 5 g of curium-244 (Fanghänel et al. 2010, p. 2948). For the implementation of a P&T fuel cycle, however, facilities able to partition several tons of minor actinides per year are necessary.

7.4 Aging of the Transuranium Vector

The isotopic composition of the fuel changes during irradiation in the reactor core. This leads to a change of the neutron multiplication factor: the reactivity swing. Isotopic fuel compositions derived from own calculations and from the literature are used for analysis of the effect of different isotope vectors on the criticality of the EFIT reactor.

7.4.1 The Reactivity Swing During Reactor Operation

It is desirable to have near stable conditions with regard to the neutron multiplication factor and the neutron flux during reactor operation. In reality, a stable neutron flux can never be achieved due to the ongoing reactions that take place in the reactor core. In general, with higher burn-up less fissile material is present and therefore fission reactions are less likely. At the same time, more and more fission products are in place that in turn act parasitic on the neutron population. Each neutron absorbed by a fission product (or any other isotope) is lost for fission as well as for energy production. It is unavoidable to replace some of the spent fuel elements with fresh fuel elements to compensate for the reactivity change after a certain time.

There are several options that can prolong the operation time of a reactor core. All depend on the fact that at beginning of the fuel cycle, extra fuel is added to the core which inserts positive reactivity. The effect of this excess positive reactivity must be mitigated by the presence of neutron absorbing material whose negative reactivity can be adjusted during core lifetime. The two usually applied options are the use of burnable neutron poisons diluted in the coolant and control rods (United States Department of Energy 1993b, p. 55ff). A neutron poison is a material with a high neutron absorption cross section which ends up being an isotope with only a low absorption cross section after neutron intake. Examples are boron or gadolinium. The more of the neutron poison is burned, the less negative reactivity is added to the core. Ideally, the burn-up of the neutron poison compensates the loss in reactivity induced by fuel burn-up.

Control rods also consist of neutron-absorbing material. They can be partially inserted into the active region of the core and hence allow for on-line adjustment of the negative reactivity they add. Compared to the dissolved neutron poisons, control rods have the disadvantage that they are not as evenly distributed in the core, which induces disruptions in the power profile.

In the case of an accelerator-driven system, the method to balance the reactivity swing is different. In a sub-critical reactor, at least in theory, a self-sustained chain reaction is not possible. The core

only multiplies the external neutrons. Hence, there is no such thing as an exponential excursion of the neutron population because the number of all neutrons is proportional to the number of external neutrons. Since the neutron yield is proportional to the beam current, the number of source neutrons can be adjusted by controlling this parameter. With increasing burn-up of the fuel in the core, the beam and subsequently the number of neutrons that are amplified can be increased up to a certain limit, resulting in a more or less constant power output of the reactor core.

The range in which the beam current can be adjusted during operation is limited and also depends on the maximum beam power. With future linear accelerator generations this range might be increased, but current research and development efforts focus mainly on the reliability of the beam. Discontinuities in the beam power (*beam dips*) lead to high temperature gradients that induce significant material stress. Great efforts are taken to reduce their number to lower values. For the MYRRHA reactor, less than ten dips per three month operation that exceed three seconds are targeted (SCK-CEN 2016). More importantly, the higher the maximum beam current, the more expensive is the linear accelerator. The particle accelerator already poses a major economic penalty on the operation of an accelerator-driven system.

In a transmutation facility supposed to only incinerate minor actinides, plutonium is added to the core to provide sufficient reactivity for operation. In principle, mostly the isotopes with an odd mass number (namely plutonium-239) are fissioned while at the same time the concentration of the even isotopes increases because of neutron absorption. Over time, the plutonium vector degenerates and in terms of criticality it can be expected that its positive reactivity worth is reduced. At the same time, it is stated in various sources that plutonium is only needed for the initial load of the transmutation facility (Barbensi et al. 2007; Mansani et al. 2012). The fast degeneration of the plutonium composition observed in thermal reactors is not supposed to appear in the transmutation facilities (Renn 2013, p. 129). One way of minimizing the reactivity swing could be the reduction of the plutonium and minor actinide ratio (Chen, Rineiski, Liu, et al. 2008). The adjustment of this ratio contradicts the main objective of maximizing the transmutation efficiency. As shown in 7.2.2, the fraction of plutonium in the fuel determines whether or not the goal of a zero plutonium balance can be reached.

The degeneration of the plutonium vector is not considered in the publicly available information on the design process for the EFIT reactor. The core design and the accompanying calculations of reactor parameters, such as the criticality and void coefficients for the EFIT reactor, are done using a plutonium and minor actinide composition derived from MOX fuel that was cooled for a certain period. But this isotopic composition of the fuel is only true for the initial load of the transmutation facility. The minor actinides have to be recycled several times to reach a significantly reduced final inventory. While they are incinerated in the transmutation facility, the plutonium is used within the commercial nuclear reactor fleet for energy production.

It will take several decades before an equilibrium cycle is reached. In an equilibrium cycle, the transmutation facilities are operated to burn the minor actinides produced in the reactor fleet. The fuel composition would then be the same for each load. Consequently, it has been shown that a minimum of five cycles are necessary to reach an isotopic equilibrium state (IAEA 2004, p. 94). The equilibrium scenario for the operation of the transmutation facilities depends heavily on the initial minor actinide stockpile, the participating partners, their objectives and the overall target of the fuel cycle (e.g. stabilization or reduction of the minor actinide inventory). This wide range of parameters is generally hard to be appropriately taken into account when designing the transmutation facility.

An estimation of the impact of the degeneration of the plutonium vector on the criticality of the EFIT reactor is conducted in the following. As a crude first estimate, plutonium compositions originating from EFIT-like fuel elements irradiated in the MYRRHA core and the initial minor actinide vector is used for criticality calculations. In a second step, it is assumed that the minor

actinides in the fuel have also been irradiated before and the criticality of EFIT using this fuel is also calculated.

The PATEROS study performed a more comprehensive simulation of the possible implementation of a transmutation fuel cycle. It reports the plutonium composition at certain time steps within their simulation period (Salvatores et al. 2008). These isotope vectors are used for additional criticality calculations.

7.4.2 Irradiation History and Criticality

The overall design of the EFIT reactor is based on a plutonium and minor actinide vector derived from an exemplary stock, coming from spent LWR fuel at a burn-up of 45 MWd/kgHM and cooled for a certain period. But this composition is only valid for one possible initial load of the reactor core. In this section it is referred to as the fresh isotopic vector. Already one irradiation cycle changes the isotopic composition and therefore the behavior of the core and its criticality. A simplified approach was taken, because it was not possible to perform burn-up calculations for the EFIT-reactor: the spent fuel from the EFIT-like fuel elements irradiated in the MYRRHA core were filled into the EFIT reactor geometry to perform criticality calculations. Therefore, the effect of irradiated plutonium and minor actinides on the criticality of the EFIT reactor could be approximated. Since the irradiation period in the EFIT core is not yet clear and to account for the higher neutron flux in the MYRRHA core, the criticality was calculated for fuel with different burn-up irradiation histories¹¹. Table 7.8 lists the composition of the plutonium vector after various irradiation times. It shows a decreasing plutonium-239 fraction. The plutonium-238 fraction increases. It is much higher than in light water reactor spent fuel. Plutonium-238 is mainly produced by breeding from neptunium-237 or via α -decay from curium-242. Both isotopes are present in an unusually high fraction due to the admixture of minor actinides into the fresh fuel. Compared to the average reactor-grade plutonium (cf. Table 5.4), there are more plutonium isotopes with an odd mass number present in the irradiated transmutation fuel. This is also the reason why a light water reactor fleet is commonly regarded as not being suitable to use the plutonium discharged from an accelerator-driven system for energy generation. The resulting plutonium isotope vector as depicted in Table 7.8 is not sufficiently fissionable in a thermal neutron spectrum.

Table 7.8.: Evolution of the plutonium vector in the P&T-fuel for different irradiation histories of the EFIT-like fuel elements in the MYRRHA IPS. All values are in weight percent and derived from irradiation of EFIT-like fuel elements in the MYRRHA IPS.

	Pu-238	Pu-239	Pu-240	Pu-241	Pu-242
0 Days	3.7	46.4	34.1	3.8	11.8
270 Days	6.4	41.7	34.7	4.0	13.1
540 Days	10.9	36.8	34.4	4.0	13.9
810 Days	14.8	32.6	34.0	4.0	14.6
1080 Days	17.9	29.1	33.8	4.0	15.2

The spent fuel is separated into different material streams after irradiation in the accelerator-driven system. It is then fabricated into fresh fuel elements for the next transmutation cycle. To obtain the best possible transmutation efficiency, it is now assumed that the fraction of plutonium to minor actinides is reset to the optimum fraction as derived based on the *42-0 concept* (cf. section 7.2.2). Yet, the calculated plutonium and minor actinide ratio might not hold true for the new composition.

¹¹ For the change in the material composition, the total neutron flux is an important factor. The exposure to a certain neutron flux can be approximated by exposure to only half of the flux but for a doubled irradiation period.

But since this ratio is a reference point of the design efforts, the fraction of 45.7 % plutonium is used in all the following calculations.

For a first set of calculations, the minor actinides are taken from the stockpile and combined with previously irradiated plutonium into fuel for the EFIT reactor. Figure 7.6 shows the evolution of the calculated k_{eff} . The irradiation period assigns the days the plutonium had been irradiated prior to fuel fabrication. With the initial composition, criticality of the system is at 0.96, a value consistent with the published values for k_{eff} (Mansani et al. 2012). With plutonium aging, criticality drops massively to a value of less than 0.92 after a previous irradiation of 1080 FPD. This reactivity swing is by far higher than values derived in other calculations for various oxide fuels rich in minor actinides (NEA 2005). For MYRRHA, a reactivity swing of 1500 pcm ($\Delta k \approx 0.015$) was calculated¹² (Sarotto et al. 2013). For EFIT, publications even list a value of only 200 pcm per cycle (Artioli et al. 2007). It seems reasonable that these are ranges controllable by the beam current than the approximately 4000 pcm visible in the calculated figures.

Table 7.9.: Evolution of the minor actinide vector in the P&T-fuel for different irradiation times. All values in weight percent. The fraction of Am-243 is constant at 16 %.

	Np-237	Am-241	Am-242m	Cm-242	Cm-243	Cm-244	Cm-245
0 Days	3.9	76.	0.25	0.	0.066	3.	1.1
270 Days	3.8	71.	1.2	2.8	0.094	4.2	1.2
540 Days	3.8	68.	2.1	3.2	0.14	5.4	1.2
810 Days	3.9	66.	2.8	3.2	0.18	6.6	1.4
1080 Days	3.9	64.	3.4	3.1	0.22	7.8	1.6

To meet the objective of significant minor actinide reduction, several irradiation periods in the reactor are necessary. Table 7.9 shows the evolution of the minor actinide vector derived from the EFIT-like fuel elements. The fraction of americium decreases while at the same time more curium is generated. Curium has large fission cross sections in fast spectrum, e.g. more than seven barn for curium-243 compared to less than two barn for plutonium-239. The combined compositions from Table 7.9 and 7.8 are used for criticality calculations of EFIT. Figure 7.6 shows the resulting values for k_{eff} .

Naturally, the initial value for k_{eff} is also 0.96, because there is no irradiation history of the fuel. But with minor actinides and plutonium previously irradiated, k_{eff} increases. As a reference value, the upper limit of 0.983 for the effective multiplication factor during design based conditions is shown as well (Mansani et al. 2012). When the EFIT-like fuel elements were irradiated in the MYRRHA reactor in-pile test sections for 540 days or more, the neutron multiplication factor of EFIT is higher than allowed during operation. Therefore, recycling of the fuel is only possible with shorter irradiation times.

Several publications on EFIT mention $k_{eff} = 0.97$ instead of 0.96 as used in the computer model of this thesis. Modifying the computer model to start at 0.97 would have led to an offset resulting in the fact that the upper limit for the reactor during design based conditions is reached after even shorter irradiation histories.

In theory, one option to stabilize the criticality level could be to mix the plutonium and minor actinides in fractions according to their effect on reactivity. Plutonium and minor actinides are separated into different material streams during reprocessing anyway. Consequently, the fraction of plutonium in the newly fabricated fuel might as well be adjusted. It would imply detailed

¹² The unit pcm assigns percent millip with the reactivity ρ defined as $\rho = \frac{k_{eff}-1}{k_{eff}}$. It represents the fractional change of the neutron population per generation (United States Department of Energy 1993b). It is zero for steady-state operation and consequently the preferred figure for automatic control of the neutron population.

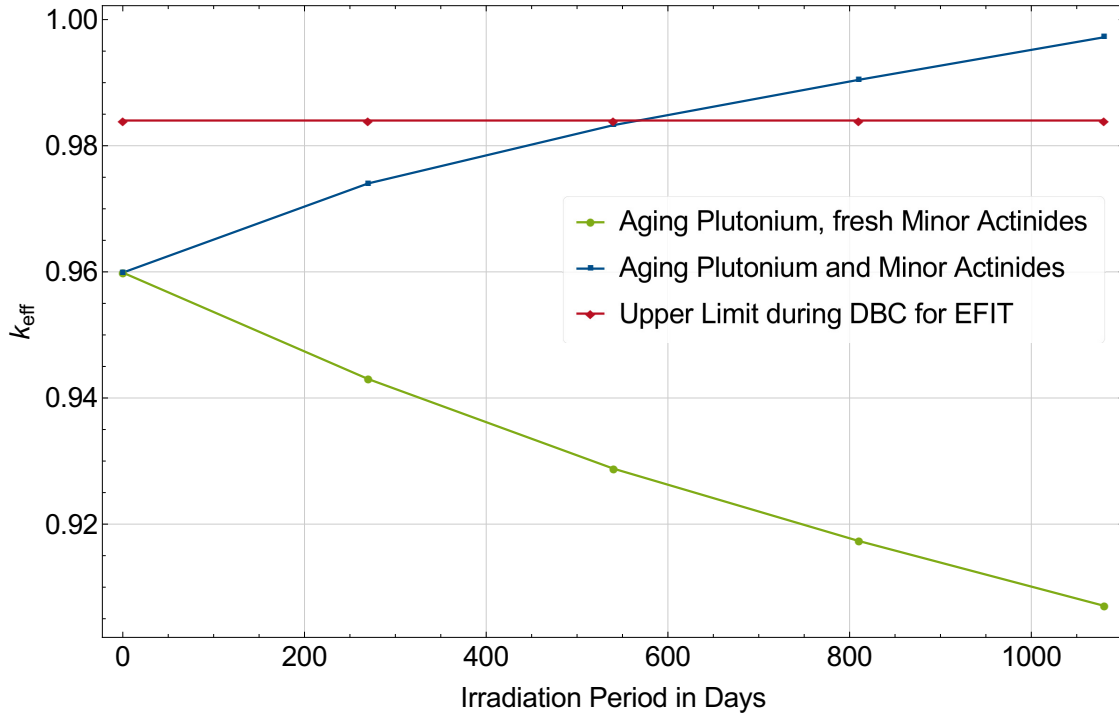


Figure 7.6.: Evolution of criticality in the EFIT reactor in dependence of the irradiation history of plutonium (plutonium and minor actinides) prior to fuel fabrication. The values derived from calculations with the initial minor actinide composition and the plutonium vector from previous irradiation periods are shown in green. The blue graph depicts k_{eff} for fuel made of both previously irradiated minor actinides and plutonium. As a reference, the upper limit for criticality during design basis conditions for EFIT is also plotted.

knowledge on the current isotopic composition, since not only the fission cross sections but also the neutron yield has to be taken into account for the new fuel. More importantly, this procedure might work against the premise for optimum minor actinide transmutation depending on the plutonium fraction in the fuel as well.

7.4.3 Plutonium Vectors from a European P&T Scenario

The previous calculations of k_{eff} for different fuel compositions are a limited approach to model the evolution of the actual fuel vector in a partitioning and transmutation scenario. For a more comprehensive picture, modeling of the whole fuel cycle including the different reactors and necessary cooling periods is advisable.

In the PATEROS study, this was done for an exemplary European scenario. Among others, the plutonium composition at certain times during the P&T implementation period were published (Salvatores et al. 2008). A double strata approach is investigated in some of the scenarios: there exist ADS for the transmutation of minor actinides while at the same time there is a fast reactor fleet present that uses the plutonium for energy generation. For the roughly 150 years of the scenario, the plutonium composition of the plutonium stock, the average plutonium composition in the fast reactor fleet and the average plutonium composition in the ADS are tabled after certain years. Table 7.10 shows the published vector for the plutonium composition in ADS fuel.

The difference to the initial plutonium vector used for the design of the EFIT reactor is evident. First and foremost, the fissile plutonium-239 fraction is increased by around 20 % while at the same time the fraction of the parasitic plutonium-240 fraction is reduced. Compared to the initial

Table 7.10.: The ADS stockpile plutonium vectors for regional scenarios given in the PATEROS report (Salvatores et al. 2008). The composition of the EFIT initial load is shown as a reference. Figures are given in weight percent.

	Pu-238	Pu-239	Pu-240	Pu-241	Pu-242
EFIT	3.77	46.56	34.10	3.82	11.74
2060	1.88	63.21	25.49	1.35	8.07
2100	1.41	58.99	30.85	0.19	8.56
2150	0.96	59.42	30.96	0.02	8.64
2190	0.70	59.64	30.98	0.00	8.68

load of EFIT, the plutonium composition stays relatively constant over the PATEROS scenario. The plutonium-239 fraction for example ranges from 60 % to 63 % while it is at 46 % in the initial load. There are no figures given for the evolution of the minor actinide vector in the stockpile.

Hence, for the calculation of k_{eff} of the EFIT reactor, the initial minor actinide composition was combined with the published plutonium vectors. Table 7.11 lists the calculated values for k_{eff} . There are only small changes in the criticality of the accelerator-driven system during the partitioning and transmutation scenario, but the values are enormously high. The value of 1.6 for k_{eff} is not only by far beyond the definition of a sub-critical reactor core, it lies also well above the range in which normal critical reactor operation takes place.

Table 7.11.: Criticality calculated for the EFIT reactor using plutonium compositions in a P&T scenario at certain years during the PATEROS implementation scenario (7.10).

	EFIT	2060	2100	2150	2190
k_{eff}	0.96	1.63	1.59	1.59	1.59

The simulation code used in PATEROS allows the adjustment of the fissile isotope fraction in the fuel in such a manner that their content remains constant with changing composition (Salvatores et al. 2008, p. 10). To do so, the code uses predefined equations for thermal and fast neutron spectrum. It is not clear to what extent these equations can be used for P&T-fuel with increased minor actinide content. Due to these uncertainties and for simplification, in the above calculations of k_{eff} no adjustment of the fissile isotope fraction in the fuel was performed.

A rough estimation of the needed reduction is done using fuel elements with transuranium elements that have been irradiated for 540 days prior to fuel fabrication. Several calculations of the neutron multiplication factor with different fissile material fractions were conducted. In the initial design, the fuel contains either 43 % or 50 % fissile isotopes, depending on the position in the core. If these fractions are reduced to 35 % and 40 %, k_{eff} results in ≈ 0.97 . In reality, such a reduction cannot be achieved without further analysis of the resulting system: the fraction of the fissile isotopes in the fuel does not only determine the criticality of the system but also influences safety relevant parameters, such as the different reactivity coefficients. Since the plutonium fraction in the fuel is based on atomic densities, the reduction of fissile isotopes leads to a comparably high increase of magnesium oxide in the fuel, if the density is set to remain constant.

The plutonium and minor actinide composition is the base to pellet composition and geometry and, subsequently, to fuel element and core design of the EFIT reactor core (cf. Figure 5 in Mansani et al. (2012)). Therefore, the reactor design is based on conditions that only mirror the initial load and not reactor operation during a more realistic scenario which was for example developed in the PATEROS study. The EFIT reactor is explicitly mentioned as the example used for accelerator-driven transmutation systems (Salvatores et al. 2008; Abderrahim 2013). Its purpose in the

implementation scenarios is minor actinide burning, exactly the task it is designed for. Still, the scenario does not match the official design description of the core.

Setting aside the possible operation, maintenance and safety implications of a reduced fissile material content, the resulting reduced minor actinide core load also influences the overall P&T scenario. All scenarios are designed that after a certain time period, either the inventory of minor actinides is stabilized or reduced to (practically) zero. From this, implementation time frames for the overall P&T strategy and the number of needed transmutation facilities are derived. A fissile material content of approximately only 80 % of the initial value is estimated to keep the reactor sub-critical. Therefore, more facilities will be needed if the same throughput shall be reached. At the same time, for an optimum load factor of the transmutation facilities, the number of facilities has to decrease over the implementation period because the minor actinide stockpiles decline. This number of facilities is of course also influenced by the fissile material inventory per accelerator-driven system transmutation facility.

7.5 Characteristics of the Spent Fuel Elements

One crucial point in assessing possible implementation scenarios for P&T fuel cycles are the objectives of the participating countries. At least in Europe, several countries phase-out nuclear energy or at least do not want to increase the nuclear share in their energy production. The objective for these countries in participating in a P&T scenario could be to deal with their spent fuel legacy. When deciding whether or not transmutation is an option, the anticipated duration until a certain P&T objective is met is of interest. One objective might for example be the reduction of the minor actinide inventory to 10 % of the initial inventory. It is already established knowledge, that several transmutation cycles in dedicated facilities are necessary, even though the number itself is unknown. The overall time is also greatly influenced by the time needed for reprocessing of the spent fuel elements and the subsequent fuel fabrication and the necessary cooling periods before doing so. Assumed values range from about two up to eight years, with eight years already considered to be a conservative estimation (Kirchner et al. 2015). For the simulation of a P&T fuel cycle scenario, an exemplary cooling period of five years and a fuel fabrication time of two years is implemented in Salvatores et al. (2008). No explanation for these values is given in the reference.

Several aspects rooted in the characteristics of the spent fuel elements influence the overall P&T scheme. It starts with transportation of the spent fuel to the reprocessing facility for which heat and neutron dose rates are limiting factors. It can always be argued that for the P&T fuel cycle and the P&T-fuel itself new technologies have to be developed and that current technology should not be the reference. As an illustration, it is true that the transportation casks used for spent fuel elements could be loaded with fewer fuel elements, allowing for higher dose and residual heat rates of single fuel elements. But for the reprocessing itself, the activity of the material is then restricted by radiation protection regulations and the used chemicals depending on the process. Once more, for the P&T fuel cycle improved partitioning processes are needed. The separation efficiency for the minor actinides is one crucial point for the whole partitioning and transmutation concept. Finally, staff in all related nuclear facilities must be protected from radiation. How this can be achieved depends heavily on the envisioned technical processes and the facility designs.

It seems like an oversimplification when several critical points are dismissed by saying that appropriate technology will be developed in due time. To illustrate possible challenges for design and development of suitable technology, in the following some of the key parameters of the spent fuel elements are analyzed in more detail. This includes the activity of the spent fuel, the residual heat from the spent fuel elements and the gamma dose rates.

7.5.1 Activity

The activity of the spent fuel is an intrinsic material property that does not depend on the geometry of the spent fuel elements. It affects the measures necessary for safe handling of the material as well as the chemicals that are used for reprocessing of the spent fuel. High radiation degrades the chemicals and they might react with the solvents in the separation process to form *red oil* which is easily exploding at temperatures above 135 °C (IRSN 2008). The activity of the spent fuel originates from two groups of elements in the fuel: the instable fission and activation products and the fissile isotopes, in this case the transuranium isotopes. The latter is also referred to as the intrinsic activity of the fuel. The contribution of the fission products rises with higher burn-up of the fuel elements since more fission products have already been produced then, while at the same time the fraction of the transuranium isotopes declines.

The activity of the spent fuel for different irradiation times is derived from the burn-up calculations for the EFIT-like fuel elements. Figure 7.7 depicts the total activity in Becquerel per volume for different times after discharge. The graphs start after a short cooling period to eliminate the contribution of the very short-lived fission products, some of them with half-lives of only several seconds. Naturally, activity coming from the fuel with a low burn-up is the smallest. With increasing burn-up, the values for the different irradiation times are converging in the long term. The longer time in the core increases the fraction of isotopes with intermediated half-lives that decay during irradiation. From the graph it is evident, that after four years other isotopes with longer half-lives become more important.

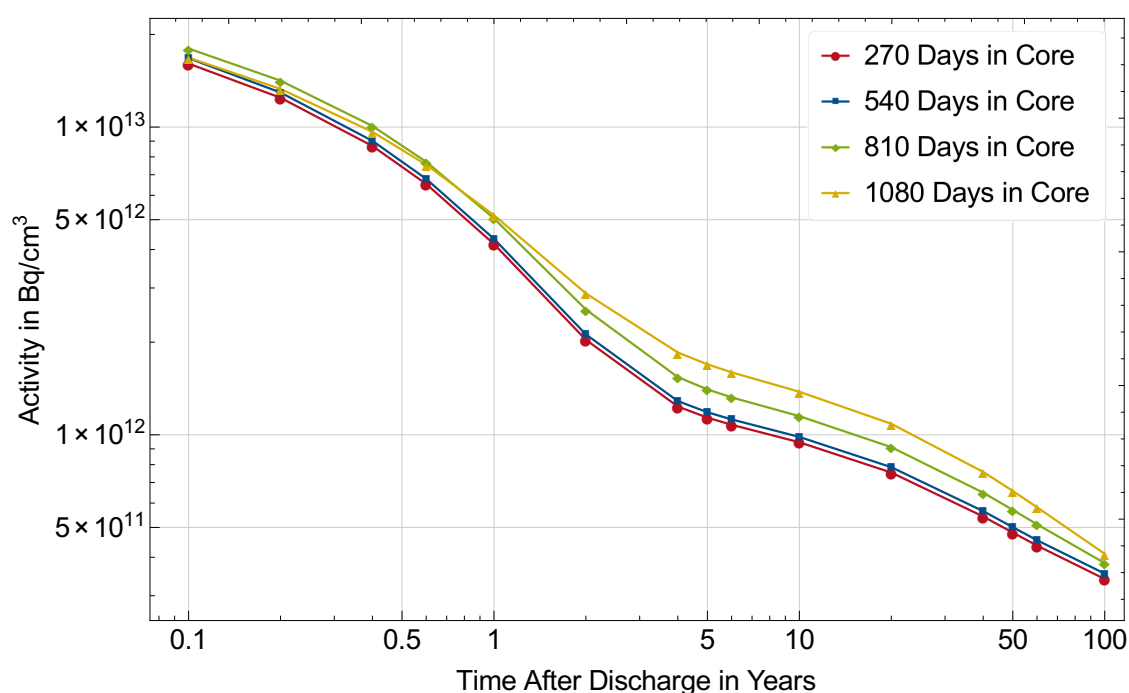


Figure 7.7.: Activity of spent P&T-fuel in dependence of the time after discharge for different irradiation times in the core. It takes almost five years for the activity to drop to one tenth of its initial value.

The combined α - and β -activity of the spent fuel is 16.8 TBq per cm³ for the spent fuel with the highest burn-up. It takes almost five years for the activity to drop to one tenth of its initial value. After a cooling period of one century, the average value is roughly 400 GBq per cm³, about 2.5 % of the initial value. Calculations were done for fuel containing 43 % and 50 % fissile material, but only the values for the higher fraction are plotted. They correspond to fuel positioned in the outer

zone of the EFIT core. Looking at the activity per volume of the spent fuel corresponding to the inner elements, the values are less than 5 % lower at all times.

It is impossible to know activity limits at the current stage of R&D activities for the P&T fuel cycle. Hence, the best option to assess the resulting values is comparison to today's conventional spent fuel. After 40 years of cooling, the spent fuel with higher burn-up from the outer zone of the transmutation facility has a combined α - and β -activity of $7 \cdot 10^{11}$ Bq/cm³. Average BWR spent fuel with a burn-up of 48 MWd/kgHM and after the same cooling period has a β -activity of $9 \cdot 10^{10}$ Bq/cm³. This value is calculated assuming an average fuel density of 10 g/cm³ (McGinnes 2002). For spent thermal reactor fuel, the α -activity is usually less than one tenth of the total activity after the cooling period of only one decade (ibid.).

Besides possible implications on reprocessing chemistry, the activity of the spent fuel is the determining factor when assessing the effects of possible nuclear accidents and the impact on workers in fuel cycle facilities. In case of release of radioactive material, the possible exposure of the public has to be calculated. Even though in this regard usually only a few isotopes are relevant, a eight-fold increase in total activity is not negligible. For the implementation of a P&T fuel cycle, there will be additional nuclear facilities at several sites, increasing the risk of exposure to larger fraction of the population.

The calculated values for the total activity and the α -activity of the spent P&T-fuel after selected cooling periods are given in Table 7.12. The α -activity is approximated by summing the activity of all transuranium elements except plutonium-241 and americium-242. This approximation is reasonable, since the transuranium elements in general account for more than 99% of the total α -activity of spent fuel in the short term (Fanghänel et al. 2010, p.2982). Also, except for plutonium-241 and americium-242, α -decay is their most likely decay mode. The branching ratio for spontaneous fission is often up to ten orders of magnitude lower. The ratio of α -activity and spontaneous fission rates changes with longer cooling periods due to the change in the most contributing isotopes. It can be seen from Table 7.12 that the contribution of the transuranium elements to the total activity increases with increasing cooling period. Directly after discharge, several short-lived fission and activation products are present in the spent fuel. With their vanishing, the contribution of the transuranium elements becomes more important. After a cooling period of 100 years, more than 80 % of the total activity is due to α -decay.

Table 7.12.: The total activity, the α -activity and the spontaneous fission rate per volume for one EFIT-like fuel element irradiated for 1080 full power days in the MYRRHA reactor. The spontaneous fission rate is calculated only considering plutonium-238, plutonium-240, plutonium-242, curium-242, and curium-244.

Cooling Period	Activity Bq/cm ³	α -Activity Bq/cm ³	Spont. Fission Rate 1/(s·cm ³)
0. years	$5.11 \cdot 10^{13}$	$9.05 \cdot 10^{12}$	$1.16 \cdot 10^6$
0.1 years	$1.68 \cdot 10^{13}$	$7.93 \cdot 10^{12}$	$1.09 \cdot 10^6$
0.6 years	$7.54 \cdot 10^{12}$	$4.19 \cdot 10^{12}$	$8.48 \cdot 10^5$
1. years	$5.17 \cdot 10^{12}$	$2.71 \cdot 10^{12}$	$7.48 \cdot 10^5$
5. years	$1.70 \cdot 10^{12}$	$9.18 \cdot 10^{11}$	$5.52 \cdot 10^5$
10. years	$1.38 \cdot 10^{12}$	$8.32 \cdot 10^{11}$	$4.56 \cdot 10^5$
40. years	$7.58 \cdot 10^{11}$	$5.37 \cdot 10^{11}$	$1.46 \cdot 10^5$
100. years	$4.10 \cdot 10^{11}$	$3.40 \cdot 10^{11}$	$1.63 \cdot 10^4$

For the spent fuel from the small, fast reactor analyzed in chapter 6, the activity 40 years after discharge is $6.34 \cdot 10^{10}$ Bq/cm³ and the α -activity $7.66 \cdot 10^8$ Bq/cm³. The absolute values are significantly lower than in the P&T-fuel. The α -decay plays a less important role in this spent fuel,

it comprises less than 1 % of the total activity. Alpha particles can be easily shielded. The α -activity is in principal relevant for the case of accidental ingestion and the interaction of the spent fuel with the reprocessing chemicals.

The neutron background originating from the spent fuel determines the required shielding for fuel handling. The higher it is, the heavier the shielding must be. Neutrons are produced in the spent fuel by spontaneous fission, nearly exclusively by plutonium-238, plutonium-240, plutonium-242, curium-242, and curium-244. Preliminary calculations were performed to show that it is sufficient to consider these five isotopes for the neutron activity of the spent fuel from the EFIT-like fuel elements. The last column of Table 7.12 lists the calculated spontaneous fission rates.

The spontaneous fission rate is $1.16 \cdot 10^6 \text{ 1/(s} \cdot \text{cm}^3)$ directly after discharge. It declines visibly, because the contributing actinides have comparably short half-lives (cf. Table 1.2). After a cooling period of 100 years, the rate is about 1.5 % of its original value. The neutron activity for the fuel during the first year after discharge from a fast breeder is reported in Orlov et al. (1974). After a cooling period of twelve months, the number of produced neutrons per second per kilogram is reported to be $0.7 \cdot 10^6$. Assuming an average MOX density of 10 g/cm^3 and approximating the average number of neutrons per fission with three, this results in a spontaneous fission rate of about $2,333 \text{ 1/(s} \cdot \text{cm}^3)$. The neutron rate generated by the fast breeder reactor fuel is more than two orders of magnitude lower than the neutron rate from the transmutation fuel after a cooling period of one year. Again, this result shows that the build-up of curium during burn-up poses severe challenges to reprocessing and fuel fabrication in a P&T fuel cycle due to its high spontaneous fission rate (cf. Table 1.2).

7.5.2 Heat Development

The residual heat from the spent P&T-fuel elements is a factor that complicates fuel handling. On-site cooling periods must be sufficiently long to allow for transportation and eventually reprocessing. Figure 7.8 depicts the evolution of the residual heat after an in-core period of 270 FPD and 1080 FPD. Almost directly after removal from the core, the P&T-fuel elements emit close to 100 kW of heat. This figure drops to a value of around 5 kW within three years. After 100 years of interim storage, the heat is only about two percent of the original value. In the first years, one main contributor to the heat is curium-242. The curium-242 is built during reactor operation via β^- -decay of americium-242. Hence the accumulation cannot be avoided if fuel enriched in minor actinides is used. In the end, it might be even necessary to rethink the use of fuel containing curium (IAEA 2015, p. 204). It is also known, that with equilibrium operation of the P&T fuel cycle, the curium content in the fuel will most likely increase (NEA 2005).

There is a rule of thumb to calculate the decay heat after shutdown for a nuclear power reactor. The decay heat usually declines to less than 1 % within one hour after shutdown (United States Department of Energy 1993b). The calculated residual heat of the spent P&T-fuel elements is, however, almost 1 kW each one year after discharge. With 180 fuel elements present in the EFIT reactor, this totals 3.6 MW or almost 1 % of the thermal output (400 MW). Therefore, the common rule of thumb cannot be applied at all to P&T-fuel.

The residual heat of the fast breeder BN-600 spent fuel elements is also plotted for a better understanding of the calculated values. It starts with 9 kW, about one tenth of the heat from the P&T-fuel elements, and declines within one year to 1 kW per element. The fuel elements of the BN-600 are small compared to modern standards. They only contain 23 kg dioxide. The P&T-fuel elements in contrast contain either 38.6 kg or 47.7 kg of fuel material in total, depending on the position in the core. Decay heat from uranium oxide elements coming from thermal reactors is even smaller, lying roughly one order of magnitude below the values for MOX and fast reactor fuel (Ade et al. 2011; Ragheb 2011).

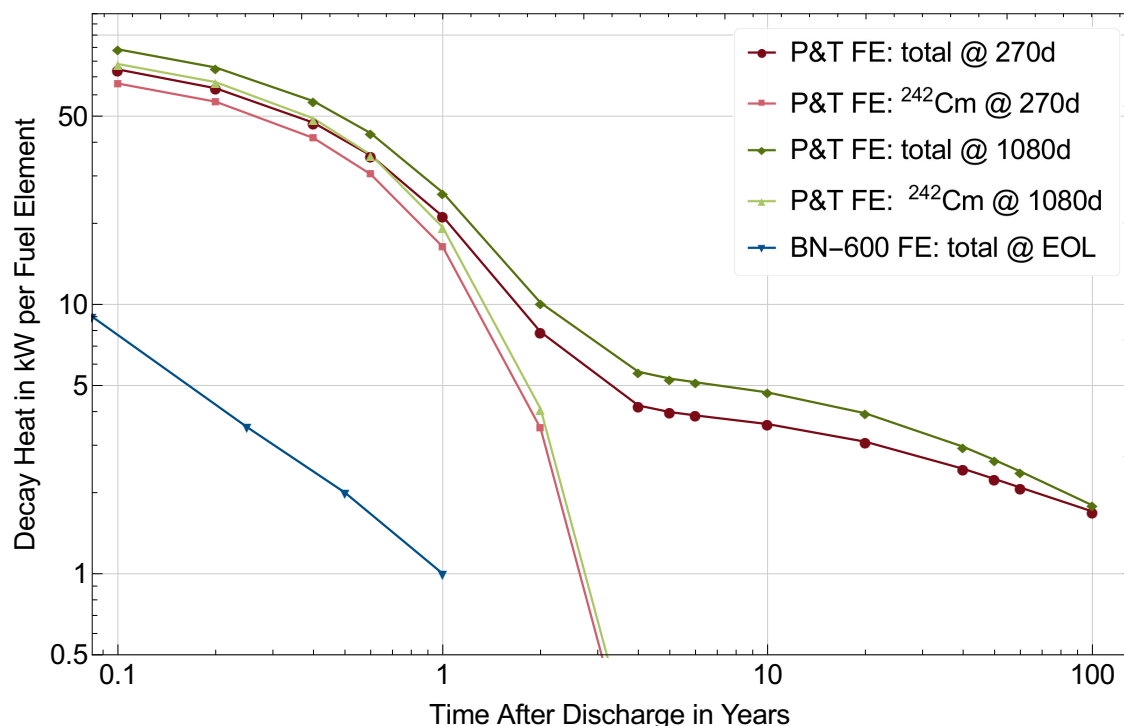


Figure 7.8.: Calculated decay heat for one P&T-fuel element after an irradiation period of either 270 FPD or 1080 FPD. The contribution of curium-242 is plotted separately. The residual heat from a BN-600 fast breeder fuel element is taken from Orlov et al. (1974).

Average values for the decay heat after certain cooling periods for exemplary bundles and elements of spent fuel are tabled in McGinnes (2002). No explicit values for MOX fuel are mentioned, only cumulative values the different types of spent fuel transportation casks containing several fuel elements each. Type number one consists of 9 UO_2 fuel elements and type number two of 3 UO_2 and one MOX element. Combining this information, reference residual heat for one MOX spent fuel elements could be derived. Even though irradiated in thermal reactors, the high fraction of plutonium results in a residual heat comparable to that of fast reactor fuel. Nevertheless, the absolute value after a cooling period of 40 years is lower than 1 kW. The MOX fuel elements contain 322 kg of spent fuel and thus significantly more than the EFIT fuel elements, but emit less heat.

P&T-fuel elements at different reactor positions (cf. Figure 7.2) are exposed to different irradiation conditions and subsequently differ in burn-up. Regarding the decay heat, these differences are very small. As shown in Figure 7.9, the heat emitted by one element from the inner and the intermediate zone is nearly the same. This changes for the outer zone, where more fissile material and consequently, after removal from the core, more fission products are present.

Table 7.13 lists exemplary figures for the residual heat after a cooling period of four years for the different fuel zones and irradiation times. Longer irradiation results in a higher generation of fission products and therefore in a higher decay heat. The overall difference between the zones and irradiation times is small compared to the impact of the duration of the cooling period after removal from the core. Examining the trend of the curves in Figure 7.8, it is also clear that the cooling period should last at least four years. After this period, the decay heat declines less quickly. Still, after five years the spent fuel elements emit several kilowatts of heat, therefore posing a challenge to cooling and transportation options.

Even when waiting for a century before reprocessing, a time span practically impossible in P&T fuel cycle scenario, the decay heat is still at least one order of magnitude higher than the one originating from conventional spent fuel elements. Even for MOX spent fuel elements, it takes less

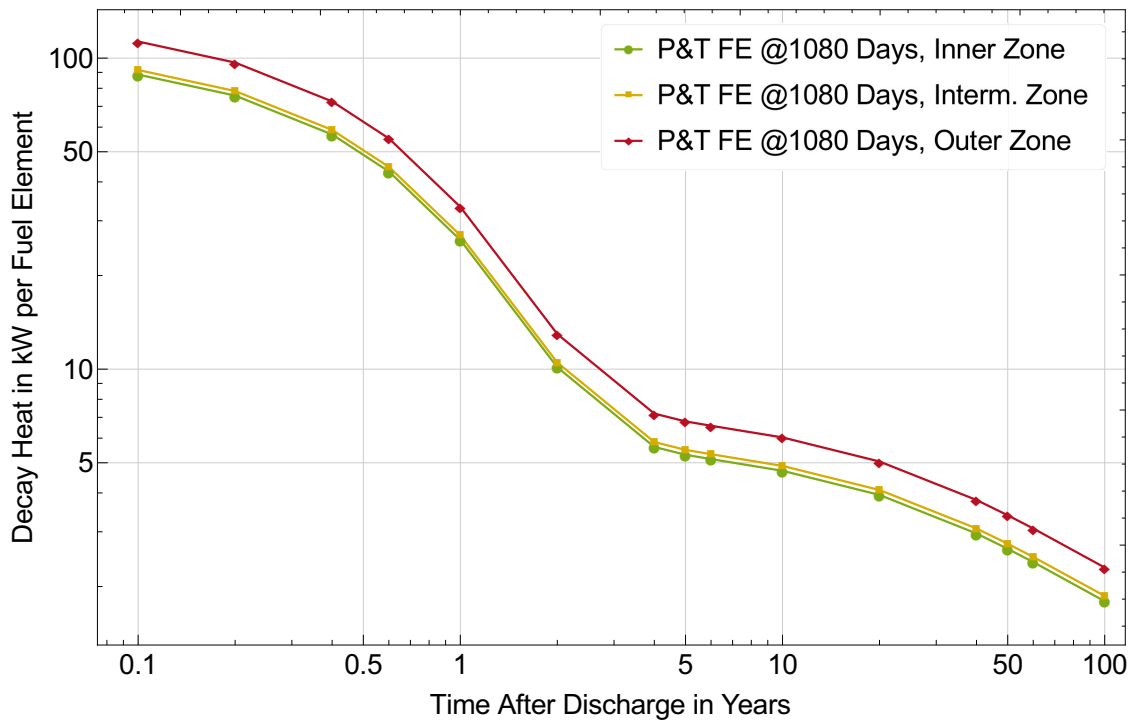


Figure 7.9.: Calculated decay heat for one EFIT fuel element from each fuel zone after an irradiation period of 1080 days. After the first four years, the decay heat declines only slowly.

than 40 years for the residual heat to fall below 1 kW. Estimations show that a P&T scenario might easily last for hundreds or even thousands of years if at the same time a nuclear reactor fleet for power generation is maintained (Lyman and Feiveson 1998; IPFM 2015b, p. 105).

Table 7.13.: Calculated decay heat for single EFIT fuel elements with different burn-ups after a cooling period of four years.

	Inner Zone	Intermediate Zone	Outer Zone
270 Days	4.2 kW	4.4 kW	5.4 kW
540 Days	4.9 kW	5.1 kW	6.2 kW
810 Days	5.3 kW	5.5 kW	6.8 kW
1080 Days	5.6 kW	5.8 kW	7.2 kW

Noteworthy, the current procedures used for calculating the decay heat for safety analysis are not appropriate for advanced fast reactors. To simplify computer simulation, pre-calculated curves for the decay heat are usually used. The American Nuclear Society provides a pre-calculated curve, the ANS-79 decay heat curve, which is by default used in the RELAP5 code for thermo-hydraulic analysis of reactor dynamics. Using this curve for advanced fast reactors, all safety limits are satisfied. Using decay data derived from calculations for advanced fast reactors, the cladding temperature limit was not met. Consequently, the standard procedures and rules of thumb for the calculation of the decay heat can especially not be used for P&T-fuel elements (Shwageraus et al. 2009).

7.5.3 Gamma Dose Rate

The last analyzed factor influencing the requirements set on spent fuel handling and reprocessing is the gamma dose rate. It is generally accepted that spent fuel elements can be seen as being

self-protecting, because they emit such high radiation dose rates that handling is only possible using specialized equipment and facilities. But a higher radiation also complicates the whole procedure of reprocessing and makes it more expensive. The penalty of plutonium rich fuel on reprocessing can already be seen by the increased needs required by MOX fuel. Consequently, MOX fuel is economically not competitive to pure uranium fuel even though its reuse of the *resource* element plutonium is advertised as being beneficial (Mueller 2013; IPFM 2015b, p. 112; Deutch 2009).

The gamma dose rates in one meter distance for EFIT fuel elements from different core positions are calculated. The results for elements from the outer fuel zone with a burn-up equaling 270 FPD and 1080 FPD of irradiation are shown in Figure 7.10. Shortly after discharge from the core, the dose rates are extraordinarily high, lying in the range of 800 Sv/hr. Due to the fast decay of short-lived fission into stable products, the dose rates decline quickly. The build-up and decay of short-lived fission products explains the different behavior of the graphs originating from high and low burn-up: The gamma dose rate is always lower for the elements that were irradiated for a shorter time period before discharge, because less fission products are produced.

During exposure in the core, mostly shorter-lived fission products already decay again. The longer the fuel element is irradiated in the core, the more the concentration of short-lived fission products approximates an equilibrium state. For the fuel with higher burn-up, the contribution of the short-lived fission products to the dose rate is thus smaller than for fuel with low burn-up. After removal from the core, the isotopes continue to decay but the effect on the derived dose rates is stronger for the case where the contribution of the short-lived fission products is higher. Consequently, the dose rates for the spent fuel elements that were irradiated only 270 days drop faster.

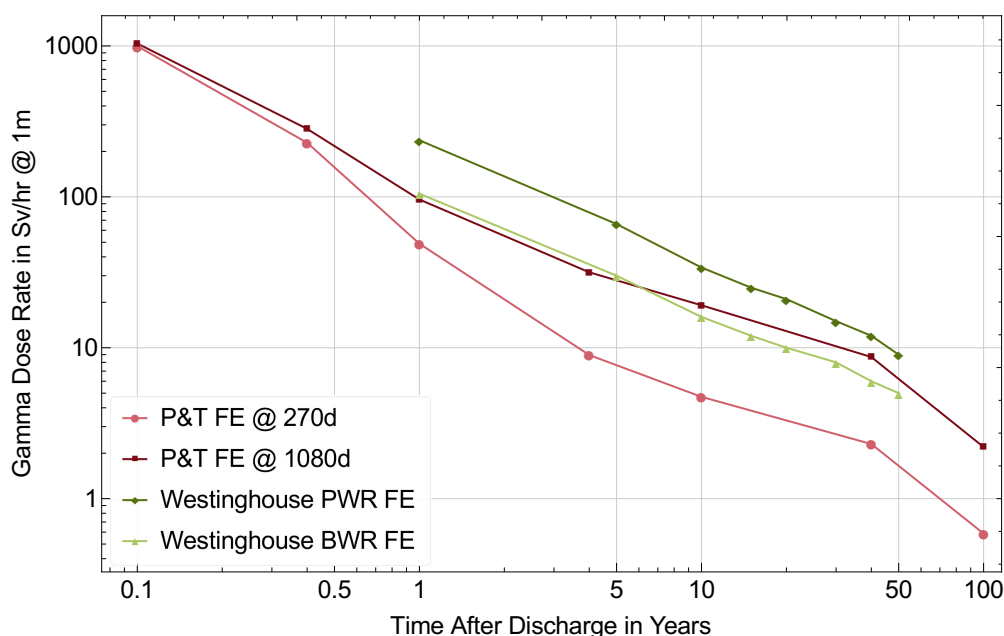


Figure 7.10.: Gamma dose rates in one meter distance for P&T-fuel elements with different burn-ups after certain cooling periods (fuel load 47.7 kg). Reference values for a Westinghouse PWR and a General Electric BWR fuel elements are also shown. BWR fuel contains also several times more heavy metal than the P&T-fuel elements (fuel load 470 kg).

The overall values are rather small compared to published values for the gamma dose rates emitted from spent fuel elements of a Westinghouse pressurized and boiling water reactor as also plotted in Figure 7.10. The values were calculated at one meter distance perpendicular to the fuel element at the center with a burn-up of 30 MWd/kgHM (Loyd et al. 1994). In general, the dose rates from a BWR are nearly twice as high as the dose rates from of a PWR spent fuel element.

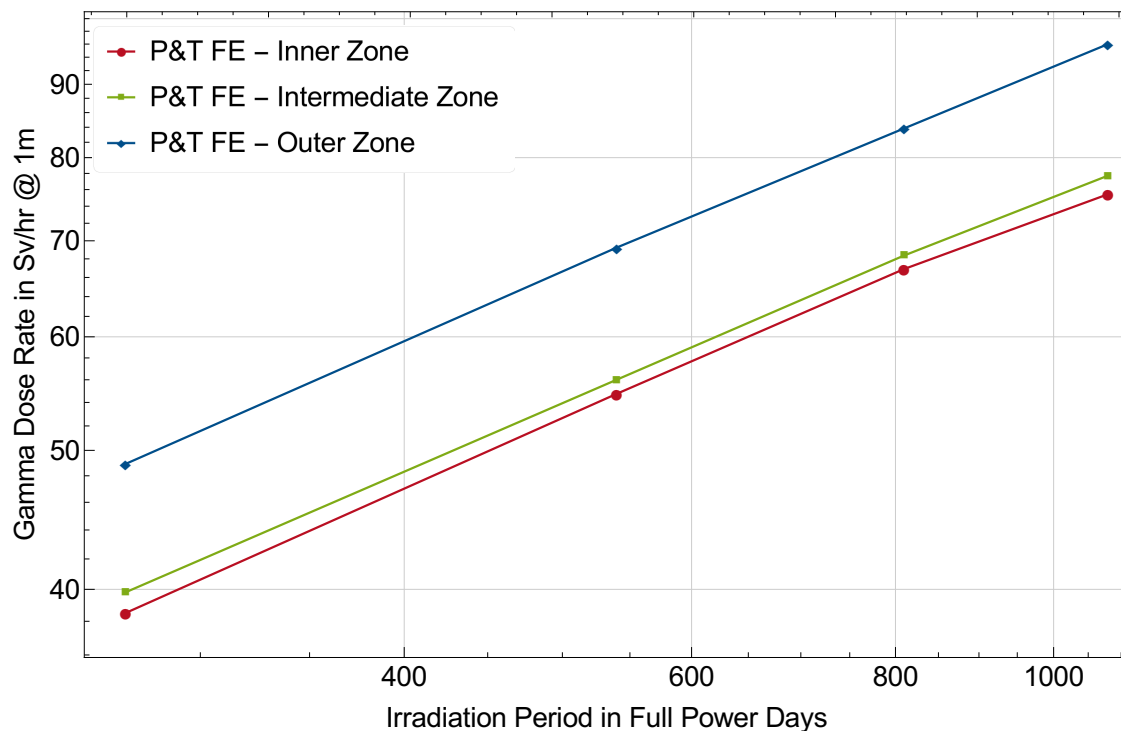


Figure 7.11.: Gamma dose rates for spent P&T-fuel elements discharged from the different zones of the EFIT core against burn-up after a one year cooling period.

The higher dose rates from the thermal reactors can be accounted to the fact that complete fuel elements are considered in this kind of analysis. Whereas a P&T-fuel element only contains 47.7 kg of fuel, the heavy metal content of the pressurized water reactor fuel elements is nearly ten times as high, weighing 470 kg (Lloyd et al. 1994). The exact heavy metal content of the BWR fuel element is not specified. But it is also several times higher than in the spent P&T-fuel elements. If the emitted gamma dose rate is normalized to the mass, neglecting the self-shielding of the fuel, the dose rates from the thermal reactor spent fuel fall significantly below the values of the spent P&T-fuel. This is in particular the case for P&T-fuel with a burn-up of 1080 FPD. Five years after discharge, the P&T fuel emits about the ten-fold dose rate per kilogram fuel than the BWR spent fuel.

The gamma dose rate from the P&T-fuel elements can also be compared to the dose rates of the BN-800 (Frieß and Liebert forthcoming 2017). Figure 5.4 shows that the BN-800 fuel elements emit a high gamma dose rate of 400 Sv/hr after a one year cooling period. This value declines quickly. After a cooling period of only five years the dose rate from the BN-800 spent fuel elements is roughly the same as the dose rate from the P&T-fuel elements after a short irradiation and it continues declining. It is unclear to what extent these values are representative for fast reactor fuel because of the weapon-grade plutonium in the BN-800 fuel elements.

In regard to the proliferation risk posed by the material contained in the spent fuel elements, an element that emits a dose rate of 1 Sv/hr or more it is usually considered to be self-protecting. The radiation requires sophisticated technology for handling and reprocessing. After one century, the gamma dose rates of the spent fuel element with the high burn-up is still higher than the threshold. Also for the shorter irradiated elements, it takes at least 50 years of cooling. In the light of accessibility of the fissile material for a potential proliferator the elements are not very attractive. The above discussed dose rates are all derived from a spent fuel element of the outer core zone. These elements contain more fissile material than elements from the inner and intermediate core zone. The influence of this increased mass is seen in Figure 7.11 after a one year cooling period. The inner and the intermediate zone differ in regard to the fraction of the fissile material in the

fuel matrix (43 % and 50 %). This difference is reflected in the decrease of the gamma dose rates originating from intermediate and inner zone spent fuel elements. The gap to the spent fuel elements is about 10 Sv/hr and does hardly depend on the burn-up in the core.

In the PATEROS study, a cooling period of five years before reprocessing is assumed for the scenario analysis (Salvatores et al. 2008). Therefore, in Table 7.14 the gamma dose rates in one meter distance for the different EFIT fuel elements are presented five years after discharge from the core. The values are calculated using the material compositions derived from the burn-up simulation of the EFIT-like fuel elements in the IPS of the MYRRHA reactor and the actual EFIT geometry. The irradiation period in the core is the most important factor when assessing the gamma dose rates. After a five year cooling period, the dose rates from spent light water reactor fuel lie in the range between 20 Sv/hr and 60 Sv/hr (Loyd et al. 1994; IPFM 2011, p. 13). Even with the highest analyzed burn-up, the P&T-fuel elements emit a lower dose rate due to their significantly lower mass per fuel element.

Table 7.14.: Calculated gamma dose rates from spent P&T-fuel elements for various irradiation times after a five year cooling period.

Burn-up	Inner Zone Sv/hr	Intermediate Zone Sv/hr	Outer Zone Sv/hr
270 Days	5.4	5.6	6.9
540 Days	10.8	11.1	13.8
810 Days	16.1	16.6	20.4
1080 Days	21.0	21.8	26.9

For the above mentioned PWR and BWR elements it is shown, that even in a conservative estimate the gamma dose rate is more than 10^5 times higher than the neutron dose rate (Loyd et al. 1994). Exemplary calculations for the P&T-fuel elements also show several orders of magnitude difference between neutron and gamma dose rate. But the significantly lower neutron dose rates do not reflect the actual problem appropriately. Neutrons cannot be shielded as easily as gamma particles. It is essentially impossible to do so within current fuel fabrication facilities.

7.6 Inventory of Long-lived Fission Products

The discussion on transmutation is mainly restricted to minor actinides and their fraction in the high level waste which will finally be sent to a deep geological repository. In this section, the influence of long-lived fission products is investigated in greater detail. First, their importance for the long-term safety analysis of a deep geological repository is explained. Then, the concentration of selected long-lived fission products in the spent P&T-fuel is calculated. The effect of a P&T fuel cycle on the total inventory of long-lived fission products which have to be sent to final storage is derived. The analysis is based on a simplified scenario for Germany.

7.6.1 Importance for Long-term Safety Analysis

The reduction of the radiotoxicity of the nuclear waste is often used to argue in favor of a P&T fuel cycle. Figure 1.1 showed that the radiotoxicity of untreated nuclear waste declines very slowly. It takes geological time scales to reach a level compared to that of a uranium ore. If the minor actinides are transmuted into stable isotopes or isotopes with a much shorter half-life, the time scale is significantly reduced. The value of transmutation of minor actinides appears obvious. But this figure mirrors a simplified case: the used definition of the radiotoxicity assumes that the total waste inventory is consumed by the population. This can be seen as a very conservative

estimation since ingestion of radionuclides yields the highest dose rates. Yet, it neglects the probability of such an ingestion. Consequently, it is usually not used as a reference value when assessing a deep geological repository in regard to the risk it would pose to future generations. If the potential exposure to the public by such a deep geological repository is to be calculated, there are many more parameters that need to be taken into account (Brasser et al. 2008). In contrast to the intrusion or repository-breach scenario, where the whole radionuclide inventory is ingested, the underlying scenario for the long term safety assessment is a leach-and-migrate scenario. In this case, the repository functions more or less as planned and is not compromised from the outside. Regardless, after a certain time span, the man-made barriers will fail. Some of the nuclides will eventually dissolve from the host matrix and will be transported to the surface where they might affect the population.

This relevant safety scenario goes beyond the sole composition of the radioactive waste in the geological repository which is used for the radiotoxicity calculation. Instead, the repository system as a whole has to be analyzed, because different nuclides behave differently in the host matrix. Possible questions are: how long will the host matrix stay intact and prevent radionuclides from diffusion and subsequent release into the biosphere? Which radionuclides are more likely to dissolve? Which release paths are dominating? The answers to these questions also depend on the geological formations, which are site-specific and might vary over time. Beside ongoing changes such as erosion and denudation processes, sudden events, such as seismic activity or volcanic eruptions, can affect the repository. The long term safety analysis of a deep geological repository tries to cover all these aspects as best as possible. Among others, it estimates the radioactive dose humans will receive in the future from the repository. Unlike the radiotoxicity index, where the value is compared to the value for an unspecified natural uranium ore, the estimated dose rate originating from the future repository is compared to what is considered to be an acceptable exposure today. This also explains why they result in very low values compared to the calculated ingestion dose rates.

The approach explained above is by far more complex than simply using the total radioactive inventory and multiplying it by the appropriate conversion factors to calculate the ingestion dose rates. It starts with the fact, that for example the host matrix in which the deep geological repository is placed must be considered. Granite, clay, salt, or tuff affect the mobility of certain nuclides differently.

But in all cases, the dose rate emitted from the deep geological repository is dominated by some long-lived fission products when looking at time scales beyond 10,000 years (IAEA 2004, p. 98). In Mol, Belgium, the clay dome repository SAFIR-2 is planned. Exemplary calculations show that, in the long term, among the most influential nuclides are selenium-79, technetium-99, tin-126, and iodine-129 (Preter et al. 2001; G. Schmidt et al. 2013). For the planned swiss deep geological repository, also to be placed in clay, selenium-79 and iodine-129 are calculated to be the most relevant isotopes after 100,000 years (Nagra 2002, p. 261). For the long-term safety of repositories in other host matrices, zirconium-93 and cesium-135 play an important role as well (IAEA 2004, p. 98). zirconium-93 is in so far interesting as it is produced by neutron irradiation of zirconium alloys which are often used as cladding material for the fuel pins.

Assuming that an efficient transmutation fuel cycle can be implemented, and that uranium, plutonium and the minor actinides are almost completely removed from the spent fuel, the main contributors to the radiotoxicity will be the fission products. Figure 7.12 shows that in this case, after 1000 years of decay, the radiotoxicity is dominated by only a few fission products for typical high level waste made from PWR spent fuel. In a time frame of up to 100,000 years, the dose rate is dominated by the technetium-99 inventory. Afterwards, iodine-129 dominates. This mirrors the fact that even the long-lived fission products greatly differ in regard to their lifetime: while technetium-99 has a half-life of 211,100 years, the half-lives of iodine-129 and cesium-135 are more than ten times longer. Table 7.15 summarizes these values.

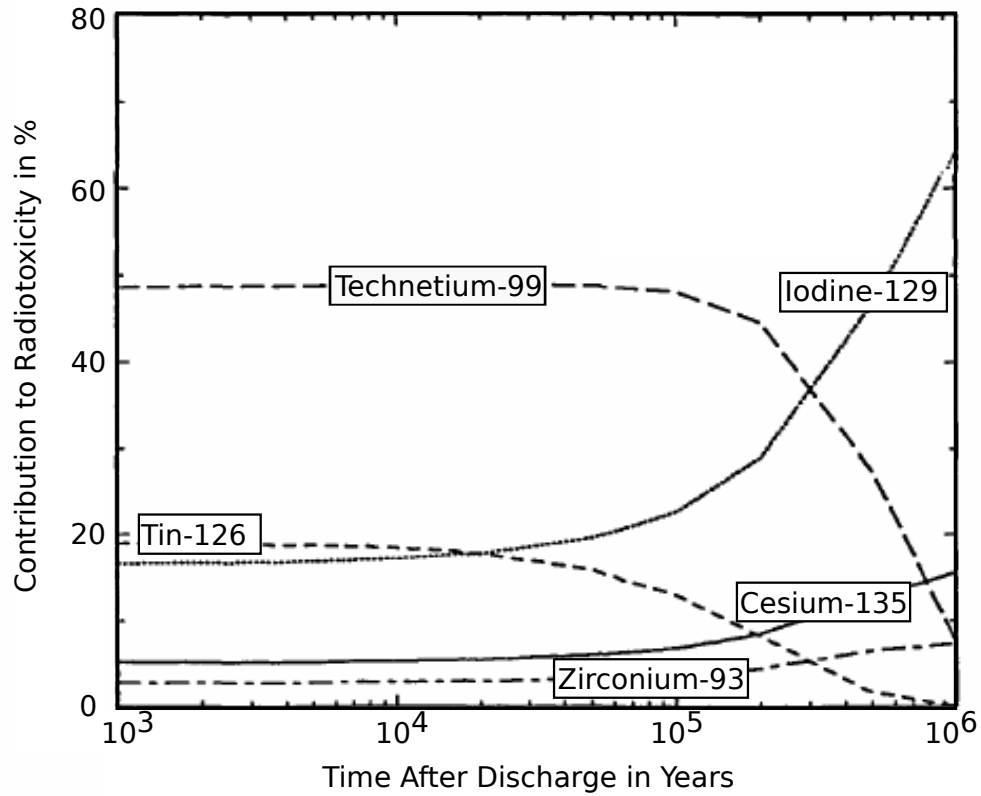


Figure 7.12.: Relative contribution of selected long-lived fission products to the total radiotoxicity if all transuranium elements are removed from the spent fuel (Kloosterman et al. 1995). The five fission products are responsible for more than 90 % of the total radiotoxicity from all fission products.

Considering the discussion above, it seems only consequent that in the original partitioning and transmutation concepts, the destruction of the long-lived fission products was included as well (NRC, Committee on Separations Technology and Transmutation Systems 1996; Jameson et al. 1992; United States Department of Energy 1999). They investigated also the transmutation of at least technetium-99 and iodine-129. When assessing the practical feasibility of the transmutation of fission products, a first step is the calculation of the transmutation half-life (NEA 2005). The transmutation half-life is a rough estimate for the time period it takes to incinerate half of the initial mass. It is defined as

$$T_{1/2}^{trans} = \frac{\ln 2}{\sigma_{n,\gamma} \cdot \Phi \cdot 3.15 \cdot 10^7} \text{ years.} \quad (7.12)$$

The transmutation half-life depends on the cross-section for (n,γ) reactions $\sigma_{n,\gamma}$ and the neutron flux Φ . Because it neglects the ongoing build-up of fission products in the core, this definition is mostly useful when looking at heterogeneous transmutation. In this case, special elements rich on the targeted nuclides are positioned in the core. Table 7.15 gives average values for the transmutation half-life in a thermal and a fast neutrons spectrum (NEA 2002, p. 265). The energy of the incoming neutrons is assumed to be 1 eV and 0.2 MeV for the two spectra. A neutron flux of $10^{14} \text{ n/(s}\cdot\text{cm}^2)$ and $10^{15} \text{ n/(s}\cdot\text{cm}^2)$, respectively, is selected.

Explicit transmutation in a nuclear reactor is only useful when the transmutation half-life is significantly shorter than the natural half-life of the targeted radionuclide. For the long-lived fission products, at least in principle this holds true for the thermal and the fast neutron spectrum. Yet, the

Table 7.15.: Characteristic values for selected long-lived fission products. The half-lives are taken from the Janis database NEA (2012b). Average isotope production from a pressurized water reactor with a burn-up of 50 MWd/kgHM is tabled in NEA (1999, p. 170). The ingestion dose and the transmutation half-lives as listed in NEA (2002, p. 265) are shown for a simplified thermal and fast neutrons spectrum. Note that a 1 GWe nuclear reactor can produce up to 8 TWh per year.

Isotope	Half-life 1000 years	Isotope Quantity kg/TWh	Ingestion Dose nSv/Bq	$T_{1/2}^{trans,thermal}$ years	$T_{1/2}^{trans,fast}$ years
Se-79	335	0.018	2.3	220	730
Zr-93	1,610	2.8	0.42	790	730
Tc-99	211	3.2	0.34	51	110
Sn-126	230	0.079	5.1	4400	4400
I-129	15,700	0.66	74	51	160
Cs-135	2,300	1.40	1.9	170	310

thermal spectrum leads to a higher transmutation efficiency, in particular for technetium-99 and iodine-129. Therefore this already contradicts the objective of efficient minor actinide transmutation in a fast neutron spectrum.

The difference between the fast and thermal transmutation half-lives of the isotopes seems small. But when considering human time scales, there is a significant difference between 51 years and 160 years for the example of iodine-129. It takes long irradiation periods for efficient reduction in the overall inventory, because the neutron absorption cross sections and thus the probability of the absorption reaction is small. However, once again, material endurance is an open question. It is impossible that cladding and structure last for such a long time, considering the heavy neutron bombardment.

One limiting factor especially in a thermal neutron spectrum is the neutron balance. Each transmutation of a fission product is a net neutron loss due to absorption since no new neutrons are produced. Even in a fast spectrum it might be necessary to add external neutrons when the transmutation of long-lived fission products is an actual objective during operation.

Additional, element specific challenges when transmuting long-lived fission products became evident over the years. One example is the long-lived cesium-135 isotope. It comprises only about 10 % of the total cesium vector in the spent fuel. Other isotopes, such as cesium-133 and cesium-134, are also present. These isotopes also absorb neutrons, producing on the one hand more cesium-135 isotopes while on the other hand parasitically using neutrons that are supposed to be used for transmutation of cesium-135. Possible transmutation schemes for cesium-135 were developed, but the general opinion is that cesium-135 transmutation is too complicated to be deployed on an industrial scale (NEA 2005, p. 215). The transmutation of technetium-99 and iodine-129 seems more feasible, but there were only limited irradiation experiments with different target materials and geometries. Iodine targets for example bear the problem that a considerable amount of xenon gas is produced during irradiation. The gas needs to be removed by venting of the target (NEA 1999, p. 171).

The emphasis has mostly shifted to the sole treatment of the minor actinides in the spent fuel because of these challenges. Therefore, current publications only discuss the incineration of minor actinides when assessing the transmutation efficiency for a certain system (Mansani et al. 2012; Mueller 2013; Renn 2013; Sarotto et al. 2013). All arguments in favor of transmutation only consider the hazard generated by a deep geological repository. However, it is acknowledged even by advocates of a P&T fuel cycle, that a deep geological repository is required.

For the design and capacity of a deep geological repository, the emitted dose rate is not the limiting factor. The initial heat generation of the spent fuel and, subsequently, of the high-level waste, is far more important in this context (Bonin 2010, p. 3307). The residual heat of typical LWR spent fuel is dominated by the more short-lived fission products, such as cesium-137 and strontium-90 (Mueller and Abderrahim 2010). Both isotopes have a half-life of about 30 years. For the P&T-fuel, the situation is different since especially curium-242 adds a significant amount of heat during this time period. While much could be gained with an extended interim storage, this would contradict the objective not to shift the burden of nuclear waste treatment to next generations. The long-term consequences are also the topic of the following section, in which findings on long-term effects caused by the generation of long-lived fission products in a P&T fuel cycle are presented.

7.6.2 Concentration of Long-lived Fission Products in the Spent P&T-Fuel

Recent publications claim that the total inventory of minor actinides in the spent fuel can be significantly reduced (Abderrahim 2013; Sarotto et al. 2013). But the argument often ends at this point. There is hardly an assessment of related effects on the spent fuel. There is only a small note saying that the disproportional generation of plutonium-238 and its effect on the decay heat from the spent fuel elements should be further investigated in NEA (2006, p. 17). Therefore, the question to which extend long-lived fission products are generated is investigated in this section. These nuclides are known to be relevant for the long-term safety analysis of a deep geological repository, as already discussed.

Usually, concentrations of long-lived fission products within the spent fuel are given in Becquerel per ton heavy metal inventory. This is an obstacle for the comparison of the fraction of long-lived fission products in the spent fuel. Only conventional nuclear fuel comprises a heavy metal matrix, P&T-fuel consists of a magnesium-oxide matrix.

For further analysis the weight percentage of single radionuclides as a part of all fission products is considered. Figure 7.13 shows the derived weight fractions for the relevant long-lived fission products in the spent P&T-fuel. It was irradiated for 1080 FPD and cooled for 40 years. Shorter irradiation periods and a cooling period of only 90 days after discharge did not alter the result visibly. Cesium-135 has the highest fraction with more than 4 %. Hence, a first result is that additional long-lived fission products are produced in a P&T fuel cycle which have to be dealt with in a deep geological repository. The fraction of selenium-79 is not shown because its concentration is 0.006 % and would appear as zero. The fact the concentration of cesium-137 is also disproportionally increased is also not depicted¹³.

For comparison, the estimated values for the German spent fuel inventory in 2022 are also plotted (Schwenk-Ferrero 2013). The list is not comprehensive regarding relevant fission products. The values for selenium-79, zirconium-93, and tin-126 are missing in the publication and therefore also in Figure 7.13. They could however be estimated using the production rates listed in Table 7.15. The total amount of fission products is not mentioned in the paper directly, but can be calculated by summing up the figures for explicitly given isotopes and "*other fission products*". For 2022, the calculated German inventory for fission products is 415.65 tons. Details are discussed later on in the following section.

There are comprehensive inventories for Swiss spent fuel elements available. They originate from pressurized water reactor uranium-oxide, boiling water reactor uranium-oxide and pressurized water mixed-oxide fuel (McGinnes 2002). In Figure 7.13 and the following, these are referred to as *Swiss PWR*, *Swiss BWR*, and *Swiss MOX*. The inventories for different burn-ups are given in Becquerel per ton heavy metal for all unstable isotopes and in mol per ton heavy metal for all stable isotopes; directly after removal from the core and after a 40 year cooling period. For this study,

¹³ Cesium-137 is the dominating contributor to the gamma dose rate exposure of workers in conventional nuclear facilities (Schwenk-Ferrero 2013).

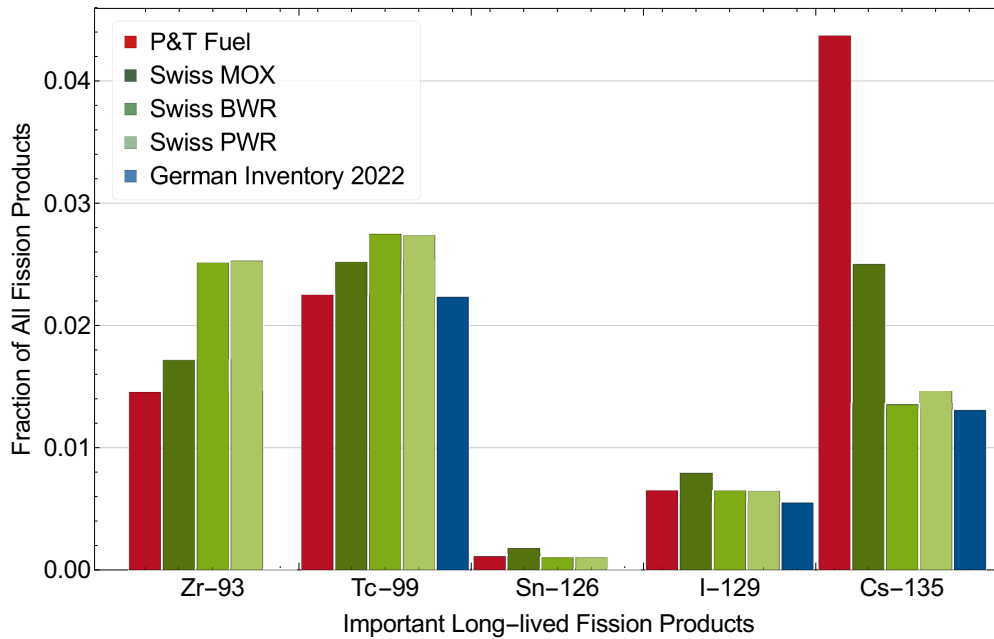


Figure 7.13.: Weight fraction of selected fission products as a part of all fission products for various types of spent fuel (see text). For the total German reference inventory expected in 2022, values for zirconium-93 and tin-126 are not published. The values for P&T-fuel are derived from the EFIT-like fuel elements after a 1080 FPD irradiation period in the MYRRHA core 40 years after discharge.

the values of a burn-up of 48 GWd/kg and a decay time of 40 years are used as reference values. In 2022, a certain (small) fraction of the accumulated spent fuel will still be originating from the core almost without cooling period. Analysis of the P&T-fuel has, however, shown that the fractions of the long-lived fission products of all fission products does hardly change in dependence of the cooling period after discharge. The focus lies on long-lived fission products. The overall amount of fission products is approximately constant because spontaneous fission and decay of the heavy metal have only low reaction rates.

Conversion of the activities and amounts of substances is done using Mathematica and the isotope half-lives implemented in the program. The calculated specific activities and masses for all considered isotopes are listed in Appendix C. Concentrations are published per 1,000 kg heavy metal. Summing up the calculated masses results in 996 kg (PWR), 995 kg (BWR) and 936 kg (MOX). The slight differences in comparison to the nominal 1,000 kg can be explained by the cut-off of unstable isotopes with an activity of less than 1 GBq/tHM and possible discrepancies in the used isotope data. Oxygen is not included in the list of isotopes for the spent fuel. All listed isotopes up to hafnium-178 are considered to be fission products. Figure 7.13 depicts the fractions for the long-lived fission products in the swiss spent fuel for the different reactor types as well.

In general, the concentrations of long-lived fission products for fuel originating from different sources are comparable. The zirconium-93 and technetium-99 fraction is higher for the spent fuel from light water reactors. The cesium-135 concentration in the P&T-fuel is present in nearly a four-fold higher concentration. Already the MOX fuel shows an increase in cesium-135 concentration. Hence this effect can most likely be attributed to the increased content of transuranium elements in the fresh fuel.

From the swiss figures, concentrations in the German spent fuel inventory can be derived for the missing three long-lived fission products selenium-79, zirconium-93, and tin-126. The German nuclear waste is modeled by combining the three vectors from BWR, PWR, and PWR-MOX spent

fuel. Therefore the fraction F_i of a certain isotope i in the German spent fuel can be estimated using equation

$$F_{Germany}^i = \kappa F_{Swiss,PWR}^i + \lambda F_{Swiss,BWR}^i + \mu F_{Swiss,MOX}^i \quad (7.13)$$

Beginning with the known fraction for technetium-99, iodine-129, and cesium-135 in the German spent fuel, it can be derived that the variables are

$$\begin{aligned} \kappa &= 0.662, \\ \lambda &= 0.058, \text{ and} \\ \mu &= 0.105. \end{aligned} \quad (7.14)$$

Table 7.16.: Concentration of long-lived fission products of all fission products in the spent fuel in weight percent. Values are given for the accumulated German spent fuel in 2022 and for P&T-fuel based on own calculations.

	Se-79	Zr-93	Tc-99	Sn-126	I-129	Cs-135
German SNF	0.004 %	2.00 %	2.23 %	0.09 %	0.55 %	1.31 %
P&T-fuel	0.006 %	1.45 %	2.25 %	0.11 %	0.65 %	4.36 %

For the German spent fuel inventory, the concentration of all six important long-lived fission products is calculated using equation 7.13 and 7.14. Results are given in Table 7.16, together with the results for the P&T-fuel derived from the simulation of EFIT-like fuel elements in the MYRRHA reactor. For all considered isotopes except zirconium-93 and in particular for cesium-135, the fraction is higher for the P&T-fuel. Since the amount of fission products increases over burn-up, the ratio of the fission products under consideration to all fission products is almost independent of burn-up. Some fission products undergo further reactions, such as neutron absorption or decay. The choice to neglect these reactions seems reasonable. It was validated by calculating the ratios also for P&T-fuel that was irradiated for shorter times in the core.

7.6.3 Total Inventory in a Simplified Scenario

As an illustration for the concentrations calculated above, the resulting total inventory for an exemplary, simplified German scenario is calculated. Table 7.17 shows an overview of the German inventory for spent nuclear fuel and high level waste. Since no explicit values for the long-lived fission products are given in Schwenk-Ferrero (2013), their total inventory is estimated using the production rates from Table 7.15. A total nuclear energy generation for Germany of 5500 TWh until 2022 is assumed and the fraction of already vitrified spent fuel is set to 39 % (Kommission Lagerung hoch radioaktiver Abfallstoffe 2016). The plutonium and minor actinide inventories will be used to calculate the additional amount of fission products resulting from two different transmutation scenarios, namely the regional and the national scenario as described in the beginning of this chapter. Here, only the spent nuclear fuel is analyzed, since the high level waste is already vitrified and cannot be irradiated again, at least not with a reasonable effort.

The scenarios are simplified, neglecting a variety of different issues: For example, there are no losses during the partitioning process, the size and number of available facilities is optimal and it is possible that the transmutation fuel cycle can continue until all targeted isotopes are transmuted. It is also assumed that the spent fuel from the last transmutation cycle does not contain any minor actinides, no final load of a transmutation facility is considered.

Table 7.17.: Accumulated German inventories in 2022, adapted from Schwenk-Ferrero (2013). Figures for long-lived fission products are estimated using production rates from Table 7.15. High level waste is already vitrified and not further considered in a P&T scenario.

Constituent	Spent Nuclear Fuel	High Level Waste
Total	10,300 t	215 t
Minor Actinides	21.5 t	6.7 t
Plutonium	131 t	0.2 t
TRU	152.5 t	6.9 t
Fission Products	415 t	207 t
Long-lived Fission Products	27.4 t	17.5 t

Although the isotopes undergo different reactions in the reactor core, this is not relevant for the following estimations. Besides the desired fission, the most likely reaction is neutron absorption. If a transuranium isotope absorbs a neutron, the resulting element will again be an unstable minor actinide or plutonium atom. Hence, the initial isotope cannot be considered to be transmuted, but it can still undergo further reactions. Since the spontaneous decay into stable products is not taken into account due to the long half-lives of the minor actinides, fission is the only reaction which results in stable or short-lived isotopes. Therefore, a nuclide is only considered to be transmuted after it fissioned, independently of previous reactions. In a first approximation, the transmutation of a given amount of transuranium elements thus results in the same amount of fission products. The advantage of this perspective is that the actual implementation, for example the number of transmutation cycles, is not relevant.

The first analyzed scenario is the regional scenario. In this case, several countries are operating one or more ADS facilities in co-operation in order to transmute their minor actinide inventories. At the same time, the existing plutonium is used in the fast reactor fleet by at least some of the partners for energy production. Therefore, Germany could irradiate all its transuranium element inventory in the transmutation facility, but would only have to take back the fission products resulting from the incineration of minor actinides. The plutonium would be used in the foreign reactor fleet. In the current design of the EFIT transmutation facility, 40.16 kg minor actinides and 1.74 kg plutonium would be fissioned per TWh of produced energy (Artioli et al. 2007). Most likely, Germany would be obliged to take back all fission products originating from the transmutation of German minor actinides, including the fission products from the plutonium fission. Thus, the mass of the initial inventory of minor actinides is increased by the factor of $42/40.16 = 1.046$ (22.5 t of fission products from 21.5 t of minor actinides). The regional scenario relies on the fact that the repeated use of plutonium in other nuclear reactors is possible and the plutonium does not degenerate as quickly as the calculations in section 7.4 imply. If this is not the case and the same reduction of the radiotoxicity is to be reached, plutonium must be incinerated as well and the regional scenario converges to a scenario where all transuranium elements should be incinerated. This is very similar to the case of a German (or any other state from Group A) national scenario.

In a national scenario, Germany is assumed to be the sole owner and operator of the transmutation facilities and the accompanying fuel cycle. In this scenario, all transuranium elements, namely the minor actinides and the plutonium, would have to be transmuted due to the renunciation of nuclear energy production. This results in an additional 152.5 tons of fission products. No correction factor is added, since it is not clear how well fitted the possible accelerator-driven system would be for that task. It is claimed that the plutonium to minor actinide ratio in the fuel for the EFIT reactor could be modified to optimize incineration of all transuranium elements (Renn 2013, p. 93). It is unclear to what extent this change of the plutonium fraction in the fuel would influence reactor design and operation.

Table 7.18.: Inventory of selected long-lived fission products for different scenarios. All values are given in tons. The figures for the phase-out scenario are derived using data from Schwenk-Ferrero (2013). Other inventories are calculated using the fractions from Table 7.16. Material already vitrified is not considered.

Constituent	Phase-Out	Regional Scenario		National Scenario	
All FPs	415	+22.5	+5.4 %	+152.5	+37 %
All LLFPs	25.7	+2.0	+ 7.8 %	+13.36	+ 52 %
Se-79	0.015	+0.0014	+9.3 %	+0.0092	+61 %
Zr-93	8.3	+0.33	+4.0 %	+2.2	+27 %
Tc-99	9.3	+0.51	+5.5 %	+3.4	+37 %
Sn-126	0.38	+0.025	+6.6 %	+0.17	+45 %
I-129	2.3	+0.15	+6.5 %	+0.98	+43 %
Cs-135	5.4	+0.98	+18.0 %	+6.6	+120 %

Table 7.18 lists the estimated inventories for the baseline phase-out, the regional, and the national scenario. Since no inventory was published for the radionuclides selenium-79, zirconium-93 and tin-126, their inventory is calculated using the fractions from Table 7.16. For the regional and the national scenario, the resulting amount of the single isotopes is calculated using the fractions derived in the previous section. The total amount of selenium-79 is two orders of magnitude lower than the amount of the other long-lived fission products except tin-126. Several tons need to be sent to a deep geological repository for all other long-lived fission products. Despite its comparatively low amounts, selenium-79 could be the dominating factor for the dose rate from a salt dome repository after around 10,000 years (Brasser et al. 2008, p. 76).

For the regional scenario, the inventory of all fission products increases by 5.4% and for the national scenario by 36.6%. From all long-lived fission products, cesium-135 is the outstanding isotope: while for the others, the total amount increases almost linearly with the total increase of fission products and for zirconium-93 even a slightly lower fraction is produced, the cesium-135 generation is disproportionally high. For the regional scenario it increases by 18% and it is twice as high in the national scenario (+120%). In a national scenario, there would be 12 tons of cesium-135 to be stored instead of only 5.4 t in the phase-out scenario. The effect of this increase on a possible deep geological repository has still to be clarified.

It is generally accepted that a deep geological repository is needed no matter what kind of fuel cycle scenario is going to be the future choice. But to what extent is the total amount going into the deep geological repository reduced? And for how long must the deep geological repository ensure the safe containment of the high-level waste? As long as the containment lasts, it does not matter how much dose-rate determining isotopes are present in the repository. But as soon as the man-made barriers start to fail, the situation changes. Cesium-135 is not one of the most mobile long-lived fission products. But since its dose-conversion factor is comparably high, it adds significantly to the dose rate exposure from a deep repository in the longer term. The generation of the long-lived nuclides zirconium-93, technetium-99, and iodine-129 in an ADS is mostly comparable to their generation in light water reactors. This implies that the total amount of isotopes relevant for the long-term safety analysis is also increased.

The minor actinide reduction in the deep geological repository is bought by an increase of the inventory of long-lived fission products. For the long term safety analysis conducted for current designs of deep geological repositories, the emerging dose rate from the repositories lies well below the regulatory guideline. But these calculations are based on current cask characteristics, comprising typical LWR spent fuel and the subsequent volume occupied by a certain amount of high level waste. The storage of spent fuel might be changed to better accommodate for the increased

residual heat and the claimed hazard reduction due to the lower minor actinide content. Reliable statements will be only possible when more information is available.

7.7 Summary

The potential implications of the implementation of a P&T fuel cycle are far reaching. It does not only require dedication to nuclear energy production for at least one additional century, it also needs all kinds of nuclear facilities that enable the handling and reprocessing of the spent fuel. Inevitably, in these facilities nuclear weapons material can be separated and processed.

Moreover, several aspects of the whole concept have not gone beyond design stage yet: among others, the accelerator-driven system, crucial to the success of P&T, only exists on paper. Due to the preliminary nature of the current knowledge, it is impossible to assess the benefits and risks of this technology in greater detail. But inconsistencies in the arguments of its proponents can be found. Burn-up simulations were performed based on models of the planned proof-of-concept accelerator-driven systems MYRRHA and EFIT. Out of the gained data, three different aspects that either affect the feasibility and/or the benefit of P&T fuel cycles are analyzed in more detail: the effect of the changing isotopic composition of the fuel on reactor criticality, the comparability of the characteristics of spent P&T-fuel elements to typical LWR spent fuel elements, and the benefit of only targeting the transmutation of minor actinides during the process compared to the remaining and newly produced long-lived fission products.

Several transmutation cycles are needed to reduce the amount of minor actinides in the high-level waste sent into a deep geological repository to a significantly lower level. The isotopic composition of the fissile material in the fuel changes during each of these cycles, also influencing criticality. Criticality calculations with fuel based on previously irradiated plutonium and minor actinides show that an adjustment of the fissile material fraction in the fuel would definitely be needed. Continuously using the same plutonium load is most likely not possible although often claimed otherwise. The neutron multiplication factor decreases heavily already after the first irradiation cycle. Minor actinide compositions generated by continuous recycling in the ADS result in positive reactivity added to the core. Even with the counterbalance of the decreasing criticality worth of the plutonium vector, the system then easily exceeds the limit for safe operation. As part of the Partitioning and Transmutation European Roadmap for Sustainable Nuclear Energy (PATEROS), the plutonium compositions at certain dates during a possible implementation scenario are given. These compositions are used for further criticality calculations. They result in $k_{eff} = 1.6$. This factor would be far too high even for a critical nuclear reactor system. To use the EFIT reactor as envisioned in these scenarios, adaptations regarding the fuel would have to be made. The reduced fissile material fraction in the fuel will inevitably increase the time frame of the P&T scenario.

In the same implementation scenario, a cooling period of five years before fuel reprocessing is assumed without further justification. Experience with MOX fuel has already shown the increased difficulties in handling fuel containing a higher plutonium fraction. To estimate the effect of the minor actinides on the spent fuel, the activity, the residual heat and the gamma dose rates from the spent P&T-fuel elements were calculated. Most outstanding is the significantly higher residual heat of the spent P&T-fuel elements. Compared to the residual heat from an exemplary fast reactor, the figures for the P&T elements are about eight times higher. This is caused to a high degree by the large amount of curium in the spent fuel. The same holds true for the spontaneous fission rate of the spent fuel and the resulting strong neutron radiation. Even though the total amount of minor actinides is reduced during irradiation in an accelerator-driven system, there actually is a curium build-up. Apparently, neither in MOX nor in P&T-fuel the transmutation of curium is favorable.

The main argument in favor of transmutation usually is the reduction of the radiotoxicity calculated using the ingestion dose rate of the spent fuel. This is based on the conservative assumption that the complete inventory is consumed by future humans. It neglects that the canister and host matrix

will not stay intact and that by a certain point in time, isotopes will dissolve, be transported to the surface, and released into the biosphere. When taking these mechanisms into account, some long-lived fission products play a more important role than the minor actinides. The most relevant radionuclides are zirconium-93, technetium-99, iodine-129, and cesium-135. Based on depletion calculations for the accelerator-driven transmutation facilities, the additional amount of these isotopes produced in a hypothetical transmutation scenario is calculated. There is a disproportionately high generation of cesium-135 in a P&T fuel cycle. The increased total inventory of long-lived fission products might be important to consider when designing and assessing the deep geological repository.

These findings show that the implementation of P&T is not as straightforward as advocates assure. Besides the known challenges such as the material endurance of the cladding materials and the separation efficiency, there are more aspects that need careful assessment and should not be left to the nuclear industry and their eager partners. Possible implications are discussed in the following chapter.



8 Conclusion

According to a many publications and discussions, fast reactors hold promises to improve safety, non-proliferation, economic aspects, and reduce the nuclear waste problems. Consequently, several reactor designs advocated by the Generation IV Forum are fast reactors.

In reality, however, after decades of research and development and billions of dollars investment worldwide, there are only two fast breeders currently operational on a commercial basis: the Russian reactors BN-600 and BN-800. Energy generation alone is apparently not a sufficient selling point for fast breeder reactors. Therefore, other possible applications for fast nuclear reactors are advocated. Three relevant examples are investigated in this thesis.

The first one is the disposition of excess weapon-grade plutonium. Unlike for high enriched uranium that can be downblended for use in light water reactors, there exists no scientifically accepted solution for the disposition of weapon-grade plutonium.

One option is the use in fast reactors that are operated for energy production. In the course of burn-up, the plutonium is irradiated which intends to fulfill two objectives: the resulting isotopic composition of the plutonium is less suitable for nuclear weapons, while at the same time the build-up of fission products results in a radiation barrier. Appropriate reprocessing technology is in order to extract the plutonium from the spent fuel.

The second application is the use as so-called nuclear batteries, a special type of small modular reactors (SMRs). Nuclear batteries offer very long core lifetimes and have a very small energy output of sometimes only 10 MWe. They can supposedly be placed (almost) everywhere and supply energy without the need for refueling or shuffling of fuel elements for long periods. Since their cores remain sealed for several decades, nuclear batteries are claimed to have a higher proliferation resistance. The small output and the reduced maintenance and operating requirements should make them attractive for remote areas or electrical grids that are not large enough to support a standard-sized nuclear power plant.

The last application of fast reactors this thesis investigates promises a solution to the problem of the radioactive waste from nuclear energy production. The separation of the spent fuel in different material streams (partitioning) and the irradiation of minor actinides in a fast neutron spectrum (transmutation) is claimed to solve this problem. Implementation of partitioning and transmutation (P&T) would require centuries of dedicated efforts, since several irradiation cycles and repeated reprocessing of the spent fuel elements between the irradiation cycles would be necessary.

For all three applications, computer models of exemplary reactor systems were set up to perform criticality, depletion, and dose rate calculations. Based on the results, a specific critique on the viability of these fast reactor applications was conducted. Possible risks associated with their deployment were investigated.

Small Modular Reactors – Nuclear Batteries

A *Super-Safe, Small and Simple* reactor promises to meet the energy demand of remote, small energy grids. The discussion of the proliferation risks associated with the spread of this kind of reactors often addresses the sealed core. The fissile material produced in the core and the possibility of breaking a seal and extracting the fuel is neglected. To address these questions, the Toshiba 4S reactor was modeled as an example of a fast small reactor with a core lifetime of 30 years and an energy output of 10 MW.

The fast SMR core is said to have a high level of proliferation resistance (IAEA 2011). Depletion calculations, however, show a production rate of more than 5 kg plutonium per year. Furthermore,

the plutonium-239 fraction in the fuel is higher than 90 % even at planned discharge from the reactor, resulting in very attractive material for a possible proliferator. Several SMR characteristics complicate the unauthorized removal: the refueling intervals are extraordinary long and in-between the core does not have to be opened for reshuffling of fuel elements. It supposedly remains sealed for the whole time. Also, the machines needed to remove the spent fuel elements are not kept at the reactor side but will be transported there only for refueling. Still, the fissile material produced in the core poses a proliferation risk.

The dose rates emitted from fuel elements 30 years after discharge are higher than 1 Sv/hr. They fulfill what is currently considered to be an important part of the spent fuel standard. Yet, there is only a one year on-site cooling period planned before the spent fuel elements are transported back to a central facility. At this point, the spent fuel elements emit about 100 Sv/hr. This of course impedes diversion of the spent fuel from the reactor site, but also complicated transportation to the reprocessing facility.

Especially if these nuclear reactors are to be deployed on a global scale, the proliferation risks imposed by the material production in the core have to be addressed. The likely detection of unauthorized fissile material diversion might discourage some actors from this pathway. But for a state determined to acquire nuclear weapons and thus most likely willing to break its obligations under the Non-Proliferation Treaty and as a consequence to face corresponding reactions from the international community, the detection might not be a prohibiting factor. In the case of an open break-out, at nearly any point of the SMR operation cycle, the state has access to significant quantities of weapon-grade plutonium. After only two years of reactor operation already more than one significant quantity (8 kg) of weapon-grade plutonium has been produced in the core.

For a state opting for this type of nuclear batteries to power its remote small grid locations, the bottleneck for acquiring nuclear weapons is not the access to fissile material but reprocessing. Due to the modularity of small reactors, deployment of several of them in one country would not raise suspicions while the latent option of becoming a nuclear weapon state would emerge. The first generation of deployed SMRs would most likely be operated in a once-through fuel cycle and their number would be limited. In such a scenario, the concept of having only central facilities for (re)fueling might be realistic and the access to sensitive technology would be limited. But it is not yet clear by whom these facilities would be owned and how safe transportation to and from reactor sites can be ensured.

For the second generation of the SMRs, a closed fuel cycle is foreseen. With the projected possible high number of deployed SMRs, several reprocessing and fuel fabrication facilities would be needed. To reduce transportation efforts, those facilities might be decentralized as well. In these scenarios, the number of states that have access to key technologies needed to acquire fissile material and build nuclear weapons increases and the obstacles for non-state actors are reduced.

SMRs can only play their economic advantage caused by their modularity if they are produced and deployed in high numbers. Thus, for the proliferation risk assessment, this should be also taken into account. Even though providing enhanced features regarding the possible proliferation of nuclear material, the overall security case is not as easily made as suggested by its proponents.

Fast Breeders: the Russian BN-800 Reactor

The BN-800 breeder reactor was awarded *Top Plant 2016* in the nuclear generation category by the POWER Magazine, the oldest American journal for the global power generation industry. This award is given to what are considered to be the most advanced and innovative projects. Among the winning attributes are the possibility to use the reactor for various purposes, including plutonium consumption (Rosatom 2017). The BN-800 is essential for Russia's efforts to dispose of its excess weapon-grade plutonium as agreed-upon in the recently suspended Plutonium Management and Disposition Agreement (PMDA) signed between Russia and the United States. Depletion calculations for the BN-800 verify the viability of this disposition method, according to the requirements set by

the PMDA. The ratio of plutonium-240 to plutonium-239 is 0.17 in the spent fuel, thus fulfilling the agreed-upon fraction of 0.1 or higher. Yet, depending on its position in the core, the plutonium content in the spent fuel amounts to 82 %-88 % and is very close to what is generally labeled weapon-grade (more than 93 % plutonium-239). After a cooling period of 30 years, the spent BN-800 fuel elements emit more than 1 Sv/hr and can therefore be considered to be self-protecting. According to IAEA regulation, they require less strict safeguards.

At the same time, in the blanket elements of the reactor attractive nuclear material is bred even when the reactor is operated with a breeding ratio below one¹. Not only is the plutonium produced in the blankets of weapon-grade quality with a plutonium-239 fraction significantly higher than 93 %, the radiation barrier also deteriorates quickly. The elements cannot be considered to be self-protecting after a cooling period of 30 years. Currently, no separation and reprocessing of blanket material is planned, but it is not clear why the blankets are necessary at all. In particular for the purpose of plutonium disposition, it would be preferable if no new weapon-grade material be bred. Further research should be done to assess the possibility of operating the BN-800 without blankets. Additionally, the introduction of inert matrix fuel could further increase the rate of achievable plutonium reduction in the reactors. Unfortunately, with the PMDA suspended in September 2016, the issue lost its urgency.

The BN-800 is planned to play a key role in Russia's efforts to establish a closed nuclear fuel cycle in the future. A closed nuclear fuel cycle always implies reprocessing of spent fuel. In the case of the breeding blankets, weapon-grade plutonium will be separated at a certain stage in the fuel cycle, which contradicts the current efforts to dispose of such material. Once the BN-800 is exported to other countries for energy production, the possible proliferation of nuclear materials becomes of even greater concern. It is widely accepted that fast reactors are more suitable for the production of nuclear weapons material. Especially for newcomers to nuclear energy, the possible advantages of fast reactors, namely the option to close the nuclear fuel cycle, seem to be a distant option. On the other hand, the operating history and economic viability of fast reactors is far worse than for light water reactors, but they offer the option of access to nuclear weapons material.

Several measures could reduce the proliferation risk of the BN-800 in the case of export. The most obvious are of course IAEA safeguards, preferably including an Additional Protocol. Until now, only China showed interest in the BN-800.

It would be advisable to achieve transparency during all steps of building the nuclear power plant, operation, and decommissioning. Comprehensive monitoring and inspection mechanisms would increase trust among the different parties and could also act as an example for other countries. As a demonstration, the precise and continuous monitoring of the reactor power output and irradiation times would provide the basis for a reliable assessment of the amount of plutonium and fission products produced in the core and blanket.

The case of the BN-800 shows that especially in the light of several newcomer countries interested in buying nuclear technology the proliferation risk has to be assessed more comprehensively. Limiting the focus to the reactor itself and the country originally developing it is not sufficient. Disadvantages of fast reactors, such as the high costs and the proliferation and safety risks, have long been known. They should not be forgotten with the new reactor generation of reactors, even though some enhanced safety and security technologies are in place.

Accelerator-Driven Systems in a P&T Fuel Cycle

Under current economic circumstances, the implementation of a transmutation fuel cycle is not competitive compared to other means of energy production. The use of plutonium in MOX fuel alone brings an economic penalty compared to the once-through fuel cycle and is motivated by other reasons such as a better resource utilization, which is necessary if nuclear power is to be used on

¹ This obvious contraction is due to the fact that for the calculation of the breeding ratio only the fissile plutonium isotopes are taken into account.

a global scale. An objective of introducing a double-strata partitioning and transmutation fuel cycle using accelerator-driven systems for the transmutation of minor actinides is the treatment of high-level waste. The implementation of such a fuel cycle requires long-term dedication to the use of nuclear energy and the deployment of all facilities that make up a closed nuclear fuel cycle. Before taking such far reaching decisions, it should be ensured that the promised benefits will hold true in reality. To date, even the proof of concept of an accelerator-driven system is pending.

An analysis of the existing literature shows that some crucial points regarding a P&T scenario are not dealt with in sufficient detail. In this thesis, a closer look was taken at some of these issues. Burn-up calculations were performed based on computer models of the European proof-of-concept reactor MYRRHA and the facility explicitly designed to be used for transmutation of minor actinides (EFIT). Both are accelerator-driven systems (ADS). They consist of a sub-critical reactor core, a spallation target to provide extra source neutrons, and a particle accelerator to provide high-energy protons for the spallation reaction. Besides some general characteristics, such as the possible transmutation rate in those reactor systems, three key issues that might affect the implementation were investigated in detail: the change in the fuel composition, the characteristics of the spent fuel elements, and the concentration of long-lived fission products in the spent fuel.

The minor actinides have to be irradiated in the ADS for several cycles. For efficient transmutation, plutonium and minor actinides must be mixed in the fuel according to fixed fractions. After each cycle, the fuel has to be reprocessed and fresh fuel elements must be fabricated. It is noteworthy, that even today's nuclear reactor fuel is only reprocessed once and its use as MOX fuel is limited to a second cycle. Calculations of the effective neutron multiplication factor k_{eff} for various fuel compositions that depend on the number of previous cycles show the influence of the changing isotope vector. The claim that one initial load of plutonium is sufficient for several irradiation cycles can not be confirmed. Moreover, criticality calculations show that using fuel compositions as published for European implementation scenarios (PATEROS) result in $k_{eff} = 1.6$. This is a much too high figure, suggesting that P&T scenarios published so far are not feasible. Calculations were done with the EFIT reactor, the reference reactor in the PATEROS study. As a consequence, major adjustments of the fissile material content in the fuel are necessary to resolve the overall reactivity problematic. This in turn might lead to performance losses regarding the intended reduction of minor actinides within one reactor cycle.

The claimed benefits of a P&T scenario are the reduction of the minor actinide inventory in the deep geological repository. After each irradiation cycle, the spent fuel elements must be cooled and reprocessed before new fuel elements can be fabricated. Since transmutation requires several cycles, the necessary cooling periods before reprocessing of the spent fuel play an important role to assess P&T scenarios. The calculations show that due to the increased residual heat of the spent P&T-fuel elements, longer cooling periods than currently assumed would be necessary. The decay heat from the spent P&T-fuel elements after a 40 year cooling period is still higher than the decay heat from spent MOX and fast reactor fuel elements, although these contain significantly more fuel. Also, the dose rates and the activity of the spent fuel would pose challenges for the overall reprocessing and fuel fabrication scheme. The build-up of curium-242 with its high spontaneous fission rate causes a strong neutron background. Thus, heavy shielding would be necessary for the processing of the spent fuel elements. The high specific power makes permanent cooling of the tools and material unavoidable during all phases.

Finally, it is questions in this thesis that the benefit of minor actinide transmutation is as significant as claimed by the proponents of P&T. With regard to the risks emerging from a deep geological repository, several long-lived fission products dominate the dose rate released to the biosphere. The production of the relevant nuclides zirconium-93, technetium-99, and iodine-129 in an ADS is mostly comparable to their generation in light water reactors. However, the fraction of cesium-135 increases four-fold. For a German P&T scenario, the cesium-135 inventory in the deep geological repository would more than double as compared to the agreed-upon phase-out scenario in which

the spent fuel elements are directly disposed. The overall inventory of long-lived fission products in a German deep geological repository would increase by more than 50 % in a P&T scenario. It can be stated that the reduction of the minor actinide inventory would be bought in exchange for an increase of the inventory of long-lived fission products. These results question the benefits of the currently researched P&T strategy that claims to reduce the nuclear waste burden.

At the current stage of P&T research and development, there are several open questions that need to be answered before actual implementation. This includes not only technical challenges as the ones already discussed. Other crucial issues are the endurance of the cladding material in the core and the partitioning efficiency realistically achievable on industrial scale. Even with all these issues resolvable, the benefit of the technology remains uncertain. Over the years, the number of targeted isotopes published in P&T schemes has declined: while in the beginning the plan was to transmute long-lived fission products as well, it now seems that even curium must be left out of the minor actinide composition because of the challenges it poses to reprocessing and fuel fabrication.

Final Remarks

Even though fast reactor research and development has a long history, operational experience of fast reactors is quite small. Since more suitable solutions exist for energy generation, in recent years additional applications have been discussed for new and emerging fast reactor designs. The examples above show that the use of fast reactors is not as straight forward and beneficial as the advocates of this technology would argue.

When looking at specific applications, fast reactors seem to offer solutions for various tasks, such as plutonium disposition, safe and secure energy supply in remote areas, and the treatment of radioactive waste. In a more comprehensive view, promises are fading and it turns out that suggested applications bear risks.

Critical fast reactors cause the spread of nuclear weapons material and, even more importantly, the technology and facilities to handle it. This is also true for fast sub-critical ADS, which would be deployed in a P&T fuel cycle. It is not yet clear in how far P&T technology can actually help to solve the nuclear waste problem. The argument in favor of nuclear waste treatment in an ADS is based on one simple index value: the radiotoxicity based on the total ingestion by humans. Besides, the development risks regarding P&T are high and it is not clear whether a P&T fuel cycle could actually be implemented in the near future. Several crucial technologies do not yet exist.

Moreover, nuclear reactors are first of all designed for energy production. Still, the vast majority of the current nuclear fleet are light water reactors and not fast breeder reactors. This might always be attributed to soft factors, such as political considerations and the public opinion. But maybe the reasons are intrinsic to the technology: fast reactors might just not be competitive for energy production. And it has not yet been proven that they are competitive in regard to emerging applications beyond power supply. In general, the new applications will lead to higher costs and risks and it sometimes seems puzzling why they are promoted by academia, industry, and policy. It also seems somehow contradictory to solve a problem, namely the excess plutonium stockpiles and the radioactive waste, by using the same technology that originally produced it.

Research efforts in this field have been going on for decades, and they have been substantially sponsored. Apart from the fact that this money is lost for other means, it could be argued that if even huge investments do not result in the desired outcome, other approaches should be tried. Critical assessment of the technology, however, is difficult as long as research is almost exclusively conducted by institutions that would benefit from a future implementation. Especially when official entities, such as the European Union, allocate funds for research and design efforts, they should take care that at least a fraction of the money also goes to independent researchers. This is the only way to guarantee that transparent and comprehensive data information and assessment is available. And only then, can society come to informed decisions on whether it supports fast reactor technologies - or not.



Bibliography

- Abderrahim, H. A. (2013). "Future Advanced Nuclear Systems and Role of MYRRHA as Waste Transmutation R&D Facility". In: *FR13: International Conference on Fast Reactors and Related Fuel Cycles: Safe Technologies and Sustainable Scenarios*. Paris, France.
- Abderrahim, H. A., D. De Bruyn, G. Van den Eynde, and S. Michiels (2013). "Transmutation of High-Level Nuclear Waste by Means of Accelerator Driven System (ADS)". In: *Digital Encyclopedia of Applied Physics*. Wiley-VCH Verlag GmbH & Co. KGaA. DOI: 10.1002/3527600434.eap723.
- Abderrahim, H. A., P. Kupschus, E. Malambu, Ph. Benoit, K. van Tichelen, B. Arien, F. Vermeersch, P. D'hondt, Y. Jongen, S. Ternier, and D. Vandeplasseche (2001). "MYRRHA: a Multipurpose Accelerator Driven System for Research and Development". In: *Nuclear Instruments and Methods in Physics Research A* 463, pp. 487–494. DOI: 10.1016/S0168-9002(01)00164-4.
- Adams, D. (1979). *The Hitchhiker's Guide to the Galaxy*. Pan Books.
- Ade, B. J. and I. C. Gauld (2011). *Decay Heat Calculations for PWR and BWR Assemblies Fueled with Uranium and Plutonium Mixed Oxide Fuel Using Scale*. ORNL/TM-2011/290. Oak Ridge National Laboratory.
- Albright, D., F. Berkhout, and W. Walker (1993). *World Inventory of Plutonium and Highly Enriched Uranium 1992*. Ed. by SIPRI. Oxford University Press.
- Amano, Y. (2013). *Statement at IAEA Ministerial Conference on Nuclear Power in the 21st Century*. International Atomic Energy Organisation. URL: <http://www.iaea.org/newscenter/statements/2013/ampsp2013n13.html> (visited on 10/31/2013).
- Artioli, C., H. A. Abderrahim, B. Glinatsis, L. Mansani, C. Petrovich, M. Sarotto, and M. Schikorr (2007). "Optimization of the minor actinides transmutation in ADS: the european facility for industrial transmutation EFIT-Pb concept". In: *International Topical Meeting on Nuclear Research Applications and Utilization of Accelerators*. Pocatello, ID, USA.
- Auger, T., G. Lorang, S. Guérin, J.-L. Pastol, and D. Gorse (2004). "Effect of Contact Conditions on Embrittlement of T91 Steel by Lead - Bismuth". In: *Journal of Nuclear Materials* 335.2, pp. 227–231. DOI: 10.1016/j.jnucmat.2004.07.025.
- Azad, A. (2012). "Generation mPower SMR Plant and FOA Progress". In: *Platts 3rd Annual Small Modular Reactors Conference*. Arlington, Virginia, USA.
- AZOM (2015). *Boron Carbide (B4C) - Properties and Information about Boron Carbide*. Material Data Sheet. Macclesfield, Cheshire, UK.
- Barbensi, A., G. Corsini, L. Mansani, C. Artioli, and G. Glinatsis (2007). "EFIT: the European Facility for Industrial Transmutation of Minor Actinides". In: *International Topical Meeting on Nuclear Research Applications and Utilization of Accelerator*. Pocatello, ID, USA.
- Bathke, C. G. (2009). "The Attractiveness of Materials in Advanced Nuclear Fuel Cycles for Various Proliferation and Theft Scenarios". In: *Proceedings of Global 2009*. Paper 9544. Paris, France.
- Bathke, C. G., B. B. Ebbinghouse, B. W. Sleasford, R. K. Wallace, B. A. Collings, K. R. Hase, M. Robel, G. D. Jarvinen, K. S. Bradley, J. R. Ireland, M.W. Johnson, A. W. Prichard, and B. W. Smith (2009). *An Assessment of the Attractiveness of Material Associated with a MOX Fuel Cycle from a Safeguards Perspective*. LA-UR-09-03637. Los Alamos National Laboratory.
- Bauer, G. S. (1998). *Physics and Technology of Spallation Neutron Sources*. PSI Bericht Nr. 98-06. Paul Scherrer Institut.
- Belgium (2016a). *Ministral Statement of Belgium at the IAEA International Conference on Nuclear Security: Commitments and Actions*.

- Belgium (2016b). *Ministral Statement of Belgium at the Preparatory Committee for the 2020 NPT Review Conference*.
- Bell, G. I. and S. Glasstone (1970). *Nuclear Reactor Theory*. Ed. by Van Nostrand Reinhold Company. Litton Educational Publishing.
- Bergmann, R. M., N. Fischer, and T. Ho (2009). *Toshiba 4S = Super-Safe, Small, and Simple*. Presentation, UX Consulting Company Research Center.
- Bonin, B. (2010). “The Scientific Basis of Nuclear Waste Managment”. In: *Handbook of Nuclear Engineering*. Ed. by D. Cacuci. Springer, pp. 3253–3420.
- Bowman, C. D. (1998). “Accelerator-Driven System for Nuclear Waste Transmutation”. In: *Annual Review of Nuclear and Particle Science* 48, pp. 505–556. DOI: 10.1146/annurev.nucl.48.1.505.
- Brasser, T., J. Droste, I. Müller-Lyda, J. Neles, M. Sailer, G. Schmidt, and M. Steinhoff (2008). *Endlagerung wärmeentwickelnder radioaktive Abfälle in Deutschland*. GRS-247. Öko-Institut e.V, Gesellschaft für Anlagen und Reaktorsicherheit (GRS) mbH.
- Brewer, R. (2009). *Criticality Calculations with MCNP5: A Primer*. LA-UR-09-00380. Los Alamos National Laboratory.
- Bruyn, D. de (2012). “MYRRHA, the Multi-purpose hYbrid Research Reactor for High-tech Applications”. In: *SILER Training Course*. Verona, Italy.
- Bruyn, D. de, H. A. Abderrahim, P. Baeten, R. Fernandez, and G. van den Eynde (2013). “Recent Design Developments of the MYRRHA Project in Belgium”. In: *Proceedings of ICAAP 2013*. Paper No.FF050. Jeju Island, Korea.
- Bureau of International Security and Nonproliferation (2017). *Russian Plutonium Disposition*. Fact Sheet. United States Department of State.
- Burnie, S. (2015). *Russian BN-800 Fast Breeder Reactor Connected to Grid*. IPFM Blog. URL: http://fissilematerials.org/blog/2015/12/russian_bn-800_fast_breed.html (visited on 02/14/2017).
- CEA Nuclear Energy Division (2012). *4th Generation Sodium-Cooled Fast Reactors - The ASTRID Technological Demonstrator*. Tech. rep. CEA.
- Chen, X., A. Rineiski, P. Liu, W. Maschek, C. M. Boccaccini, F. Gabrielli, and V. Sobolev (2008). “Design and Safety Studies on an EFIT Core with CERMET Fuel”. In: *International Conference on Reactor Physics*. Interlaken, Switzerland.
- Chen, X., A. Rineiski, W. Maschek, P. Liu, C. M. Boccaccini, V. Sobolev, F. Delage, and G. Rimpault (2011). “Comparative Studies of CERCER and CERMET fuel for EFIT from the Viewpoint of Core Performance and Safety”. In: *Progress in Nuclear Energy* 53, pp. 855–861. DOI: 10.1016/j.pnucene.2011.05.031.
- Chihara, L. (2010). “Utilization of 4S Reactor for Resource Sustainability and Proliferation Resistance”. Presentation. The University of Tokyo.
- Cinotti, L., C. F. Simth, and C. Artioli (2010). “Lead-Cooled Fast Reactor (LFR) Design: Safety, Neutronics, Thermal Hydraulics, Structural Mechanics, Fuel, Core, and Plant Design”. In: *Handbook of Nuclear Engineering*. Ed. by Dan Gabriel Cacuci. Springer Science + Business Media LLC, pp. 2750–2840.
- Cochran, T. B. et al. (2010). *Fast Breeder Reactor Programs: History and Status*. Research Report 8. International Panel on Fissile Materials.
- Committee on International Security and Arms Control (1994). *Management and Disposition of Excess Weapons Plutonium*. Ed. by D.C. National Academy Press Washington. DOI: 10.17226/2345.
- (2000). *The Spent-Fuel Standard for Disposition of Excess Weapon Plutonium: Application to Current DOE Options*. Ed. by D.C. National Academy Press Washington. DOI: 10.17226/9999.
- Deutch, J. M. et al. (2009). *Update of the MIT 2003 Future of Nuclear Power*. An Interdisciplinary MIT Study. MIT Energy Initiative.
- Di Maria, S., M. Ottoline, E. Malambu Mbala, M. Sarotto, and D. Castelliti (2012). “Neutronic Characterization and Decay Heat Calculations in the In-Vessel Fuel Storage Facilities

- for MYRRHA/FASTEF". In: *Energy Conversion and Management* 64, pp. 522–529. DOI: 10.1016/j.enconman.2012.05.001.
- Digges, C. (2016). *Russia Trumpets Dubious Success in Weapons Plutonium Destruction Agreement*. Bellona. URL: <http://bellona.org/news/nuclear-issues/2016-06-russia-trumpets-dubious-success-in-weapons-plutonium-destruction-agreement> (visited on 04/27/2017).
- DOE, U.S. (2012). *Small Modular Reactor Design Program*. United States Department of Energy. URL: <http://www.grants.gov/search/search.do?oppId=138813&mode=VIEW> (visited on 07/08/2013).
- Englert, M. (2009). "Neutronenphysikalische Simulationsrechnungen zur Proliferationsresistenz nukleare Technologien". PhD Thesis. Technische Universität Darmstadt.
- Englert, M., F. Frieß, and M. V. Ramana (2017). "Accident Scenarios Involving Pebble Bed High Temperature Reactors". In: *Science & Global Security* 25.25 (1), pp. 42–55. DOI: 10.1080/08929882.2017.1275320.
- Eriksson, M., J. Wallenius, M. Jolkkonen, and J. E. Cahalan (2005). "Inherent Safety of Fuels for Accelerator-Driven Systems". In: *Nuclear Technology* 151.3, pp. 314–333. DOI: 10.13182/NT05-A3654.
- Fanghänel, T., J.-P. Glatz, R.J.M. Konings, V. V. Rondinella, and J. Somers (2010). "Transuranium Elements in the Nuclear Fuel Cycle". In: *Handbook of Nuclear Engineering*. Ed. by Dan Gabriel Cacuci. Springer Science + Business Media LLC, pp. 2935–2998.
- Fassnacht, F. (2013). "Plutonium Production in Small Modular Reactors (SMR) - the Case of Toshiba 4S". Master's Thesis. Technische Universität Darmstadt.
- Fazio, C. (2007). "Introduction". In: *Handbook on Lead-bismuth Eutectic Alloy and Lead Properties, Materials Compatibility, Thermal-hydraulics and Technologies*. Ed. by OECD/NEA Nuclear Science Committee. Nuclear Energy Agency, pp. 1–9.
- Frieß, F. and M. Kütt (2016). "BN-800: Spent Fuel Dose Rates and the Plutonium Management and Disposition Agreement". In: *Science & Global Security* 24.3, pp. 204–209. DOI: 10.1080/08929882.2016.1235391.
- (forthcoming 2017). "The Role of the BN-800 Fast Reactor in a Non-Proliferation Scenario". In: *International Conference on Fast Reactors and Related Fuel Cycles, (FR17)*. Paper 219. Yekaterinburg, Russian Federation.
- Frieß, F., M. Kütt, and M. Englert (2015). "Proliferation Issues Related to Fast SMRs". In: *Annals of Nuclear Energy* 85, pp. 725–731. DOI: 10.1016/j.anucene.2015.06.028.
- Frieß, F. and W. Liebert (2015). "Transmutation of Minor Actinide and Long-Lived Fission Product in a Generic Accelerator Driven System (ADS)". In: *Proceedings of Global 2015*. Paris, France.
- (forthcoming 2017). "Implications of Partitioning and Transmutation on Reprocessing and Fuel Fabrication". In: *International Conference on Fast Reactors and Related Fuel Cycles, (FR17)*. Paper 68. Yekaterinburg, Russian Federation.
- Gandini, A. and M. Salvatores (2002). "The Physics of Subcritical Multiplying Systems". In: *Journal of Nuclear Science and Technology* 39.6, pp. 1–28. DOI: 10.1080/18811248.2002.9715249.
- Gen IV International Forum (2009). *GIF R&D Outlook for Generation IV Nuclear Energy Systems*. Report. Gen IV International Forum.
- (2016). *2015 GIF Annual Report*. Report. Gen IV International Forum.
- Gibney, E. (2015). "Why Finland Now Leads the World in Nuclear Waste Storage". In: *Nature*, Nature News. DOI: 10.1038/nature.2015.18903.
- Gilinsky, V., M. Mille, and H. Hubbard (2004). *A Fresh Examination of the Proliferation Dangers of Light Water Reactors*. Tech. rep. The Nonproliferation Policy Education Center.
- Glaser, A. (1998). "Abbrandrechnung für ein System zur Eliminierung von Waffenplutonium". PhD thesis. Technische Universität Darmstadt.

-
- Glaser, A., L. B. Hopkins, and M. V. Ramana (2013). “Resource Requirements and Proliferation Risks Associated with Small Modular Reactors”. In: *Nuclear Technology* 184, pp. 121–129.
- Glaser, A., M. V. Ramana, A. Ahmad, and R. Socolow (2015). *Small Modular Reactors - A Window on Nuclear Energy*. Tech. rep. andlinger center.
- Governments of the United States and Russia (2000). *Plutonium Management and Disposition Agreement*.
- (2010). *Plutonium Management and Disposition Agreement as Amended by the 2010 Protocol*.
- Guertin, A., M. Dierckx, R. Stieglitz, F. Roelofs, and V. Moreau (2011). “XT-ADS Windowless Spallation Target Design and Corresponding R&D Topics”. In: *Technology and Components of Accelerator-driven Systems*. Nuclear Energy Agency, pp. 335–345.
- Haeck, W. (2008). *VESTA User’s Manual, Version 2.0.0*. DSU/SEC/T/2008. Institute for Radiological Protection and Nuclear Safety.
- (2011). *VESTA User’s Manual, Version 2.1.0*. DSU/SEC/T/2011-81. Institute for Radiological Protection and Nuclear Safety.
- Hartigan, K., C. Hinderstein, A. Newman, and S. Squassoni (2015). *A New Approach to the Nuclear Fuel Cycle*. Rowman & Littlefield.
- Hinton, J.P., R.W. Barnard, D.E. Bennett, R.W. Crocker, M.J. Davis, H.J. Groh, E.A. Hakkila, G.A. Harms, W.L. Hawkins, E.E. Hill, L.W. Kruse, J.A. Milloy, W.A. Swansiger, and K.J. Ystesund (1996). *Proliferation Vulnerability Red Team Report*. Sandia Report SAND97-8203. Sandia National Laboratories.
- Holdmann, G. (2011). *Small Scale Modular Nuclear Power: an Option for Alaska?* Tech. rep. University of Alaska et al.
- Holdren, J. P., J. F. Ahearne, R. J. Budnitz, M. M. May, and J. J. Taylor (1995). *Management and Disposition of Excess Weapons Plutonium: Reactor Related Options*. Tech. rep. Committee on International Security and Arms Control, National Academy of Sciences.
- Horner, D. (2015). *S. Korea, U.S. Sign Civil Nuclear Pact*. Arms Control Association. URL: https://www.armscontrol.org/ACT/2015_0708/News/South-Korea-US-Sign-Civil-Nuclear-Pact (visited on 05/13/2017).
- IAEA (2001). *IAEA Safeguards Glossary - 2001 Edition*. International Nuclear Verification Series No. 3. International Atomic Energy Agency, Vienna, Austria.
- (2004). *Implications of Partitioning and Transmutation*. IAEA-TECDOC-435. International Atomic Energy Agency, Vienna, Austria.
- (2006). *Fast Reactor Database 2006 Update*. IAEA-TECDOC-1531. International Atomic Energy Agency, Vienna, Austria.
- (2007). *Status of Small Reactor Designs Without On-Site Refuelling*. IAEA-TECDOC-1536. International Atomic Energy Agency, Vienna, Austria.
- (2008). *Thermophysical Properties of Materials for Nuclear Engineering: A Tutorial and Collection of Data*. IAEA-THPT. International Atomic Energy Agency, Vienna, Austria.
- (2011). *Status Report 76 - Super-Safe, Small and Simple Reactor (4S)*. Tech. rep. International Atomic Energy Organisation.
- (2012a). *Status of Fast Reactor Research and Technology Development*. IAEA-TECDOC-1691. International Atomic Energy Agency, Vienna, Austria.
- (2012b). *Status of Small and Medium Sized Reactor Designs - A Supplement to the IAEA Advanced Reactors Information System (ARIS)*. Supplement to the IAEA Advanced Reactor Information System (ARIS). International Atomic Energy Agency, Vienna, Austria.
- (2012c). *Structural Materials for Liquid Metal Cooled Fast Reactor Fuel Assemblies - Operational Behaviour*. Nuclear Energy Series No. NF-T-4.3. International Atomic Energy Agency, Vienna, Austria.

-
- (2013). *The Agency's Activities on Small and Medium Sized Reactors (SMRs) to support Member States*. International Atomic Energy Agency, Vienna, Austria. URL: <http://www.iaea.org/NuclearPower/SMR/activities/index.html> (visited on 05/15/2014).
 - (2014). *Advances in SMR Technology Development*. Supplement to the IAEA Advanced Reactor Information System (ARIS). International Atomic Energy Agency, Vienna, Austria.
 - (2015). *Status of Accelerator Driven Systems Research and Technology Development*. IAEA-TECDOC-1766. International Atomic Energy Agency, Vienna, Austria.
 - (2016). *Advances in Small Modular Reactor Technology Developments*. Supplement to the IAEA Advanced Reactor Information System (ARIS). International Atomic Energy Agency, Vienna, Austria.
 - (2017). *Potential Advantages & Perceived Challenges (IAEA Observation)*. International Atomic Energy Agency, Vienna, Austria. URL: https://www.iaea.org/NuclearPower/Downloadable/SMR/files/8_Perceived_advantages_and_challenges.pdf (visited on 04/28/2017).
 - ican (2016). *UN General Assembly Approves Historic Resolution*. URL: <http://www.icanw.org/campaign-news/un-general-assembly-approves-historic-resolution/> (visited on 05/03/2017).
 - ICRP (1996). “Conversion Coefficients for Use in Radiological Protection Against External Radiation”. In: *ICRP Publication 74* 26.3/4.
 - (2010). “Conversion Coefficients for Radiological Quantities for External Radiation Exposures”. In: *ICRP Publication 116, Annals of the ICRP* 40.2-5, pp. 1–257.
 - IPFM (2007). *Global Fissile Material Report 2007*. Report. The International Panel on Fissile Materials.
 - (2010). *Fast Breeder Reactor Programs: History and Status*. Report. The International Panel on Fissile Materials.
 - (2011). *Managing Spent Fuel from Nuclear Power Reactors - Experience and Lessons from Around the World*. Report. The International Panel on Fissile Materials.
 - (2013). *Global Fissile Material Report 2013*. Report. The International Panel on Fissile Materials.
 - (2015a). *Global Fissile Material Report 2015*. Report. The International Panel on Fissile Materials.
 - (2015b). *Plutonium Separation in Nuclear Power Program - Status, Problems and Prospects of Civil Reprocessing Around the World*. Report. The International Panel on Fissile Materials.
 - IPFM Blog (2012). *China Delays Purchase of Russian Fast Neutron Reactors*. International Panel on Fissile Materials. URL: http://fissilematerials.org/blog/2012/05/china_delays_purchase_of_.html (visited on 02/14/2017).
 - (2016). *Russia Suspends Implementation of Plutonium Disposition Agreement*. International Panel on Fissile Materials. URL: http://fissilematerials.org/blog/2016/10/russia_suspends_implement.html (visited on 02/14/2017).
 - IRSN (2008). *Risks of Explosion Associated with "Red Oils" in Reprocessing Plants*. Technical Note. Institut de Radioprotection et de Sûreté Nucléaire.
 - Jameson, R. A., G. P. Lawrence, and C. D. Bowman (1992). “Accelerator-Driven Transmutation Technology for Incinerating Radioactive Waste and for Advanced Application Power Production”. In: *Nuclear Instruments and Methods in Physics Research B* 68, pp. 474–480. DOI: 10.1016/0168-583X(92)96126-J.
 - Jonter, T. (2008). “Nuclear Non-Proliferation - a Brief Historical Background”. In: *Nuclear Safeguards and Non-Proliferation*. Ed. by G. Janssens-Maenhout. European Communities, pp. 9–28.
 - Kang, J., T. Suzuki, S. Pickett, and A. Suzuki (2002). “Spent Fuel Standard as a Baseline for Proliferation Resistance in Excess Plutonium Disposition Options”. In: *Science & Global Security* 37.8, pp. 691–696. DOI: 10.1080/18811248.2000.9714945.
 - Kankeleit, E., C. Küppers, and U. Imkeller (1993). *Report on the Useability of Reactor Plutonium in Weapons*. Tech. rep. Institut für Kernphysik, Technische Hochschule Darmstadt.

-
- Kelly, J. E. (2013). “DOE Strategic Vision for Small Modular Reactors”. In: *4th Annual Platts SMR Conference*. Washington, D.C., USA.
- (2014). “Generation IV International Forum: A Decade of Progress through International Cooperation”. In: *Progress in Nuclear Energy* 77, pp. 240–246. DOI: 10.1016/j.pnucene.2014.02.010.
- Kessides, I. N. and V. Kuznetsov (2012). “Small Modular Reactors for Enhancing Security in Developing Countries”. In: *Sustainability* 4, pp. 1806–1832. DOI: 10.1080/18811248.2000.9714945.
- Kilaru, B., M. Mavricek, Y. Szeto, and M. Yanamandala (2010). *Increasing Nuclear Power Use in the United States*. Report. University of Chicago.
- Kirchner, G., M. Englert, C. Pistner, B. Kallenbach-Herbert, and J. Neles (2015). *Gutachten "Transmutation"*. Assessment Report. Institut für angewandte Ökologie und Universität Hamburg, Zentrum für Naturwissenschaft und Friedensforschung.
- Kloosterman, J. L. and J. M. Li (1995). *Transmutation of Tc-99 and I-129 in Fission Reactors*. A Calculational Study, ECN-R-95-002. The Netherlands Energy Research Foundation ECN.
- Kommission Lagerung hoch radioaktiver Abfallstoffe (2016). *Verantwortung für die Zukunft*. Abschlussbericht der Kommission Lagerung hoch radioaktive Abfallstoffe. Geschäftsstelle K-Drs. 268.
- Krieger, H. (2012). *Grundlagen der Strahlungsphysik und des Strahlenschutzes*. Ed. by Springer Spektrum.
- Kurata, Y., T. Takizuka, T. Osugi, and H. Takano (2002). “The Accelerator Driven System Strategy in Japan”. In: *Journal of Nuclear Materials* 301, pp. 1–7. DOI: 0.1016/S0022-3115(01)00731-0.
- Kütt, M. (2007). “Proliferationsproblematik beim Umgang mit Plutoniumbrennstoffen: Abbrandrechnungen zur Rolle von ^{238}Pu ”. Bachelor’s Thesis. Technische Universität Darmstadt.
- (2011). “Neutronic Calculations: Proliferation Risks of Fast Reactors”. Master’s Thesis. Technische Universität Darmstadt.
- Kütt, M., F. Frieß, and M. Englert (2014). “Plutonium Disposition in the BN-800 Fast Reactor: an Assessment of Plutonium Isotopic and Breeding”. In: *Science & Global Security* 22.3, pp. 188–208. DOI: 10.1080/08929882.2014.952578.
- Leyen, P. (2012). “MYRRHA Current Design and Design Challenges”. In: *Gen 4-Seminar*. Risø, Denmark.
- Liebert, W. (2005). “Proliferationsresistenz: Risiken und notwendige Schritte zur effektivem Eindämmung der nuklearen Proliferation”. In: Neuneck, Götz and Christian Mölling. *Die Zukunft der Rüstungskontrolle*. Nomos.
- Liebert, W. and J. C. Schmidt (2015). “Demands and Challenges of a Prospective Technology Assessment”. In: Scherz, C., T. Michalek, L. Hennen, L. Heáková, J. Hahn, and S. Seitz. *The Next Horizon of Technology Assessment*. Prag: Technology Center ASCR, pp. 331–340.
- Lovering, J. R., A. Yip, and T. Nordhaus (2016). “Historical Construction Costs of Global Nuclear Power Reactors”. In: *Energy Policy* 91, pp. 371–382. DOI: 10.1016/j.enpol.2016.01.011.
- Lovins, A. (1980). “Nuclear Weapons and Power-Reactor Plutonium”. In: *Nature* 283, pp. 817–823. DOI: 10.1038/283817a0.
- Loyd, W.R., M.K. Sheaffer, and W.G. Sutcliffe (1994). *DoseRate Estimates from Irradiated Light-Water-Reactor Fuel Assemblies in Air*. UCRL-ID-115199. Lawrence Livermore National Laboratory.
- Lyman, E. (2013). *Small Isn’t always Beautiful*. Report. Union of Concerned Scientists.
- Lyman, E. and H. Feiveson (1998). “The Proliferation Risks of Plutonium Mines”. In: *Science & Global Security* 7, pp. 119–128.
- Makhijani, A. (2013). *Light Water Designs of Small Modular Reactors: Facts and Analysis*. Tech. rep. Institute for Energy and Environmental Research.
- Makhijani, A., L. Chalmers, and B. Smith (2004). *Uranium Enrichment - Just Plain Facts to Fuel an Informed Debate on Nuclear Proliferation and Nuclear Power*. Tech. rep. Institute for Energy and Environmental Resrach.
-

-
- Mansani, L., C. Artioli, M. Schikorr, G. Rimpault, C. Angulo, and D. de Bruyn (2012). "The European Lead-cooled EFIT plant: an Industrial Scale Accelerator-driven System for Minor Actinide Transmutation". In: *Nuclear Technology* 180, pp. 241–263.
- Martínez-Val, J. and H. A. Abderrahim (2008). *D6.2 P&T Roadmap proposal for Advanced Fuel Cycles leading to a Sustainable Nuclear Energy*. Syntheses Report. Sixth Framework programme - Partitioning and Transmutation European Roadmap for Sustainable nuclear Energy (PATEROS).
- Maschek, W., X. Chen, F. Delage, and A. Fernandez-Carretero, D. Haas, C. Matzerath Boccaccini, A. Rineiski, P. Smith, V. Sobolev, R. Thetford, and J. Wallenius (2008). "Accelerator Driven Systems for Transmutation: Fuel Development, Design, and Safety". In: *Progress in Nuclear Energy* 50, pp. 333–340. DOI: 10.1016/j.pnucene.2007.11.066.
- McCarty, R. D. (1972). *Thermophysical Properties of Helium-4 from 2 to 1500 K with Pressures to 1000 Atmospheres*. U.S. Department of Commerce.
- McGinnes, D.F. (2002). *Model Radioactive Waste Inventory for Reprocessing Waste and Spent Fuel*. Technical Report 01-01. National Cooperative for the Disposal of Radioactive Waste.
- Mills, A. (2012). *B&W Selected as Winner of DOE's Small Modular Reactor Program*. Babcock & Wilcox. URL: http://www.babcock.com/news_and_events/2012/20121120a.html (visited on 07/08/2013).
- Mueller, A. C. (2013). "Transmutation of Nuclear Waste and the future MYRRHA Demonstrator". In: *Journal of Physics: Conference Series* 420. DOI: 10.1088/1742-6596/420/1/012059.
- Mueller, A. C. and H. A. Abderrahim (2010). "Transmutation von radioaktivem Abfall". In: *Physik Journal* 9.11, pp. 33–38.
- Musiol, G., J. Ranft, R. Reift, and D. Seeliger (1988). *Kern- und Elementarteilchenphysik*. VCH.
- Nagra (2002). *Demonstration of Disposal Feasibility for Spent Fuel, Vitrified High-level Waste and long-lived Intermediate-level Waste (Entsorgungsnachweis)*. Tech. rep. National Cooperative for the Disposal of Radioactive Waste.
- NEA (1995). *Physics of Plutonium Recycling, Plutonium Recycling in Pressurized-water Reactors, a Report, Volume II*. OECD Document. Nuclear Energy Agency / Organisation for Economic Co-Operation and Development.
- (1999). *Actinide and Fission Product Partitioning and Transmutation - Status and Assessment Report*. Tech. rep. Nuclear Energy Agency / Organisation for Economic Co-Operation and Development.
 - (2002). *Accelerator-driven Systems (ADS) and Fast Reactors (FR) in Advanced Nuclear Fuel Cycles*. Comparative Study. Nuclear Energy Agency / Organisation for Economic Co-Operation and Development.
 - (2005). *Fuels and Materials for Transmutation*. Status Report. Nuclear Energy Agency / Organisation for Economic Co-Operation and Development.
 - (2006). *Physics and Safety of Transmutation Systems*. Status Report. Nuclear Energy Agency / Organisation for Economic Co-Operation and Development.
 - (2012a). *Actinide and Fission product partitioning and transmutation - Eleventh Information Exchange Meeting*. Tech. rep. Nuclear Energy Agency / Organisation for Economic Co-Operation and Development.
 - (2012b). *Joint Evaluated Nuclear Data Library for Fission and Fusion Applications*. Data Library. Nuclear Energy Agency / Organisation for Economic Co-Operation and Development.
- Nikitin, M. B. (2012). *North Korea's Nuclear Weapons: Technical Issues*. Report for Congress. Congressional Research Service.
- NRC (2012). *Super-Safe, Small and Simple (4S)*. United States Nuclear Regulatory Commission. URL: <http://www.nrc.gov/reactors/advanced/4s.html> (visited on 12/10/2012).
- NRC, Committee on Separations Technology and Transmutation Systems (1996). *Nuclear Wastes: Technologies for Separations and Transmutation*. The National Academies Press.
- Nuclear Energy International Magazine (2017). *Fast Reactions*. URL: <http://www.neimagazine.com/features/featurefast-reactions-4899798/> (visited on 02/14/2017).
-

-
- NuScale Power, LCC (2013). *U.S. DOE Awards Funding for NuScale Power's SMR Technology*. URL: <http://www.nuscalepower.com/news20131212.aspx> (visited on 05/15/2014).
- Obama, B. (2012). *National Security Speech at the National War College*. Speech.
- Obbink, H. G. (2017). *Wunderland Kalkar*. URL: <https://www.wunderlandkalkar.eu/de> (visited on 05/01/2017).
- Office of Nuclear Energy (2017). *Small Modular Reactors (SMRs)*. U.S. Department of Energy. URL: <https://www.energy.gov/ne/nuclear-reactor-technologies/small-modular-nuclear-reactors> (visited on 04/28/2017).
- Official Journal of the European Union (2013). *Council Directive 2013/59/EURATOM*. Legislation. EURATOM.
- O'Meara, S. (2013). *SMR and Advanced Reactor Deployment in the USA*. Report. Nuclear Energy Insider.
- Orlov, V. V., O. D. Bakumenko, E. M. Ikhlov, M. Y. Kulakovskij, M. F. Troyanov, and A. G. Tsykunov (1974). *Physical Peculiarities of the Fast Power Reactor Fuel Cycle*. Tech. rep. International Atomic Energy Agency, Vienna (Austria).
- Palazzo, S., K. I. Velkov, G. Lerchl, and K. van Tichelen (2013). "Analyses of the MYRRHA Spallation Loop Using the System Code ATHLET". In: *Annals of Nuclear Energy* 60, pp. 274–286. DOI: 10.1016/j.anucene.2013.05.010.
- Pellaud, B. (2002). "Proliferation Aspects of Plutonium Recycling". In: *C. R. Physique* 3, pp. 1067–1079. DOI: 10.1016/S1631-0705(02)01364-6.
- Pelowitz, D. B. (2011). *MCNPX User's Manual, Version 2.7.0*. LA-CP-11-00438 LA-CP-11-00438. Los Alamos National Laboratory.
- Pistner, C. (1998). "Entwicklung und Validierung eines Programmsystems zur Zellabbrandrechnung plutoniumhaltiger Brennstoffe". Diploma Thesis. Technische Universität Darmstadt.
- (2006). "Neutronenphysikalische Untersuchungen zu uranfreien Brennstoffen". PhD Thesis. Technische Universität Darmstadt.
- Plutonium Disposition Working Group (2014). *Analysis of Surplus Weapon-Grade Plutonium Disposition Options*. Report. U.S. Department of Energy.
- Podvig, P. (2016). *Can the US-Russia Plutonium Disposition Agreement be Saved?* Bulletin of the Atomic Scientists. URL: <http://thebulletin.org/can-us-russia-plutonium-disposition-agreement-be-saved9389> (visited on 04/27/2017).
- Popov, S. G., V. K. Ivanov, J. J. Carbajo, and G. L. Yoder (2000). *Thermophysical Properties of MOX and UO₂ Fuels Including the Effects of Irradiation*. ORNL/TM-2000/351. Oak Ridge National Laboratory.
- Porollo, S. I., Y. V. Konobeev, and F. A. Garner (2009). "Swelling and Microstructure of Austenitic Stainless Steel ChS CW after High Dose Neutron Irradiation". In: *Journal of Nuclear Materials* 393, pp. 61–66. DOI: 10.1016/j.jnucmat.2009.05.005.
- Preter, P. de, P. Lalioux, and W. Cool (2001). *Technical overview of the SAFIR 2 report*. Safety Assessment and Feasibility Interim Report 2. ONDRAF/NIRAS.
- Prinja, A. K. and E. W. Larsen (2010). "General Principles of Neutron Transport". In: *Handbook of Nuclear Engineering*. Ed. by Dan Gabriel Cacuci. Springer Science + Business Media LLC, pp. 428–542.
- Pusa, M. (2013). "Numerical Methods for Nuclear Fuel Burnup Calculations". PhD thesis. Aalto University.
- Ragheb, M. (2011). *Decay Heat Generation in Fission Reactors*. <http://www.ewp.rpi.edu/hartford/ernesto/F2011/EP/MaterialsforStudents/Petty/Ragheb-Ch8-2011.PDF>.
- Ramana, M. V., L. B. Hopkins, and A. Glaser (2013). "Licensing Small Modular Reactors". In: *Energy* 61, pp. 555–564. DOI: 10.1016/j.energy.2013.09.010.

- Ramana, M. V. and Z. Mian (2014). “One Size Doesn’t Fit All: Social Priorities and Technical Conflicts for Small Modular Reactors”. In: *Energy Research and Social Science* 2, pp. 115–124. DOI: 10.1016/j.erss.2014.04.015.
- Reaktor-Sicherheitskommission and Strahlenschutzkommission, Germany (2002). *Gemeinsame Stellungnahme der RSK und der SSK betreffend BMU-Fragen zur Fortschreibung der Endlager-Sicherheitskriterien*.
- Renn, O. et al. (2013). *Partitionierung und Transmutation - Forschung - Entwicklung - Gesellschaftliche Implikationen*. acatech Studie. Deutsche Akademie der Technikwissenschaften.
- Robel, M., J.-S. Choia, B.B. Ebbinghaus, B. W. Sleaforda, C. G. Bathke, B. A. Collinsc, Z. Beauvais, K. R. Haseb, A. W. Prichardc, and J. A. Blinka (2013). *A Safeguards and Security Assessment Comparing the Nuclear Material Attractiveness of Unirradiated and Irradiated Fuels Associated with Existing Power Reactors and Potential Future Small Modular Reactors*. LLNL-CONF-639792. Lawrence Livermore National Laboratory.
- Romero, E. M. González and H. A. Abderrahim (2007). *D1.1 Rational and Added Value of P& T for Waste Management Policies*. Deliverable D1.1. Sixth Framework programme - Partitioning and Transmutation European Roadmap for Sustainable Nuclear Energy (PATEROS).
- Rosatom (2017). *Modern Reactors of Russian Design*. URL: <http://www.rosatom.ru/en/rosatom-group/engineering-and-construction/modern-reactors-of-russian-design/> (visited on 02/14/2017).
- Rossa, R. (2011). “Study of Some Aspects of Proliferation Resistance of the MYRRHA facility”. Master’s Thesis. Politecnico di Torino.
- Rouault, J. (2010). “Sodium Fast Reactor Design: Fuels, Neutronic, Thermal-Hydraulics, Structural Mechanics and Safety”. In: *Handbook of Nuclear Engineering*. Ed. by Dan Gabriel Cacuci. Springer Science + Business Media LLC, pp. 2321–2710.
- Rubbia, C., J. A. Rubio, S. Buono, F. Carminati, N. Fiétier, J. Galvez, C. Gelés, Y. Kadi, R. Klapisch, P. Mandrillon, J. P. Revol, and Ch. Roche (1995). *Conceptual Design of a Fast Neutron Operated High Power Energy Amplifier*. CERN/AT/95-44(ET). European Organisation for Nuclear Research.
- Salvatores, M., M. Meyer, V. Romanello, L. Boucher, and A. Schwenk-Ferrero (2008). *Results of the Regional Scenarios Studies*. Deliverable 2.2. Sixth Framework programme - Partitioning and Transmutation European Roadmap for Sustainable Nuclear Energy (PATEROS).
- Şarer, B., S. Şahin, Y. Çelik, and M. Günay (2013). “Evaluation of Integral Quantities in an Accelerator Driven System Using Different Nuclear Models Implemented in the MCNPX Monte Carlo Transport Code”. In: *Annals of Nuclear Energy* 62, pp. 382–389. DOI: 10.1016/j.anucene.2013.05.045.
- Sarotto, M. (2012). “MYRRHA-FASTEF FA/Core Design”. In: *International Workshop on Innovative Nuclear Reactors cooled by HLM: Status & Perspectives*. Pisa, Italy.
- Sarotto, M., D. Castelliti, R. Fernandez, D. Lamberts, E. Malambu, A. Stankovskiy, W. Jaeger, M. Ottolini, F. Martin-Fuertes, L. Sabathe, L. Mansani, and P. Baeten (2013). “The MYRRHA - FASTEF cores Design for Critical and Sub-critical Operational Modes (EU FP7 Central Design Team Project)”. In: *Nuclear Engineering and Design* 256, pp. 184–200. DOI: 10.1016/j.nucengdes.2013.08.055.
- Schlichting, K. W., N. P. Padture, and P. G. Klemens (2001). “Thermal Conductivity of Dense and Porous Yttria Stabilized Zirconia”. In: *Journal of Materials Science* 36, pp. 3003–3010. DOI: 10.1023/A:1017970924312.
- Schmidt, G., G. Kirchner, and C. Pistner (2013). “Endlagerproblematik - Können Partitionierung und Transmutation helfen?” In: *Technikfolgenabschätzung - Theorie und Praxis* 22, pp. 52–58.
- Schneider, M. and A. Froggatt (2016). *The World Nuclear Industry*. Status Report. Mycle Schneider Consulting.

- Schwenk-Ferrero, A. (2013). "German Spent Nuclear Fuel Legacy: Characteristics and High-Level Waste Management Issues". In: *Science and Technology of Nuclear Installations*. DOI: 10.1155/2013/293792.
- SCK-CEN (2016). *MYRRHA - Proton Beam Specifications*. Belgian Nuclear Research Center. URL: http://myrrha.sckcen.be/en/Engineering/Accelerator/Beam_specifications (visited on 05/25/2016).
- (2017). *MYRRHA: Multi-Purpose Hybrid Research Reactor for High-Tech Applications*. Belgian Nuclear Research Center. URL: <http://myrrha.sckcen.be/> (visited on 04/20/2017).
- Seltborg, P. (2005). "Source Efficiency and High-Energy Neutronics in Accelerator-Driven Systems". PhD thesis. Department of Nuclear and Reactor Physics, Royal Institute of Technology, Stockholm.
- Shwageraus, E. and P. Hejzlar (2009). "Decay Heat in Fast Reactors with Transuranic Fuels". In: *Nuclear Engineering and Design* 239.12, pp. 2646–2653. DOI: 10.1016/j.nucengdes.2009.07.010.
- Sobolev, V. (2005). "Fuel Design for the Experimental ADS MYRRHA". In: *Technical Meeting on Use of LEU in ADS*. Vienna, Austria: IAEA.
- Sobolev, V. and G. Benamati (2007). "Thermophysical and Electric Properties". In: *Handbook on Lead-bismuth Eutectic Alloy and Lead Properties, Materials Compatibility, Thermal-hydraulics and Technologies*. Ed. by OECD/NEA Nuclear Science Committee. Nuclear Energy Agency, pp. 25–99.
- Sobolev, V., W. Uyttenhove, W. Maschek, A. Rineiski, X. Chen, J. Wallenius, A. Fokau, and F. Delage (2010). "Optimisation of the EFIT Fuel Design". In: *Technology and Components of Accelerator-Driven Systems - Workshop Proceedings*. DOI: 10.1787/9789264117297-en.
- Sokova, E. (2010). *Plutonium Disposition*. NTI Analysis. URL: <http://www.nti.org/analysis/articles/plutonium-disposition-14/> (visited on 05/28/2017).
- Stankus, S. V., R. A. Khairulin, A. G. Mozgovoy, V. V. Roshchupkin, and M. A. Pokrasin (2008). "The Density and Thermal Expansion of Eutectic Alloys of Lead with Bismuth and Lithium in Condensed State". In: *Journal of Physics: Conference Series* 98. DOI: 10.1088/1742-6596/98/6/062017.
- Stock, R. (2013). "Generation IV Nuclear Reactors". In: *Encyclopedia of Nuclear Physics and its Application*. Ed. by Reinhard Stock. Wiley-VCH Verlag GmbH & Co. KGaA, pp. 665–688.
- Subki, H. (2016). "Technology Development Status Report - Small Modular Reactors". In: *The 10th GIF-IAEA Interface Meeting*. Vienna, Austria.
- Svensk Kärnbränslehantering AB (2011). *Long-term Safety for the Final Repository for Spent Nuclear Fuel at Forsmark, Volume III*. Technical Report TR-11-01.
- Tabirian, A. (2016). *U.S.-Russian Plutonium Disposition Deal Collapses Under Weight of MOX Battle*. Exchange Monitor. URL: <http://www.exchangemonitor.com/publication/nsd/u-s-russian-plutonium-disposition-deal-collapses-weight-mox-battle/> (visited on 04/28/2017).
- Takubo, M. and F. von Hippel (2016). *Future of Japan's Monju Plutonium Breeder Reactor under Review*. International Panel on Fissile Materials. URL: http://fissilematerials.org/blog/2016/09/future_of_japans_monju_pl.html (visited on 05/15/2017).
- The Yomiuri Shimbun (2013). *Toshiba Developing Small N-reactor - Reactor to Be Used to Mine Oil Sands in Canada; Initial Operation by 2020 Eyed*. Daily Yomiuri Online. URL: <http://archive.is/ZsklU> (visited on 02/03/2014).
- ThyssenKrupp Materials (2011). *Werkstoffdatenblatt Legierter warmfester Stahl*. Werkstoffdatenblatt.
- Tichelen, K. van, H. A. Kupschus Pand Abderrahim, A. Klujkin, and E. Platacis (2001). "MYRRHA: Design and Verification Experiments for the Windowless Spallation Target of the ADS Prototype MYRRHA". In: *Fourth International Meeting on Accelerator Driven Transmutation Technologies and Applications*. Reno, NV, United States.
- Toshiba (2013). *Submittal of Technical Report "Design Description of the 4S Instrumentation and Control System"*. Letter.
- Tosoh Corp (2017). *Basic Grades - TZ-3Y-E, TZ-3YB-E*. Material Data Sheet. Bound Brook, NJ, USA.

- Traub, R. J. (2010). *Calculating of Ambient ($H^*(10)$) and Personal ($H_p(10)$) Dose Equivalent from a ^{252}Cf Neutron Source*. PNNL-19273. Pacific Northwest Laboratory.
- Trumbull, T. H. and D. R. Harris (2005). *The Effect of Material Homogenization in Calculating the Gamma-Ray Dose from Spent PWR Fuel Pins in an Air Medium*. LM-05K034. Lockheed Martin Cooperation and Rensselaer Polytechnic Institute.
- Tsuboi, Y., K. Arie, N. Ueda, T. Grenci, and A. M. Yacout (2012). "Design of the 4S Reactor". In: *Nuclear Technology* 178.2, pp. 201–217. DOI: 10.13182/NT10-74.
- Tsujimoto, K., T. Sasa, K. Nishihara, H. Oigawa, and H. Takano (2004). "Neutronics Design for Lead-Bismuth Cooled Accelerator-Driven System for Transmutation of Minor Actinide". In: *Journal of Nuclear Science and Technology* 41.1, pp. 21–36. DOI: 10.1080/18811248.2004.9715454.
- Turinsky, P. (2010). "Core Isotopic Depletion and Fuel Management". In: *Handbook of Nuclear Engineering*. Ed. by Dan Gabriel Cacuci. Springer Science + Business Media LLC, pp. 1241–1312.
- Uffelen, P. van, R. J.M. Konings, C. Vitanza, and J. Tulenko (2010). "Analysis of Reactor Fuel Rod Behavior". In: *Handbook of Nuclear Engineering*. Ed. by Dan Gabriel Cacuci. Springer Science + Business Media LLC, pp. 1519–1627.
- United Nations (2017). *Draft Convention on the Prohibition of Nuclear Weapons*. UN Document A/CONF.229/2017/CRP1.
- United States Department of Energy (1993a). *DOE Fundamentals Handbook - Nuclear Physics and Reactor Theory, Volume 1*. U. S. Department of Energy.
- (1993b). *DOE Fundamentals Handbook - Nuclear Physics and Reactor Theory - Volume 2*. U. S. Department of Energy.
- (1996). *Plutonium: The First 30 Years*. DOE/DP-0137. Department of Energy.
- (1999). *A Roadmap for Developing Accelerator Transmutation of Waste (ATW) Technology*. Report to Congress, DOE/RW-0519. U.S. Department of Energy.
- (2011). *Nuclear Materials Control and Accountability*. DOE-STD-1194-2011 DOE-STD-1194-2011. United States Department of Energy.
- (2014). *Small Modular Reactors (SMRs)*. U.S. Department of Energy: Small Modular Reactor Program. URL: <https://smr.inl.gov/Content.aspx?externalID=E9DB092D-00ED-46B3-B396-5861817DAD20> (visited on 05/17/2017).
- Uyttenhove, W. (2016). "Reactivity Monitoring of Accelerator-Driven Nuclear Reactor Systems". PhD thesis. Technische Universiteit Delft.
- Uyttenhove, W., V. Sobolev, and W. Maschek (2011). "Optimisation of Composite Metallic Fuel for Minor Actinide Transmutation in an Accelerator-Driven System". In: *Journal of Nuclear Materials* 416, pp. 192–199. DOI: 10.1016/j.jnucmat.2010.11.093.
- Vassil'kov, R. G. and V. I. Yurevich (1990). "Neutron Emission from an Extended Lead Target under the Action of Light Ions in the GeV Region". In: *ICANS-XI International Collaboration on Advanced Neutron Sources*. Tsukuba, Japan.
- Wallenius, J. (2012). "Physics of Americium Transmutation". In: *Nuclear Engineering and Technology* 44.2, pp. 199–206. DOI: 10.5516/NET.01.2012.505.
- Ward, D. C. (2009). *Impact of Switching To The ICRP-74 Neutron Flux-To-Dose Equivalent Rate Conversion Factors at the Sandia National Laboratory Building 818 Neutron Source Range*. Sandia Report SAND2009-1144. Sandia National Laboratories.
- Wilson, N. (2016). *Could Nuclear Power and the Co-Generation Be the Key to a Truly Emission-Free Oil Sands? Alberta Oil - The Business of Energy*. URL: <https://www.albertaoilmagazine.com/2016/04/nuclear-power-co-generation-key-truly-emissions-free-oil-sands/> (visited on 02/09/2017).
- World Nuclear Association (2017a). *Fast Neutron Reactors*. World Nuclear Association. URL: <http://www.world-nuclear.org/information-library/current-and-future-generation/fast-neutron-reactors.aspx> (visited on 04/25/2017).

-
- World Nuclear Association (2017b). *Russia's Nuclear Fuel Cycle*. World Nuclear Association. URL: <http://www.world-nuclear.org/information-library/country-profiles/countries-o-s/russia-nuclear-fuel-cycle.aspx> (visited on 02/14/2017).
- (2017c). *Safety of Nuclear Power Reactors*. World Nuclear Association. URL: <http://www.world-nuclear.org/information-library/safety-and-security/safety-of-plants/safety-of-nuclear-power-reactors.aspx> (visited on 04/25/2017).
 - (2017d). *Small Nuclear Power Reactors*. World Nuclear Association. URL: <http://www.world-nuclear.org/information-library/nuclear-fuel-cycle/nuclear-power-reactors/small-nuclear-power-reactors.aspx> (visited on 04/28/2017).
- World Nuclear News (2010). *Joint Venture Launched for Chinese Fast Reactor*. World Nuclear Association. URL: http://www.world-nuclear-news.org/C-Joint_venture_launched_for_Chinese_fast_reactor-3004104.html (visited on 02/14/2017).
- Yacout, A. M. (2008). *Long-Life Metallic Fuel for the Super Safe, Small and Simple (4S) Reactor*. AFT-2008-000056. Toshiba Corporation and Central Research Institute of Electric Power Industry.

A Acronyms

ADS	Accelerator-Driven System
BOC	Begin of Cycle
BOL	Begin of Life
BR	Breeding Ratio
BWR	Boiling Water Reactor
CR	Control Rods
EFIT	European Facility for Industrial-sized Transmutation
EOL	End of Life
eV	Electron Volt
FE	Fuel Element
FP	Fission Product
FPD	Full Power Days
GIF	Generation IV International Forum
IAEA	International Atomic Energy Agency
IPS	In-pile Test Sections
IRSN	French Institute for Radiological Protection and Nuclear Safety
LBE	Lead-Bismuth Eutectic
LLFP	Long-lived Fission Product
LWR	Light Water Reactor
MOX	Mixed Oxide Fuel
MW/kgHM	MegaWatt days per Kilogramm Heavy Metal
MYRRHA	Multi Purpose Hybrid Research Reactor for High-tech Applications
(N)NWS	(Non-)Nuclear Weapon State
NPT	Treaty on the Non-Proliferation of Nuclear Weapons
NRC	Nuclear Regulatory Commission
PMDA	Plutonium Management and Disposition Agreement
P&T	Partitioning and Transmutation
PuMA	Plutonium and Minor Actinides
PWR	Pressurized Water Reactor
R&D	Research and Development
RDD	Radiation Dispersion Device
SMR	Small, Modular Reactor
UO ₂	Uranium Oxide Fuel



B MCNPX Input Files

For the two specific cases of gamma dose rate calculations and the simulation of a spallation source, the Data Card Block from the MCNPX input files is given. The material compositions as a part of the block were omitted. The number of source particles was determined in preliminary calculations.

Data Card Block for Spontaneous Fission Source

```
c =====
c transport gamma particles (photons)
MODE P
c number of starting particles
NPS 1000000
c print and dumb cycle
PRDMP 2j 1
c Activation control
c create delayed photons from fission and non-fission events
c sample gammas using models based on line-emission data
ACT FISSION=p NONFISS=p DG=LINES
c =====
c Source Definition
c spontaneous photons in the fuel. Each fuel pin listed separately
sdef par=sp pos=d1
SI1 L -9.541 0.          96 &
[...]
SP1 1 167r
c =====
c Tally cards
FC5 Tally in 1m distance (ring)
F5z:p 145 100 2
c Energy bins for dose calculation with different coefficients in mathematica
E0  0.100e-1 0.150e-1 0.200e-1 0.300e-1 0.400e-1 0.500e-1
    0.600e-1 0.800e-1 0.100e+0 0.150e+0 0.200e+0 0.300e+0
    0.400e+0 0.500e+0 0.600e+0 0.800e+0 0.100e+1 0.150e+1
    0.200e+1 0.300e+1 0.400e+1 0.500e+1 0.600e+1 0.800e+1
    0.100e+2
c print activities of the materials from sp source + universe map
Print 44 128
c =====
```

Data Card Block for Spallation Source

```
c =====
c transport neutrons, protons, and pions
MODE N H /
c increase upper limit for neutron energy (default: 100 MeV)
PHYS:N 1000. j j
c increase upper limit for proton energy increased (default: 100 MeV)
PHYS:H 1000. j j
c select Bertini, ISABEL, CEM03 or INCL4 model; CEM03, highly recommended
c default: elastic scattering for neutrons and protons
c default: pre-equilibrium model after intranuclear cascade
c default: Bertini model for nucleons and pions and ISABEL for other particles
LCA 8j 1
c number of starting particles
NPS 7000
c print and dump cycle
PRDMP j -30 j 1
c =====
c Source Definition
c 600 MeV proton beam, donut shape, constant distribution
SDEF sur 40 erg 600. dir 1 vec 0. 0. -1 pos 0. 0. 106. par 9 rad=D1
SI1 2.5 5
SP1 0 1
c =====
c Tallies automatically added by VESTA
```

C Specific Activities

Isotope	Specific Activity in Bq/kg	Isotope	Specific Activity in Bq/kg
H-3	$3.56 \cdot 10^{17}$	U-234	$2.30 \cdot 10^{11}$
C-14	$1.7 \cdot 10^{14}$	U-235	$8.00 \cdot 10^{07}$
Cl-36	$1.2 \cdot 10^{12}$	U-236	$2.39 \cdot 10^{09}$
Ar-39	$1.26 \cdot 10^{15}$	U-238	$1.24 \cdot 10^{07}$
Fe-55	$8.80 \cdot 10^{16}$	Np-237	$2.60 \cdot 10^{10}$
Co-60	$4.19 \cdot 10^{16}$	Pu-238	$6.33 \cdot 10^{14}$
Ni-59	$3.0 \cdot 10^{12}$	Pu-239	$2.30 \cdot 10^{12}$
Ni-63	$2.10 \cdot 10^{15}$	Pu-240	$8.40 \cdot 10^{12}$
Se-79	$5.68 \cdot 10^{11}$	Pu-241	$3.84 \cdot 10^{15}$
Kr-85	$1.45 \cdot 10^{16}$	Pu-242	$1.46 \cdot 10^{11}$
Sr-90	$5.09 \cdot 10^{15}$	Am-241	$1.27 \cdot 10^{14}$
Y-90	$2.0 \cdot 10^{19}$	Am-242m	$3.88 \cdot 10^{14}$
Zr-93	$9.30 \cdot 10^{10}$	Am-243	$7.37 \cdot 10^{12}$
Nb-93m	$8.83 \cdot 10^{15}$	Cm-242	$1.23 \cdot 10^{17}$
Nb-94	$6.93 \cdot 10^{12}$	Cm-243	$1.87 \cdot 10^{15}$
Tc-99	$6.34 \cdot 10^{11}$	Cm-244	$3.00 \cdot 10^{15}$
Pd-107	$1.9 \cdot 10^{10}$	Cm-245	$6.3 \cdot 10^{12}$
Cd-113m	$8.31 \cdot 10^{15}$	Cm-246	$1.1 \cdot 10^{13}$
Sn-121	$3.55 \cdot 10^{19}$		
Sn-121m	$2.0 \cdot 10^{15}$		
Sn-126	$4.57 \cdot 10^{11}$		
Sb-125	$3.84 \cdot 10^{16}$		
Sb-126	$3.11 \cdot 10^{18}$		
Sb-126m	$2.89 \cdot 10^{21}$		
Te-125m	$2.26 \cdot 10^{33}$		
I-129	$6.54 \cdot 10^{09}$		
Cs-134	$4.79 \cdot 10^{16}$		
Cs-135	$4.2 \cdot 10^{10}$		
Cs-137	$3.21 \cdot 10^{15}$		
Ba-137m	$1.99 \cdot 10^{22}$		
Pm-147	$3.43 \cdot 10^{16}$		
Sm-151	$9.9 \cdot 10^{14}$		
Eu-152	$6.44 \cdot 10^{15}$		
Eu-154	$1.00 \cdot 10^{16}$		
Eu-155	$1.80 \cdot 10^{16}$		
Ho-166m	$6.64 \cdot 10^{13}$		
Hf-178m	$1.59 \cdot 10^{33}$		

The specific activities were calculated using isotope half-lives and masses as implemented in Mathematica.



Acknowledgements

This work would not have been possible without the IANUS group of the Technische Universität Darmstadt. Becoming a member of this group was one of the best decisions I made during my time at the university. Countless meetings, discussions, and seminars broadened my horizon and deepened my understanding of the world.

Special credit is due to Prof. Franz Fajara. He supported this work from the beginning. With the future of IANUS unclear, he took all efforts to ensure the successful outcome of my dissertation. From the beginning, Matthias Englert helped in shaping the actual research project. He always found time for discussion and supervision. Without him, I might as well still be postponing the final writing of this thesis. I enjoyed working with Moritz Kütt. He was not only very helpful in ongoing tech and computer support, his comments greatly improved my work. I want to thank them both for the fruitful collaboration.

Still a Master's student, Prof. Wolfgang Liebert invited me to Vienna to present my work. His interest in my research never ceased. His input and knowledge shaped the final outcome of this work. After we moved to Vienna, I was warmly welcomed in his research group. All colleagues from the Institute for Safety/Security and Risk Sciences at the BOKU Vienna together make going to work each day really enjoyable. They have an open door and mind to answer literally any question. I would especially like to thank Nikolaus Müllner and Klaus Gufler who spent hours in supporting my research and provided valuable feedback.

I am grateful to Nikolaus Arnold, Christopher Fichtlscherer, Bartłomiej Gruchalski, Regina Hagen, and Larissa Zajicek who helped in finding all the little imperfections in the near final version of this thesis.

Prof. Barbara Drossel agreed to be my supervisor already at an early stage. I am thankful for her ongoing interest and support. Prof. Alfred Nordmann generously continued financing my research including several travels after restructuring IANUS. Even though working under different objectives, the new IANUS members welcomed me whenever I visited Darmstadt.

Through all my (educational) career, my parents supported me in letting me make my own decisions. I believe, they still cannot fathom some of them. My siblings had different approaches in supporting me, ranging from the least possible distraction from work over German grammar support to messages containing countless emojis. Thanks to all of them.

Last but not least I am grateful to my husband Johannes for his ongoing love and support. Over the years, he became an expert in proof-reading my work. He spent hours on chasing my mistakes. He moved with me to Vienna and took care of the smartest and most beautiful of all children, our daughter Inara. She touched my heart in a way I never thought possible before.



Curriculum Vita

Personal Data

Name: Friederike Renate Frieß, neé Fassnacht
Date of Birth: September 28, 1986
Place of Birth: Cuxhaven, Germany
Nationality: German

Education

Since 2014 Research Assistant at the Institute for Safety and Risk Sciences,
University of Life Sciences and Natural Ressources (BOKU), Vienna
Since 2013 Research Assistant at IANUS, Technische Universität Darmstadt
2011-2013 Master Programme in Physics, Technische Universität Darmstadt
2009-2010 ERASMUS Student at the Technical University of Denmark
2007-2011 Bachelor Programme in Physics, Technische Universität Darmstadt
2006-2007 Bachelor Programme in Mechanical Engineering,
Vienna University of Technology
1997-2006 Secondary School Kronberg Gymnasium Aschaffenburg



Erklärung zur Dissertation

Hiermit versichere ich, die vorliegende Dissertation ohne Hilfe Dritter nur mit den angegebenen Quellen und Hilfsmitteln angefertigt zu haben. Alle Stellen, die aus Quellen entnommen wurden, sind als solche kenntlich gemacht. Diese Arbeit hat in gleicher oder ähnlicher Form noch keiner Prüfungsbehörde vorgelegen.

Darmstadt, den 13.6.2017

(Friederike Renate Frieß, M.Sc.,)
